Strathclyde Business School

Department of Management Science

A Data-Driven Framework Using AI Predictive Models to evaluate Charterer Satisfaction in the LNG Shipping Industry

BY

Marios Ignatios Gaitanos

A thesis in fulfilment of the requirements for the degree of Doctor of Business Administration

Glasgow, UK

2026

Declaration of Authenticity and Author’s Rights

This thesis is the result of the author’s original research. It has been composed by the author and has not been previously submitted for examination which has led to the award of a degree.

Signed: Marios Ignatios Gaitanos

Date: 24th January 2026

Acknowledgement

Firstly, I would like to express my deepest gratitude to my supervisors, Professor Dr. Robert Van der Mear and Professor Dr. Iraklis Lazakis, for their invaluable guidance, continuous support, and generous contribution of time and expertise throughout my research. Their patience, helpful feedback, and encouragement have played a key role in shaping my academic journey, while allowing me the chance to follow my own research ideas. I am especially thankful for our many meetings and discussions, which were always insightful and filled with overwhelming support that helped me stay focused and confident throughout this work.

My heartfelt love and gratitude go to my family, whose constant support has been the foundation of all my achievements. To my parents, for their endless sacrifices, patience, and belief in me. To my brothers and their wives, thank them for your understanding, motivation, and the happiness you bring into my life. A special dedication goes to my nieces, for their joyful presence and innocent smiles.

Finally, I am truly grateful to my close friends for their friendship, understanding, and encouragement throughout this journey as well. Their kindness, good times, and support have made this experience both meaningful and memorable.

Abstract

The thesis addresses the need for a structured, data-driven approach to evaluating charterer satisfaction in the LNG shipping industry and so it introduces a framework called the Charterer Satisfaction Index (CSI). The CSI incorporates vessel performance predicting models that account for fuel consumption during laden passages, heel amount (fuel consumption in ballast condition), estimated discharging quantity, and the vessel's emission footprint for each voyage. These models are critical to charterers' decision-making in optimizing logistics efficiency. The charterers' scope of work involves making decisions to match cargo requirements, originating from commodity traders who arrange cargo deals, with suitable vessels for cargo shipment (offered by shipping companies). By applying the results of predictive models, charterers can increase their income, while shipping companies can enhance their reputation. The CSI measures the deviation between predicted and actual performance values for each model, where smaller deviations indicate higher levels of satisfaction, reflecting more efficient decision-making by charterers, while larger deviations indicate lower satisfaction, indicating that the matching process is not optimized. To achieve this, a quantitative methodology is applied, supported by predictive machine learning modeling and high-frequency AI-driven data analysis. Seven machine learning models, Linear Regression, Lasso Regression, Gradient Boosting Regressor, AdaBoost Regression, XGBoost, Random Forest, Histogram-Based Gradient Boosting Regressor (HGBR), Light GBM using Root Mean Squared Error (RMSE), Coefficient of Determination (R^2), and Mean Absolute Error (MAE). Among these, the Random Forest model consistently emerges as the best performing, achieving R^2 values ranging from 0.985 to 0.997 across three case studies conducted on three LNG vessels under both laden and ballast conditions. The case studies, based on two years of operational voyage data, demonstrate the robustness and predictive accuracy of the framework. Furthermore, expert interviews with industry professionals significantly contribute to the research, as their input guides both the selection of models for evaluating charterer satisfaction in terms of logistics efficiency and the weighting of each model's

relative importance within that assessment. The CSI is properly structured to capture and evaluate charterer satisfaction in a practical, realistic, and industry-relevant manner.

Table of Contents

List of Figures

List of Table

List of Abbreviations

ADEBOOST	Ade boosting
ADLM	Adaptive Learning Method
AHP	Analytical Hierarchy System
AI	Artificial Intelligence
ALS	Air Lubricating system
ANN	Artificial of Neural Network
AR	Auto Regressive
ATSP	Asymmetric Traveling Salesman Problem
B/T	Beam-to-Draft ratio
BBMS	Black-Box Models
BILSTMS	Bidirectional Long Short-Term Memory
BOG	Boil-Off Gas
BP	Back propagation
BPM	Business Process Management
BPNN	Back Propagation Neural Network
BRI	Belt and Road Initiative
C2H6	Ethane
C3H8	Propane
CAPEX	Capital Expenses
CATBOOST	Categorical Boosting
CBM	Cubic Meters
CBM	Cubic Meters
CH4	Methane

CII	Carbon Intensity Indicator
CNN	Convolutional Neural Network
CO_2	Carbon Dioxide
CODLAG	Coded Lag
COG	Course over Ground
COVID-19	Coronavirus Disease 2019
CP	Prismatic Coefficient
CPU	Central Processing Unit
CSI	Charterer Satisfaction Index
CVN	Cargo for Vessel Needs
CW	Coefficient Waterplane
DBA	Doctor of Business Administration
DCS	Data Collection System
DEA	Data Envelopment Analysis
DELM	Deep Extreme Learning Machines
DFDE	Dual Fuel disele engine
DG	Diesel Generator
DQ	Discharging Quantity
DSS	Decision Support System
DT	Decision Tree
EDA	Exploratory Data Analysis
EDM	Expectancy-Disconfirmation Model
EDQ	Estimated Delivered Quantity
EEOI	Energy Efficiency Operational Index

EFB	Exclusive Feature Bundling
EPS	Earnings per Share
ESG	Environmental, Social, and Governance
ET	Extra Trees
ETR	Extra Trees Regressors
EU ETS	European Union Emissions Trading System
EWMA	Exponential Weighted Moving Average
FCR	fuel consumption rates
FFD	Free-Form Deformation
FFNN	feedforward neural network
FNN	feed neural network
FNN	Feed-Forward Neural Networks
FOC	Fuel oil Consumption
FRB	Fuzzy Rule Base
FW	Fresh Water
GAM	Generalized Additive Models
GBM	Grey-Box Model
GBR	Gradient Boosting Regression
GCU	Gas Combustion Unit
GDPR	General Data Protection Regulation
GE	General Electric
GHG	Greenhouse gases
GKNN	Global K-Nearest Neighbor
GMM	Gaussian Mixture model

GOSS	Gradient-based One-Side Sampling
GP	Gradient Boosting
GPR	Gaussian Regression
GPS	Global Positioning System
GPU	Graphics Processing Unit
GR	Gradient Boosting
GTT	Gaztransport & Technigaz
HFO	Heavy Fuel Oil
HGBR	Histogram-Based Gradient Boosting Regressor
HHV	Higher Heating Value
HR	Human Resources
HRM	Human Resource Management
HSQE	Health, Safety, Quality, and Environmental Management
IAS	Integrated Automation Systems
IBS	Inboard Sensor
IGC	International Gas Carrier Code
IMO	International Maritime Organization
ISM	International Safety Management
IT	Information Technology
KNN	K-Nearest Neighbor
KRLS	Kernel-Based Regularized Least Squares
KW	Kilowatt
L/B	Length-to-Beam ratio
LASSO	Least Absolute Shrinkage and Selection Operator

LB	Light GBM
LCB	Center of Buoyancy
LD	Low Duty compressor
LGBM	Light Gradient Boosting Machine
LHV	Lower Heating Value
LNG	Liquefied Natural Gas
LO	Lubricating Oil
LSHFO	Low Sulfur Heavy Fuel Oil
LSMGO	Low Sulfur Marine Gas Oil
LSTM	Long Short-Term Memory
MAE	Mean Absolute Error
MAPE	Mean Absolute
MCDM	multi-criteria decision-making
ME	Main engine
ME-GA	M-type engine with low-pressure Gas Admission
MGO	Marine Gas Oil
ML	Machine Learning
ML/AI	machine learning/artificial intelligence
MLP	Multilayer Perceptrons
MLPR	Multi-Layer Perceptron Regression
MLPS	Multilayer Perceptrons
MLRA	Multiple Linear Regression Analysis
MMBTU	Milion British Thermal Unit
MOPSO	Multi-Objective Particle Swarm Optimization

MPR	Multi Linear Regression
MR	Multi Regression
MRV	Monitoring, Reporting, and Verification
MSE	Mean Squared Error
MT	Metric Tonnes
MTL	Multi-Task Learning
N2	Nitrogen
N_2O	Nitrous Oxide
NAN	Not A Number
NBOG	Natural Boil Off Gas
NG	Natural Gas
NN	Neural Network
NOAA	National Oceanic and Atmospheric Administration Ocean data
NOX	Nitrogen Oxides
NYSE	New York Stock Exchange
OLS	Ordinary Least Squares.
OM	Operation Management
OPEX	Operating Expenses
OSV	Offshore Support Vessel
P/E	Price-to-Earnings Ratio
PCA	Principal Component Analysis
PCTC	Pure Car and Truck Carrier
PPR	Projection Pursuit Regression
PROMEETHEE	Preference Ranking Organization Method for Enrichment Evaluations.

QES	Quantity Expansion or Shrinkage
R^2	Coefficient of Determination
RF	Random Forest
RFR	Random Forest Regressors
RMSD	Root Mean Square Error
RMSE	Root Mean Square Error
RPM	Per Mean Minute
RPM	Revolutions Per Minute
RSM	Response Surface Methodology
RSME	Root Mean Square Error
SERVQUAL	Service Quality Model
SFC	Ship Fuel Consumption
SFOC	Specific Fuel Oil Consumption
SMR	Single Mixed Refrigerant
SMS	Safety Management System
SOG	Speed Over Ground
SOM	Shipping Operation Management
SOOP	Speed Optimization Over a Path
SOX	Sulfur Oxides
SPC	Statistical Process Control
SPM	Ship Performance Monitor
SVM	Support Vector Machine
SVR	Support Vector Regression
TOPSIS	Technique for Order Preference by Similarity to Ideal Solution

TTW	Tank-to-Wake
U.S.	United States
UNCTAD	United Nations Conference on Trade and Development
VLCC	Very Large Crude Carrier
VLSFO	Very Low Sulfur Fuel Oil
WBM	White Box Models
WNNS	Wavelet Neural Networks
WTT	Well to tank
WTW	Well-to-Tank
XDF	expandable Dual-Fuel
XGBOOST	Extreme Gradient Boosting

1. Chapter 1 – Introduction

1.1 Introduction

This chapter presents as an introduction to the thesis, including the research background and offering introductory insights into the study's focus area. Also, it includes an outline of the thesis structure with a description of each chapter, as well as the main aim and objectives of the research

1.2 Research Background

This thesis examines the area of the cargo transportation service with a focus on maritime shipping. Among the various transport modes, air, road, and sea, this study concentrates on sea freight due to its dominance in global trade. Currently, maritime transport accounts for over 80% of worldwide cargo movement, owing to its extensive route networks, cost efficiency, environmental sustainability and strong safety record. (Zhang, et al., 2024b)

Maritime cargo transportation is a critical component of global trade, connecting a complex ecosystem of stakeholders. Commodity traders, being part of stakeholders, initiate this chain by purchasing and selling physical shipments domestically and internationally. Commodity traders also leverage global supply chains to meet cargo receivers' needs, capitalizing on arbitrage opportunities and globalization's reach to source raw materials efficiently (Huang, et al., 2005; Milberg, 2008). Charterers, as stakeholders in the maritime cargo transportation, then match shipment requirements with available vessels, often operating within the same organizations as traders. Last but equally important as the other stakeholders, shipping companies execute and manage vessel operations, ensuring the physical movement of goods (Stopford, 2009). The efficient collaboration and interconnection of the stakeholder network are vital for optimizing international commerce.

The thesis focuses on the shipping company stakeholders. Specifically, this part of global trade provides a variety of vessel sizes to meet market needs. Larger vessels are commonly preferred due to their ability to benefit from economies of scale, which result in lower per-unit costs as the volume of transported goods increases goods (Stopford, 2009). Smaller vessels, however, are favored for shorter distances and ports with strict limitations. Nowadays, the shipping market provides modern and efficient vessel services that contribute to environmental sustainability and produce relatively low emissions (Ahmed, et al., 2023; Bicer & Dincer, 2018). Also, it offers advancements in vessel technology which have improved the speed, reliability, and accessibility of sea services (Atieh, 2021). Moreover, it is important to highlight that there are various types of vessels, each designed to transport specific types of cargo such as oil, bulk commodities, containers, and gas.

Shipping companies' core scope is to make efficient strategies concerning vessel characteristics such as size, type and technology to capitalize on market demand. Once a vessel is built and operational, these companies need to ensure high-quality maritime services through successful vessel operations to gain a competitive edge. Conversely, poor service can severely damage a company's reputation, leading to significant financial losses and operational disruptions.

The study mainly examines the services of vessels that specifically transport cargo gas, known as LNG vessels. This type of cargo is carried in a liquefied phase, known as Liquefied Natural Gas (LNG). The need for LNG transportation has emerged more recently due to the growing of its demand, largely driven by its characteristics. LNG is considered a cleaner and more sustainable energy source, making it increasingly popular for use in both transportation of any kind of means (both at sea and on roads) and industrial applications. Thus, it investigates the mechanisms through which shipping companies can attain high services standards in LNG transportation by leveraging data-driven approaches. By adopting the latest technological trends, particularly the use of Artificial Intelligence (AI), the study can achieve higher accuracy in vessel performance analysis, gaining valuable insights to support operational decision-making and goals of a shipping company.

Thus, this thesis develops a framework called the Charterer Satisfaction Index (CSI), which evaluates charterers' satisfaction. The charterers' scope of work involves making decisions to match cargo requirements, originating from commodity traders who arrange transportation deals, with suitable vessels for cargo shipment (offered by shipping companies). To make efficient decisions that maximize their income, charterers require accurate and specific vessel performance information to plan and allocate resources effectively. The provided information includes predictions of vessel performance, and the CSI measures the deviation between actual and predicted values.

A low CSI indicates that the vessel performs consistently with its expected operational profile, allowing charterers to make informed and accurate commercial decisions regarding voyage planning, cargo allocation with the most suitable vessel, bunker management, and emissions compliance. This improves operational efficiency, reduces commercial uncertainty, strengthens long-term relationships between charterers and shipowners, and increases the likelihood of repeat business. In practical terms, a low CSI signifies that the predicted vessel performance closely matches the actual performance, that means the voyage implementation is according to the plan.

Conversely, a high CSI indicates larger deviations between predicted and actual vessel performance, reflecting lower charterer satisfaction. Such deviations may lead to increased fuel costs, inaccurate cargo planning, scheduling disruptions, reduced voyage profitability, and lower confidence in future vessel nominations. As a result, charterers face greater commercial uncertainty, making it more difficult to optimize cargo trades and maximize financial returns.

From the shipowner's perspective, the CSI can serve as a decision-support tool to continuously monitor operational performance, benchmark vessels across the fleet, identify performance deficiencies, and support operational and investment decisions aimed at improving fleet efficiency. Consistently achieving a low CSI can enhance a shipping company's reputation for reliability, strengthen its commercial competitiveness, improve customer retention, and contribute to its long-term financial sustainability and market growth.

From the charterer's perspective, the CSI provides an objective indicator of a vessel's operational reliability. A consistently low CSI increases confidence that the vessel will perform as expected, enabling charterers to make more informed vessel selection and cargo allocation decisions for future trades while reducing operational and commercial risk.

Hence, in this research, charterer satisfaction is defined as the extent to which a vessel's operational performance meets the charterer's expectations and supports efficient commercial decision-making. It reflects how accurately a shipping company can deliver the performance characteristics that charterers rely upon when selecting a vessel for a specific trade route.

The scope of charterer satisfaction in this study is specifically limited to voyage performance and encompasses four measurable dimensions for fuel consumption during laden passages, heel amount (which represents both the fuel consumed and the quantity of LNG retained on board to meet the vessel’s needs during ballast conditions, as analyzed in later chapters). These performance factors are selected because of their direct influence on voyage economics, contractual performance, and logistics planning. These models are developed using machine learning techniques to provide highly accurate predictive insights into vessel performance. This operational definition provides the foundation for the development of the proposed CSI framework.

To support the development of the CSI, interviews were conducted with 12 LNG shipping experts to validate the selected evaluation criteria and determine their relative importance through the Analytic Hierarchy Process (AHP). The interviews are not intended to identify the research topic or establish the conceptual framework; rather, they serve to confirm the relevance and suitability of the four predefined performance criteria and to derive their corresponding weights for incorporation into the CSI.

The number of 12 expert interviewees is considered sufficient because the purpose of the interviews is to gather expert opinions rather than achieve statistical generalisation. The experts are selected based on their experience in LNG shipping and chartering. During the interviews, the responses are very similar, with the experts consistently identifying the same key criteria for evaluating charterer satisfaction.

1.3 Thesis Outline

This thesis comprises five chapters that outline the implementation and presentation of the research, as the headers are defined in the Figure 1.1.

Chapter 1 – Introduction: This chapter introduces the overall scope and context of the research. It outlines the significance of the maritime shipping industry and presents the research aim and objectives. It also sets the foundation for the subsequent chapters.

Chapter 2 – Shipping Market and Shipping Operation Management: This chapter provides an overview of the shipping market and its key sectors, together with a review of shipping operation management. These areas provide the necessary background for understanding the dynamics, operational characteristics, and management practices of the shipping industry.

Chapter 2 – Literature and Critical Review: This chapter provide a comprehensive literature and critical review on vessel performance. Moreover, it includes a market analysis of key sectors within the shipping industry and review shipping operations management. These elements are essential for enhancing the reader's understanding of the industry's dynamics.

Chapter 3 – Literature and Critical Review: Vessel Performance and Charterer Satisfaction: This chapter provides a comprehensive literature and critical review focusing on vessel performance and charterer satisfaction. It examines existing studies on vessel performance assessment and prediction, including the application of machine learning models, as well as research related to service quality and customer satisfaction in shipping.

Chapter 4 – Case Study Implementation: This chapter presents the practical application of the research methodology of framework (CSI), as described in the Chapter 4, using real-world LNG shipping data. It outlines the implementation process highlighting how the framework performs under actual operational conditions. There are three CSI results based on three LNG vessels. Specifically, each vessel is evaluated in two conditions: laden (loaded) and ballast (unloaded), resulting in three separate case studies.

Chapter 5 – Findings and Discussion: This final chapter summarizes the key findings of the research, highlights their significance for the shipping industry, and assesses the effectiveness of the proposed framework. It also reflects on the study's limitations and offers recommendations for future research directions.

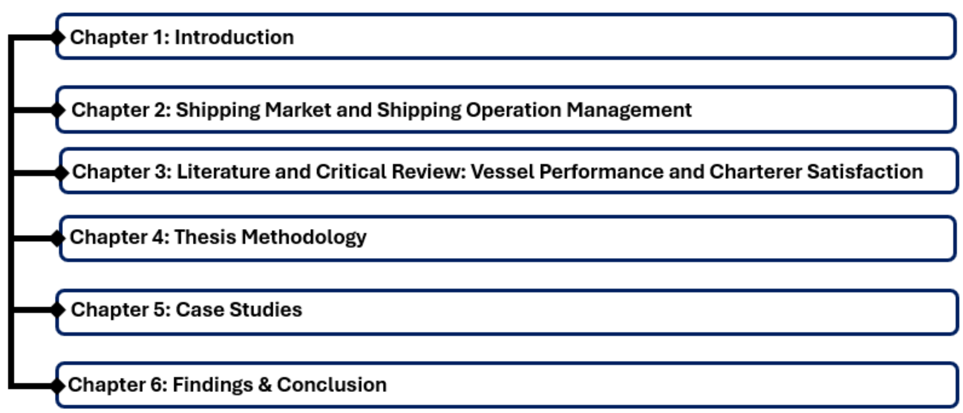

Figure 1.1 Chapters' headers.

1.4 Main aim and objectives

This research aims to develop a structured and AI-driven framework named CSI for evaluating charterer satisfaction with a focus on the Liquefied Natural Gas (LNG) shipping industry.

The objectives of this research are to ensure a comprehensive and systematic approach to the endeavor of developing CSI framework as follows:

1. Conduct a comprehensive literature and critical review to analyze existing scholarly information on vessel performance to understand the current academic landscape and inform the framework's development.
2. Design a structured, data-driven framework to evaluate charterer satisfaction. This involves detailing the methodical approach and components for transforming raw data into actionable insights.
3. Identify the set of models to be included in the framework based on insights from industry experts obtained through structured interviews.
4. Apply and validate the framework using LNG shipping datasets under real-world conditions, presenting these as case studies through analysis.
5. Validated the CSI results using statistical processes and interviews, incorporating feedback from industry experts and conducting a sensitivity analysis.

1.5 Research Gap

This study makes several contributions to both academia and industry in the context of LNG shipping by linking vessel operational performance with charterer satisfaction through a data-driven framework. The main contributions are categorised into practical, methodological, and academic dimensions, as outlined below.

i. Practical Contribution

The study develops the first Charterer Satisfaction Index (CSI) for LNG shipping, providing shipping companies and charterers with an objective, AI-driven decision-support tool. The CSI enables the evaluation and benchmarking of vessel operational performance and supports vessel selection by assessing how closely predicted performance aligns with actual operational outcomes.

ii. Methodological Contribution

The research proposes a novel framework that integrates machine learning-based predictions of fuel consumption, heel quantity, Estimated Discharging Quantity (EDQ), and emissions calculations with the Analytic Hierarchy Process (AHP). By combining predictive analytics with expert-derived weighting of performance criteria, the framework provides a transparent and systematic approach for translating multiple operational performance indicators into a single CSI.

iii. Academic Contribution

The study extends the literature on customer satisfaction in maritime transport by introducing an objective, operational performance-based approach to assessing charterer satisfaction. It complements traditional perception-based satisfaction models by demonstrating how machine learning, predictive analytics, and expert judgment can be integrated into a unified framework specifically developed for LNG shipping.

1.6 Summary

Chapter 1 highlights the critical role of maritime shipping in global trade, with over 80% of cargo transported by sea, and emphasizes the importance of vessel services in enhancing maritime efficiency and competitiveness. Moreover, it outlines the research background with a focus on the growing use of Artificial Intelligence (AI) to enhance vessel performance services, particularly in ways that benefit charterers and shipping companies. Also, the chapter presents the thesis aim and sets out the research objectives as an important insight of the research. Finally, it serves as an introduction to Chapter 2 which includes the literature and critical Review of thesis research area.

2. Chapter 2 - Shipping market and Shipping Operation Management

2.1 Introduction

Chapter 2 provides a comprehensive literature and critical review, focusing on three interconnected pillars: Shipping Market Analysis across major sectors, Shipping Operations Management, and Vessel Performance using machine learning models. The first two pillars are analysed in Chapter 2, while Vessel Performance is examined separately in Chapter 3. Figure 2.1 illustrates this comprehensive view of the shipping industry, where the convergence of these three pillars, highlighted by the yellow frame, defines the focus of the thesis.

Figure 2.1. The three foundational pillars of the literature and critical review, their interrelations, and the central intersection—highlighted in dark yellow—which delineates the specific focus of this research.

2.2 Shipping market: Demand and Supply Dynamics

This section examines key shipping sectors in tramp market, Tankers, Dry, and LNG, across four segments: freight rates, scrap, second-hand, and new building. It identifies major factors driving global shipping market based on demand and supply.

In the context of shipping market analysis of this section of chapter, one of the most academic resources is Stopford's book (2009) that provides a comprehensive overview of the key markets within the shipping industry. Additionally, several papers from the bibliography are used to contribute to the analysis of the shipping market, as shown in the following pages. For the research conducted, a range of digital libraries and academic databases are utilized to access scholarly articles, theses, and books. Key resources included ResearchGate, Google Scholar, Academia.edu, IEEE Xplore, SpringerLink, ScienceDirect, Wiley Online Library, JSTOR, and Taylor & Francis Online, all of which provided valuable peer-reviewed materials and academic insights (ResearchGate, 2024; Scholar, 2024; Academia.edu, 2024; IEEE Xplore, 2024; SpringerLink, 2024; ScienceDirect, 2024; Wiley Online Library, 2024; JSTOR, 2024; Taylor & Francis Online, 2024). These platforms are valuable for accessing a wide range of academic work, allowing researchers to upload and share their work with a broad audience. In addition, University's machine research via Strathclyde Business School's platform, named "Myplace" have been used proposing respective paper. Moreover, a significant database for shipping market analysis over the years is Clarkson, which is utilized for the following analysis. Relevant figures and data are derived from their reports, serving as primary sources for this research, Clarkson (2024).

More specifically, this section analyzes the principles of demand and supply dynamics in the shipping market, which together determine the equilibrium point that ultimately sets the daily freight rate. Demand in the shipping market refers to the need for vessel services, specifically the transportation of cargo. It is directly tied to cargo demand, or the volume of goods requiring shipment; an increase in cargo demand typically leads to higher shipping demand. Supply in the shipping market, on the other hand, is related to fleet productivity, which depends on factors such as vessel utilization, size, speed, time spent loading and unloading cargo operation, and also maintenance schedules. The number of vessels available in the market also plays a crucial role, fluctuating due to growth cycles and vessel lifespans (typically around 20 years before retirement). Measuring supply is complex due to these dynamic factors. Common indicators include the number of ships, total deadweight tonnage, and the fleet's ton-mile capacity. In addition to the existing fleet, two forward-looking indicators are particularly important when evaluating future shipping supply: the orderbook and the age profile of the fleet. The orderbook represents vessels that have been contracted but not yet delivered and therefore provides an indication of future fleet expansion, whereas the age profile indicates the potential removal of capacity through vessel demolition, particularly during periods of weak freight markets or increasingly stringent environmental regulations. Consequently, future shipping supply should be assessed not only by the current fleet but also by the balance between expected newbuilding deliveries and anticipated demolition activity.

Moreover, as a guiding theoretical principle, the interaction among the freight, newbuilding, second-hand and demolition markets can be explained through shipping-cycle theory (Stopford, 2009). Rising shipping demand or the prospect of higher freight rates often prompts shipowners to order new vessels to capitalize on anticipated profits. At the same time, stronger freight markets increase second-hand vessel values because existing vessels can immediately benefit from improved earnings. However, newbuilding vessels require a considerable construction period before entering service, creating a time lag between investment decisions and the actual increase in fleet capacity. If market demand weakens before these vessels are delivered, the industry may experience oversupply, resulting in declining freight rates and lower vessel values. Conversely, declining freight rates lead to increased scrapping of older, less efficient ships, thereby reducing market supply. During market downturns, second-hand vessels often become more attractive than new buildings because they involve lower capital investment, lower financial risk and immediate availability for employment, despite potentially higher maintenance requirements. These markets are closely interconnected, dynamically responding to fluctuations in freight rates and broader economic trends. Therefore, freight rates, newbuilding activity, second-hand transactions and demolition should not be viewed as independent markets but as interrelated components of the shipping cycle that continuously influence the evolution of fleet supply.

2.2.1 Bulk Carriers

This subsection presents a concise analysis of the dry bulk market over recent decades. The following analysis outlines trends in market demand and supply, alongside key global events that have significantly shaped the market.

The dry bulk market, centered on transporting commodities like coal, iron ore, and grain, is significantly influenced mainly by global infrastructure development, population growth and trading patterns (UNCTAD, 2024). Infrastructure projects, such as highways, bridges, railways, and ports, drive demand for raw materials like steel and cement, increasing the need for bulk carriers to transport iron ore, a key cargo in the market. Population growth further amplifies this demand, as rising global populations require more agricultural products, like grain, and energy resources, such as coal, necessitating bulk carriers to move these commodities from production to consumption regions (Michail & Melas, 2021). Additionally, changing trade patterns, driven by economic growth in emerging markets, regional trade agreements, and technological advancements, reshape the volume and routes of bulk commodity flows, prompting adjustments in bulk carrier demand to meet new and expanding trade channels (Algieri, et al., 2022).

Figure 2.2 presents to be a multi-axis bar and line graph displaying indices and values related to the bulk shipping industry over several decades, from 1976 to 2023. It uses a dual y-axis format to accommodate the different scales of data represented: the left y-axis for the New Building Price Index, Secondhand Price index and scrap values, and the right y-axis for the historical earnings, freight rate market, which are notably in scale compared to the prices and values on the left.

The Average Capesize Long-Run Historical Earnings (yellow line) represent the freight market, fluctuating between $6,500/day and $113,000/day over the years, as shown in the figures. Early 2000, in 2002, earnings surged from $13,000/day to $70,000/day within two years, 5.5 times more. After a brief downturn in the freight market, earnings spiked again in 2006, rising from $40,000/day to over $110,000/day, the highest rate in recent decades, an increase of more than 175% during the global commodities boom. However, following the 2008 global financial crisis, earnings plummeted by 95%, falling back below $7,000/day. This sharp decline highlights the freight market's sensitivity to global economic conditions, as reduced shipping demand significantly impacts profitability. In 2013, China's Belt and Road Initiative (BRI) also influenced global trade and shipping routes. The BRI expanded infrastructure across Asia, Europe, and Africa, increasing demand for bulk shipping of construction materials like steel, cement, and coal. During this period, freight rates are relatively low, around $6,500/day, but they doubled to $13,500/day, a 100% increase driven by rising demand for these projects. Finally, from 2020 to 2022, the COVID-19 pandemic caused unprecedented disruptions in global supply chains. Shipping demand collapsed as economies went into lockdown and global trade slowed. However, a rapid recovery followed, fueled by supply chain bottlenecks and a sharp rebound in commodity demand. Simultaneously, the Russia-Ukraine War (2022) further disrupted the shipping industry, particularly the grain market, as Ukraine, one of Europe's key grain exporters, is severely impacted. While this affected Capesize freight rates, the impact is even more pronounced on smaller vessel sizes.

The Dry Cargo Newbuilding Price Index (blue bars) shows long-term upward and downward trends, fluctuating due to global events. In the 1980s, the index fell from 137 to 99 (25% increase), a significant decline, but it later fluctuated between 99 and 192 in 2007 with some fluctuations in between, peaking due to high freight rates driven by the global commodities boom from China's economic expansion. In 2019, due to low freight rates caused by the COVID-19 pandemic, the index remained low without any further investment from shipping companies for a new building vessel at there was a uncertainty in the freight market. However, with expectations of higher freight rates, later the index rose from 139 in 2020 to 191 in 2023 (37% increase).

The Bulk Carrier Secondhand Price Index (orange bars) followed a pattern similar to that of the dry freight market, rising steadily from the late 1970s through the 1980s and ranging between 12 and 60 (400% of increase) by 1991. During the 1990s, secondhand prices experienced moderate fluctuations, a 120% increase, ranging from 60 to 133, with the peak occurring in 1995. From the early 2000s to 2007, the index rose significantly, peaking at 462, driven by strong freight market conditions. Following the 2008 financial crisis, the market saw a sharp decline, with the index falling to 78 by 2015. In subsequent years, values fluctuated between 78 and 172 (an increase of 120%), closely tracking freight market movements. The Secondhand Price Index serves as an alternative to investing in newbuild ships, providing shipowners with a quicker way to capitalize on favorable freight rates without the long lead times associated with new vessel construction.

The Capesize Scrap Value (grey line) showed a more stable trend compared to the price indices, ranging from 32 in the 1990s to 35, with fluctuations in between, and peaking at 37 in 1994. Later, notable peaks occurred in 2007, 2011, and 2021, reaching values of 104, 112, and 126, respectively. Unlike freight rates, which are primarily driven by demand for shipping services, scrap values are mainly influenced by the market value of materials, particularly steel, together with demand from ship-recycling yards. When global steel prices increase, the value of these materials rises, enabling demolition yards to offer higher prices for obsolete vessels. Consequently, higher scrap values do not necessarily indicate stronger demand for maritime transport but rather improved economic returns from vessel demolition. At the same time, weak freight markets often encourage shipowners to scrap older and less efficient vessels because the expected earnings from continued operation are lower than the value that can be realised through demolition. Therefore, scrap values are influenced by both conditions in the materials market and shipping-market fundamentals, rather than by shipping-service demand alone.

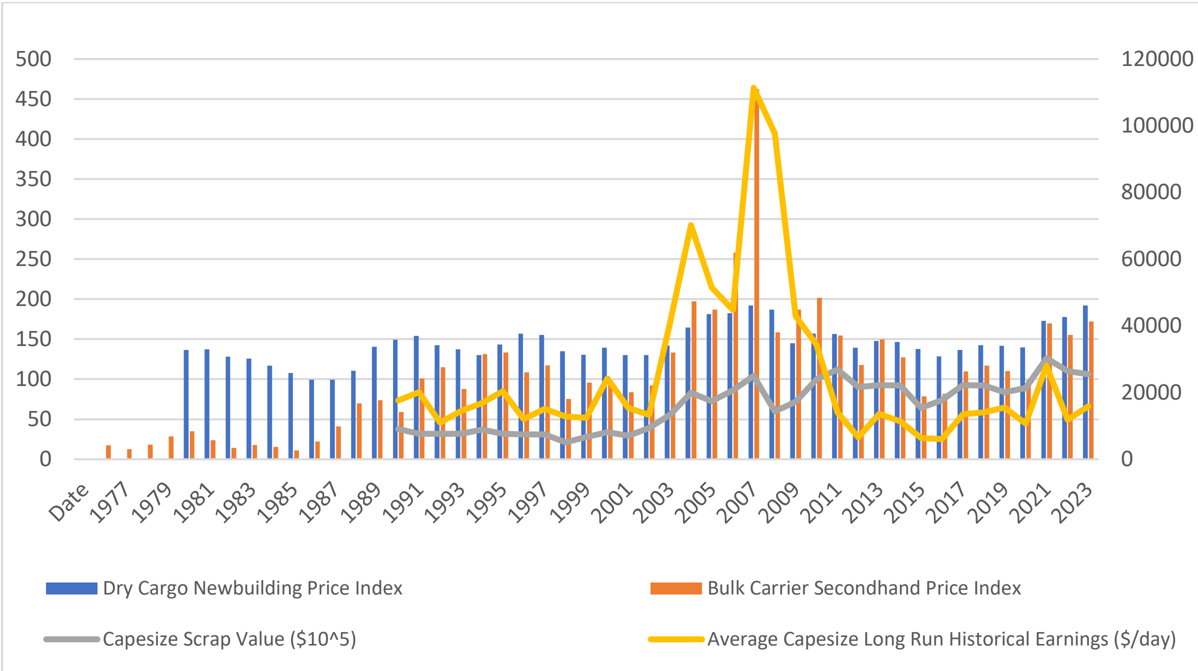

Figure 2.2. Dry Cargo Market (Freight, Second-hand, Scrap and Newbuilding prices). , data from Clarkson (accessed May 2024).

2.2.2 Tankers

Moreover, Tanker's market analysis is carried out following which is the market that focused on transport liquid oil cargoes, primarily crude oil and petroleum products (UNCTAD, 2024). This subsection explores the demand and supply dynamics in the tanker market.

The tanker market, like the dry bulk market, is driven by cargo demand, which is shaped by geopolitical events (Argyriou, 2023). Conflicts, political tensions, or trade disputes in oil-producing regions can disrupt supply chains, impacting tanker demand. Sanctions or regional conflicts may reduce oil exports, lowering tanker needs, while alternative routes or sources can increase demand, creating opportunities for shipping companies. Moreover, oil price fluctuations significantly impact tanker demand. Higher oil prices often encourage producers to increase output, boosting the need for tankers to transport larger volumes. Conversely, lower prices can lead to reduced production and decreasing tanker demand. Price volatility influences decisions on whether to scrap older vessels or invest in newer, more efficient ones. In addition, environmental regulations and the push for sustainable shipping are reshaping the tanker market. Stricter emission standards are prompting tanker owners to retrofit vessels with emission-reducing technologies or invest in eco-friendly newbuilds. These changes could tighten the supply of compliant vessels, potentially driving up charter rates for those meeting regulatory standards. Also, shifting energy consumption patterns further influence the tanker market. Growing global energy demand is likely to increase the need for crude oil and petroleum products, driving tanker demand. However, the transition toward renewable energy and natural gas could reduce oil demand over time, potentially impacting the tanker market in the long term.

Following the market principles, Figure 2.3 illustrates Average Earnings of All Tankers ($/day) from 1990 to 2024 which highlights significant fluctuations influenced by global events. In the early 1990s, earnings averaged around $18,000/day but rose sharply following the End of the Cold War, as global trade expanded. The Gulf War (1990-1991) caused short-term volatility, but markets stabilized quickly, limiting its long-term impact on earnings.

By 2003, the Iraq War pushed earnings from $17,000/day to almost $55,000/day, a more than 220% increase due to oil supply disruptions and heightened demand for tankers. This surge is followed by a slight decline, but earnings remained above $35,000/day through the mid-2000s.

In 2008, earnings peaked again at $52,000/day, driven by the global commodities boom. However, the Global Financial Crisis (2008-2009) caused a sharp collapse, with earnings dropping to $15,000/day. This reflected reduced global oil demand and oversupply of shipping capacity.

A gradual recovery followed, with earnings reaching $36,000/day by 2015, due to o the Shale Revolution and increased U.S. oil exports. However, the COVID-19 pandemic, period 2019 to 2022, caused another collapse, with earnings plunging by 76%, from $25,000/day to around $6,000/day in 2021.

The market rebounded sharply, with earnings rising to $38,000/day by 2022, around 500% increase from the pandemic low. The Russia-Ukraine War further boosted earnings, as the shift in oil and LNG flows increased demand for tankers. By 2024, earnings stabilized around $40,000/day, reflecting a strong recovery in global trade, energy market shifts, and new environmental regulations affecting shipping capacity.

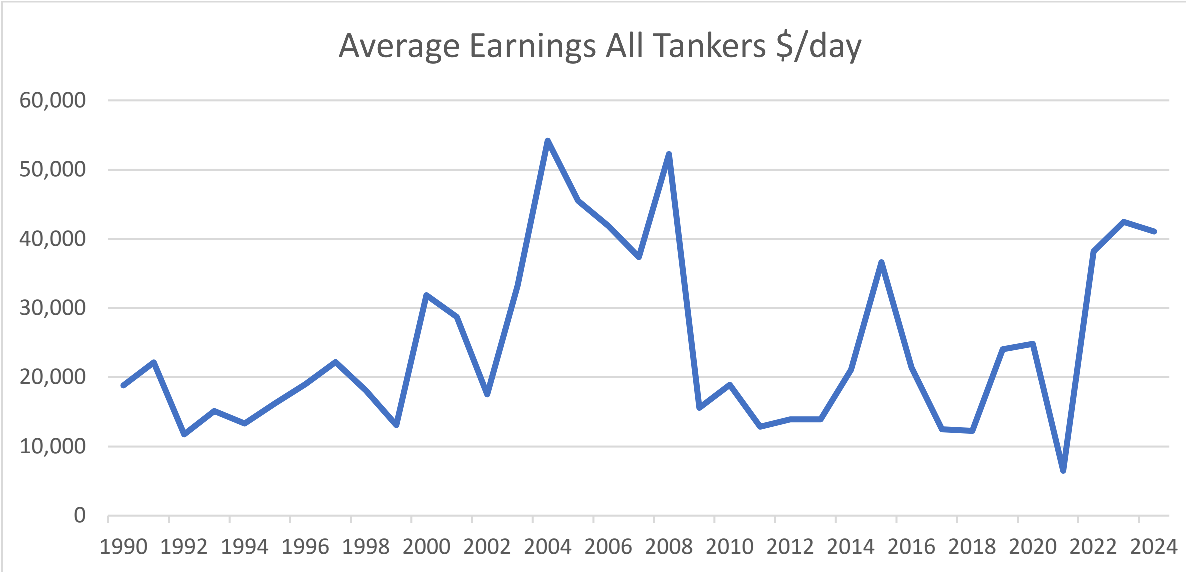

Figure 2.3. Tanker Market with Freight value. , data from Clarkson (accessed May 2024).

Moreover, Figure 2.4 illustrates three key market metrics for tanker ships from 1976 to 2023. The Tanker Secondhand Price Index (Blue Line) tracks the price trends of secondhand tankers. The Oil Tanker Newbuilding Price Index (Orange Line) monitors the cost of new oil tankers. Additionally, the VLCC Scrap Value ($m, Grey Line) reflects the scrap value of Very Large Crude Carriers (VLCCs).

The Oil Tanker Newbuilding Price Index (orange line) starts at a lower level in 1976, around 50 units, and increases over time. It remains particularly steady at a high level during the late 1990s into the 2000s. The index peaks around 2008 at approximately 250 units, then declines sharply to 150 before rising again to around 210 units toward 2023, following the trends in freight rates.

Like the Newbuilding Price Index, the Secondhand Price Index Index (Blue Line), it starts at a lower range about 13 in 1976 and shows a general upward trend to 250 until 2008. Followed by a period of significant volatility, with notable peaks occurring after 2008 and again in the early 2020s. The general trend suggests fluctuations in market demand and supply dynamics for secondhand tankers, with peaks often correlating with broader economic booms and downturns. The correlation between the new building and secondhand price defines that both markets are affected by similar economic forces.

The VLCC Scrap Value (grey line) generally followed the trends of secondhand and newbuilding prices, although it is still influenced by similar demand-supply dynamics. Between

1976 and 2000, the scrap value remained relatively stable, starting at around \$3 million and rising to \$4.85 million, with brief peaks in 1980 and 1990 at \$7 million and \$8.5 million, respectively. However, in the early 2000s, the trend shifted upward, reaching approximately \$27 million by 2008, an increase of about 210%, driven by the global economic boom and high demand for steel. Following this period, a financial crisis occurred, causing scrap values to fall by around 65% to about \$9 million. By 2023, the scrap value had recovered, reaching approximately \$28 million fueled by continued steel demand and the scrapping of older vessels.

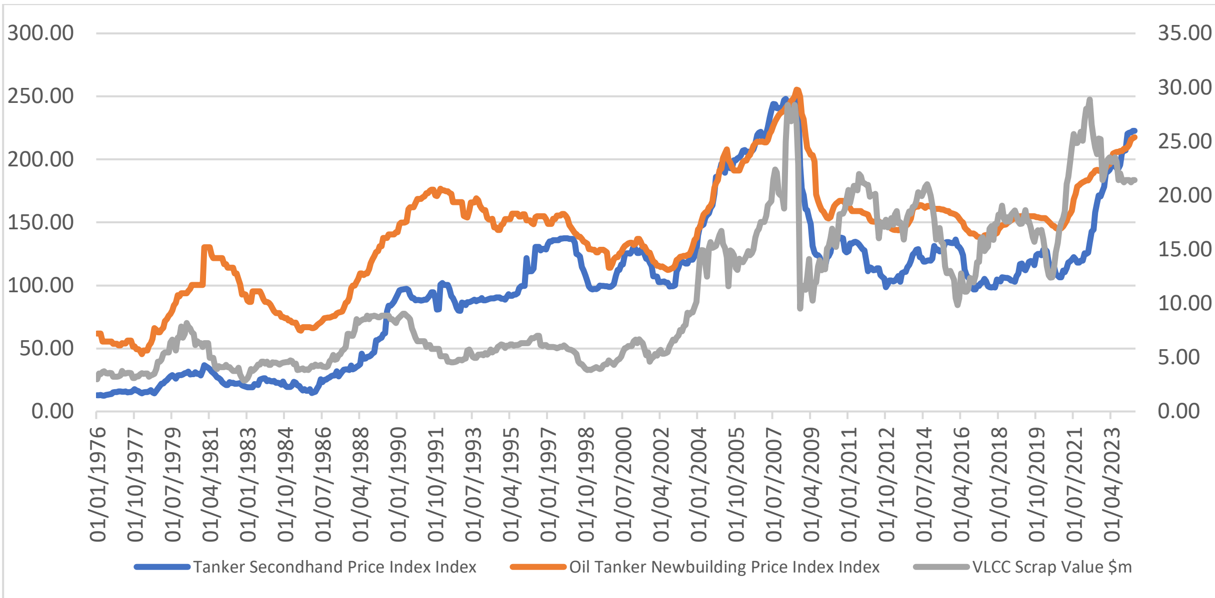

Figure 2.4. Tanker Market (Second-hand, Scrap and Newbuilding prices). , data from Clarkson (accessed May 2024).

2.2.3 Liquefied Natural Gas (LNG) Carriers

The LNG carrier market, a key focus of this thesis, involves specialized vessels designed to transport liquefied natural gas (Molnar, 2022). The growing role of natural gas as a cleaner energy source, the development of new LNG projects, and advancements in LNG shipping technology are driving market growth (Botão, et al., 2023).

The increasing importance of natural gas as a cleaner energy source, significantly boosts demand for LNG carriers, driven by its lower carbon footprint compared to coal and oil. As nations strive to reduce greenhouse gas emissions, this shift in energy preferences increases the need for LNG carriers to transport natural gas from production hubs to consumption centers. Furthermore, the development of new LNG projects, including the construction and expansion of export terminals and the establishment of import facilities in countries diversifying their energy mix, further heightens the demand for carriers to meet rising production and distribution needs. Concurrently, advancements in LNG shipping technology, such as more efficient containment systems, advanced propulsion methods, and enhanced operational capabilities, improve vessel performance and cost-effectiveness (Adekoya, et al., 2024). These innovations encourage shipowners to invest in modern, high-performance LNG carriers, thereby sustaining and driving demand for cutting-edge vessels in the market.

Figure 2.5 depicts the growth of the global seaborne LNG trade from 1990 to 2024 across key metrics such as world seaborne LNG trade (million cubic) and world seaborne LNG trade billion tone-miles. The figure highlights a steady increase in LNG cargo demand market, with upward trends in all metrics reflecting rising freight demand. The miles covered by LNG vessels closely align with this trend, supporting the expansion of the market. This growth underscores the increasing reliance on LNG as a vital energy source, driven by global efforts to transition to cleaner fuels.

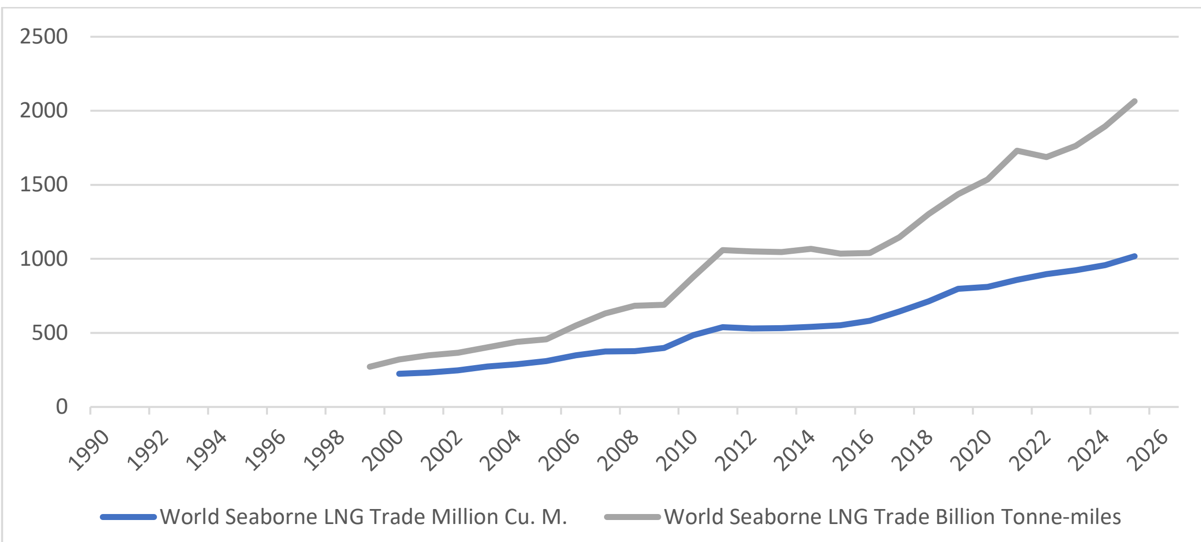

Figure 2.5. LNG carrier market analysis: supply and demand. , data from Clarkson (accessed May 2024).

Following Figure 2.6 shows freight rate from different sizes of LNG vessel and time of contract for the last twenty years. Firstly, the LNG 145K CBM 1-Year Time Charter Rate (grey line) tracks the rate for smaller 145K CBM vessels for a short time contract, with data providing a market overview from 2015 to 2024 based on availability. These ships follow the same general trends as their larger counterparts. At the beginning of the observed period, rates are relatively low, around $20,000/day, but gradually increased, peaking at $57,000 in 2019 and $66,000 in 2023. By 2024, the freight rate had declined to approximately $38,000/day. Overall, fluctuations ranged between $20,000/day and $66,000/day over the last decade. This pattern suggests that smaller capacity vessels tend to command lower charter rates, reflecting the market's preference for larger ships, which offer greater cargo capacity and operational efficiency.

The LNG 160K CBM 1-Year Time Charter Rate (dark blue line) represents the daily rate for a 1-year time charter of a 160K CBM LNG carrier. Starting at approximately $35,000/day in 2005, the rate gradually increased to $61,000/day by 2024. The rate peaked at nearly $135,000/day during both 2012 and 2022, reflecting periods of heightened demand. Between 2015 and 2017, the rates declined to around $31,000/day.

The LNG 174K CBM 1-Year Time Charter Rate (orange line) follows a similar pattern but at generally higher levels, reflecting the premium for the larger 174K CBM vessels even the contracts are short time. The data covers the period from 2019 to 2024. Rate variability mirrors that of the 160K CBM ships, however, the larger capacity vessels command higher charter rates, especially during periods of market tightness, such as in 2022 when the rate reached $172,000/day.

On the other hand, the LNG 160K CBM 3-Year Time Charter Rate (yellow line) reflects the rates for longer-term charters of 160K CBM LNG carriers, with market data spanning from 2010 to 2024. These rates exhibit less volatility compared to shorter-term charters, highlighting the typical discount associated with longer-term commitments. Fluctuations range between $63,000/day and $116,000/day, with notable peaks in 2011 at $116,000/day and in 2023 at $102,000/day.

Similarly, the LNG 174K CBM 3-Year Time Charter Rate (light blue line) reflects the rates for long-term charters of 174K CBM LNG carriers, with market data spanning from 2021 to 2024. This trend underscores the market's continued preference for larger vessels, which offer greater operational efficiency over time. In recent years, rates have fluctuated between $83,000/day and $134,000/day, with a peak occurring in 2023 at $134,000/day.

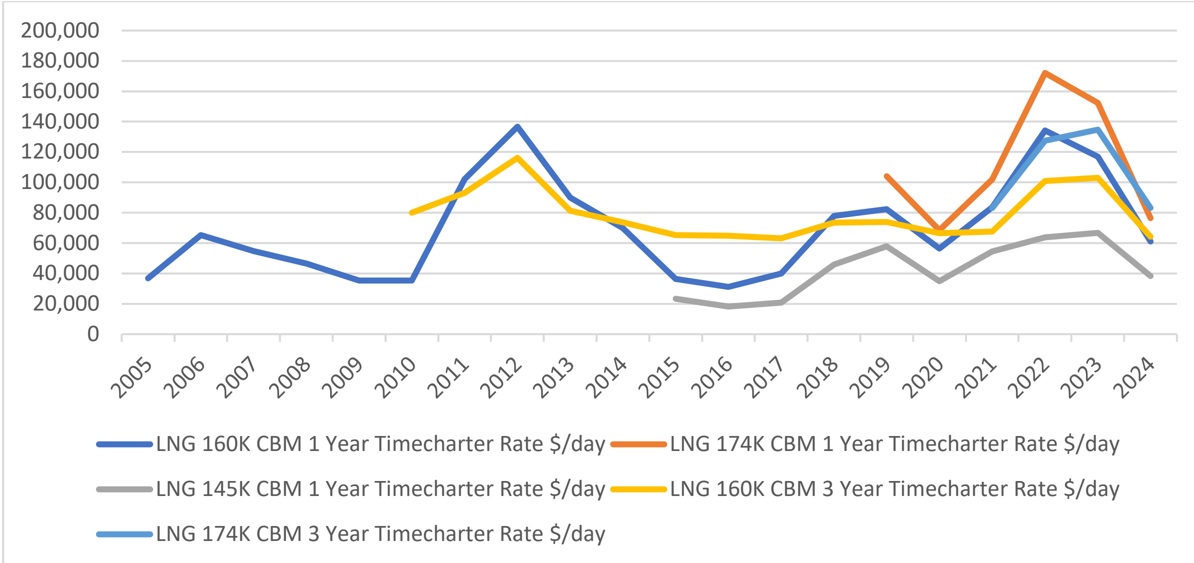

Figure 2.6. LNG Vessels Time Charter rate analysis.   , data from Clarkson (accessed May 2024).

In recent years, global crises like the COVID-19 pandemic, the Russia-Ukraine war, and the energy crisis have greatly affected the LNG shipping market. The pandemic disrupted supply chains, causing a sharp drop in shipping demand and charter rates, but these quickly recovered due to ongoing higher LNG demand. The Russia-Ukraine war in 2022 led Europe to increase LNG imports, boosting reliance on LNG carriers. The energy crisis caused natural gas prices to rise, especially in Europe, which strengthened LNG trade as energy sources shifted globally. At the same time, efforts to reduce emissions have made LNG an important cleaner fuel for shipping, resulting in increased demand. Overall, freight rates have followed a clear upward trend, showing how major global events shape the dynamic LNG shipping market.

2.3 Shipping Operation Management (SOM)

This section explores Shipping Operations Management (SOM) by applying Operations Management (OM) principles and theories that are particularly relevant to the shipping industry. OM is a well-established academic field, extensively explored in literature and education (Visvikis & Panayides, 2017).

Similarly to section "2.3 Shipping market: Demand and Supply Dynamics", a range of digital libraries and academic databases are utilized for this research to access scholarly articles and books. Therefore, for the section "2.3 Shipping Operation Management (SOM)", indicative keywords such as *"operations management objectives in shipping," "maritime operational* *efficiency,"* and *"shipping process optimization."* have been used. The significance of OM's key elements prompted further investigation in the section "2.3.1 Key elements of Shipping Operation Management", using keywords such as *"core elements of shipping operations," "maritime operational frameworks,"* and *"shipping management principles".* Also, the section "2.3.2 Economic benefits" examines the economy within maritime operations using terms such as "*circular economy in shipping*", *"shipping economy" and "shipping business,".* Additionally, the broader economic benefits of shipping operations, analyzed in this section, are searched based on the phrase "*shipping industry financial performance"* ensuring a thorough and focused review.

Related to Operations Management (OM) definition, it can be viewed as a science, applying systematic, evidence-based methods to optimize processes and support decision-making. More specifically, it involves designing, producing, and delivering products and services efficiently across all stages of the supply chain. As Ivanov et al. (2021) note, OM aligns operations with customer needs and sustainability goals. In the shipping industry, OM plays a crucial role in managing risks, reducing costs, and enhancing performance (Mitroussi, 2013; Tsarouhas, 2023). It ensures reliable, cost-effective, and high-quality services, supporting competitiveness in the global market (Salah, et al., 2023).

Operations Management (OM) has evolved significantly since its origins, driven by the goal of delivering goods and services that meet customer needs. Its journey began in 1776 with Adam Smith's concept of the "Specialization of Labor in Manufacturing" and extends to the 2010s with the advent of the "Worldwide Communication Internet of Things" (Graves, 2021). Over time, OM has continuously advanced, emphasizing product quality, production volume, human factors, digitalization, environmental and social responsibility, operational efficiency, cybersecurity, safety, and integrated management systems. Within the shipping industry, this evolution has also been driven by increasingly demanding charterers, particularly major tanker customers, who require higher standards of safety, operational reliability, environmental performance and service quality. Furthermore, the introduction of international regulations and industry standards, including SOLAS, MARPOL, the ISM Code and STCW, has fundamentally transformed shipping operations by promoting standardized safety, environmental protection and risk management practices. Equally important has been the ability of shipping companies to develop skilled personnel capable of implementing and operating new technologies, digital systems and management frameworks, ensuring that technological and regulatory developments are effectively translated into improved operational performance.

It is necessary for the two key focus areas of SOM to be analyzed. The first one is related to five objectives which are vital for maintaining daily operational efficiency and enhancing overall business competitiveness, ensuring that customer expectations are consistently met or exceeded (Stopford, 2009).

In the shipping industry, meeting customer expectations starts with delivering high-quality goods and services (first objective) that fulfill their intended purpose. This is pivotal to ensuring vessel performance and operational safety. Within Shipping Operations Management, these objectives are achieved through Health, Safety, Security, Quality and Environmental (HSSQE) management systems, which provide a structured framework for managing operational risks, regulatory compliance and continuous improvement. Adhering to strict quality and safety standards together with effective security and environmental management not only satisfies customers but also builds trust and secures a competitive advantage. In an industry where incidents such as oil spills, security threats or safety failures can result in severe financial penalties, operational disruptions and lasting reputational damage, prioritizing HSSQE performance is critical for maintaining market share and long-term business sustainability. Additionally, quality extends to effective communication with customers, ensuring clarity and responsiveness throughout the service process.

The second key objective in shipping services is optimizing speed rather than simply maximizing vessel velocity. In modern shipping operations, speed is determined through a trade-off between transit time, fuel consumption along with its relative costs and contractual delivery requirements. This balance has become increasingly important following periods of high fuel-oil prices and stricter environmental regulations, as excessive speed substantially increases fuel consumption and emissions. Consequently, shipping companies seek the optimum operating speed that satisfies customer requirements while maintaining cost-efficient operations. This optimisation is increasingly supported by weather-routing systems, voyage optimisation software, high-frequency data acquisition systems and real-time vessel performance monitoring, which enable operators to continuously adjust speed according to weather conditions, sea state and operational constraints. Therefore, speed optimisation has evolved from simply reducing voyage duration to achieving the most efficient balance between service quality, fuel consumption and environmental performance. Speed and reliability remain important time-related characteristics of shipping services and continue to provide a competitive advantage in the market (Notteboom, 2006).

Also, dependability (third objective) is vital for consistently meeting delivery commitments, fostering customer trust, and building a reputation for reliability. This consistent performance provides a strategic advantage, setting operations apart from competitors. Key indicators, encompassing both core and supplementary attributes, evaluate the overall consistency in customer service delivery and efficient transportation processes. Dependability is key to operational excellence and building customer trust (Prokofieva, 2020).

Moreover, flexibility is another critical attribute (forth objective) in shipping operations, enabling adaptation to unexpected challenges or unique customer needs. The ability to customize operations and respond swiftly enhances customer service, increases satisfaction, and provides a competitive advantage (Lin, et al., 2020).

The objectives of reliability, flexibility, safety, and quality in shipping, combined with the concept of "value" (fifth objective) directly influence customer satisfaction through the cost of transporting cargo between ports (Phan, et al., 2020). Charterers, tasked with arranging cargo transportation, are highly cost-sensitive, as voyage expenses significantly impact overall service costs (Lirn & Wong, 2013).

While, the second key focus area of a shipping company is to optimization operating costs, and Shipping Operations Management plays a vital role in achieving this through strategic cost-efficiency measures. Several common and effective practices adopted by shipping companies are further analyzed, focusing on cost control.

Initially, the first practice is related to optimization, which is a primary strategy, focusing on the efficient management of ships by controlling and monitoring in short terms high-cost resources which are the crew, maintenance and also fuel consumption of the vessels. Specifically, effective recruitment strategies for crew and office staff help maintain operations within budget, avoiding overstaffing and keeping daily costs manageable. Moreover, related to the fuel consumption of the vessel improved routing, slow steaming, or adopting alternative fuels can significantly lower expenses. Lastly, effective maintenance and scheduling of ships minimize breakdowns, delays, and unplanned downtime is another strategy. Predictive maintenance and investments in modern, fuel-efficient vessels reduce repair costs and enhance operational efficiency.

However, the most critical aspect between these two key focus areas is the trade-off that exists between them. Balancing cost efficiency and customer satisfaction in the shipping industry requires a comprehensive, multi-faceted approach. For instance, choosing between older and newer vessels is a key strategic decision for shipping companies. However, vessel-acquisition strategies vary considerably depending on the financial capability, commercial strategy and risk appetite of each shipowner. The decision is not simply a comparison between the lower acquisition cost of an older vessel and the higher capital investment of a newbuilding. Market conditions, asset-value volatility and sale-and-purchase (S&P) opportunities often play a decisive role. Second-hand vessels can generate immediate cash flow because they are available for immediate employment, allowing owners to capitalize quickly on favourable freight-market conditions. In contrast, newbuildings require a significant construction period before delivery but may provide superior fuel efficiency, lower operating costs, improved environmental performance and longer-term competitiveness.

Also, balancing transit speed and fuel efficiency is also crucial. Rather than maximizing vessel speed, operators increasingly seek the optimum balance between voyage duration and fuel consumption, supported by weather-routing systems, voyage optimisation software and real-time data-acquisition technologies. However, once a vessel is operating under a time charter, speed requirements are normally determined by the charterer, who specifies the required voyage schedule or arrival window. Consequently, the shipowner or technical manager primarily focuses on operating the vessel as efficiently as possible within the charterer's commercial instructions by optimising fuel consumption, routing and overall vessel performance. Fast shipping improves customer satisfaction but raises fuel and operational costs, whereas slow steaming reduces fuel consumption and emissions but may extend delivery times. Environmental compliance introduces another trade-off. Meeting regulations often means investing in green technologies such as LNG or hydrogen propulsion, which raises costs but avoids penalties and supports brand reputation. Automation and Artificial Intelligence can boost operational efficiency, improve decision-making and support real-time monitoring through digital technologies. While highly standardised automated processes may reduce flexibility in specific operational tasks (a static operational perspective), digital technologies simultaneously enhance the ability of shipping companies to respond dynamically to changing weather conditions, market requirements and operational constraints. Therefore, technology should be viewed not as reducing operational flexibility, but as transforming flexibility through improved information, faster decision-making and data-driven operational optimisation.

2.3.1 Key elements of Shipping Operation Management

Success in Operations Management depends on effective procedures, a well-defined business structure and culture (Wu, et al., 2019; Salah, et al., 2023). A company's strategy and policies also significantly influence OM performance and its core objectives. The following subsection explores the key elements essential to achieving these goals.

2.3.1.1 Structure

According to Ivanov et al., (2021), Operations Management helps a shipping company succeed by ensuring a clear and effective organizational structure. This structure defines roles and responsibilities across departments, enabling smooth coordination, efficient decision-making, and better resource management. A well-organized company can improve communication, optimize operations, and quickly adapt to challenges, all of which support achieving business goals effectively.

Operations Management specifically defines that the company's structure can be based on three main pillars as a general model: Marketing, Operations, and Finance. The importance of each pillar and how the company/organization supports them may vary due to the proper utilization of human resources and the market demands in which the company or organization operates (Ivanov, et al., 2021).

The book by Visvikis and Panayides (2017) include foundational concepts of ship management as well as reviews of shipping company operations. Specifically, there is a reference which discusses commercial management as it is pivotal for the economic effectiveness of shipping operations, focusing on maximizing revenue through efficient chartering strategies, and customer relationship management (Assimenos, 2017). Furthermore, Ajayi and Udeh (2024) addresses crew operations management, highlighting its importance for operational efficiency and safety. Effective management ensures that all crew members are competent, well-trained, and ready for their duties onboard. Additionally, technical operations management, as covered by Lazakis et al. (2010) encompasses all technical aspects of ship machinery and structure management, ensuring that vessels are well-maintained, regulatory-compliant, and prepared for safe operations. Rinaldy (2022) explores safety and security in shipping operations, which are crucial for protecting both assets and lives within maritime activities. This segment emphasizes the implementation of practices that reduce operational risks and comply with international safety standards. Lastly, the nationality of ships and marine insurance, discussed by Aladwan (2020), focus on how a ship's nationality determines its legal status and regulatory obligations, which in turn affects its operations, safety, and associated insurance costs.

Drawing on the structures of Greek companies as described in the paper by Lazakis and Van Der Meer (2023) which provides a general structure of a company analyzing each department separately (Figure 2.7). More specifically, a shipping company based on the market challenges includes departments that address the commercial and strategic aspects of the business, such as the Chartering department and is under the Marketing framework. Additionally, the Operational aspect of a shipping company is included by a variety of the departments, which concentrates on the input view of operational functions encompasses the Operations, Technical, HSSQE (Health, Safety, Security, Quality, and Environmental management), Crew, Insurance, Legal, HR (human resources), IT (Information Technology) and Purchasing departments. The primary objective of these departments is to ensure the maximization of outputs, namely the shipping services provided by the vessels. Therefore, these departments must guarantee smooth, safe, and secure cargo transportation from one area to another, emphasizing the importance of operational efficiency, safety protocols, and security measures in facilitating effective logistics. Lastly, the Accounting/Financial department focuses on accounting matters, company cash flow and assurance of the proper receipt of the income on time and generally related to asset management.

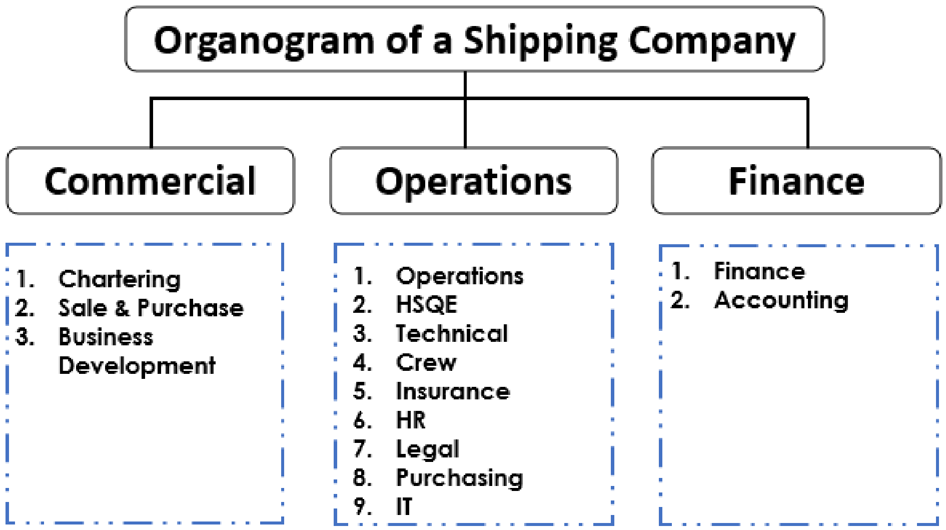

Figure 2.7. Organogram of a shipping company.

2.3.1.2 Culture

The culture of a shipping company does affect the operation management. Lazakis and Van Der Meer (2023) examine how the organizational structures of Greek-owned shipping companies contribute to their successful business performance despite global shipping challenges. This paper focuses on Greek culture, highlighting specific characteristics that influence how companies are managed in Greece. Also, Progoulaki and Theotokas (2010) discussed the role of Human Resource Management (HRM) in accordance to culture as well, in securing a competitive advantage within the shipping industry. Their paper suggests that culture can be seen as a strategic resource, providing a company with a unique identity and operational efficiency that competitors find difficult to copy.

As Theotokas, et al. (2024) explains that organizational culture impacts various dimensions within companies, including their effectiveness, strategic approaches, behavior, communication, and decision-making processes. In their study, Xi et al. (2021) investigate the strategic alignment of human resource management with organizational goals, emphasizing a supportive culture that prioritizes high performance, continual enhancement, and active employee engagement. Gabel-Shmueli et al. (2019) emphasize also that the organizational culture within multinational corporations significantly influences employee work engagement. Additionally, the study explores cultural intelligence, the ability to work effectively across diverse cultures, and examines whether it enhances employee engagement.

In conclusion, literature and critical reviews highlight that selecting a specific management culture in a shipping company is essential because it directly influences company outcomes. The internal culture shapes employee behaviors and decision-making, which significantly impacts service quality and overall company performance. A strong, positive culture fosters engagement, innovation, and operational efficiency, helping shipping companies maintain competitive advantage and meet market demands effectively.

2.3.1.3 Process

This section further analyzes organizational processes, exploring their role in enhancing performance. Nigam, et al. (2016) define processes of tasks and activities, both formal and informal, that transform inputs into outputs.

The articles Kit-Fai Pun et al. (2003) and Rinaldy (2022) examine the proper application of Safety Management Systems (SMS) in the shipping industry. It explores the structured processes and benefits of implementing SMS. The authors likely highlight how these systems manage operational risks, enhance safety at sea, and improve ship and crew performance, emphasizing the role of systematic safety practices in fostering a safer and more efficient shipping industry. Similarly, Wagner and Wiśnicki (2022) underscore the importance of SMS for defining the scope of work, analyzing hazards, developing and implementing controls, and enhancing feedback systems to ensure continuous improvement. Kartal and Bayramoğlu (2024) describe a Safety Management System (SMS) as a comprehensive framework that organizations adopt to promote workplace health and safety while preventing incidents and accidents. By proactively managing risks, SMS creates a safer work environment and reinforces public trust in organizational practices.

Additionally, Sanchez-Gonzalez et al. (2022) note that Business Process Management (BPM) provides a scientific approach to tracking organizational workflows and procedures, ensuring consistent outcomes, and identifying opportunities for improvement. This makes BPM an effective method for understanding the operational dynamics of maritime shipping companies.

2.3.1.4 Strategy

A shipping company's strategy aligns with its vision and mission, guiding efforts to achieve competitive success and market advantage (Ricardianto, et al., 2023). Novaselić et al. (2018) describe strategic management as a critical process where top management sets and pursues major goals and initiatives. Genç (2024) defines it as establishing long-term objectives, implementing actions, and allocating resources to secure competitive advantage and growth. According to Weiser et al (2020), strategy functions as a framework for coordination and adaptation within a dynamic environment.

In addition, Phuong (2024) adds that strategy encompasses overarching goals and policies critical to a company's success or failure. Once established, a strategy should remain stable, fostering a shared understanding of how to thrive in a competitive market. This focused approach keeps a company effective and adaptable in achieving its business goals in a dynamic landscape.

2.3.1.5 Policy

A shipping company must maintain clear and robust policies to ensure safety, security, and environmental protection, aligning with both international and regional regulations as well as charterers' operational and vetting requirements. These policies provide a structured framework to identify, assess and mitigate operational risks and security threats, while fostering a culture of compliance and responsibility. Although well-designed policies significantly reduce the likelihood of operational incidents and their consequences, they do not eliminate the possibility of accidents, which may still occur due to unforeseen circumstances or human and technical failures. For instance, adherence to standards set by the International Maritime Organization (IMO), such as the International Safety Management (ISM) Code, together with charterer requirements and company-specific procedures, provides a structured management framework for safe ship operations and pollution prevention (IMO, 2023). However, safe operations are achieved not merely through compliance with written procedures, but through their effective implementation, including crew training, risk assessment, internal audits, continuous monitoring, corrective actions and the development of a strong safety culture. By implementing comprehensive policies, shipping companies can enhance operational efficiency, protect crew and cargo, and maintain public trust in their practices (Kartal & Bayramoğlu, 2024).

To address the complexities of diverse regulatory requirements, policy frameworks in the maritime sector need continuous improvement. Nõmmela and Kõrbe Kaare (2022) suggest enhancing these frameworks to better navigate varying regulatory landscapes, identifying gaps in current policy-making processes. This also includes responding to evolving charterer expectations, which frequently exceed minimum regulatory requirements by introducing additional standards for safety, environmental performance, cybersecurity and operational reliability. Also, integrating advanced risk assessment tools and stakeholder collaboration can strengthen policy effectiveness, ensuring shipping companies remain adaptable and compliant in a dynamic global market (Wagner & Wiśnicki, 2022).

2.3.2 Economic benefits

Building on the earlier sections, which included a literature review of Shipping Operation Management objectives and key elements, it's equally critical for a shipping company to effectively manage its finances. This section explores the economic benefits of sound financial management for a shipping company.

First, a vessel's expenses must be defined, which are categorized into three types: capital expenses (CAPEX), operating expenses (OPEX), and voyage expenses. Capex represents the largest cost, covering the purchase price of second-hand vessels or construction costs for new builds, plus any interest fees. OPEX includes the ongoing costs of daily operations, such as crew wages, maintenance, lubricants, insurance, and provisions like food and water. Voyage costs, which vary by trip, are additional expenses beyond OPEX. These may include canal tolls, pilotage fees, cargo handling, port rentals, and bunkering (the fuel oil for the ship's main engine and diesel for auxiliary systems) (Stavroulakis & Papadimitriou, 2022).

As a vessel ages, its cost structure changes considerably. A case study presented by Stopford (2009) compares the annual costs of three Capesize bulk carriers aged 5, 10 and 20 years. Although the total daily cost of the 20-year-old vessel is approximately 13% lower than that of the newer vessels, this reduction is primarily attributable to substantially lower capital costs rather than lower operating expenses. The capital expenditure (CAPEX), which includes depreciation and financing costs, accounts for approximately 47% of the total daily cost of the 5-year-old vessel but only about 11% for the 20-year-old vessel. In contrast, operating expenditure (OPEX), including crew, maintenance, repairs, insurance and other day-to-day operating costs, increases from approximately 18% of total costs for the 5-year-old vessel to around 31% for the 20-year-old vessel. Voyage costs, which primarily comprise bunker fuel, port charges and canal dues, also represent a larger proportion of the total costs for the older vessel (approximately 40%) than for the newer vessel (approximately 33%). Therefore, the comparison does not suggest that older vessels are less costly to operate; rather, it demonstrates that lower capital costs can offset higher operating and voyage costs, resulting in a different overall cost structure. Consequently, the business case for acquiring new or older vessels depends on the balance between capital investment, operating efficiency and expected market conditions.

To extend the analysis beyond operating expenses, a financial overview of GasLog Ltd. is provided by which is a liquefied natural gas (LNG) shipping company listed on the New York Stock Exchange (NYSE). This analysis provides additional insights into the market for better understanding of the reader. GasLog Ltd., founded in 2001 and based in Piraeus, Greece, offers liquefied natural gas (LNG) shipping and vessel management services to charterers.

To ensure sustainability, a shipping company must earn revenue, known as freight, via the vessels services. Moreover, a shipping company must assess all costs, capital, operating, and voyage costs, alongside freight revenue to evaluate its financial viability. This information enables the company to assess the sustainability of its investments. To provide deeper insight into GasLog Ltd.'s financial performance, key metrics such as the Price-to-Earnings (P/E) ratio, which compares the company's share price to its earnings per share, and the Basic Earnings per Share (EPS), which reflects the net income per outstanding share of common stock annually (Kimmel, et al., 2022), are analyzed below:

Figure 2.8 illustrates the P/E ratio history for GasLog Partners from 2014 to 2023. Starting at a peak of around 200 in 2014, reflecting a high valuation relative to earnings, the P/E ratio dropped sharply to below 50 by 2016. It continued to decline, stabilizing between 10 and 20 from 2017 to 2021. A slight uptick to around 20 occurred in 2021, followed by a dip below 10 in 2022, and a minor recovery to approximately 10 by 2023. This overall downward trend indicates a lower valuation relative to earnings over the decade.

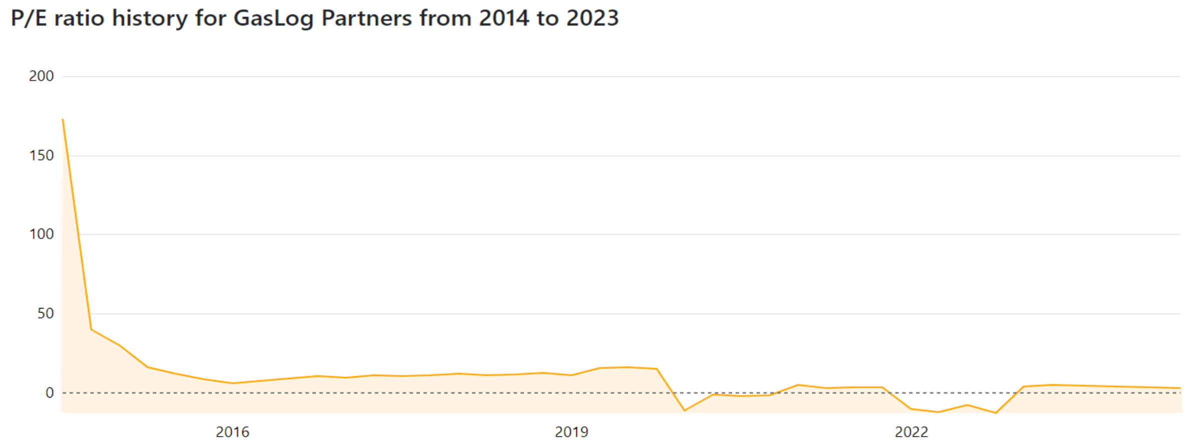

Figure 2.8. P/E ratio history for GasLog Partners from 2014 to 2023. Source: GasLog Ltd. (2023) (accessed May 2024).

In contrast, Figure 2.9 shows the EPS history for GasLog Partners over the same period. The EPS began at around $1 in 2014, peaked at nearly $2.00 by 2016, and remained relatively stable through 2018. A significant decline followed, with EPS falling to a low of approximately -$1.00 around 2020, reflecting a net loss per share. Recovery started in 2021, with EPS returning to around $0 by 2022 and rising steadily to $1.79 by 2023. This trend highlights significant volatility, with a sharp dip in 2019-2020, followed by a consistent upward trajectory in later years.

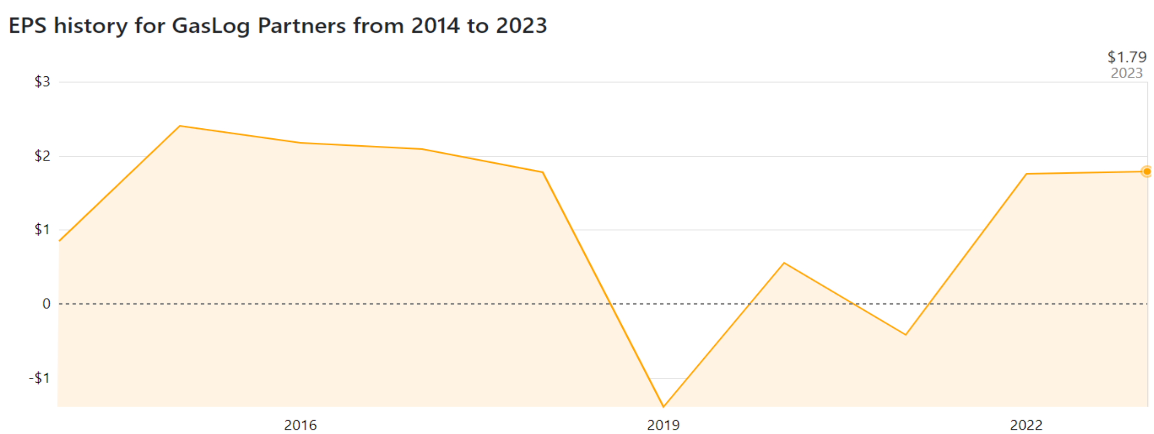

Figure 2.9. EPS history GasLog Partners from 2014 to 2023. Source: GasLog Ltd. (2023).

Based on this brief analysis, GasLog Partners shows sustainability over the years. The recent EPS recovery to $1.79 by 2023 and slight cost optimization reflect improved financial health and resilience. However, significant volatility in earnings, including a notable loss in 2019, largely due to the COVID-19 crisis that began impacting markets in early 2020, led to a temporary decline in profitability. Additionally, the low P/E ratio, indicating cautious investor confidence, suggests that the company has not been consistently sustainable. To achieve long-term sustainability, GasLog Partners must maintain profitability, manage costs effectively and build greater investor trust amidst the cyclical LNG shipping market.

However, to enhance sustainability, maintain economic benefits, and uphold their reputation, GasLog and other shipping companies must foster strong relationships with their customers (charterers). It has been reviewed through literature and critical analysis that customer satisfaction models help shipping companies align their services with customer expectations to ensure sustainable performance.

2.4 Summary

Chapter 2 provides a comprehensive bibliographic review of the shipping market and its major sectors, as well as shipping operations management. The following chapter extends the literature review by examining vessel performance assessment through machine learning models and charterer satisfaction, which together constitute the other key pillars of the research as Figure 2.1 illustrates. Collectively, these research areas establish the theoretical, operational, and analytical foundations of the thesis and support the development of the proposed Charterer Satisfaction Index (CSI).

3. Chapter 3 – Literature and Critical Review: Vessel Performance and Charterer Satisfaction

3.1 Introduction

Chapter 3 critically reviews the literature on the key research pillar of vessel performance and charterer satisfaction. It examines machine learning approaches for vessel performance prediction together with established service quality and customer satisfaction models relevant to shipping.

3.2 Vessel Performance: Advanced Vessel Analytics with AI and Statistics

This thesis section examines vessel performance, the third primary focus pillar of literature and critical review. Vessel performance is closely tied to Operations Management, focusing on how efficient services are delivered to Charterers for cargo transport.

Vessel Performance is studied based on relevant literature using keywords like: "Vessel Performance", "Ship Energy Efficiency", "Fuel Consumption Analysis", "Weather Impact", "Speed-Power Relationships", "Data-Driven Maritime Performance", "Performance Prediction Models", "Ship Monitoring Systems" and "Environmental Footprints". Scholarly articles and books are accessed via online libraries as used in "2.2 Shipping market: Demand and Supply Dynamics" and "2.3 Shipping Operation Management (SOM)" as well.

Therefore, a literature and critical review is conducted, analyzing 87 papers published in recent years. Figure *3.1. Histogram with year categories of papers that are used in literature and critical review.*

illustrates the number of research papers per year from 2008 to 2025. The data reveals a steady increase in academic output, with a significant rise after 2020. This upward trend reflects growing interest in academic research, particularly in vessel efficiency and sustainability, highlighting its importance in the shipping industry.

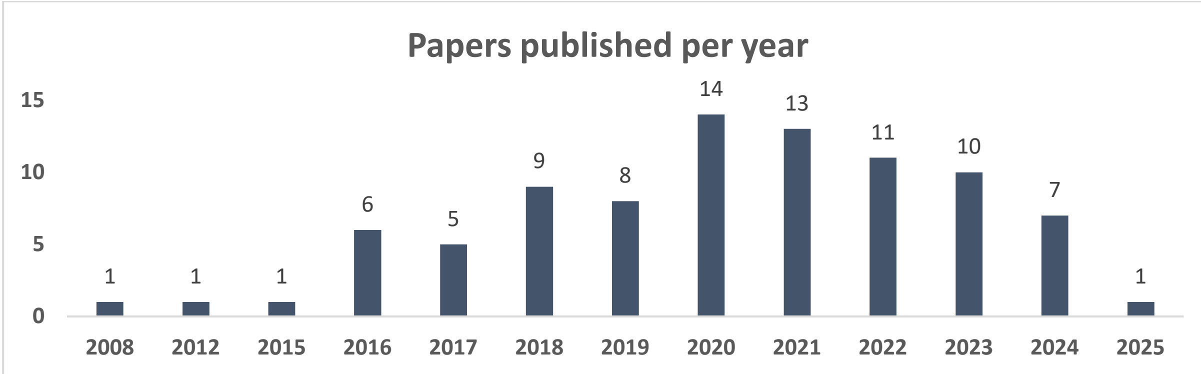

Figure 3.1. Histogram with year categories of papers that are used in literature and critical review.

3.2.1 Vessel Performance: Literature Review

The literature review has been organized based on vessel performance assessment. It includes studies focused on predicting or optimizing aspects such as fuel consumption, power usage, speed, costs, or environmental conditions, primarily in relation to different types of vessels, such as bulk carriers, tankers, and container ships. A key focus is the methodology used in these studies, particularly the application of artificial intelligence (AI), including machine learning, deep learning, and neural networks, along with the specific techniques employed.

The first category of vessel performance assessment addressed in the literature review pertains to the predictive analysis of vessel performance, with a particular emphasis on fuel consumption and energy efficiency. Predictive analysis in vessel performance involves using historical data, machine learning, and statistical algorithms to forecast future behaviors of a ship efficiency under different conditions. However, there are also challenges, such as the need for high-quality, consistent data, significant upfront investment in technology and training, and potential inaccuracies in predictions due to unforeseen variables. Overall, predictive analysis empowers smarter, data-driven decision-making in maritime operations, though it requires careful implementation and monitoring.

Specifically, Uyanık et al. (2020) developed data-driven models to predict fuel consumption of vessel using operational data (using noon reports, logbooks, sensor data) from a container vessel. Their approach included data pre-processing, correlation analysis (identifying key parameters like engine cylinder values, scavenge air, cooling water, and shaft indicators), and K-fold cross-validation. Multiple machine learning algorithms are tested, including Linear Regression, Ridge Regression, LASSO, Support Vector Regression (SVR), Tree-Based models, and Boosting methods, with Multiple Linear and Ridge Regression by demonstrating exceptionally low errors (RMSE ≈ 0.0001, MAE ≈ 0.002–0.003) and achieving nearly perfect accuracy ($R^2 \approx 99.999\%$).

Cepowski and Chorab (2021) used Artificial Neural Networks (ANNs) to estimate fuel consumption for bulk carriers, tankers, and container ships. Trained on ship speed and capacity, simple linear ANNs provided accurate results with errors of 3–7% for bulk carriers and tankers, and up to 10% or more for container ships. The models are useful for ship design, planning, and emissions studies. Moreover, Ahlgren et al. (2019) applied machine learning to predict fuel oil consumption on a Baltic Sea cruise ship, aiming to improve energy efficiency and reduce costs without extra hardware. The authors used AutoML to train models on engine data and aggregated fuel use over 12–96-hour intervals. The best-performing model, Linear SVR, achieved high accuracy ($R^2 > 0.99$), even with sparse 96-hour data.

Also, Du et al., (2022) conducted a study that utilized sensor and meteorological data from two 9,200-TEU containerships to predict fuel consumption. By fusing onboard sensor data with public weather data, nine datasets are created and analyzed using Machine Learning models such as Extra Trees (ET), Gradient Boosting (GB), Extreme Gradient Boosting (XG), LightGBM (LB), Artificial Neural Networks (ANN), Random Forest (RF), and Support Vector Machines (SVM). Key factors included speed, draft, trim, and sea conditions. The best dataset yielded R^2 values of 0.999–1.000 (train) and >0.966 (test), with RMSE below 0.75 ton/day and MAE under 0.52 ton/day. A key challenge noted is the need for at least five months of sensor data for effective model training. Perera and Mo (2016) study evaluated ship performance and navigation behavior to enhance energy efficiency and reduced fuel use and emissions, using data from a bulk carrier. The methodology first applied Gaussian Mixture Models (GMMs) to cluster operational data into engine load regions, then used Principal Component Analysis (PCA) within each cluster to uncover hidden parameter relationships. PCA acted as the core analytical tool, revealing correlations among draft, speed, shaft speed, and fuel consumption. Results showed that combining GMM and PCA improves interpretability and performance analysis. Challenges include managing nonlinear, unstructured data and detecting sensor faults.

Li et al. (2021) developed an Elastic Net regression model to predict ship fuel consumption using two months of ferry navigation data. They combined LASSO and Ridge regression to address multicollinearity and perform feature selection. The model achieved strong accuracy ($R^2 = 0.90$, RMSE = 4.95), outperforming LSTM and BPNN in interpretability. Challenges included multicollinearity and sensor data preprocessing. Moreover, Chen et al. (2023) applied machine learning to predict fuel consumption of a tugboat operating in Singapore port waters, using ship-related (speed, engine power) and meteorological (wind, tide, temperature, humidity) data. Four models, Support Vector Regression (SVR), Ridge Regression, Random Forest (RF), and Artificial Neural Network (ANN), are evaluated through data cleaning, splitting, cross-validation, and testing. Random Forest consistently delivered the best performance, and incorporating weather data improved all models' accuracy. Key challenges included the precision of meteorological inputs and sensitivity to abnormal data.

In addition, prediction of yacht energy consumption using real operational data to support early-stage design and reduce environmental impact is conducted by Odendaal et al. (2023). Focusing on a Feadship fleet yacht, the study used a Grey-Box Modelling (GBM) approach—combining physics-based White-Box Models (WBM) with Artificial Neural Network-based Black-Box Models (BBM). Using ten months of data, GBMs outperformed standalone models, achieving propulsion and auxiliary power prediction errors within 3% and 7%, respectively. Besides that, Papandreou & Ziakopoulos (2022) focused on predicting Main Engine Fuel Oil Consumption (FOC) for Very Large Crude Carrier VLCCs to reduce costs and emissions. Using operational sensors and basic weather data (e.g., speed through water, wind conditions, draft, trim, drydock interval, and vessel state), they evaluated Multivariate Polynomial Regression (MPR), Artificial Neural Networks (ANNs), and eXtreme Gradient Boosting (XGBoost). Data are averaged at 15-minute intervals. XGBoost performed best, predicting FOC within 5% accuracy over 86% of the time. The study highlighted the value of using readily available onboard data, with case studies for both laden and ballast voyages.

It is worth noting that Gkerekos et al. (2019) compared machine learning models to predict the ship main engine fuel oil consumption (FOC), aiming to reduce costs and emissions. Using data from noon reports and Automated Data Logging and Monitoring (ADLM) systems, they tested models such as Support Vector Machines (SVM), Random Forest Regressors (RFR), Extra Trees Regressors (ETR), and Artificial Neural Networks (ANN). Operational data, such as weather conditions, speed, sailing distance, and drafts, is used for training. ETR and RFR performed best, with ADLM data improving accuracy by 7% and reducing data requirements by up to 90%.In like manner, Hu, et al. (2019) used Back-Propagation Neural Networks (BPNN) and Gaussian Process Regression (GPR) to predict enroute ship fuel consumption.

Including environmental data improved accuracy, with GPR slightly outperforming BPNN (R^2 = 0.9887 vs. 0.9817). However, BPNN is better suited for real-time use due to GPR's longer runtime.

Likewise, Hu et al. (2021) developed a hybrid model to predict fuel consumption using sensor data from an ocean-going container ship, aiming to support energy savings and emission reduction. The proposed hybrid model outperformed individual models, ranking best overall, followed by Extremely Randomized Trees (ET), XGBoost (XGB), Random Forest (RF), Artificial Neural Networks (ANN), Support Vector Machines (SVM), and Multiple Linear Regression (MLR). Data cleaning improved the coefficient of determination (R^2) from 0.78 to 0.92. The hybrid model achieved the highest accuracy (mean R^2 = 0.99) and demonstrated greater stability with lower error variability compared to single models like Extremely Randomized Trees (ET), making it highly effective for operational fuel prediction.

Ilias et al. (2023) created a machine learning model to predict fuel use for both the main and auxiliary engines on fishing vessels. They used a method called multitask learning (MTL), which allows one model to learn and predict several related tasks at once. Their model, called MTL-Double Encoders, uses two parts: one to find patterns shared between both engines, and one to focus on the differences. This helped the model make better predictions. They also used a type of model called a transformer, which is good at finding important patterns in large sets of data. Furthermore, Jeon et al. (2018) focused on predicting main engine fuel consumption using big data analysis to enhance smart ship operational efficiency. Data from a specific vessel, including ship state, engine operation, speed, and weather,is processed through a framework involving denoising, clustering, compression, and expansion. They developed a regression model using an Artificial Neural Network (ANN) and compared it with Polynomial Regression (PR) and Support Vector Machine (SVM). The ANN outperformed both in accuracy and efficiency, achieving approximately 5–10% lower prediction error. Challenges included hyperparameter selection and model explainability.

In addition, Ji (2021) developed machine learning models to predict marine fuel consumption and exhaust emissions (CO_2, CH_4, N_2O, black carbon) for assessing the sustainability of the global LNG carrier fleet. The Gaussian Process Regression (GPR) models demonstrated high accuracy, with ensemble methods excelling in fuel consumption prediction and Rational Quadratic GPR alongside Boosted Trees performing best for emission estimates. The analysis is based on data from 435 LNG carriers, achieving R^2 values above 0.95 and reducing prediction errors by 5–10%. Besides that, Tran (2019) developed a prediction model for low-sulfur fuel oil consumption on the bulk carrier M/V NORD VENUS (80,000 DWT) to support cost savings and MARPOL Annex VI compliance. The study used an Artificial Neural Network (ANN) and compared it to traditional statistical regression methods, including linear and polynomial regression. Using recorded fuel consumption data, the ANN model showed superior reliability and accuracy, making it more effective for predicting low-sulfur fuel use in emission control areas.

Similarly, Tran (2021) aimed to predict main diesel engine fuel oil consumption for a bulk carrier in Vietnam to enhance energy efficiency and reduce emissions. The study used a Monte Carlo simulation for data generation and an Artificial Neural Network (ANN) with back-propagation for prediction, validated with two years of non-log data. Under various engine loads (65%, 85%, 100%), the ANN model outperformed traditional statistical methods in accuracy and reliability for energy management. However, Xie et al. (2023) developed models to predict ship fuel consumption using data from an oil tanker, aiming to improve energy efficiency and reduce emissions. The study combined a white-box model (mathematical, physics-based) with black-box machine learning models: Random Forest (RF) and Extreme Gradient Boosting (XGBoost). Input data included ship sensor readings, model test results, and weather conditions. A Kwon formula-based data cleaning method is used to exclude noisy data from dynamic sailing. Results showed strong performance: the white-box model achieved an R^2 of 0.9977, while XGBoost and RF reached 0.9954 and 0.9922, respectively. Cleaning further improved accuracy, highlighting the importance of preprocessing in noisy maritime data environments.

Notably, Fam et al. (2022) proposed a data-driven framework to improve energy efficiency by predicting fuel consumption using telemetry data from 9,000 TEU container ships. The method combined simplified Kernel Density Estimation with an Artificial Neural Network (ANN), using inputs like vessel speed, draft, sea current, and wind. The ANN effectively predicted fuel use and captured varying fuel-speed curves across sea conditions, with $R^2 \approx 0.8675$. The study highlighted the challenge of limited data for distinguishing operational profiles and validated the model across open-sea and close-sea journeys. Moreover, Le et al. (2020) estimated fuel consumption for container ships in Korea to improve energy efficiency and reduce emissions.

Using operational data from 100–143 vessels (with a case study of five), they compared two Artificial Neural Network (ANN) models and two Multiple Linear Regression (MLR) models. ANN using four inputs, sailing time, speed, cargo weight, and capacity, outperforming MLR models, achieving the lowest Mean Absolute Percentage Error (MAPE).

Also, Le et al., (2024) paper predicts ship fuel use and reduces emissions by using machine learning. The study compared Huber Regression and Light Gradient Boosting Machine (LGBM) models against a linear regression baseline. Both models handled non-linear data well, but Huber Regression performed best, achieving an R^2 of 0.979 and RMSE of 2.278, outperforming LGBM ($R^2 = 0.917$, RMSE = 4.55). Graphical validation confirmed Huber's accuracy. While vessel details are not specified, the model is suited for real-time fuel estimation in complex marine operations. Likewise, Karagiannidis and Themelis (2021) predicted main engine fuel consumption and speed loss for a container ship to improve energy efficiency and reduce emissions. Using high-frequency sensor data, they applied Feed-Forward Neural Networks (FNNs) within a data-driven propulsion modeling framework. Rigorous data pre-processing, filtering, validation, and statistical checks, proved crucial, significantly boosting model accuracy. The study highlights data quality as a key challenge and demonstrates the effectiveness of ANN models when paired with clean, well-processed data.

Moreover, Kee et al. (2018) predicted fuel consumption for in-service tugboats operating on the Rejang River and Straits of Malacca using operational data (distance, time, speed, deadweight, wind speed). They compared an Artificial Neural Network (ANN) with back-propagation to Multiple Linear Regression (MLR), applying outlier removal in pre-processing. The ANN model outperformed MLR ($R^2 = 0.9253$ vs. 0.9085), capturing the complex nonlinear dynamics of tugboat operations. The case study supports ANN use in fuel-saving decision-making, though accounting for multiple interacting factors remains a challenge. Peng et al. (2020) focused on predicting ship energy consumption in port to enhance operational efficiency and support green port initiatives, using data from vessels at Jingtang Port, China. They applied several machine learning models, including Random Forest, Gradient Boosting, Linear Regression, Back-Propagation (BP) Network, and K-Nearest Neighbors, using 15 input features. Key predictors identified are net tonnage, deadweight tonnage, actual weight, and facility efficiency. Notably, doubling facility efficiency reduced ship energy consumption by 34.17% at berth and 8.41% in port. These findings offer valuable insights into green port development strategies.

To add to this, Petersen et al. (2012) proposed a machine learning approach to predict main energy consumption under realistic operating conditions, aiming to optimize efficiency and reduce costs. Using high-quality sensor data from a ferry and a product tanker, they applied Neural Networks for both real-time and predictive modeling. The study highlights the effectiveness of machine learning in improving operational decision-making and indirectly reducing fuel use and emissions. In like manner Su et al. (2025) focused on predicting fuel consumption costs for PCTC (Pure Car/Truck Carrier) vessels to reduce operational expenses and address emission concerns. Using a dataset of 16,189 observations from 2012–2021, they evaluated 18 machine learning models, emphasizing deep learning. CatBoost outperformed all models with an R^2 of 0.976. Key predictors included distance, sea days, speed (most influential), duration, and port days. The study fills a gap in research on PCTC energy efficiency.

In addition, Zhang et al. (2024) focused on predicting ship fuel consumption (SFC) under real operational conditions to support decarbonization and improve efficiency. Using big data from a Kamsarmax bulk carrier (266 variables from sea trials), the study applied a Decision Tree (DT) for feature selection and trained a Bi-directional Long Short-Term Memory (Bi-LSTM) network with an attention mechanism. The model outperformed traditional and deep learning methods, achieving a low average prediction error of 0.98% and strong generalization across eight international voyages. Key challenges included managing complex big data and abnormal fluctuations.

Also, Wang et al. (2018) predicted ship fuel consumption using data from 97 container ships across 884 voyages to reduce costs and emissions. They preprocessed data with Z-score standardization and applied several models, including LASSO regression (which also performs variable selection), Artificial Neural Networks (ANN), Support Vector Regression (SVR), and Gaussian Process (GP) regression. The LASSO model outperformed others, achieving the lowest Root Mean Square Deviation (RMSD) of 7.4 and Mean Absolute Error (MAE) of 4.9. It effectively addressed multicollinearity among input variables and identified key features influencing fuel use. The main challenge is managing multicollinearity in data. Moreover, Zhao et al. (2021) focused on predicting fuel consumption for an inland river cruise ship to enhance energy efficiency and reduce emissions. Using real operational data (e.g., engine speed, wind, water conditions), they tested six models: Multi-Layer Perceptron, Decision Tree, Random Forest, K-Nearest Neighbor, Extra Trees, and Support Vector Regression. Extra Trees and

Random Forest models showed the highest accuracy. A key challenge is the increased training time of Random Forest and SVR with larger data volumes. The study used voyage data from Chongqing to Yichang.

In a comparable manner, Işıklı et al. (2020) used Response Surface Methodology (RSM) to estimate fuel consumption on a bulk carrier using noon report data. They modeled key factors like speed, Revolutions Per Minute (RPM), draft, and cargo load, capturing non-linear and interactive effects. Results showed fuel consumption decreases with speed up to a threshold, then increases. While RPM had little direct impact, its interactions influenced fuel use. RSM proved effective despite data and complexity challenges, supporting energy-efficient and eco-friendly decision-making. Also, Karatuğ and Arslanoğlu (2020) analyzed ship fuel consumption for a large dry-bulk carrier using engine data collected over five months. The Multiple Linear Regression (MLR) model performed well, achieving an RMSE of 2.82 and MAE of 1.43, closely matching actual consumption. Key challenges included handling complex interactions among influencing factors.

Moreover, Uyanik et al. (2019) predicted ship fuel consumption to reduce costs and CO_2 emissions using actual voyage noon report data from a commercial vessel. The study applied Multiple Linear Regression (MLR) as a machine learning model, trained and tested on split datasets. The model produced efficient results, achieving a Root Mean Squared Error (RMSE) of 1.61 for fuel consumption prediction. Furthermore, Guo et al. (2022) combined ship hydrodynamic models with Random Forest to estimate fuel consumption and emissions using AIS, vessel data, and metocean conditions. Proposed hybrid model, VERDE, accurately predicted power and fuel use for cargo ships, outperforming the Cubic Rule (a traditional mode). Errors ranged from -3% to -11.6%, compared to up to -30.8% for the Cubic Rule. Challenges included missing data, input uncertainties, and limited validation data.

Moreover, Nwaoha et al. (2017) developed a combined Fuzzy Rule Base (FRB) and Utility Theory (UT) algorithm to predict fuel consumption rates (FCR) for diesel-poared marine vessels. This approach handles uncertainty by integrating factors like machinery condition, hull and propeller status, and metocean conditions. In a case study comparing two LNG vessels, the model showed that Vessel #1(0.4662) performed more efficient than Vessel #2 (0.4081), indicating that Vessel #1 is more fuel-efficient. In addition, Shokohian et al. (2024) improved prediction of ship fuel consumption for Low Sulfur Heavy Fuel Oil (LSHFO) using data from

29 bulk carriers. They evaluated six machine learning models—Multiple Linear Regression (MLR), Decision Tree (DT), Random Forest (RF), Support Vector Regression (SVR), K-Nearest Neighbors (KNN), and XGBoost, using K-fold cross-validation and hyperparameter tuning via Grid Search. Data preprocessing involved cleaning, encoding, and scaling. XGBoost and RF performed best, with tuned R^2 values of 95.82% and 95.62%, respectively. Challenges included managing multiple influencing factors and validating results rigorously.

Likewise, Xie et al. (2023) developed fuel consumption prediction models for an oil tanker to support energy conservation and emission reduction. They combined a physics-based white-box model with machine learning black-box models, XGBoost and Random Forest (RF), using sensor and ship test data. A novel Kwon formula-based data-cleaning method addressed noise from acceleration/deceleration. The white-box model had ~4% error, while XGBoost and RF achieved high accuracy ($R^2 = 0.9977$ and 0.9922). After cleaning, XGBoost maintained strong performance ($R^2 = 0.9954$). Challenges included noisy data and cleaning limitations.

Additionally, Perera and Mo (2020) explored the use of big data and machine learning/artificial intelligence (ML/AI) to support the digitalization of the shipping industry, aiming to enhance energy efficiency, reliability, and reduce fuel use and emissions. Using data from a bulk carrier, they applied Gaussian Mixture Models to cluster operational modes and Singular Value Decomposition for structural analysis. The model successfully identified operational clusters and key parameter correlations. Challenges included handling erroneous data, visualizing high-dimensional clusters, and integrating weather data. Likewise, Yoo and Kim (2019) aimed to improve ship energy efficiency by accurately estimating powering performance under real-world conditions using operational and weather data from a containership. They employed a Gaussian Process (GP) model, integrating domain knowledge and regularization to address overfitting and uncertainty. The GP model outperformed a polynomial model in predicting speed and engine power, though challenges remained in managing overfitting and environmental variability.

Moreover, Gómez et al. (2016) proposed a machine learning system using Artificial Neural Networks (ANNs) to forecast operational parameters in container terminals, aiming to optimize vessel productivity during loading and unloading. While not directly focused on fuel or emissions, enhanced terminal efficiency contributes to overall energy and cost savings. Their nine-step framework, applied to historical terminal and climate data, achieved 96% correlation and 94% accuracy. Major challenges included inconsistent data, 68% is discarded, and varying sampling frequencies. The case study is based on a semi-automated terminal in Spain. In a related effort, Yan, et al. (2015) used a Backpropagation ANN to assess energy efficiency in inland river ships via the Energy Efficiency Operational Indicator (EEOI). Trained on data from a Yangtze River passenger ship, the model predicted EEOI, fuel use, and voyage speed with high accuracy. Sensitivity analysis showed that water current speed influenced efficiency nearly as much as engine speed. Key challenges involved modeling complexes, nonlinear relationships in river navigation.

Building upon the general principles of predictive analytics, this review now shifts to a critical examination of studies focused on ship speed prediction. These studies explore various modeling approaches, including process-based, data-driven, and hybrid models, to forecast ship speed accurately under different conditions. Their findings contribute to enhancing navigational efficiency and operational decision-making in maritime transport. Specifically, vessel speed prediction supports performance assessment, as shown in several studies and more specifically, Bassam et al. (2023) proposed an Artificial Neural Network (ANN) model to predict ship speed under real conditions, aiming to optimize performance and reduce fuel use, costs, and emissions. Using high-frequency data from the ferry M/S Smyril, the best-performing ANN,featuring two hidden layers with 100 neurons each, achieved an R^2 of 95% and an RMSE of 0.96 knots. It outperformed SVM and tree ensemble models, demonstrating strong potential for voyage planning and optimization.

Likewise, Abebe et al. (2020) developed machine learning models to predict ship speed over ground (SOG) using one year of AIS and marine weather data from 76 vessels. They tested various regression models, including Linear Regression, Decision Trees, and ensembles like Gradient Boosting, XGBoost, Random Forest, and Extra Trees Regressor (ETR). Using Bayesian optimization and cross-validation, ensemble models achieved high accuracy (R^2 > 97%), with ETR performing best (R^2 = 0.9847) and consistent across vessel types and routes. Also, Baressi Šegota et al. (2020) developed a Multilayer Perceptron (MLP) neural network to accurately predict vessel speed, supporting energy-efficient route planning. Focusing on a frigate with a combined diesel-electric and gas (CODLAG) propulsion system, they optimized MLP configurations using publicly available propulsion data. The best model achieved a very low Mean Absolute Error (MAE) of approximately 0.00014% of the speed range. Challenges included hyperparameter tuning for optimal performance.

Additionally, Bassam et al. (2022) developed a machine learning approach to predict ship speed for performance optimization and emissions reduction. Using operational data from the ferry M/S Smyril, they found that Gaussian Process Regression (GPR) with a Matérn (Exponential) kernel performed best, achieving an R^2 of 0.91 and RMSE of 0.91 knots. This model outperformed linear regression, regression trees, ensemble trees, and SVMs, demonstrating high accuracy under real operating conditions. Also, Zentai and Toka (2023) predicted boat speed in the SailGP high-performance sailing championship to enhance operational performance. Using high-resolution data from Race 4 of the 2021 Bermuda event, they applied Gradient Boosting, Random Forest, and a stacked model with a feature analysis highlighted factors like daggerboard rake angle. The stacked model performed best ($R^2 = 0.97$, MSE = 3.2). A key challenge is limited access to confidential SailGP data.

Moreover, Coraddu et al. (2019) estimated speed loss due to marine fouling to improve ship efficiency, reduce fuel use, and lower emissions using operational data from two Handymax chemical/product tankers. They developed a Data-Driven Digital Twin employing Deep Extreme Learning Machines (DELM), trained on clean hull data to predict speed and analyze fouling impact via robust regression. DELM outperformed ISO 19030 standards, accurately capturing performance trends and hull cleaning events. Challenges included managing sensor data noise and uncertainty over extended periods. However, Moreira et al. (2021) developed an ANN model to predict a container ship's speed and fuel consumption, aiming to optimize voyage operations, improve energy efficiency, and reduce emissions. Trained using the Levenberg–Marquardt algorithm, the model used inputs like engine torque, shaft RPM, wave height, wave period, and wave encounter angle. The data-driven approach included steps like clustering and compression of big data. Results showed high accuracy ($R = 0.9999$), outperforming polynomial regression and SVMs. The study used simulation data, with references to pilot demonstrations.

Correspondingly, Lang et al. (2021) used supervised machine learning to predict ship speed-power performance at sea, aiming to support energy efficiency and emissions reduction. Using five years of operational and metocean data from a global chemical tanker, they compared models including XGBoost, neural networks, SVMs, and statistical regression. XGBoost delivered the best results ($R^2 = 0.9952$, RMSE = 88.6 kW, MAE = 42.1 kW), followed by neural networks ($R^2 = 0.9905$) and SVR ($R^2 = 0.9928$), all outperforming linear regression ($R^2 = 0.6120$).

Following, the review further extends to a critical examination of relevant power prediction studies, highlighting major methodologies such as data-driven models, regression formulas, and artificial neural networks, as well as challenges like varying accuracy across ship types and the need for optimal input parameters to improve prediction reliability. However, Kim et al. (2020) developed a Support Vector Regression (SVR) model to predict propulsion power for a 200,000-ton bulk carrier. Using onboard sensor and National Oceanic and Atmospheric Administration Ocean data (NOAA) ocean data, the SVR model achieved strong performance with an R^2 of 89.78% and an RMSE of 54 kW. In comparison, the traditional ISO15016 method showed much lower accuracy, with an R^2 of 30.23% and RMSE of 985 kW. Key challenges include incorporating vessel condition factors such as hull roughness and exploring other machine learning approaches.

Also, Okumuş and Ekmekçioğlu (2021) estimated main engine power for general cargo ships using machine learning to support eco-friendly design and cost reduction. Using data from 2,286 ships, they compared Polynomial Regression, K-Nearest Neighbors (KNN), and Gradient Boosting Machine (GBM) models. GBM performed best, achieving an R^2 of 0.991, RMSE of 415.66, and MAE of 267.39. Moreover, Liang et al. (2022) predicted ship propulsion power using Random Forest Regression (RFR) to support fuel consumption and emission reduction goals set by the International Maritime Organization (IMO). The study utilized a large dataset from 231 ships of various sizes, integrating AIS, weather, and onboard data. Using scikit-learn and Spark MLlib for processing, the RFR model achieved a strong test R^2 of 0.9238. Challenges included managing the volume and quality of big data.

Also, Valchev et al. (2022) developed a short-term forecasting model for vessel electrical power generation to improve operational efficiency and reduce emissions. Using high-fidelity sensor data from a Royal Netherlands Navy Oceangoing Patrol Vessel with hybrid propulsion, they applied Kernel-Based Regularised Least Squares (KRLS), a kernel-based machine learning method. The model achieved high accuracy with MAPE under 1% for 30-second forecasts and around 2% for 2-minute forecasts, effectively predicting load changes even during maneuvers. A key challenge is incorporating environmental data due to limited sampling rates.Furthermore, Mocerino and Rizzuto (2021) predicted total installed power on modern cruise ships to support emission estimation and regulatory compliance. Using data from 129 ships, they applied Multiple Linear Regression (MLR), based on speed and passenger count, achieved strong performance with an R^2 of 0.884 and a residual standard deviation of 6.705 MW. The model outperformed other methods, with residual errors three times lower, despite challenges like dataset generation, multicollinearity, and managing residuals.

Likewise, DeKeyser et al. (2022) modeled the speed–power relationship to optimize fuel use and emissions. Using in-service data from various vessel types, they compared a simple neural network (NN) to traditional semi-empirical methods. The NN, trained on filtered data including wind and wave effects, outperformed traditional approaches, achieving a MAPE of 7.4% versus over 10%. Key challenges included the need for large, high-quality datasets and the interpretability of ML outputs. Similarly, Abreu et al. (2023)developed a data-driven method to predict ship stay time in Brazilian ports, aiming to improve operational efficiency and logistics planning. Using 2018 cargo movement data, they tested machine learning classifiers like decision trees and random forests. The random forest model performed best, achieving over 73% accuracy, with geography and cargo type as key features. Challenges included data uncertainties and missing weather information.

Beyond prediction, a substantial body of literature also focuses on optimizing vessel performance to achieve enhanced fuel efficiency, reduced operational costs, and minimized environmental impact. However, challenges remain implementation can be complex, requiring seamless integration with onboard and remote monitoring systems for maximum effectiveness. Additionally, optimization models may overlook unpredictable external factors, such as extreme weather, which can affect efficiency. More specifically, several papers employing AI-based approaches have been reviewed regarding the optimization of energy management and reducing fuel and emission impact as well. Farag & Ölçer (2020) aimed to improve operational energy efficiency and reduce fuel and Greenhouse gases (GHG) emissions for a VLCC tanker with a case study of two voyages. It developed a combined Artificial Neural Network (ANN) and Multi-Regression (MR) model using onboard and hindcast data. Trained on one voyage and validated on another, the model predicted ship power and fuel use with 99.6% accuracy, outperforming a standalone ANN. In a Just-In-Time scenario, it projected 24.24% fuel saving. A key challenge is ensuring diverse training data for robust ANN performance.

Likewise, Beşikçi et al. (2016)developed an Artificial Neural Network (ANN)-based decision support system to enhance ship energy efficiency and reduce fuel consumption. Using noon report data from a cargo vessel, the ANN is trained on variables such as ship speed, draft, wind speed/direction, and engine load. The model achieved high prediction accuracy, with an R^2 value of 0.96 and a Mean Absolute Percentage Error (MAPE) of 2.82% for fuel consumption. These results demonstrated the ANN's potential to support real-time, data-driven decision-making onboard. However, the study is limited to a single-vessel case study, indicating the need for further validation across diverse ship types and routes. Moreover, based on paper's, Yan et al. (2024), they aimed to enhance ship energy efficiency and reduce fuel and emission costs in line with IMO regulations, using data from a Capesize bulk carrier. A customized ANN model, called DK-ANN, integrates data from noon reports, AIS, and weather forecasts while embedding domain knowledge. It outperforms traditional models with a MAPE of 7.5% and supports optimization models that showed 2–3% cost and up to 15% emission reductions. A key challenge is the limited quality and quantity of noon report data compared to sensor data.

Equally, Hu et al. (2022) proposed a two-step strategy to enhance ship energy efficiency by predicting and optimizing fuel consumption, aiming to reduce operational costs and GHG emissions. Using real-world data from two bulk carrier voyages, they developed a hybrid machine learning model combining Extra Trees (ET), Random Forest (RF), and XGBoost (XGB), with a Multiple Linear Regression (MLR) meta-model. The process involved data cleaning, transformation, feature selection, model training, and trim optimization via enumeration. The hybrid model outperformed seven individual models, ET, RF, XGB, ANN, SVM, Ridge, and MLR, in both accuracy and robustness. 2 case studies were conducted, and it improved MAPE by 0.20% to 54.08% on Voyage 1 and by 0.64% to 57.53% on Voyage 2, compared to the standalone models. This confirms the hybrid approach's effectiveness over conventional and advanced single-model methods. Also, Ruan et al. (2024) developed a grey-box model (GBM) to accurately predict fuel consumption for wing-diesel hybrid vessels, focusing on optimizing operations and reducing emissions. Using noon report data from a VLCC (2019–2021), they integrated aerodynamic wing features related to fuel savings with six machine learning algorithms (Decision Tree, Random Forest, Support Vector Regression, Ridge, LASSO, Elastic Net) in series and parallel GBM frameworks. The best model, a parallel GBM with Random Forest and wing fuel savings, reduced RMSE by 41.7%. Data quality from non-reports remains a challenge.

Sun et al. (2019) aimed to optimize ship energy efficiency by minimizing the EEOI using a Back Propagation Neural Network (BPNN) optimized with a Genetic Algorithm. Trained on operational data from the bulk carrier YUMING, the model identified optimal engine speeds under varying conditions. Specifically, reducing RPM from 127 to 122 loaded EEOI from 9.66 to 6.79. The approach proved effective despite challenges like noisy data and environmental complexity. Additionally, Wang et al. (2016) focus on real-time ship energy efficiency optimization to enhance marine economic performance and reduce CO_2 emissions. Using data from a cruise ship on the Yangtze River, the approach employs a Wavelet Neural Network (WNN) to predict short-range environmental conditions like wind speed and water depth. These predictions inform a real-time model to optimize engine speed for maximum efficiency. Results show the method effectively reduces fuel consumption by up to 19.04% per unit distance in ideal cases.

Also, Xie et al. (2023) study having the same scope, focusing on an ocean-going oil tanker. Using an XGBoost model to predict fuel consumption, the methodology includes data preprocessing, model training, and optimization of speed and trim. A smoothing technique Exponential Weighted Moving Average (EWMA) addressed prediction noise. Results showed high model accuracy ($R^2 = 0.9958$), with joint speed–trim optimization achieving up to 12.30% fuel savings before smoothing. Challenges included noisy data, step effects in predictions, and practical trim adjustment limits. Pagoropoulos et al. (2017) aimed to boost energy efficiency in shipping by improving both technical and crew-related practices. Focusing on tankers, they studied how ships manage onboard power, especially electricity production. They used a machine learning model, Multi-Class Support Vector Machine (SVM), trained on noon report data, with Penalized Linear Discriminant Analysis (PLDA) for selecting key features. For a single vessel, savings could reach $50,000 per year. Key challenges included spotting inefficient operations and handling complex ship data, using information from five tankers.

In addition, Papageorgiou (2020) used Ship Performance Monitor (SPM) software with linear regression to analyze vessel sensor data and track long-term performance trends, focusing on hull and propeller condition. The system identified speed losses of over 4% annually and 11.7% over 2.5 years, highlighting optimization potential. By enabling timely maintenance, SPM supported data-driven performance recovery, reducing fuel use and emissions. However, hybrid approach for optimizing vessel performance in regard to energy efficiency and fuel consumption is presented. Yan et al., (2020) study proposes a two-stage hybrid model to enhance energy efficiency for a dry bulk ship, aiming to cut fuel use and CO_2 emissions. In Stage 1, a Random Forest regressor predicts fuel consumption using factors like speed, cargo weight, and weather, achieving a 7.91% MAPE and outperforming ANN, LASSO, and SVR. Stage 2 uses these predictions for speed optimization to minimize fuel use while meeting arrival times. Case studies over two 8-day voyages showed 2–7% fuel savings. Challenges include non-report data limitations, integrating diverse factors, and the need for vessel-specific models.

Also, Fan et al (2020) developed a physical/empirical energy efficiency model for a 53,000-tonne bulk carrier, aiming to reduce fuel consumption and CO_2 emissions. The model incorporates cargo load, speed, and random environmental factors (e.g., wind, waves) using Monte Carlo simulations in MATLAB/Simulink. Validated against real voyage data, the model showed good accuracy, with an average fuel consumption error of ~6.46%. Challenges include environmental and sensor-related data uncertainties, requiring preprocessing. The case study focuses on a Chinese coastal bulk carrier. Moreover, Leifsson et al. (2008) aimed to optimize vessel operations for energy efficiency amid rising fuel costs and environmental pressures, using data from the container ship *Dettifoss*. The study applied a grey-box modeling approach, combining a physics-based white-box model with a data-driven feedforward neural network (FFNN). Results showed a ~65% reduction in fuel consumption prediction error (RMSE) with modest improvement in speed prediction. Challenges included noisy data and limited input variation affecting model training.

Brandsæter and Vanem (2018) used machine learning models—Linear Regression, Generalized Additive Models (GAM), and Projection Pursuit Regression (PPR)—to predict ship speed using shaft thrust and weather data. They analyzed 10 months of sensor data from an ocean-going ship and found that including environmental factors greatly improved accuracy, especially in rough weather. GAM performed best, boosting accuracy by up to 41%. The study shows how valuable large, high-quality data is for improving ship performance and energy efficiency through data-driven methods. A notable study on statistical approach related to speed optimization is addressed by He et al. (2017).The Speed Optimization Over a Path (SOOP) problem focuses on minimizing fuel costs and emissions for vessels on fixed routes with time windows and speed limits. Rather than using machine learning, a conquer algorithm is applied, leveraging the problem's convex structure. A real-world case study on a cargo ship showed the method's practical benefits, with a 0.24% fuel reduction achieved by allowing flexibility in port time window constrain

Lee et al., (2018) developed a Decision Support System (DSS) to optimize ship speed, aiming to cut fuel costs and emissions without affecting service quality. They used big weather data and operational records from a liner shipping company on a Mediterranean–Black Sea route. Using a method called Multi-Objective Particle Swarm Optimization (MOPSO), the system balanced fuel savings with schedule demands. It gave better estimates, especially on longer trips. Key challenges included dealing with complex weather data and uncertainties at ports. Also, Öztürk & Başar, (2022) aimed to reduce air pollution and operational costs by predicting fuel oil consumption (FOC) using data from 19 container ships. They applied Multiple Linear Regression Analysis (MLRA) and Artificial Neural Networks (ANN) to 24 months of voyage data, including RPM, pitch, draft, trim, and weather. ANN outperformed MLRA, with model accuracy between 76–90%. Predicted energy savings are up to 32–37% (RPM), 6.5–8% (trim), 7–12% (weather routing), and 6–8% (ballast). Challenges included data limitations and the need for more detailed voyage parameters.

Moreover, Cepowski & Drozd (2023) aimed to optimize ship fuel consumption and reduce emissions by accurately estimating fuel use. Using over 105,000 data points from a 4,800 TEU container ship, they developed ANN and Multiple Nonlinear Regression models based on factors like RPM, trim, draught, hull fouling, and environmental conditions. The ANN model achieved more efficiently with high accuracy (MAPE ~6%, RRMSE ~7%, $R^2 = 0.93$). The study highlighted financial impact, estimating that a 1% fleet-wide fuel reduction could yield USD 17.5 million in annual profit. As well, Bui-Duy & Vu-Thi-Minh, (2021) focused on minimizing fuel costs and emissions for container ships on Asian liner routes. They used a deep-learning ANN to predict fuel consumption and Random Forest for variable importance analysis, based on historical voyage, weather, and capacity data. The predicted fuel costs are then used to solve an Asymmetric Traveling Salesman Problem (ATSP) for route optimization. The ANN model achieved high accuracy (MAPE 5.89%, ~95% accuracy). In a case study, the optimized route yielded an estimated fuel cost of USD 98,769.6.

Also, Chaal (2018) focused on reducing fuel consumption and emissions using machine learning models (including K-Nearest Neighbours (KNN), Decision Tree (DT) with AdaBoost, and Artificial Neural Network (ANN)) trained on VLCC historical operational data and applied on the same vessel a case study. ANN performed best and is combined with a Genetic Algorithm to optimize operations, achieving up to 3.13% fuel savings through trim optimization. Challenges included data quality issues and limited operational condition coverage. Similarly, Gonzalez et al. (2018) used high-frequency sensor data to compare the performance of two similar LNG carriers on the same route. They analyzed fuel use, trip time, and environmental conditions. One ship is clearly more efficient, using less fuel and arriving faster. The study showed how detailed data can reveal performance differences and help find ways to save fuel. Filtering the large and complex dataset is key to getting useful results.

While optimization of vessel performance addressed based on trim of the vessel. Tu et al (2023) proposed a machine learning approach to predict optimum trim for container ships, aiming to minimize resistance and improve fuel efficiency, cutting costs and emissions. Using model test data, they trained four models, such as BPNN, Decision Tree, Random Forest, and KNN. Random Forest performed best ($R^2 = 0.905$, MSE = 0.0074), with trim prediction accuracies of 85.71% and 88.89% for 4700-TEU and 13500-TEU ships. Finally, Coraddu et al., (2017) paper's applied data analytics and machine learning to predict fuel consumption and optimize trim for a Handymax tanker, aiming to improve energy efficiency and reduce emissions. Three modeling approaches are compared: White Box (physics-based), Black Box (data-driven), and Gray Box (hybrid). The Gray Box Model matched the Black Box Model's accuracy with less data and lower computational cost. Among all models, Random Forest performed best. Trim optimization based on these models showed potential fuel savings of over 2%.

stly, a comprehensive literature review was conducted to collect and analyze relevant prediction studies utilizing statistical methods in vessel analytics. This review highlights various methodologies, including spatial-temporal data analysis, big data integration, and risk assessment models, which contribute to a deeper understanding of vessel performance. Mao et al. (2016)used different models, including Linear Regression and AR (1), to predict ship speed and improve arrival time estimates. They used one year of data from a container ship and found that including weather factors like waves, wind, and currents gave better results than using engine RPM alone. AR (1) model, using speed from 15 minutes earlier, had a small error in predicting travel distance—only 3.15 km—helping with more accurate route planning.

Additionally, Simonsen et al. (2018) modeled cruise ship fuel consumption and CO_2 emissions using AIS and technical data from ships operating in Norwegian waters. The study applied regression models—an IMO-based model for at-sea consumption and a multivariate regression model for in-port (hoteling) use—emphasizing speed and hoteling as key factors. Model C, a two-stage regression developed using data from MS Finnmarken, a 25,000 GT coastal cruise ship, is best suited for smaller vessels. In contrast, Model A, based on the IMO fuel consumption formula, is more appropriate for larger diesel-electric ships. Based on validation results, Model C provided the most accurate estimates for MS Finnmarken, with total fuel consumption just 3.5% below the actual value and per-nautical-mile emissions within 1% of the measured figure. For larger vessels like the Norwegian Star—a ~91,000 GT cruise ship operated by Norwegian Cruise Line with a diesel-electric power system, Model A is recommended, as it better accounts for the separation between propulsion and hotel energy demands.

To add this, Bialystocki and Konovessis (2016) estimated ship fuel consumption to improve efficiency, reduce costs, and address environmental impacts using 418 noon reports from a Pure Car and Truck Carrier (PCTC). Their statistical method applied empirical corrections for draft, current, and weather conditions to the fuel data. Their regression formula relating corrected fuel consumption to speed, achieved an R^2 of 0.8829. The method is validated on the case ship and a sister vessel. Challenges included data quality and accounting for variable environmental factors. Moreover, Le et al. (2020) developed simplified statistical regression models to estimate fuel consumption for ocean-going container ships across five TEU-based size groups. Using historical voyage data (speed, time, distance, fuel use), each model showed a cubic relationship between speed and fuel consumption. The models achieved high adjusted R^2 values (>90%) and MAPE between 11.62% and 20.71%, indicating strong predictive performance. Key challenges included limited technical data and data noise.

Dev and Saha (2021) used Multiple Linear Regression to estimate the weight of ship engines during early design. They analyzed data from over 3,000 main and 300 auxiliary diesel engines using power, RPM, and cylinder count. While MLR showed high accuracy (R^2 up to 0.97), it had large errors when validated. The study shows how hard it is to predict engine weight due to data variability, especially without AI. By the same token, for calculating ship resistance and effective power, Widodo et al. (2022) focused on predicting the ship form factor, which indirectly affects fuel consumption and operational costs. Using data from 60 displacement ship models tested at the HTL-BRIN laboratory, the study applied Multiple Linear Regression (MLR) with Ordinary Least Squares (OLS) and stepwise variable selection. The resulting regression equation predicted the form factor based on variables including Length-to-Beam ratio (L/B), Beam-to-Draft ratio (B/T), Block Coefficient (CB), Longitudinal Center of Buoyancy (LCB), Prismatic Coefficient (CP), and Waterplane Coefficient (CW). The model showed a good fit with an R-squared of approximately 0.86. Challenges included acquiring sufficient, normally distributed data and addressing outliers, multicollinearity, heteroscedasticity, and autocorrelation in the analysis.

Furthermore, Perera and Mo (2018) focus on analyzing ship performance to support energy-efficient operations. The study is vessel-specific, examining the speed–power relationship of a bulk carrier under varying wind conditions. It employs statistical analysis of operational data, primarily speed, engine power, wind speed/direction, and uses visualization tools like histograms and contour plots to reveal parameter correlations and detect anomalies or sensor faults. Results show that wind profiles significantly affect performance and that effective data cleaning is critical for reliable analysis. A key challenge is managing complex, noisy ship data and accurately identifying erroneous readings. The case study is based on real-world data from the bulk carrier.

Moreover, Cai et al. (2024) use statistical analysis to predict vessel energy efficiency by detecting anomalies in noon reports and sensor data. The method introduces indicators based on deviations from a calibrated speed–power–RPM model (Trinity model). Applied to four vessels, it identifies reliable sensors (e.g., torsion meter over fuel flow). Challenges include data complexity, subjective thresholds, and the need for expert input. Also, Zaman et al. (2017) developed a statistical system to improve ship energy efficiency and regulatory compliance by automatically identifying operational modes using sensor data (fuel flow, GPS). Using methods like Statistical Process Control (SPC) and correlation analysis, the system creates vessel-specific profiles for real-time mode detection. Validated on the *RV Princess Royal* and an Offshore Support Vessel (OSV), it achieved up to 98.3% accuracy, correcting manual log errors and supporting fuel/emission reporting.

3.2.2 Vessel Performance: Critical review

A literature review of the studies presented above is an important part of this thesis. It involves the systematic collection and analysis of relevant studies, including the methods applied, key findings, and identified limitations. By synthesising insights from the existing literature, the thesis establishes a strong research foundation, identifies gaps in current knowledge, and highlights areas where the present research can provide valuable contributions to the field. More specifically, the gaps are presented as follows:

i. Fuel-consumption prediction

Fuel-consumption prediction represents the most extensively investigated area of vessel-performance research. The reviewed studies apply methods ranging from conventional linear and polynomial regression to Artificial Neural Networks, Support Vector Regression, Gaussian Process Regression, Random Forest, Extra Trees, XGBoost, LightGBM and hybrid grey-box models.

Several studies demonstrate that relatively simple statistical models can produce acceptable results when the relationships between variables are stable and the input data are carefully prepared. Uyanık et al. (2019; 2020), Karatuğ and Arslanoğlu (2020), Işıklı et al. (2020), Li et al. (2021) and Wang et al. (2018), for example, employed Multiple Linear Regression, Ridge, LASSO, Elastic Net or Response Surface Methodology. These approaches offered interpretability and enabled the identification of important explanatory variables, including vessel speed, draught, cargo load, engine parameters and environmental conditions. LASSO and Elastic Net were particularly useful where multicollinearity existed because they combined prediction with feature selection.

However, the performance of regression-based models was not consistent across the studies. Although Uyanık et al. (2020) reported exceptionally high predictive accuracy, other statistical studies produced more moderate results or experienced substantial errors during external validation. This variation indicates that a high coefficient of determination in one dataset does not establish that a method is universally suitable. Linear and polynomial models are constrained by their assumptions regarding functional form and may not adequately represent the nonlinear interactions between speed, propulsion demand, draught, weather, hull condition and fuel consumption. Their results are therefore most reliable when the operational range is limited and the underlying relationships remain stable.

Artificial Neural Networks were widely used because of their ability to model nonlinear relationships. Cepowski and Chorab (2021), Ahlgren et al. (2019), Jeon et al. (2018), Tran (2019; 2021), Kee et al. (2018), Le et al. (2020), Beşikçi et al. (2016), Öztürk and Başar (2022) and Cepowski and Drozd (2023) generally found neural-network models to outperform conventional regression approaches. The studies reported prediction errors commonly within approximately 3–10%, although the precise level depended on vessel type, operational coverage and data quality. These results demonstrate that neural networks are well suited to complex vessel-performance relationships.

Nevertheless, their methodological advantages are accompanied by important limitations. Neural networks require sufficiently large and representative datasets, careful selection of architecture and hyperparameters, and effective control of overfitting. They also provide less transparent explanations of how individual variables influence predictions. Studies using only one vessel, a restricted route or a narrow engine-load range may consequently produce accurate results within their training conditions but remain uncertain when applied to different ships or operating profiles. This limits their immediate transferability to fleet-wide or commercial applications.

Tree-based ensemble models, including Random Forest, Extra Trees, Gradient Boosting, XGBoost, LightGBM and CatBoost, emerged as particularly strong alternatives. Chen et al. (2023), Gkerekos et al. (2019), Du et al. (2022), Zhao et al. (2021), Shokohian et al. (2024), Su et al. (2025) and Papandreou and Ziakopoulos (2022) reported that ensemble models frequently outperformed linear regression, Support Vector Regression and standalone neural networks. Their strength lies in capturing nonlinear relationships and interactions without imposing a predetermined functional structure. Random Forest and Extra Trees also demonstrate relative robustness to noisy data, while boosting methods can provide high predictive precision through the sequential correction of model errors.

The findings support the inclusion of ensemble learning in the present research. However, very high values of R^2 reported by several studies must be interpreted carefully. In some cases, predictive performance approached 0.99 or above, but the studies differed significantly in their definitions of the target variable, data aggregation intervals, train–test procedures and operational coverage. Results obtained from randomly divided high-frequency observations may partly reflect temporal similarity between training and test datasets. They are not necessarily equivalent to successful prediction on completely unseen voyages, routes, seasons or vessels. The present study therefore requires an independent unseen dataset and voyage-level case-study validation rather than relying only on conventional random train–test splitting.

ii. Importance of data source and preprocessing

A consistent finding across the literature is that data quality often influences performance more strongly than the choice between advanced algorithms. Gkerekos et al. (2019) showed that automated data-logging information improved prediction accuracy compared with noon reports, while Hu et al. (2021) demonstrated that data cleaning substantially increased model performance. Xie et al. (2023) similarly found that eliminating observations affected by acceleration and deceleration improved the reliability of both physics-based and machine-learning models. Karagiannidis and Themelis (2021), Perera and Mo (2018; 2020), Cai et al. (2024) and Zaman et al. (2017) also emphasised filtering, anomaly detection, operational-mode classification and sensor validation.

High-frequency sensor data provide detailed information about rapid changes in speed, power, fuel flow, draught and weather. They are therefore more appropriate for identifying nonlinear operational relationships than aggregated noon reports. However, high-frequency datasets contain noise, frozen signals, missing observations, autocorrelation and measurements recorded during non-representative operating conditions. Large datasets do not automatically produce reliable models unless observations are correctly filtered and aligned.

Noon reports provide a simpler and more stable data structure, but they depend on manual reporting and aggregate vessel behaviour over long periods. They may conceal short-term operational changes and can introduce subjective reporting errors. Studies based solely on noon reports therefore offer useful voyage-level insights but may lack the resolution required for accurate real-time prediction.

The reviewed evidence directly informs the methodology of the proposed CSI framework. It supports the use of validated high-frequency operational and weather data, systematic missing-value treatment, operational-mode filtering, outlier analysis, feature reduction and independent validation. The literature also demonstrates that methodological transparency is necessary because prediction results cannot be assessed without information about dataset size, frequency, preprocessing, data splitting, cross-validation and hyperparameter optimisation.

iii. Environmental and operational variables

Another common finding is that vessel performance cannot be predicted reliably using speed and engine variables alone. Du et al. (2022), Chen et al. (2023), Hu et al. (2019), Brandsæter and Vanem (2018), Yoo and Kim (2019), Abebe et al. (2020) and Lang et al. (2021) found that the inclusion of weather and sea-state information improved model accuracy. Wind, waves, currents, water depth and sea conditions affect resistance, propulsion power, speed loss and fuel consumption.

The studies nevertheless reveal a methodological trade-off. Environmental data improve the physical completeness of a model, but they also introduce measurement uncertainty. Weather observations may originate from different spatial and temporal resolutions than vessel sensor data, while forecast or hindcast information may not accurately represent the conditions encountered by the vessel. The addition of environmental variables can therefore increase both explanatory power and data complexity.

The evidence supports the inclusion of environmental and operational information during model development, but it also indicates that the final predictor set should be selected through systematic analysis rather than by retaining every available variable. Excessive numbers of correlated or low-quality inputs may increase computational complexity and overfitting without improving unseen performance. This is directly relevant to the proposed framework, which reduces the initial high-dimensional sensor dataset to a manageable group of operationally meaningful features.

iv. Vessel speed and propulsion-power prediction

The vessel-speed literature demonstrates that machine-learning models can accurately predict speed over ground, speed loss and speed–power relationships. Bassam et al. (2022; 2023), Abebe et al. (2020), Baressi Šegota et al. (2020), Coraddu et al. (2019), Moreira et al. (2021) and Lang et al. (2021) used neural networks, Gaussian Process Regression, ensemble trees and digital-twin approaches. Ensemble and nonlinear models generally outperformed basic linear methods, particularly when weather, propulsion and hull-condition variables were incorporated.

Power-prediction studies reached similar conclusions. Kim et al. (2020), Okumuş and Ekmekçioğlu (2021), Liang et al. (2022), Valchev et al. (2022), Mocerino and Rizzuto (2021) and DeKeyser et al. (2022) showed that Support Vector Regression, Gradient Boosting, Random Forest, neural networks and kernel methods can predict propulsion or electrical power more accurately than traditional empirical formulas in many operational settings.

These studies are relevant because speed and power are principal determinants of fuel consumption. They support the treatment of fuel use as an outcome of interacting navigational, environmental and machinery variables. However, speed or power prediction alone does not provide the commercial information required by LNG charterers. Charterers ultimately require estimates expressed as voyage fuel requirements, LNG heel, expected cargo delivery and emissions. Consequently, speed and power models provide analytical foundations for the CSI but do not independently constitute a charterer-satisfaction framework.

v. Physics-based, black-box and grey-box models

The literature distinguishes between white-box, black-box and grey-box modelling. Physics-based white-box models are transparent and can remain meaningful outside the exact conditions represented in the training data. However, they require accurate technical parameters and may simplify complex real-world interactions. Purely data-driven black-box models are flexible and often more accurate within the observed operating domain, but their predictions are dependent on data representativeness and may be difficult to interpret.

Grey-box approaches seek to combine these strengths. Leifsson et al. (2008), Coraddu et al. (2017), Odendaal et al. (2023), Xie et al. (2023), Guo et al. (2022) and Ruan et al. (2024) integrated physical principles with machine-learning components. These studies generally reported improved accuracy, reduced data requirements or greater operational interpretability than single-method approaches.

Despite these advantages, hybrid models can be difficult to construct, calibrate and maintain because errors may arise from both physical assumptions and learned components. Their application may also require vessel-specific technical information that is not consistently available across a fleet. For the present research, the literature supports testing a range of transparent and nonlinear algorithms before selecting the best-performing method. It does not establish that a more complex hybrid structure will necessarily provide greater practical value for the CSI.

vi. Prediction compared with optimisation

A substantial section of the literature extends prediction into operational optimisation. Farag and Ölçer (2020), Hu et al. (2022), Yan et al. (2020; 2024), Xie et al. (2023), Sun et al. (2019), Wang et al. (2016), Tu et al. (2023), Coraddu et al. (2017), Lee et al. (2018) and Bui-Duy and Vu-Thi-Minh (2021) used predictions to optimise speed, trim, routing, engine settings or arrival times. Reported savings ranged from modest improvements of approximately 2–3% to much larger theoretical reductions under selected scenarios.

These results demonstrate that accurate predictions can support operational decisions and generate financial and environmental benefits. Nevertheless, estimated savings are often scenario-dependent and may assume that a vessel can freely alter speed, trim or route. In commercial operations, such decisions are constrained by charter-party requirements, arrival windows, terminal schedules, cargo conditions, safety limits and weather. Theoretical optimisation results therefore cannot always be interpreted as practically achievable savings.

The distinction between prediction and optimisation is important for the CSI. The proposed framework does not primarily attempt to prescribe an optimal route, speed or trim. Instead, it evaluates whether the performance information supplied before a voyage corresponds sufficiently closely to actual voyage outcomes. This orientation is more directly aligned with charterers' vessel-selection and cargo-planning decisions.

LNG-specific vessel-performance literature

Only a limited proportion of the reviewed studies focus specifically on LNG carriers. Ji (2021) analysed fuel consumption and emissions across a large LNG carrier fleet, Nwaoha et al. (2017) compared the relative fuel efficiency of two LNG vessels, and Gonzalez et al. (2018) used high-frequency data to compare the performance of similar LNG carriers. These studies confirm that data-driven analysis can be applied to LNG shipping and can identify differences in fuel efficiency and environmental performance.

However, the LNG studies remain limited in relation to the operational and commercial characteristics of LNG chartering. LNG carriers differ from conventional vessels because the cargo can also serve as fuel, boil-off gas must be managed continuously, and cargo consumed during both laden and ballast passages directly affects the quantity available for discharge and the heel retained for subsequent operations. Existing studies mainly examine general fleet emissions, comparative efficiency or fuel consumption. They do not integrate fuel use with heel requirements, estimated discharging quantity and voyage emissions within a common commercial evaluation.

This limitation is central to the research gap. The wider vessel-performance literature provides strong methods for predicting individual technical outcomes, but it does not capture the interdependency of LNG cargo management, propulsion requirements, delivered quantity and charterer decision-making.

vii. General methodological limitations

Across the literature, several recurring methodological limitations are identified. First, many studies are vessel-specific. Models developed from one vessel, one route or a limited number of voyages may perform well within that operational domain but have uncertain generalisability. Even studies involving larger fleets frequently combine vessels with different designs and operational profiles, potentially concealing vessel-specific relationships.

Second, reporting is inconsistent. Some studies do not clearly state dataset size, sampling frequency, train–test proportions, cross-validation procedures, hyperparameter settings or the exact treatment of missing and abnormal observations. This restricts reproducibility and makes direct comparison difficult.

Third, model-performance metrics are not standardised. Studies report R^2, RMSE, MAE, MAPE, correlation or percentage accuracy using targets expressed in different units and levels of aggregation. A higher R^2 in one study cannot therefore be interpreted automatically as superior practical performance to a lower R^2 reported elsewhere.

Fourth, several studies report exceptionally high accuracy without validating the models on fully independent voyages or vessels. Random division of temporally related observations can overstate generalisation because neighboring records may share almost identical operating conditions.

Fifth, optimisation studies frequently report potential savings under modelled scenarios rather than savings verified through subsequent vessel operation. Their results demonstrate analytical potential but not necessarily realised commercial benefits.

Finally, most studies evaluate success technically through prediction error, fuel saving or emission reduction. Few assess whether the resulting information improves the experience or satisfaction of the customer receiving the shipping service.

3.3 Charterer Satisfaction

3.3.1 Literature Review: Charterer Satisfaction

The development of the Charterer Satisfaction Index (CSI) is supported by established theories that explain the relationship between service quality, performance, expectations, and customer satisfaction. Building upon these theoretical foundations, the present research integrates these concepts into the LNG shipping context by proposing the relationship Predicted Vessel Performance with Actual Vessel Performance and its relative Performance Deviation that concludes to the Charterer Satisfaction. This approach provides a theoretical bridge between established customer-satisfaction literature and objective vessel operational performance, enabling charterer satisfaction to be evaluated through measurable performance outcomes rather than relying exclusively on subjective customer perceptions.

Notable and well-known models for monitoring shipping company performance in relation to customer loyalty include the Service Quality Model (SERVQUAL), the Expectancy-Disconfirmation Model (EDM), and the Kano Customer Satisfaction Model. Each model addresses specific aspects of customer satisfaction and service quality, providing a framework for evaluating and improving shipping services to better meet customer expectations

The SERVQUAL model, developed by Parasuraman et al. (1988) assesses service quality across five dimensions: tangibles, reliability, responsiveness, assurance, and empathy. In shipping, it is widely used to evaluate customer satisfaction through aspects such as vessel condition, on-time delivery, and staff professionalism, offering a clear way to assess and improve service quality (Thai, et al., 2014).

Similarly, the Expectancy-Disconfirmation Model (EDM), proposed by Oliver (1980), evaluates satisfaction by comparing pre-service expectations with post-service performance, making it particularly relevant in shipping where timely delivery and cargo safety are critical (Dolzhenko, et al., 2025). A positive disconfirmation, such as an early shipment arrival, exceeds expectations, boosting customer satisfaction and fostering long-term loyalty, which supports sustainability.

Moreover, the Kano Model, introduced by Kano et al. (1984) categorizes customer needs into must-be, one-dimensional, and attractive attributes, helping shipping companies innovate and differentiate their services (Yuen & Thai, 2015).

However, several studies have applied customer satisfaction and service-quality approaches specifically within the shipping industry. Thai (2008) developed and empirically tested a maritime service-quality framework, demonstrating that service quality in maritime transport can be evaluated through dimensions associated with resources, outcomes, processes, management, image, and social responsibility. This study provided an important foundation for adapting general service-quality concepts to the specific characteristics of maritime transportation.

Building on the application of service-quality concepts in shipping, Yuen and Thai (2015) investigated the relationship between service quality and customer satisfaction in liner shipping using data collected from 183 liner shippers. Their findings identified reliability, speed, responsiveness, and value as the four principal dimensions of service quality, with reliability having the strongest influence on customer satisfaction. The study demonstrated that operationally relevant characteristics of shipping services, particularly reliability and time-related performance, can significantly influence customers' overall evaluation of shipping companies.

Similarly, Huang et al. (2015) examined service-quality assessment within the liner shipping industry by considering customer requirements and the technical and managerial characteristics of shipping services. Their approach further demonstrated the importance of translating customer requirements into measurable shipping-company performance attributes.

More specifically, Hirata (2019) investigated the relationship between service characteristics and customer satisfaction in the container liner shipping industry. The study showed that the quality of customer service representatives, digitalisation, and sales representatives were among the most influential characteristics affecting customer satisfaction. This research demonstrates that customer satisfaction in shipping is influenced by a combination of service delivery, communication, and organisational capabilities rather than by price considerations alone.

The importance of customer satisfaction has also been examined in situations where shipping service performance does not meet customer expectations. Hirata (2020) investigated service recovery and customer satisfaction in container liner shipping and found that the timeliness of communication was the most significant service-recovery attribute. The study further demonstrated that effective recovery actions following service failures can improve customer satisfaction, highlighting the importance of responsiveness in the relationship between shipping companies and their customers.

More recently, the relationship between service quality, satisfaction, and loyalty has been extended to the digital services offered by shipping companies. Chao et al. (2024) examined the e-commerce platforms of major liner shipping companies and found that e-service quality positively influences both customer e-satisfaction and e-loyalty, while trust moderates the relationship between satisfaction and loyalty. These findings further support the broader relationship between shipping-company service performance, customer satisfaction, and subsequent customer loyalty.

Further research has examined the relationship between service quality, customer satisfaction, and customer loyalty specifically within shipping and maritime transportation. These studies demonstrate that customer satisfaction in shipping is influenced by a combination of operational reliability, service responsiveness, communication, service recovery, digitalisation, and the overall quality of the service provided.

Lobo (2010) examined service quality from the perspective of shippers using container shipping lines. The study evaluated different components of the shipping service, including sales and marketing, cargo booking, documentation, operations, and claims handling. The findings indicated differences in customer evaluations across these service components, with personal visits and claims handling receiving comparatively lower assessments. The study demonstrated that customers evaluate shipping companies through multiple service-performance characteristics rather than through transportation outcomes alone.

Yeo, Thai and Roh (2015) investigated the relationship between port service quality and customer satisfaction in Korean container ports. Using data from 313 members of the Korean Port Logistics Association and Partial Least Squares Structural Equation Modelling (PLS-SEM), the authors identified port service quality as a multidimensional construct. Management, image, and social responsibility were found to have significant positive effects on customer satisfaction, demonstrating that customer satisfaction in maritime transportation is influenced by both operational and organisational dimensions.

Yuen and Thai (2015) investigated service quality and customer satisfaction specifically in liner shipping. Based on responses from 183 liner shippers, the study identified reliability, speed, responsiveness, and value as the four principal dimensions of shipping service quality. Reliability was identified as the strongest determinant of customer satisfaction, followed by speed and responsiveness, demonstrating the importance of operational and time-related performance in customers' evaluations of shipping companies.

Similarly, Hirata (2019) examined service characteristics and customer satisfaction in the container liner shipping industry. The study mapped service-quality dimensions to specific characteristics of container shipping services and found that the quality of customer service representatives, digitalisation, and sales representatives were the three most influential factors affecting customer satisfaction. The findings demonstrate that customer satisfaction in shipping reflects both operational service delivery and the quality of interactions between shipping companies and their customers.

Chao, Lin and Sun (2019) extended the customer-satisfaction literature by examining service recovery and customer loyalty among liner shipping users. Using Structural Equation Modelling (SEM), the study demonstrated that service recovery positively influences customer loyalty and that this relationship is mediated through customer satisfaction and satisfaction following recovery. This suggests that customer satisfaction not only reflects the initial quality of shipping services but also plays an important role in maintaining long-term customer relationships following service failures.

Research on maritime service quality has also demonstrated the need for industry-specific measurement frameworks. Thai (2008) developed the ROPMIS model specifically within maritime transport using data involving shipping companies, port operators, freight forwarders, and logistics service providers. The resulting framework identified six dimensions of maritime service quality: resources, outcomes, process, management, image, and social responsibility. The study demonstrated that conventional service-quality principles can be adapted to reflect the particular operational and organisational characteristics of maritime transportation.

The relationship between customer satisfaction and loyalty has subsequently received increased attention within shipping research. Chao, Yu and Wei (2024) investigated the e-commerce platforms of major liner shipping companies and established a relationship between e-service quality, e-satisfaction, and e-loyalty. Their findings demonstrated that e-service quality positively influences both customer satisfaction and loyalty, while trust plays a moderating role in the relationship between satisfaction and loyalty. This provides further evidence that satisfaction can operate as an intermediate mechanism through which shipping-company performance influences customer retention.

More recent studies have continued to investigate the relationship between maritime service quality and satisfaction. Research on container port service quality has demonstrated that different combinations of service-quality attributes can generate customer satisfaction, suggesting that maritime customers assess service providers through several interconnected dimensions rather than through a single performance characteristic.

Furthermore, Caterina and Efrata (2026) examined the relationships between logistics service quality, service costs, customer satisfaction, dependency, and customer loyalty within the container shipping industry. Using a sample of 225 service users and SEM, the study found significant relationships between several service-quality dimensions, satisfaction, and customer loyalty. Importantly, the study employed Expectancy-Disconfirmation Theory, providing evidence of the applicability of expectation–performance principles within a container-shipping environment.

Collectively, these studies demonstrate that service quality, customer satisfaction, and customer loyalty have been extensively investigated within maritime transportation, container shipping, liner shipping, and port services. Existing studies have identified factors such as reliability, speed, responsiveness, service recovery, communication, digitalisation, value, management, and corporate image as important determinants of customer satisfaction. Nevertheless, these studies predominantly evaluate performance through customer perceptions, questionnaire-based service-quality measures, or service characteristics. Comparatively limited attention has been given to integrating customer-satisfaction theory with objective vessel operational performance indicators and evaluating satisfaction through the difference between expected or predicted and actual vessel performance.

3.3.2 Critical Review: Charterer Satisfaction

Collectively, these studies demonstrate that customer satisfaction and service quality have been extensively examined within maritime transport, liner shipping, container shipping, and port services. Existing research has identified several factors that influence customers' evaluations of shipping services, including reliability, responsiveness, communication, service speed, service recovery, digitalisation, value, and the quality of interactions between shipping companies and their customers. Models such as SERVQUAL, Expectancy-Disconfirmation, Kano, and maritime-specific service-quality frameworks have provided important theoretical and empirical foundations for understanding how customers develop expectations, evaluate the services received, and subsequently form satisfaction and loyalty towards shipping service providers.

However, the existing literature predominantly assesses customer satisfaction through subjective and perception-based measures, typically collected through questionnaires, interviews, or customer evaluations of service characteristics. Although factors such as reliability, timely delivery, responsiveness, and service efficiency may indirectly reflect the operational performance of a shipping company, they generally represent customers' perceptions of performance rather than objectively measured vessel performance. Consequently, relatively limited attention has been given to operational indicators that can be quantitatively measured at vessel level, such as fuel consumption, cargo-related performance, voyage efficiency, and environmental performance. This creates a separation between the literature concerned with vessel operational performance and predictive analytics and the literature concerned with customer satisfaction and service quality.

Therefore, an important research opportunity exists to integrate these two areas by incorporating objectively measured vessel operational performance into the assessment of charterer satisfaction. In particular, limited research has investigated whether the difference between a vessel's expected or predicted performance and its actual achieved performance can provide a quantitative indication of charterer satisfaction. Such an approach extends traditional perception-based satisfaction frameworks by introducing measurable operational evidence into the evaluation process. This provides the foundation for developing a more objective and data-driven approach to charterer satisfaction in shipping, in which multiple vessel-performance criteria can be evaluated collectively and compared with expected performance to determine the extent to which the vessel meets the charterer's operational and commercial expectations.

3.4 Research gap emerging from vessel-performance and charterers satisfaction literature

The vessel-performance literature therefore provides the analytical capability required to construct reliable predictions, but not the commercial mechanism required to evaluate the shipping service from the charterer’s perspective. This unresolved connection between predictive vessel analytics and charterer satisfaction constitutes the principal gap addressed by the CSI framework. Therefore, the literature provides four main foundations for the proposed CSI as follows:

First, it demonstrates that fuel consumption and related operational performance can be predicted using statistical and machine-learning techniques. This supports the development of predicted benchmark values against which actual LNG vessel performance can be compared.

Second, the repeated success of Random Forest, Extra Trees, XGBoost and other ensemble techniques justifies comparing linear, regularised, boosting, neural-network and tree-based models rather than selecting one algorithm in advance. The model should be chosen empirically using consistent validation metrics and unseen data.

Third, the literature establishes that data preprocessing, feature selection, environmental information and operational-state classification are necessary for credible performance prediction. These findings inform the CSI data-processing methodology and validation procedure.

Fourth, the reviewed studies confirm the commercial importance of fuel consumption, cargo-related energy requirements and emissions. Nevertheless, they normally treat these performance variables separately and evaluate them from the perspective of technical efficiency rather than charterer satisfaction.

Accordingly, the literature supports the predictive component of the proposed research but does not provide the complete framework required for LNG chartering. Existing studies can predict how much fuel a vessel may consume, how speed and power respond to operational conditions, and how operating changes may reduce fuel use or emissions. They do not determine how deviations between information provided before the voyage and actual performance influence the charterer’s evaluation of the service.

The proposed CSI addresses this limitation by moving beyond isolated technical predictions. It integrates the deviations between predicted and actual values for laden fuel consumption, ballast heel requirements, estimated discharging quantity and voyage emissions. These dimensions are then combined according to their relative importance to charterers. Therefore, the contribution of the CSI is not the prediction of vessel performance alone, but the translation of prediction reliability into a structured, quantitative and commercially relevant evaluation of charterer satisfaction.

3.5 Summary

In summary, the chapter demonstrates that vessel performance and customer satisfaction have largely been studied separately. This research gap provides the foundation for integrating predicted and actual vessel performance with charterer satisfaction through the proposed Charterer Satisfaction Index (CSI). The following chapter presents the research framework of the thesis and describes the methodology adopted for its development and implementation.

4. Chapter 4 – Thesis framework

4.1 Introduction

Chapter 4 presents the development of the research framework, providing an understanding of the methodology and its practical considerations. It presents the framework's description, the research methodology, and an analysis of the overall process.

4.2 Thesis framework description

Building on the comprehensive literature review and critical evaluation presented in Chapter 4 and 3, this study addresses critical research gaps in evaluating the charterer satisfaction relative to vessel performance in maritime shipping operations using Artificial Intelligence techniques. This sub-section outlines the thesis framework to provide the reader with a general understanding of the study, and with a brief overview of topics that will be analyzed in detail in the following sections.

The study begins by identifying the fundamental aspects of vessel performance as the central focus of this research. As per Figure 4.1, vessel performance can be broadly split into four categories: technical performance, operational performance, environmental compliance performance, and commercial performance.

The technical parameters of vessel performance, especially those tied to fuel consumption, are vital for all vessel operations, including propulsion and onboard auxiliary systems, both central to this thesis. These parameters encompass factors such as hull and propeller condition, engine efficiency, the functionality of onboard sensors and equipment, and maintenance schedules. While, operational performance encompasses all voyage execution characteristics, extending beyond basic navigation to include critical aspects such as vessel routing (including speed and weather parameters), LNG cargo management, trim optimization and bunkering strategies. Moreover, environmental compliance performance, an increasingly significant dimension in modern shipping, encompasses emissions reporting, CO_2 management, and ESG (Environmental, Social, and Governance) reporting. Lastly, commercial performance reflects the vessel's ability to meet contractual obligations and maintain charterer satisfaction. This involves monitoring the execution of charter party agreement, managing pre- and post-fixture of the contract for vessel's activities, and ensuring service reliability. In conclusion, all categories of vessel performance are directly related to each other, and each can influence the others.

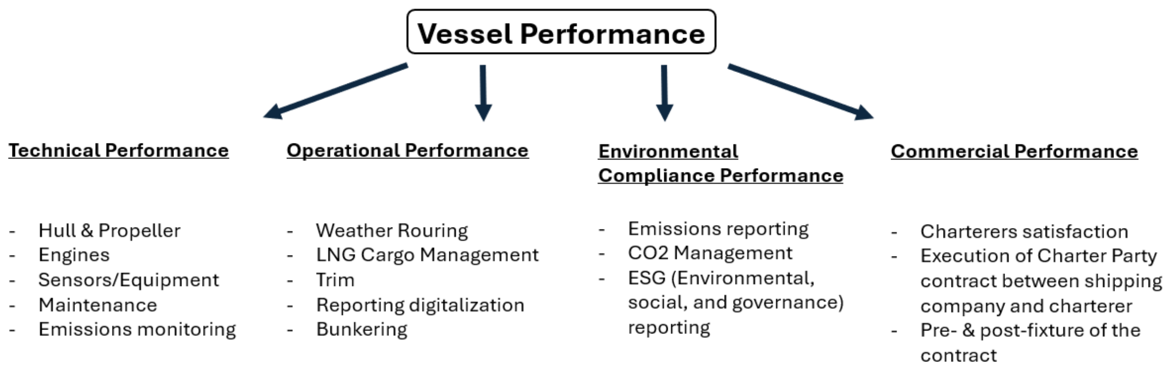

Figure 4.1. Vessel Performance Key Dimensions (Technical, Operations, Environmental & Compliance, Commercial). .

Taking vessel performance categories into account helps the reader better understand the research framework, called the Charterer Satisfaction Index (CSI). CSI is primarily grounded in commercial performance, as it incorporates with other performance such as technical, operational and environmental compliance.

In practice, CSI plays a vital role in maritime commercial operations as it evaluates charterers satisfaction according to charterers' profitability through the decision making of vessel-cargo matching. When evaluating a cargo request, charterers rely on the vessel characteristics to select the most suitable option, requiring accurate performance predictions well in advance of voyage execution from shipping companies (who offer the vessel to charterer). Thus, CSI monitors the gap between actual and predicted performance information. The closer the predicted outcomes are to the actual results, the higher the level of charterer satisfaction, as accurate forecasting enables optimal decision-making in matching vessels with specific cargo requirements. This commercial framework delivers dual benefits: it provides charterers with essential operational advantages while simultaneously enhancing shipping companies' profitability and strengthening their market reputation.

Comprehensive market interviews are conducted with industry stakeholders to identify the most critical performance information for charterer satisfaction across all categories. The results of this process include fuel consumption, heel amount (the remaining amount on board of LNG after the cargo discharge), LNG discharging efficiency, and emission footprint. Briefly, these factors represent the essential information charterers require to make efficient decisions, ultimately enabling them to maximize profitability.

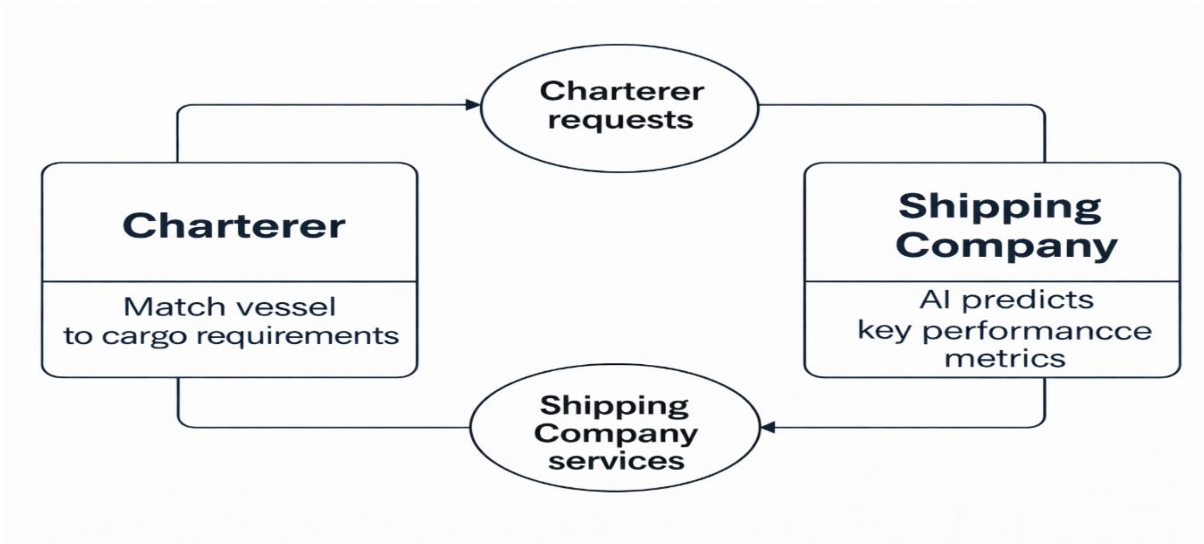

Figure 4.2. Charterers and shipping company cooperation related to voyage plan efficiencies process.

Figure 4.2 presents the key vessel performance information important to charterers. Hence, the first critical vessel performance information is briefly presented. A shipping company must provide charterers in advance with the vessel's estimated fuel consumption for the voyage from Port A to Port B for cargo delivery. This voyage is referred to as the laden or loaded vessel condition, as the vessel is transporting cargo to the discharging port. Fuel consumption encompasses the energy required for the main propulsion system, powered by the main engine. Additionally, diesel generators are essential for supplying power to auxiliary systems, including mainly cargo handling systems, engine room equipment, and bridge instruments. However, the uniqueness of LNG vessels is related to their fuel source, which comes from the LNG cargo they transport. A key feature of these vessels is their use of natural boil-off gas (NBOG) from LNG cargo, which is generated through cargo evaporation during the voyage. More technical details review of LNG vessels outlining the power supply of vessels to engine in Chapter 5, section 5.2 "LNG Operational Context and Utilization Patterns".

Also, another key vessel performance information provided to Charterers is the heel amount. It is the LNG cargo quantity that remains after the cargo delivery to the discharging port. The remaining quantity of cargo, referred to as the heel, is primarily utilized for vessel propulsion and operational requirements during the unloaded (ballast) passage from Port B back to Port A, or to an alternative loading port such as Port C (i.e., either the same or a different loading port). More technical details review of LNG vessels features is included in Chapter 5, section 5.2 “LNG Operational Context and Utilization Patterns”.

Additionally, LNG discharging quantity is another critical vessel performance information that is important for charterers. It is calculated based on the loaded quantity, accounting for the consumption of LNG cargo due to vessel’s need (main and auxiliary engines) during the voyage, as previously described in the fuel and heel quantity. This is crucial for charterers because it reflects their commitment to cargo receivers and they are responsible for ensuring the proper delivery of an agreed quantity, which the receivers have paid for. More technical details review of LNG vessels is included in Chapter 5, section 5.2 “LNG Operational Context and Utilization Patterns”.

The final performance criterion considers the vessel’s emission footprint, reflecting its environmental performance during the voyage. While shipping regulations address emissions such as CO_2, SOx, and NOx, methane (CH_4) slip is also particularly relevant for LNG-fuelled vessels, as unburned methane may be released during combustion and fuel handling. This research uses CO_2 emissions as the main indicator because verified CO_2 data are consistently available and aligned with IMO CII and EU MRV requirements. Methane slip is acknowledged as an important environmental factor and is proposed for inclusion in future extensions of the CSI framework when reliable operational data become available.

The emission footprint is discussed in many academic studies, as described in the literature review in Chapter 3. For further technical details, refer to Chapter 5, section 5.2, titled “LNG Operational Context and Utilization Patterns.

In conclusion, it is important to mention that the techniques used in the thesis to ensure high accuracy of results are based on employing Artificial Intelligence methods. These methods take into account historical operational data and benchmark the predictions against statistical evaluation metrics such as R^2, RMSE (Root Mean Square Error), and MAE (Mean Absolute Error) to guarantee the reliability of the results. The literature review provides benchmarking of these statistical evaluation metrics, validating their effectiveness in assessing prediction accuracy and ensuring model validity.

4.3 Research Methodology

This section presents the research methodology of the Charterer Satisfaction Index (CSI), outlining the structured framework and systematic process by which thesis index is designed, conducted, and analyzed, following Goundar's approach (2012) and is summarized in the Table 4.1.

Initially, the primary focus of the research methodology of CSI is justification for this study, which lies in the growing need to further develop the research area of LNG vessel performance. Through the implementation of this research, commercial vessel performance can be significantly improved, offering substantial benefits to charterers. Specifically, charterers are able to make more efficient decisions when matching cargo requirements with the most suitable and available vessels. This improved efficiency translates into stronger economic outcomes for charterers and so they can be satisfied with the shipping company services.

Following this, the research design needs to be defined, which is based on a quantitative approach. This is the most appropriate method for generating the CSI. The choice of a quantitative approach aligns with the research's objective of producing actionable insights through structured data analysis and predictive modeling.

Moreover, the research methodology includes a defined research population and two different interview processes, as described in Appendices 1 and 2 related to CSI development, and Appendices 18 and 19, which address the sensitivity analysis of the CSI results.

Regarding the first interview process, 12 professionals with varied experience, backgrounds, and perspectives on vessel performance were involved. Specifically, as shown in Figure 4.3, which illustrates the interviewees' backgrounds and the number of participants, there are four (4) individuals at management level (Top Management in a shipping company) and 5 (five) employs of a shipping company with technical background as team leaders with more than 15 years of experience in the shipping industry. Also, there are 3 (three) ex-Mariner/Captains who have previously served as vessel masters, 2 (two) senior-level personnel/team leaders from a chartering company and finally 2 (two) Captains actively executing their duties onboard vessels (Figure 4.3).

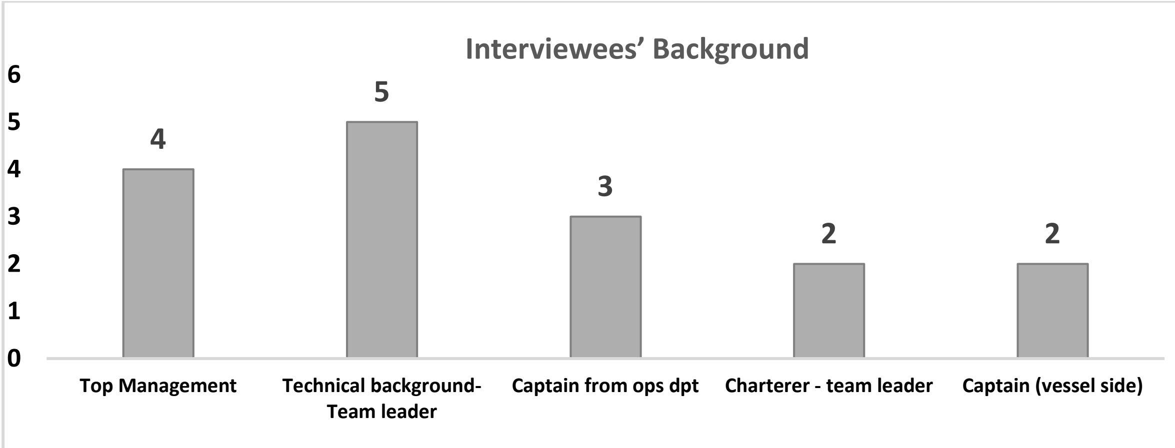

Figure 4.3 Interviewee's background related to CSI development.

The interview process consisted of two main components essential for CSI implementation. Both were designed to maintain consistency across sessions while allowing flexibility to capture detailed expert insights. The first component focused on identifying the models to be incorporated into the CSI, with further details provided in Appendices 1 and 2. Experts also assigned weights to each model based on the relative importance of factors contributing to the overall CSI, as discussed in Section 4.4.2, CSI Formulation. All interviews were conducted remotely via video conferencing platforms such as Zoom and Microsoft Teams, following semi-structured protocols.

The 12 participants were selected through purposive expert sampling based on their experience in LNG shipping operations, chartering, commercial management, and vessel performance. The sample was considered adequate because the study aimed to obtain expert judgement rather than statistical generalisation. Adequacy was also supported by response convergence, as the later interviews identified no new criteria beyond the four main themes: fuel consumption, heel quantity, estimated discharging quantity, and emissions.

The interview evidence was systematically coded and translated into AHP criteria and weights. First, the interview responses were reviewed and coded to identify common statements related to LNG vessel operational and commercial performance. Similar responses were grouped into broader themes, resulting in four main criteria consistently identified by the experts: Fuel Consumption, Heel Amount, Estimated Discharging Quantity, and Emission Footprint. These four themes were then directly used as the criteria in the AHP analysis.

Following this process, the participants compared the four criteria using Saaty's nine-point pairwise comparison scale to indicate their relative importance to charterer satisfaction. The individual expert responses were combined using the geometric mean to create a group comparison matrix, from which the final AHP weights were calculated. The consistency of the comparisons was also checked using the Consistency Ratio (CR < 0.10). Finally, these weights were incorporated into the Charterer Satisfaction Index (CSI) to represent the relative importance of each vessel performance criterion (Appendix 1 and 2).

Related to the second interview process, as shown in Figure 4.4, the distribution of participants by functional role indicates that office-based captains form the largest group (three), followed by onboard captains (two). In addition, there were two participants from the office side, one from the commercial department and one from general management.

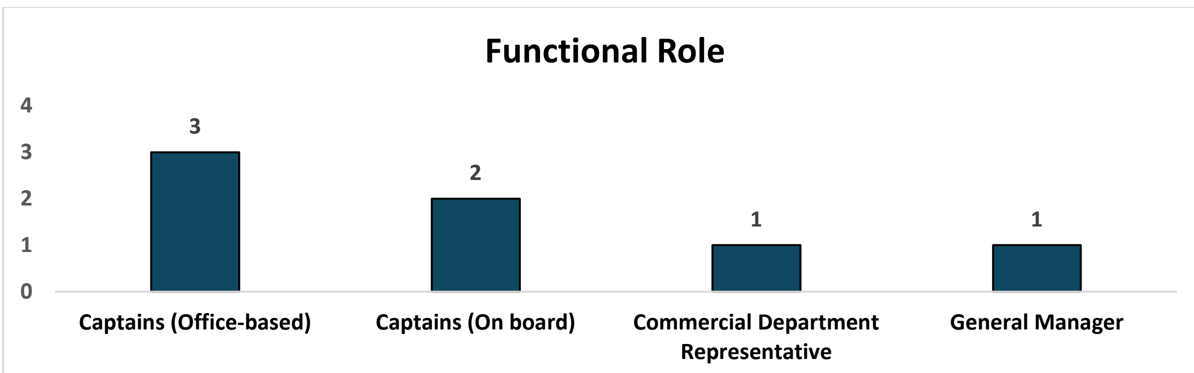

Figure 4.4. Interviewee's background related to CSI results.

This process involves conducting a sensitivity analysis of the CSI thesis framework, requiring the identification of results based on expert experience and the definition of associated logical values and business practice implications.

The next component of the research design addresses data collection for implementing research projects. This study utilized vessel operational data (primary data), sourced from the Ascenz Marorka platform, to support the analysis, an affiliate of GTT (Gaztransport & Technigaz). GTT is a leading French engineering company specializing in membrane containment systems for the transport and storage of liquefied gases, particularly Liquefied Natural Gas (LNG). With decades of expertise and innovation, GTT plays a critical role in supporting the maritime and energy sectors in their energy transition efforts. The company is widely recognized for its commitment to safety, performance, and sustainability, offering a broad portfolio of technologies and digital solutions that help shipping companies optimize operations and reduce environmental impact. Therefore, Ascenz Marorka delivers advanced maritime data intelligence and vessel performance solutions. The platform offers shipowners and operators real-time monitoring, voyage optimization, and fuel consumption analysis tools, enabling more informed decision-making by leveraging machine learning and big data analytics. Thus, the dataset provided by Ascenz Marorka includes data from Integrated Automation Systems (IAS) sensor readings and professional weather data, collected at 15-minute intervals.

The dataset provided by the Ascenz Marorka platform is of high quality, as the platform ensures its reliability through its own validation processes. The vessels selected for this thesis project were chosen based on the accuracy of their dataset values, ensuring that vessels with incorrect or faulty parameter entries were excluded.

Therefore, the quality of the Ascenz Marorka dataset was assessed through the platform's validation procedures applied to key vessel parameters, including SOG, STW, shaft RPM, shaft power, main engine fuel consumption, and forward and aft draft. Vessels with significant faulty or unreliable parameter records were excluded from the analysis. The validation process considered four main data-quality checks:

1. Out-of-bounds values: Measurements were checked against predefined realistic or vessel-specific operational limits. Values outside these limits were flagged as potentially incorrect. For example, unrealistic vessel speed, shaft RPM, fuel consumption, or draft values may indicate sensor or data-transmission errors.

2. Frozen values: Parameters remaining unchanged for an unusually long period, when normal operational variation would be expected, were identified. For example, identical shaft power or RPM readings over an extended sailing period may indicate a frozen sensor or communication issue.

3. Cross-validation: Related operational parameters were compared to assess their consistency. For example, when the vessel is sailing at a certain speed, corresponding values of shaft RPM, shaft power, and main engine fuel consumption are expected. A high vessel speed combined with zero RPM or fuel consumption would therefore be considered inconsistent.

4. Missing data: Periods in which expected sensor measurements were not received or recorded were identified. Such gaps may result from sensor failures, communication interruptions, or data-transmission problems and directly affect dataset completeness.

Data quality was expressed as the percentage of valid measurements relative to the total expected measurements:

Data Quality (%) = (Valid Measurements / Total Expected Measurements) × 100

A score of 100% represents the optimal condition, where all expected measurements are available and pass the applicable validation checks. For this research, the following thresholds were applied: ≥95% = Good Data Quality, 85–<95% = Acceptable Data Quality, and <85% = Poor Data Quality. Therefore, "close to 100%" indicates datasets with very few missing, invalid, frozen, or inconsistent measurements, with ≥95% considered sufficiently reliable for vessel performance analysis.

No separate independent measurement campaign or third-party verification was conducted. Therefore, the assessment of data quality was based primarily on the completeness, operational plausibility, and internal consistency of the recorded vessel data according to the above validation criteria.

Also, this study employs a strong analysis on primary data for the development of machine learning models for fuel prediction. The methodological approach includes regression analysis and predictive modeling using machine learning techniques. The objective is to apply advanced technological methods to structured datasets to generate actionable insights and develop predictive tools tailored to the context of LNG commercial performance.

However, assumptions and key criteria form an integral part of the research methodology and must be clearly defined. Specifically, the selected machine learning models assume the availability of a large, high-quality dataset with consistent patterns between operational variables and fuel consumption. It is also assumed that past voyage data can be used to predict future fuel use under similar conditions. Key criteria for selecting models should be defined to ensure prediction accuracy and the ability to handle complex subjects. Techniques such as feature cross-validation, hyperparameter optimization are applied to meet the assumptions and enhance model performance.

The research design, defined within the research methodology, outlines the tools implemented by CSI. For quantitative analysis and model development, Python is the primary programming language used. Essential libraries include Pandas~~,~~ NumPy, and scikit-learn for implementing machine learning algorithms. The analyses pf the dataset and models are primarily developed using Google Colab (Google Colaboratory, 2025), a cloud-based, user-friendly environment that supports efficient code execution and collaborative work. Generally, Google Colab is often compared to Jupyter Notebook, which is used locally on a computer. It is also compared to Kaggle Notebooks, which are designed for data competitions and datasets, and to local IDEs which require setup on a personal machine. Unlike these options, Colab is cloud-based, requires no installation, and enables easy collaboration, making it especially practical for research. Additionally, Microsoft Excel is employed as a complementary tool for performing basic calculations. In this study, Excel is specifically used to implement parts of the research framework, calculate the Charterer Satisfaction Index (CSI), and conduct the Analytic Hierarchy Process (AHP) to determine the relative weights of models.

The research design also defines the CSI practical exercise, which involves three case studies conducted using operational data from three different LNG vessels. Each vessel was examined under two different conditions, laden and ballast. These case studies demonstrate the predictive models' accuracy and highlight their practical application in real-world scenarios.

Final step is the validation of the methodology is to evaluate the performance and accuracy of the selected models, key evaluation metrics have been used, including R^2 (coefficient of determination), MAE, and RMSE. These are a common and well know metrics used in the validation of model results with R^2 to indicate how well the model explains the variability of the target variable, with values closer to 1 signifying a better fit. MAE provides the average magnitude of the errors between predicted and actual values, offering a straightforward interpretation of prediction accuracy. Finally, RMSE gives greater weight to larger errors by squaring them before averaging and taking the square root, making it particularly useful when large deviations are undesirable. Together, these metrics provide a comprehensive validation of the model's predictive capabilities and allow for comparison with the findings of existing studies in the relevant literature.

Table 4. 1 Research Methodology flowchart.

Research Methodology	Application in the Study
Justification for the Research	The research methodology of CSI focuses on improving LNG vessel performance to enhance commercial efficiency. This allows charterers to better match cargo with suitable vessels, leading to stronger economic outcomes and greater satisfaction with shipping services
Research Design	The research adopts a quantitative design, best suited for generating the CSI and providing actionable insights through structured data analysis and predictive modeling.
Data collection	Data was collected via purposive sampling from two primary sources: (1) Operational data from LNG vessels, recorded at 15-minute intervals through the Ascenz Marorka platform; (2) Expert interviews with 12 professionals from management, chartering, and onboard roles for CSI development and also another interview process from experts related to sensitivity analysis of CSI results.
Data Analysis	The research design includes instrumentation for quantitative analysis, primarily using Python with libraries such as Pandas, NumPy, and scikit-learn. Analyses are developed in Google Collab, while Microsoft Excel supports basic calculations, CSI computation, and the Analytic Hierarchy Process (AHP) for weighting models.
Selection of Methods and Techniques	This study analyzes primary data to develop machine learning models for fuel prediction, applying regression and predictive techniques to generate actionable insights and tools for improving LNG vessel performance.
Assumptions and Criteria	The methodology relies on assumptions, including access to a large, high-quality dataset and the use of past voyage data to predict future fuel consumption. Model selection is based on accuracy and ability to handle

Research Methodology	Application in the Study
	complexity, supported by techniques like cross-validation, and hyperparameter optimization to improve performance
Quantitative vs Qualitative	The methodology is quantitative, as it focuses on numerical data, statistical and machine learning modeling. Qualitative input is based on expert insights to CSI.
Quantitative Criteria (validation of the results)	The final step is methodology validation using R^2, MAE, and RMSE. R^2 measures how well the model explains variability, MAE shows average prediction error, and RMSE emphasizes larger errors. Together, these metrics ensure robust evaluation and enable comparison with existing studies.

4.4 Thesis Framework implementation

This section outlines the implementation of the thesis framework, beginning with the definition of the CSI formulation Specifically, CSI consists of four models that define actual and predicted vessel performance values, where less deviation indicates a better index and higher satisfaction for charterers.

Table 4. *2 Thesis Framework implementation flowchart.* presents the framework implementation flowchart, outlining the step-by-step structure of the thesis. These steps are further analyzed in the next section of this chapter. The process begins with the formulation and definition of the Charterer Satisfaction Index (CSI). To support the application of subsequent CSI models, fuel consumption prediction is first required. This is followed by data collection, where the necessary datasets are sourced and prepared, along with data preprocessing and feature engineering to ensure the data is cleaned, transformed, and optimized for modeling. The next stage focuses on predictive fuel consumption of the vessel, involving the application of machine learning models and relative evaluation of the results. Once fuel prediction is completed, the framework progresses to applications, starting with the fuel model for laden and heel model corresponding to the ballast condition, followed by the integration of an estimated

discharging model. Finally, the emission footprint model is implemented to assess environmental impact, linking vessel performance with sustainability outcomes.

Table 4. 2 Thesis Framework implementation flowchart.

Thesis Sections	Thesis Description
1. CSI Formulation	a. Definition and formulation of the Charterer Satisfaction Index (CSI).
2. Prediction of Fuel consumption	a. Data collection: Sourcing and preparation of the fuel model dataset. b. Data Preprocessing & Feature Engineering: Cleaning, transforming, and selecting relevant features for modeling. c. Predictive Model Development & Evaluation: Building and evaluating the performance of predictive models.
3. Fuel in laden model	a. Application of the model
4. Heel model	a. Application of the model
5. Estimated Discharging Quantity Model	a. Application of the model
6. Emission footprint model	a. Application of the model

In conclusion, as a summary according to Figure 4.5 presents the complete methodological framework adopted in this research and illustrates the sequential integration of key performance metrics used to develop the Charterer Satisfaction Index (CSI). The research begins with a comprehensive literature review, which identifies the research gap and establishes the theoretical foundation of the framework. Subsequently, semi-structured interviews with industry experts are conducted to capture practical knowledge regarding the operational factors that most significantly influence charterer satisfaction. The interview data are then analysed through thematic coding, allowing recurring concepts to be grouped into four principal evaluation criteria: Fuel Consumption, Heel Amount, Estimated Discharging Quantity, and Emission Footprint. These criteria form the hierarchical structure of the Analytical Hierarchy Process (AHP), through which pairwise comparisons are performed to determine their relative importance and derive the final weighting coefficients.

In parallel, the quantitative component of the research utilizes high-frequency operational data collected from three LNG carriers over a two-year period. The collected datasets undergo a comprehensive preprocessing procedure, including data cleaning, missing value treatment, feature selection, transformation, and dataset preparation. The processed data are subsequently used to develop machine learning prediction models for each of the four performance criteria. The predicted operational values are then compared with the corresponding actual voyage performance values to quantify the prediction deviations.

The final stage of the framework integrates the prediction deviations with the AHP-derived weights to construct the Charterer Satisfaction Index (CSI), thereby producing a single performance indicator representing the overall level of charterer satisfaction for each voyage. The robustness of the framework is assessed through model validation using established performance metrics, including RMSE, MAE, and the coefficient of determination (R^2), together with cross-validation procedures. Furthermore, the CSI methodology is evaluated through sensitivity analysis and expert validation interviews to confirm the practical relevance of the weighting structure and the resulting satisfaction scores. Finally, the framework provides an interpretable decision-support tool that enables shipping companies and charterers to evaluate vessel performance, compare voyage efficiency, and identify opportunities for operational improvement.

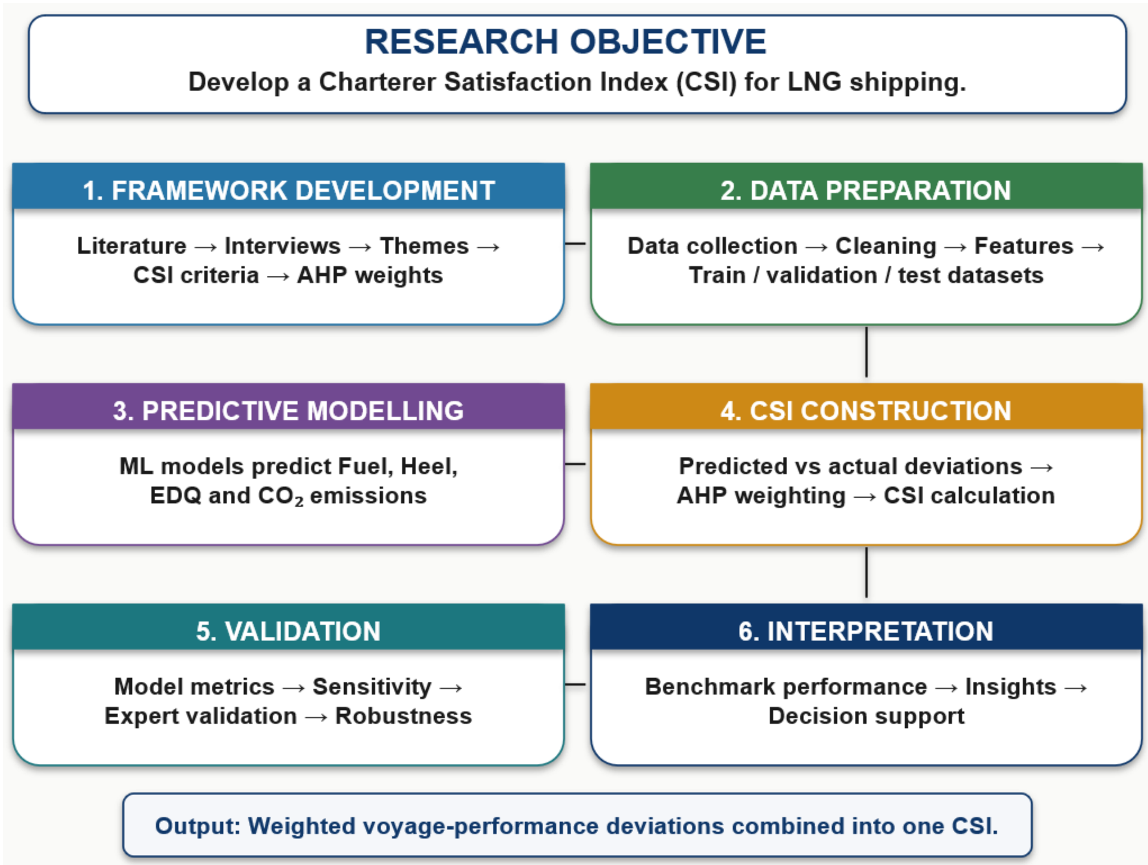

Figure 4.5, Flowchart presentation with the thesis framework

4.4.2 CSI Formulation

This thesis focuses on the LNG market with the aim of improving a shipping company's revenue through commercial operations, presenting a framework designed to enhance client satisfaction and loyalty. This section explains in detail the Charterer Satisfaction Index (CSI), which monitors the charterer satisfaction.

In practice, CSI constitutes the research framework, developed through a structured series of steps. Each stage is clearly explained to facilitate understanding of the model's functionality as follows:

Step 1: Model Definition for CSI Implementation

Evaluation of Charterer satisfaction is defined as the deviation between predicted and actual values of the models' research. Smaller deviations indicate higher satisfaction, enabling optimal decision-making for vessel-cargo matching.

Therefore, the CSI are calculated using models which a percentage deviation formula by comparing predicted values to actual values, as follows:

Fuel in laden Deviation = (|Predicted Fuel - Actual Fuel|) / Actual Fuel

Heel (in ballast) Deviation = (|Predicted Heel - Actual Heel|) / Actual Heel

EDQ Deviation = (|Predicted DQ - Actual DQ|) / Actual DQ

Emission footprint Deviation = (|Predicted Emissions - Actual Emissions|) / Actual Emissions

Model results are expressed as absolute values to show deviations between predicted and actual performance. If fuel consumption or heel quantity is lower than predicted, it reduces the total discharging quantity and affects commercial outcomes, since less LNG cargo can be sold than expected. If they are higher than predicted, it signals inefficiency and excess consumption. In both cases, performance is negatively impacted. The ideal outcome is for predicted and actual values to match, ensuring accuracy, transparency, and reliability in vessel performance reporting.

Step 2: Application of Weights in Model results

CSI accounts for the varying significance of each model by assigning appropriate weights. Therefore, Interviews were conducted to gather relevant feedback from LNG industry experts. A total of 15 professionals provided responses regarding the importance of the model results as described in the section "4.3 Research Methodology". The focus of the interviews was to determine whether deviations in specific vessel performance models, such as fuel consumption, heel quantity, discharging quantity, or emissions footprint, carry equal weight in influencing charterer satisfaction, or whether some of them are considered more critical than others. The experts came from a diverse range of professional backgrounds, including top management, operations and technical managers, vessel operators, and crew members. This diversity ensures a comprehensive perspective on how charterer satisfaction is perceived across different organizational levels and functional roles.

The weight factors were analyzed using the Analytic Hierarchy Process (AHP), a structured decision-making method that is widely recognized for its simplicity, consistency, and ability to handle qualitative data. AHP was selected over other multi-criteria decision-making (MCDM) methods, such as TOPSIS, PROMETHEE, or DEA, due to its suitability for situations where subjective expert judgment is required to prioritize complex factors. AHP is particularly effective in this context because it translates pairwise comparisons into a consistent set of weight factors. Appendix 1 presents the full details of the interview structure, comparison matrices, and the calculation steps used to derive the final weights, while Appendix 2 shows the corresponding results.

Step 3. Final Index form: All vessel performance metrics deviations are multiplied by their respective weights and then summed up to produce the final Charterer Satisfaction Index (CSI):

CSI = {w1 * [(|Predicted Fuel - Actual Fuel|) / Actual Fuel]} + {w2 *[(|Predicted Heel - Actual Heel|) / Actual Heel]} + {w3 * [(|Predicted EDQ – Actual EDQ|) / Actual DQ]} +

{w4 * [(|Predicted Emission - Actual Emission|) / Actual Emission]}

Where,

W1 = this weight is related to the fuel quantity performance metrics

W2 = this weight is related to the heel quantity performance metrics

W3= this weight is related to the discharging quantity performance metrics

W4 = this weight is related to the emission quantity performance metrics

4.4.3 Prediction of Fuel consumption

Prediction of fuel consumption is the key metric for applying then the models of CSI. The methodology is based on established literature and a thorough critical review, ensuring the model's foundation is solidly supported by scholarly research.

Initially, it is necessary to provide insights into LNG cargo in relation to fuel consumption. LNG vessels transport natural gas in liquid form, known as LNG. During voyages and cargo transfer operations, a portion of the cargo is consumed as fuel. Specifically, fuel consumption on LNG vessels primarily relies on boil-off gas (BOG), the evaporated fraction of LNG. This BOG is recovered and used as the main fuel source for both propulsion and onboard power, making it a critical component of the vessel's energy system. Indicative figures show that the full cargo capacity is 98.5%, corresponding to 174,500 m^3. Under laden conditions, and depending on voyage characteristics, a vessel traveling at around 17 knots consumes BOG at an approximate daily rate of 0.085%, equivalent to about 65 m^3 of LNG. Further details on BOG generation onboard are provided in Section 5.2 of this thesis.

Thus, this section is focused on the fuel prediction which is based on the referenced literature used for machine learning model development, which follows technically a structured and methodical pipeline to ensure an accurate and reliable results, as shown in Figure . The pipeline for developing a fuel prediction model starts with data acquisition, detailing data sources, types, frequency, and quality. Next, data pre-processing cleans the dataset by removing inconsistencies, handling missing values, filtering noise, and standardizing formats using Python libraries via Google Collab.

Briefly, some technical aspects of the machine learning model, which will be elaborated in the following sections, relate to the dataset. It is split into training and testing subsets so that the training set is used to build and optimize the model through hyperparameter tuning, while the testing set assesses performance on unseen data. Evaluation is carried out using metrics such as MAE, RMSE, and R^2 to measure predictive accuracy. This pipeline, from data acquisition to evaluation, ensures a robust fuel prediction system. The subsequent sections provide detailed explanations of each step, along with the tools and methodologies applied. Figure 4.6 presents all the above information to provide a clearer understanding of the pipeline process.

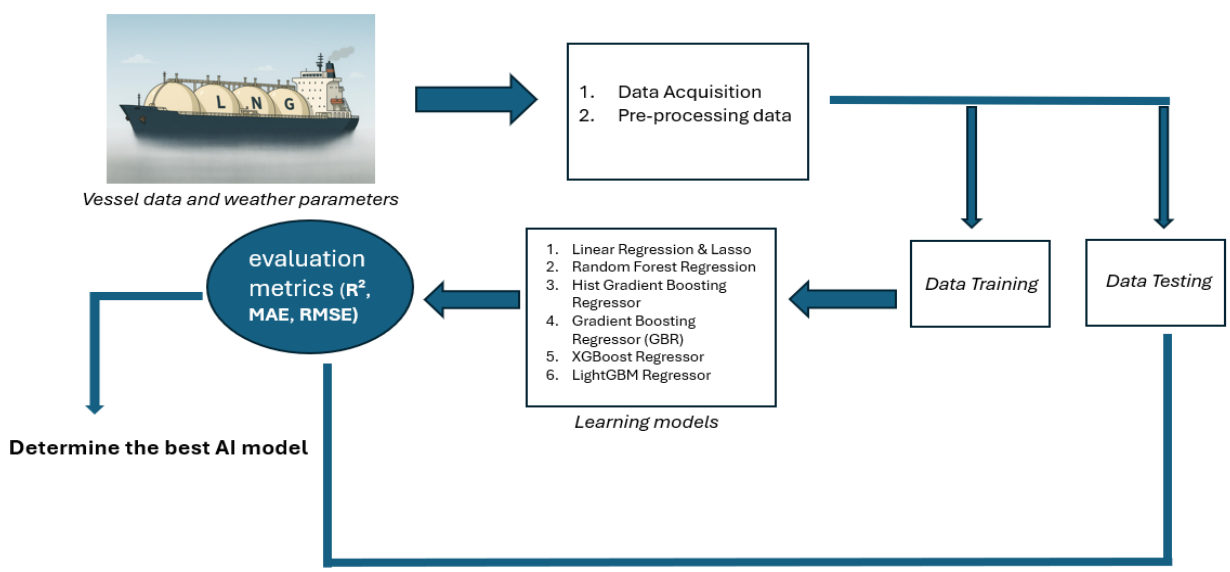

Figure 4.6. Pipeline for fuel consumption model generation.

4.4.3.1 Data Acquisition

Data acquisition is an essential process because it forms the foundation for accurate analysis and model generation. It is closely tied to the quality and characteristics of the dataset, which encompasses the variety of raw signals collected and the frequency of data points recorded.

Therefore, a reliable platform is established as part of the research framework, and data acquisition begins with the collection of information sourced from the Ascenz Marorka platform, an affiliate of GTT, as defined in the section 4.3. The platform gathers data from various LNG vessels through their Integrated Automation Systems (IAS), which consolidate inputs from onboard sensors.

The IAS is a centralized control and monitoring system that integrates various shipboard sensors to enable efficient, safe, and automated vessel operations. It is particularly critical on LNG carriers due to the complexity of their cargo and machinery systems. Specifically, these sensors monitor critical components, such as the engine, bridge, and cargo tanks, collecting essential data that drives operational efficiency and safety. For the engine, sensors track parameters like fuel consumption rates, exhaust gas temperatures, and engine RPM (revolutions per minute), which are vital for optimizing performance and detecting potential mechanical issues. On the bridge, sensors provide navigational data, including the vessel's speed over ground, heading, and rudder angle, ensuring precise course management and collision avoidance. For the cargo tanks, sensors measure variables such as tank pressure, temperature, and liquid levels of LNG, which are crucial for maintaining cargo integrity and preventing hazardous conditions during transport. Together, this detailed data from each category enables real-time monitoring and informed decision-making across the vessel's operations.

To maintain reliability, the sensors are regularly calibrated and maintained, ensuring precise readings is vital for safe and efficient operations. Continuous calibration further enhances the system's precision, always guaranteeing trustworthy data. The Ascenz Marorka platform employs its own methods to evaluate the validity and credibility of the data (it has been further analyzed in section 4.3.

In addition to onboard sensor data, environmental conditions play a significant role in the analysis. These conditions are provided by the Ascenz Marorka platform as well. By analyzing

IAS data and environmental variables, there is a holistic approach and a comprehensive understanding of the vessel's operational dynamics.

For effective analysis, all aforementioned data, both sensor-based and environmental, are collected at frequent intervals to capture detailed vessel behavior. An indicative frequency of every 15 minutes is considered appropriate, aligning with standards observed in similar research from the literature review. To clarify, there are studies that use high-frequency data with deviations of only a few seconds between data points. This approach is typically used when there are significant fluctuations between points. In such cases, collecting data every 15 minutes is sufficient, as the conditions do not change very dynamically. This high-frequency data collection enables a thorough examination of the parameters influencing vessel performance based on similar research in the literature review.

To ensure a balanced, reliable, and relevant analysis, this thesis collects exactly two years of vessel data. This timeframe is sufficient to capture operational trends, seasonal patterns, and maintenance cycles. Using less than two years of data could overlook important seasonal variations and reduce the statistical significance of performance assessments.

4.4.3.2 Exploratory data analysis & data preprocessing

This section focuses on comprehensive dataset handling, covering essential preprocessing stages such as Data Collection, Data Exploration, Data Cleaning, Data Transformation, Data Reduction, and Data Splitting, following the pipeline process outlined by Peace et al. (2024). Each of these steps plays a critical role in ensuring that the data is accurate, consistent, and properly structured to support effective and reliable machine learning model development.

So, this section covers a process which is a matter of handing the rows and features in a proper way. As per diagram Figure 4.7, which shows a dataset structured in N rows (where N is representing individual records, e.g., vessel details) and X columns (X are representing different variables/features).

Handling rows in a dataset represents individual records that often need to be addressed before building a machine learning model. Missing or incomplete rows reduces the quality of training data, so they need to be either filled with estimated values (imputation) or removed if they are not useful. Duplicate rows can create bias in the model, making some patterns appear more significant than they are. Outliers, extreme or unusual values in rows, can distort the model's predictions if not handled properly.

However, handing variables, or features, represent the measurable characteristics in the dataset. Handling missing values in columns is also important, as ignoring them can lead to incomplete learning. Furthermore, not all variables are equally useful—irrelevant, redundant, or highly correlated variables can add noise, slow down training, and reduce accuracy. Feature selection or dimensionality reduction techniques can be used to simplify the dataset while retaining the most important information.

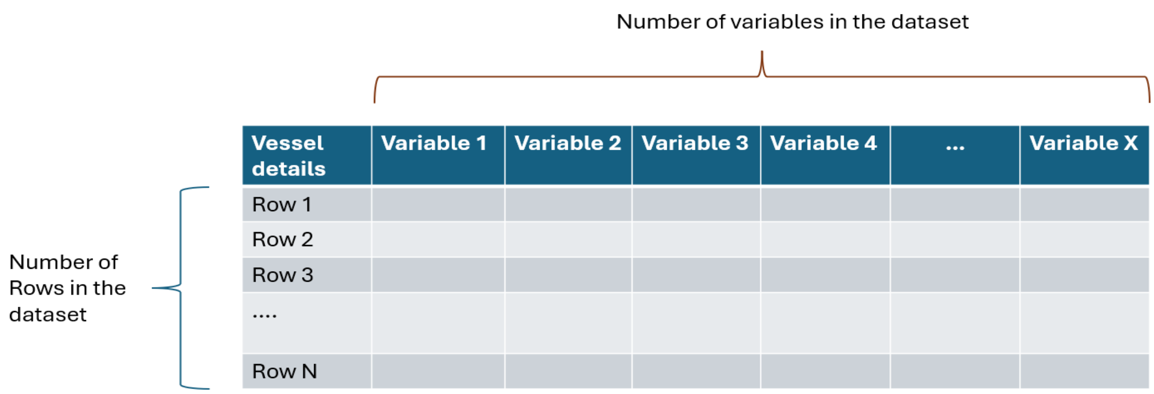

Figure 4.7. Handling N rows and X variables.

First step of the data preprocessing is the data analysis. As described in Section 4.3, the data analyzed originates from an Excel dataset uploaded into a Python-based online application, which is called Google Colab (Google Colaboratory, 2025). The dataset is structured and supervised, collected from various vessel sensors to support model development. Key considerations in handling this data include ensuring high quality, addressing ethical concerns such as privacy and General Data Protection Regulation (GDPR) compliance, particularly as no vessel names or identifiers are referenced, and maintaining data diversity.

Next are the data exploration step and descriptive analysis. Firstly, it is understanding the data types, numeric, categorical, date, and determining their proper management ensuring a systematic and efficient workflow. Also, Exploratory Data Analysis is applied which aims to understand the data by identifying patterns, trends, outliers, relationships, and distributions. Descriptive statistics play a crucial role in validating the reliability and consistency of a dataset. By examining measures such as averages, ranges, and maximum values, one can assess whether the data aligns with expected operational behavior and unit standards. For example, identifying typical consumption rates and peak usage periods helps confirm that the data reflects realistic system performance and is suitable for further analysis.

The next step in the pipeline is data cleaning. When missing data is minimal and non-systematic, simple imputation methods, such as replacing missing values with the median or mean based on skewness report for the dataset can be applied. When the skewness value is close to zero (between -0.5 and +0.5), the data is approximately normally distributed, and the mean can be safely used for imputation. If the skewness is moderate (between -1 and -0.5, or between +0.5 and +1), the data is slightly asymmetric, and in such cases, the median is generally more robust than the mean. For highly skewed distributions (less than -1 or greater than +1), where the data shows a strong long-tail effect, the median is the preferred imputation method.

In some cases, entire fields related to sensor-based measurements may be missing, likely due to data never being recorded. Such fields can be excluded from modeling if they do not provide meaningful information. So, features with more than 60% of missing values are removed. Outlier detection is also crucial to differentiate between true anomalies and valid operational conditions; for example, negative or zero values in certain technical variables may represent specific operational states rather than errors and should be retained. In addition, duplicate detection is performed to identify and remove redundant rows.

Furthermore, when preparing data for machine learning models, consideration of data transformation is necessary, as next steps of pre-processing of dataset. While tree-based algorithms are generally robust to differences in feature scales, linear models, such as those employing regularization techniques, require standardization to ensure that all features contribute equally. In such cases, features are typically transformed to have zero mean and unit variance to prevent scale from biasing the model. Subsequently, Feature engineering is proceeding as a critical step in enhancing model performance by transforming raw data into meaningful inputs that better capture the underlying drivers of the target variable.

In the context of fuel consumption modeling, categorical indicators representing different operational modes (e.g., “At Sea” vs. “In Port”) can help capture contextual variations in system behavior, such as shifts in dominant fuel-consuming components. Therefore, data collected while the vessel is docked, engaged in cargo operations, maneuvering, waiting at anchor, or drifting is excluded, as the model focuses solely on consumption during sailing periods. Thesis retained only the cases where the GPS speed is greater than 5, which is the minimum speed of LNG.

After preprocessing, the next step is data reduction. The goal is to shrink the dataset so the model runs more efficiently. Irrelevant variables, such as cargo tank measurements and cofferdam sensor data, are removed. Highly correlated variables are also checked, and only the most useful ones are kept for model development. This reduction is done using correlation analysis. Also, related features are grouped to guide this process. Typical groups include speed (GPS and log speed), engine data (power, fuel consumption, running hours), and environmental factors (wind, waves, current, swell). In such cases, one representative feature is retained from each group, such as selecting one speed measure, or features are combined meaningfully, for example, by using ratios. For example, if two wave features are available, such as height and frequency, they can be combined to create a new feature representing their ratio in m/s.

Right after preprocessing, the dataset is initially split, with 10% set aside as unseen data to be used later in case studies. The remaining 90% is further divided into 80% for training and 20% for testing, aligning with standard practices. For model evaluation, 10-fold cross-validation is employed as a standard approach, appropriate for the size and structure of the dataset.

Table 4. 3 Exploratory data analysis & data preprocessing flowchart. .

Step	Title	Description
1	Data Analysis	The first step is data collection. As described in Section 4.3, the dataset comes from an Excel file uploaded into Google Colab. It is a structured, supervised dataset collected from vessel sensors, containing 894 features. Key considerations include data quality, privacy and GDPR compliance (no vessel identifiers are used), and ensuring diversity to support robust and fair model development.
2	Data Exploration	The next step is data exploration and descriptive analysis. This involves checking data types (numeric, categorical, date) for proper handling, and applying exploratory analysis to spot patterns, trends, outliers, and distributions. Descriptive statistics, such as averages and ranges,

Step	Title	Description
		validate data reliability and confirm that values, like consumption rates and peak usage, reflect realistic system performance
3	Data Cleaning	The next step is data cleaning. Minimal missing data is handled with simple imputation (e.g., mean or median), while fields with over 60% missing values are removed. Sensor fields with no recorded data are excluded if not meaningful. Outlier detection ensures valid operational states (e.g., zero or negative values) are not mistaken for errors. Duplicate rows are also identified and removed.
4	Data Transformation	Data transformation ensures features are on comparable scales, essential for linear models, by standardizing them to zero mean and unit variance. Feature engineering then creates inputs that better capture drivers of fuel consumption. Operational modes (e.g., 'At Sea' vs. 'In Port') are considered, but only sailing data is used, with cases retained where GPS speed exceeds 5 knots, the LNG minimum.
5	Data Reduction	After preprocessing, data reduction improves efficiency by removing irrelevant variables and filtering correlated ones. Features are grouped (e.g., speed, engine data, environment), with one representative retained or combined, such as creating a wave height-to-frequency ratio in m/s.
6	Data Splitting	After preprocessing, 10% of the data is set aside as unseen for case studies, while the remaining 90% is split into 80% training and 20% testing. Model evaluation uses 10-fold cross-validation, suited to the dataset’s size and structure

4.4.3.3 Learning algorithms

The next step of prediction model is based on literature and critical review, AI models, particularly those under the supervised learning category, have become essential tools for predicting fuel consumption in maritime vessels (Melo, et al., 2024). These models leverage historical data to identify patterns and make accurate predictions, enabling more efficient and environmentally conscious operations with financial benefits.

In this section of the chapter, there is an overview of machine learning models that used for prediction of fuel consumption, explaining their operating principles, advantages, and limitations. Initially, linear regression and Lasso regression are presented, emphasizing simplicity and feature selection, respectively. Then, ensemble methods are analyzed, including Gradient Boosting, AdaBoost, XGBoost, Random Forest Regression, Histogram-Based Gradient Boosting Regressor (HGBR), and LightGBM Regressor, which combine multiple models for improved accuracy and robustness (Table 4.4). Overall, the sources compare these techniques, offering a comprehensive understanding of their applications in predictive modeling.

Thus, Linear Regression is a widely used algorithm due to its simplicity and interpretability. It performs well when there is a linear relationship between input features and the target variable. Its coefficients offer insights into feature importance, making it especially useful in applications that require model transparency. However, it assumes linearity, is sensitive to outliers, and can struggle with multicollinearity among features. It is best suited for situations where interpretability and a linear data structure are priorities. (Shikhman & Müller, 2020).

The formula for a multiple linear regression model is:

$y = \beta 0 + \beta 1 x 1 + \beta 2 x 2 + \cdots + \beta n x n$

Where:

y is the target variable (dependent variable),

$x1, x2, \ldots, xnx\_1, x\_2, \ldots, x\_nx1, x2, \ldots, xn$ are the input features (independent variables),

$\beta 0$ is the intercept.

$\beta 1, \beta 2, \ldots, \beta n$ are the coefficients that represent the relationship between each feature

and the target variable.

Linear regression uses Ordinary Least Squares (OLS) to determine the best-fitting line. OLS minimizes the absolute value of the squared residuals (the differences between the measured and the estimated values). The procedure allows the model to find the line that best describes the relationship between the input features and the target variable. Figure 4.8 shows a graphical representation of the least square line.

$$RSS = \sum(yi - \hat{y}i)^2$$

Where:

RSS *is the residual sum of squares.*

yi are the true values of the target variable.

$\hat{y}i$ are the predicted values.

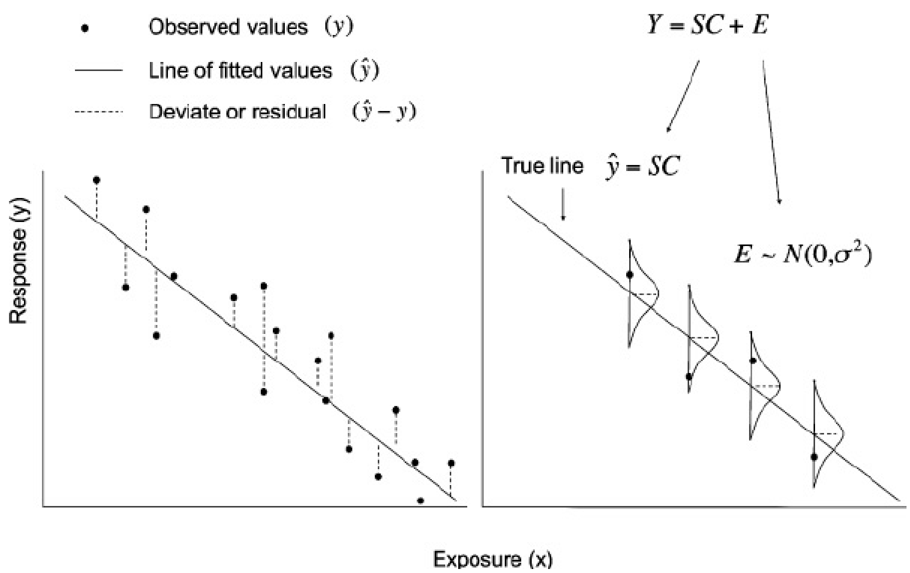

Figure 4.8. Graphical representation of the least squares line fitting in an example of simple linear regression. Source: (Ravani, et al., 2008).

Related to Lasso Regression, it extends linear regression by adding L1 regularization, which reduces the coefficients of less important features, sometimes to zero, effectively performing feature selection. This makes it valuable for datasets with many features, particularly when some may be irrelevant. Its performance, however, depends heavily on the regularization parameter and requires feature scaling to avoid biased results. Lasso is ideal when dimensionality reduction and simpler models are desired (Ranstam & Cook, 2018; Lee, et al., 2018).

The function for lasso regression combines the least squares error with an L1 penalty:

$$Loss = \sum(yi - (\beta 0 + \sum \beta j\, xij))2 + \lambda \sum|\beta j|$$

Where:

The first term represents the ordinary least squares (OLS) loss, as in linear regression.

The second term is the $L1$ penalty term, where λ is a regularization parameter that controls the strength of the penalty.

Lasso regression operates by penalizing the absolute size of the coefficients. When lambda is large, it pushes the coefficients towards zero, and some of them can even be pushed to be exactly equal to zero, and hence they are not included in the model.

Ensemble models combine multiple base learners to improve predictive accuracy and reliability. One of the most well-known is the Gradient Boosting Regressor (GBR), which builds models step by step, correcting errors from earlier ones (Figure 4.9). It works well for capturing complex, non-linear patterns and is especially effective on structured data in table form. However, it is computationally demanding and sensitive to parameter settings (Ganaie, et al., 2021; Crawford, et al., 2019).

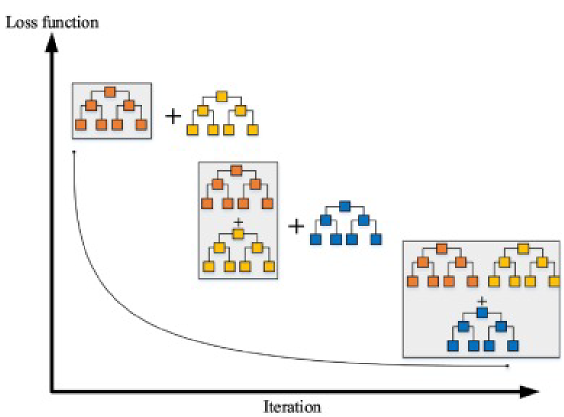

Figure 4.9. Diagrammatic representation of the Gradient Boosting technique. Source: Hoang and Tran (2023).

Also AdaBoost, another ensemble technique, improves model performance by focusing on training examples that were predicted incorrectly. It's especially useful for imbalanced or noisy datasets, where it emphasizes hard-to-predict instances. Nonetheless, its sensitivity to outliers and the risk of overfitting with too many complex models can be drawbacks. AdaBoost is a strong choice for binary classification tasks with challenging class distributions (Simidjievski et al., 2016; Figueiredo et al., 2018; Hao et al., 2020).

Moreover, XGBoost (Figure 4.10) builds upon gradient boosting with added efficiency and scalability. It incorporates L1 and L2 regularization, handles missing values automatically, and allows for parallel training. It's especially suitable for high-dimensional datasets and large-scale applications. Despite its complexity and demand for computational resources, it is widely favored in competitions and production environments for its speed and predictive power (Mitchell & Frank, 2017; Niazkar et al., 2024; Budholiya et al., 2020; Pan et al., 2022; Paleczek et al., 2021).

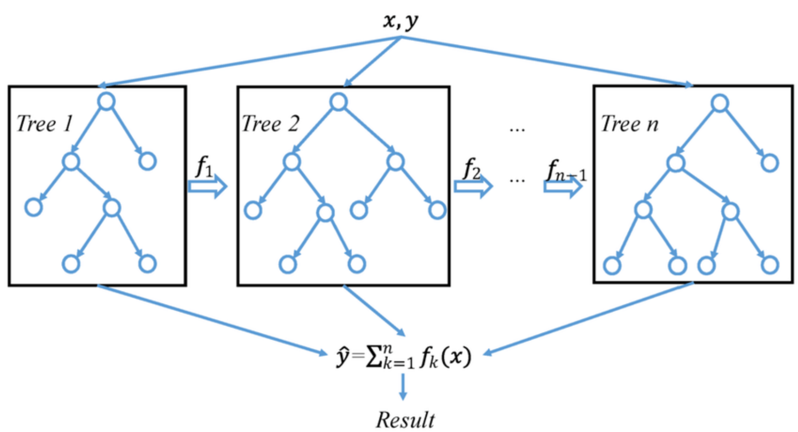

Figure 4.10. A general architecture of XGBoost. Source: Wang et al. (2024).

However, Random Forest Regression (Figure 4.11) constructs an ensemble of decision trees and aggregates their predictions to produce more stable and accurate results. It handles non-linear relationships well, resists overfitting, and provides feature importance scores. However, it can be memory-intensive and less interpretable compared to simpler models. It is best used when model stability and feature analysis are important, particularly with complex datasets (Wang et al., 2021; Jain et al., 2021; Özen, 2024).

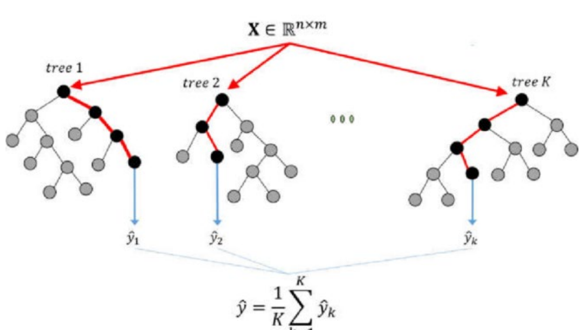

Figure 4.11. Diagrammatic representation of a Random Forest in regression problems. Source: Aldrich (2020).

Also, Histogram-Based Gradient Boosting Regressor (HGBR) is optimized for large datasets. By using histogram binning, it improves training speed and reduces memory usage while maintaining high accuracy. It handles categorical variables and missing data natively and includes regularization to prevent overfitting. Though it may lose some precision due to binning and is less interpretable, it's well-suited for fast, large-scale regression tasks.

Lastly, LightGBM is a highly optimized gradient boosting framework designed for speed and scalability. It uses leaf-wise tree growth and advanced techniques like Gradient-based One-Side Sampling (GOSS) and Exclusive Feature Bundling (EFB), allowing it to train quickly on large, feature-rich datasets. It supports GPU acceleration and offers fine-grained control over hyperparameters. However, it may be overfit on small datasets and is less interpretable. LightGBM is an excellent choice when working with massive, structured data where speed, memory efficiency, and high accuracy are essential.

Table 4. 4 Learning Model review.

Model	Pros	Cons	Best Use Case
Linear Regression	Simple, interpretable, efficient, works well with linear data, easy to understand variable impact.	Assumes linearity, sensitive to outliers and multicollinearity.	When linear relationships and interpretability are important.
Lasso Regression	Performs feature selection via L1 regularization, simplifies model, reduces overfitting.	Requires parameter tuning, sensitive to feature scaling.	When working with many features and needing dimensionality reduction.
Gradient Boosting Regressor	High accuracy, captures complex non-linear patterns, good for structured data.	Computationally intensive, needs careful hyperparameter tuning.	For high-accuracy tasks with complex, structured datasets.

Model	Pros	Cons	Best Use Case
AdaBoost	Focuses on misclassified instances, handles noisy and imbalanced data well.	Sensitive to outliers, can overfit with complex or too many models.	Binary classification with noisy or imbalanced data.
XGBoost	Highly efficient, scalable, regularized, handles missing values, fast with large datasets.	Complex tuning, resource-intensive for large datasets.	Large-scale, high-dimensional tasks requiring performance and accuracy.
Random Forest Regression	Robust, handles non-linear data, provides feature importance, less prone to overfitting.	Less interpretable, slower predictions, high memory usage with many trees.	When needing robust predictions and feature importance insights.
Histogram-Based Gradient Boosting Regressor (HGBR)	Fast training, memory-efficient, handles categorical and missing data, regularized.	Some information loss due to binning, less transparent, tuning required.	Large, mixed-type datasets requiring speed and memory efficiency.
LightGBM	Extremely fast and scalable, uses advanced optimizations, GPU support, high accuracy.	Risk of overfitting on small data, complex to tune, high memory usage with large data.	Large, structured datasets where speed and scalability matter most.

After running the said models, the results are carried out based on the statistical evaluation metrics. The best-performing model is assessed using R^2, Mean Absolute Error (MAE), and Root Mean Square Error (RMSE), with the final selection determined by MAE for its direct interpretation of average prediction error in the testing process. Furthermore, a hyperparameter fine-tuning process was performed to optimize the model, leading to improved results and enhanced overall performance of the best model. Hyperparameter is a standard process which is and external configuration settings of a machine learning model that control how the model learns from data and by adjust the parameters the model can increase the results.

4.4.4 Fuel in laden model

The fuel model includes only the total consumption during the laden passage required by the vessel. Therefore, it uses the results from the section "*Prediction of Fuel Consumption*" for one vessel condition, while the other condition (ballast) is considered in the heel model. To avoid any overlap, the fuel model follows this approach.

4.4.5 Heel Model

Heel management is a critical aspect of LNG carrier operations, ensuring sufficient LNG is retained on board after loading to meet all operational needs during the ballast passage. Accordingly, the thesis framework includes a prediction model for heel quantity, as this is considered a key performance metric in satisfying charterer requirements. Effective heel management requires accurate predicting the necessary amount: excessive heel remaining on board upon arrival at the loading port reduces the capacity for new LNG and may cause financial losses, while insufficient heel prevents the vessel from being properly prepared for the next loading operation and may also compromise propulsion and other daily operational needs.

Vessel preparation requires that all cargo tanks be properly cooled down before receiving new cargo. To facilitate this, charterers often retain a portion of LNG, known as heel, after cargo discharge. The heel is typically stored in one of the vessel's four tanks, which minimizes vaporization by limiting evaporation to a single tank and thereby optimizes cargo handling. However, this approach allows the remaining tanks to warm up. To mitigate this, the residual LNG in the heel tank is used by the crew to maintain low temperatures in the other cargo tanks with stripping pumps and spray nozzles to inject LNG from the heel tank so that the vessel is well prepared for loading the new cargo (Piasecki, et al., 2021).

Once the cargo tanks are emptied, their temperatures naturally rise toward ambient conditions, often exceeding 0°C. Therefore, they must be cooled back down to cryogenic conditions before the vessel can proceed with the next loading operation. A control cooling of cargo tanks helps prevent structural damage to the tanks that could occur due to rapid thermal contraction or expansion of tank materials (Smajla et al., 2019; Voudolon, 2000). This pre-cooling process is essential and is mandated by the IGC Code to ensure that the tanks are thermally ready for handling cryogenic cargo (Piasecki, et al., 2021).

Figure 4.12 illustrates that it takes approximately eight and a half hours for the vessel to lower the cargo tank temperature from about 20°C to below –130°C, the required temperature for the vessel to be ready for cargo loading. Each vessel is equipped with its own cooling tables, which serve as operational guides for carrying out this procedure. These cooldown tables are specific to each type of tank and are provided by the tank manufacturer, particularly those designed for membrane-type tanks (Bejger and Piasecki, 2020). The tables are unique because they depend on various factors, including tank size, construction, the number and size of spray nozzles, and the pressure of the liquefied natural gas supplied. Generally, the tables specify how many cubic meters of LNG, or how much thermal energy, are required to lower the tank temperature by one degree Celsius. On average, tank cool down from the temperature +40°C to a temperature -130°C requires (Piasecki, et al., 2021) approximately 800 m³ (assuming an average LNG density of 450 kg/m³ and a heating value of 55 MJ/kg or about 18,800 MMBtu) of liquefied gas for all tank~~s~~. Specifically, Figure 4. demonstrates the horizontal axis represents temperature in °C and the vertical axis represents the time required. The curve illustrates the time needed for the cargo tank to cool down.

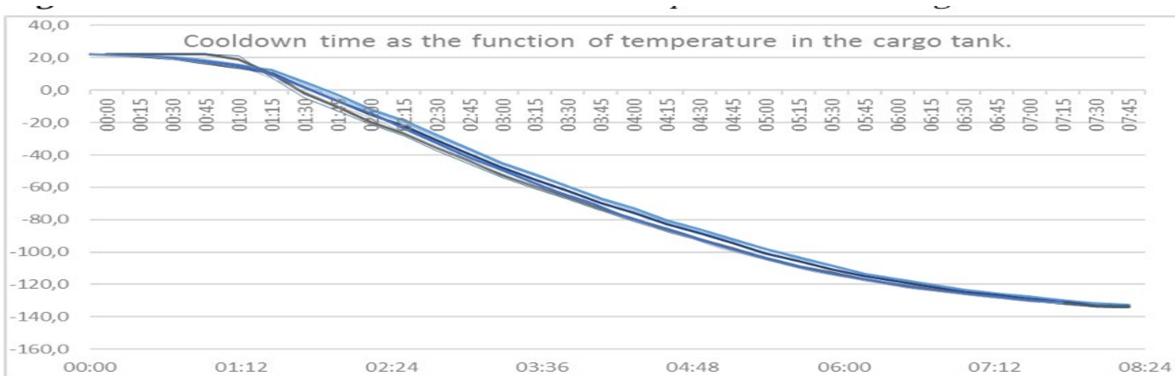

Figure 4.12. Cooling down time as the function of temperature in the cargo tanks. Source: Piasecki et al (2021).

Therefore, heel management includes both the quantity of LNG required for vessel daily operation including propulsion and the amount needed to prepare the vessel before arrival at the loading port, as shown in Figure 4..

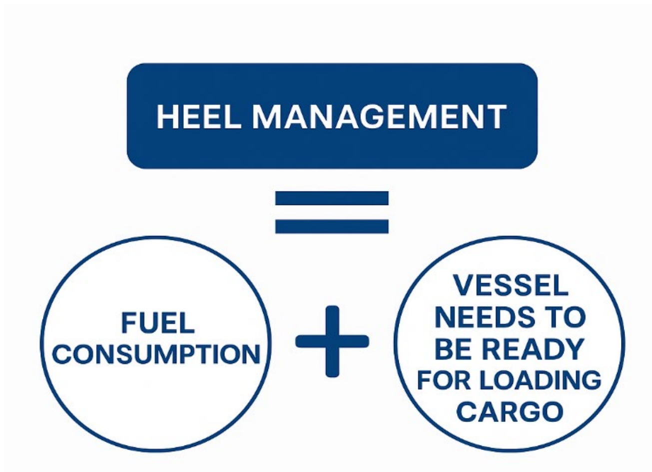

Figure 4.13. Heel Management: LNG quantity as Fuel consumption and vessel preparation for loading cargo.

However, the LNG quantity required for cargo-tank cool-down is excluded from the heel prediction model. The heel model considers only the LNG consumed during the ballast voyage for propulsion. The main reason for this exclusion is that cool-down consumption depends on several voyage-specific and thermodynamic parameters, including the cargo-tank temperature, LNG composition and calorific value, spray-system performance, and the loading terminal's required tank temperature. Accurately modelling this process would therefore require additional thermodynamic information, including LNG composition data obtained from a chromatograph or gas analyser, which was not available in the datasets used in this study.

The exact quantity consumed during the cool-down process is difficult to determine because tank cooling is performed through the spray system, whereby LNG is sprayed into the cargo tanks and partially vaporises as it absorbs heat from the warmer internal surfaces. During spraying, cargo-tank pressure increases as part of the liquid LNG evaporates. The resulting vapour may subsequently be consumed for propulsion or other vessel requirements. Any excess vapour that is not immediately required may remain within the cargo tanks or be processed through the reliquefaction system. Energy consumption associated with reliquefaction is already considered within the model, while the quantity remaining as vapour could potentially be estimated through changes in cargo-tank pressure.

Overall, the excluded cool-down quantity is expected to have a limited effect on the calculated heel quantity and is unlikely to materially influence the overall CSI results. Nevertheless, future research could improve the accuracy of the heel model by separately quantifying LNG used during cargo-tank cool-down through the integration of spray-system operation, tank-temperature and pressure variations, vapour consumption, LNG composition, and reliquefaction data.

4.4.6 Estimated Discharging Quantity model

The last vessel performance model is related to the LNG Cargo Discharging Quantity which is a critical value representing the planned amount of LNG cargo to be discharged at the receiving port. High accuracy of prediction for the discharging quantity of LNG cargo is crucial for charterers as it directly influences their income and fulfillment of commercial commitments regarding the agreed LNG quantity.

The formula for calculating the Estimated Discharging Quantity (EDQ) is based on the loaded quantity minus the total amount of LNG cargo consumed by the vessel's engines during laden and ballast passages, while also accounting for the thermal expansion or shrinkage factor that may affect the volume. EDQ is based on the fuel model, section 4.4.3 which refers to the fuel consumed in the laden and ballast passage.

Related to the thermal factor that affects the LNG cargo volume, when the temperature of LNG increases, its molecules gain energy and move farther apart, causing the liquid to expand and occupy a larger volume. For LNG, which is stored at extremely low temperatures (-162°C), even a small temperature increase can lead to a measurable increase in volume. Conversely, when the temperature decreases, the molecules move closer together, reducing the volume of the liquid. This shrinkage occurs if the LNG is cooled further during storage or transport. For instance, according to Wood [2021], the density of an LNG cargo, which typically ranges between 430 and 470 kg/m^3, depends on its temperature and decreases at a rate of approximately 1.35 kg/m^3 per 1°C. Thus, for a temperature increase of 0.1°C, the corresponding percentage increase in volume for an LNG cargo of 174,500 m^3 is approximately 0.0287% at an initial density of 470 kg/m^3 (equivalent to about 50.1 m^3), and approximately 0.0314% at an initial density of 430 kg/m^3 (equivalent to about 54.8 m^3).

Another parameter affecting EDQ is the Gas Combustion Unit (GCU), a safety system on board used when cargo tank pressure becomes too high. This situation occurs when the amount of boil-off gas (BOG) exceeds the engines' consumption needs. The excess gas is then burned in the GCU to safely relieve pressure inside the tanks.

Based on all the overmentioned and its principles, the formula is as follows.

Estimated Discharging Quantity (EDQ) = LD – CVN - QES – GCU amount

Where:

- Loaded cargo: The total quantity of liquefied natural gas (LNG) loaded at the loading port. Simply, it is considered the quantity with which the vessel begins the passage.

-Cargo for Vessel Needs (CVN): The LNG used for the vessel's operational requirements, including propulsion and generator power in both passages, laden and ballast.

-Quantity Expansion or Shrinkage (QES): The quantity of LNG affected by thermal expansion or shrinkage, accounting for volume changes due to temperature fluctuations. During transportation, LNG typically warms, resulting in volume expansion.

GCU amount: this is related to the GCU amount which the vessel may consume for safety reasons. This amount should be excluded from the EDQ model as cannot be predicted.

4.4.7 Emission footprint model

The emission footprint model is the next key vessel performance metric that charterers need to be informed about prior to voyage execution, and it is therefore included in the thesis framework. This model is important as charterers increasingly require detailed information on a vessel's emissions for each voyage, both for commercial and environmental considerations. In recent years, emissions have become one of the most critical aspects of the shipping industry.

The shipping industry's environmental objectives are increasingly aligned with global efforts to reduce greenhouse gas (GHG) emissions. Under the IMO's revised GHG framework, international shipping is required to progressively reduce emissions towards net-zero by around 2050. The main GHGs considered are carbon dioxide (CO_2), methane (CH_4), including methane slip, and nitrous oxide (N_2O), while other important air pollutants, such as sulfur oxides (SOx) and nitrogen oxides (NOx), are addressed separately under maritime regulations.

In this research, the emission model quantifies only direct CO_2 emissions using an LNG emission factor of 2.75 kg CO_2/kg fuel. This factor represents CO_2 generated during LNG combustion and does not account for methane slip, which refers to unburned methane released through the exhaust. Methane slip can vary depending on engine technology, engine load, operating mode, and machinery condition and can influence the overall environmental performance of LNG-fuelled vessels. Therefore, the emission results of this thesis should be interpreted as Tank-to-Wake CO_2 estimates rather than complete CO_2-equivalent or Well-to-Wake GHG emissions. Future development of the CSI framework could incorporate verified engine-specific CH_4 and N_2O emission factors and express the overall emission footprint in tonnes of CO_2 equivalent (CO_2e).

Reducing emissions assists vessels comply with IMO regulations and meet decarbonization targets for sustainable operations. In shipping, sustainability considers not only the fuel used but also the environmental impact during the fuel production. As per Figure4.14, fuel performance is assessed in three stages: Well-to-Tank (WtT) for production and supply emissions, Tank-to-Wake (TtW) for emissions during operation, and Well-to-Wake (WtW) as the full lifecycle view. LNG is seen as a cleaner alternative to conventional fuels like VLSFO and LSMGO, as it can lower GHG emissions across all these stages.

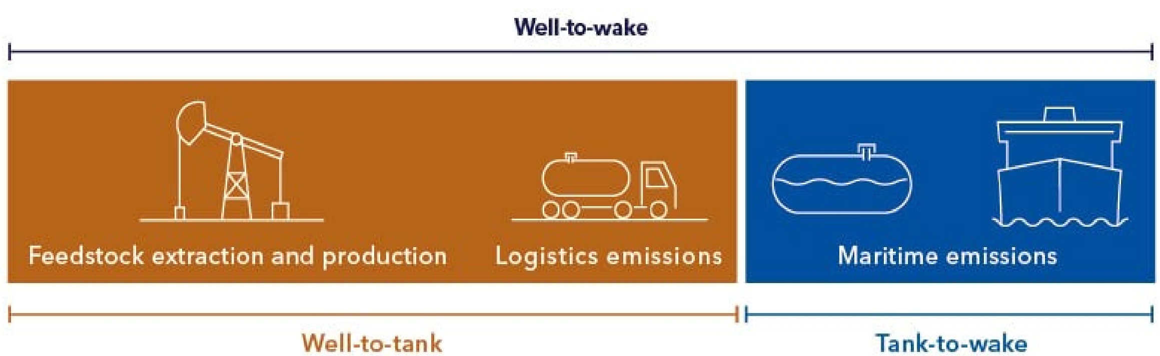

Figure 4.14. Illustration of the Well-to-Wake emission framework, covering production, distribution/transport, and operational emissions. Source DNV [2025].

Considering all the above, this thesis focuses on CO_2 emissions due to their prominence as recognized IMO and it is a key emission metric for the whole LNG market stakeholders, including charterers, shipping companies, and cargo owners. CO_2 is also the primary emission metric used in various emissions indices and regulatory frameworks, such as the Monitoring, Reporting, and Verification/Data Collection System (MRV/DCS) [European Parliament and

Council of the European Union, 2015], Carbon Intensity Indicator (CII) [IMO, 2021], FuelEU Maritime [European Parliament and Council of the European Union, 2023], and the European Union Emissions Trading System (EU ETS) [European Parliament and Council of European Union, 2003]

For an accurate emission calculation of CO2 in LNG vessel operations, it is essential to consider the voyage characteristics, type and quantity of fuel used from the vessel. So, CO_2 formula is as follows:

Fuel Consumption (tonnes) x Emission Factor (tonnes CO2/ tone of fuel)

Where:

- Fuel consumption (tons) refers to the total quantity of LNG used by the vessel's engine or any other type of fuel.
- Emission factor is as per the type of fuel used. In this case, the fuel is LNG which has a standard emission factor of 2.75 tons of CO2 per ton of LNG.

In maritime transport, the emission factor differs depending on the fuel type used by vessel. The primary fuel types in use are Liquefied Natural Gas (LNG), Very Low Sulfur Fuel Oil (VLSFO), and Low Sulfur Marine Gas Oil (LSMGO). These fuels differ significantly in their carbon dioxide (CO_2) emission factors: LNG emits 2.75 kg of CO_2 per kilogram of fuel, while VLSFO and LSMGO emit 3.114 kg and 3.206 kg respectively, as per Table 4.5. These values are crucial for assessing the environmental impact of marine fuels. Therefore, LNG demonstrates environmental advantages over conventional marine fuels as its lower CO_2 emission factor translates to a reduced carbon footprint per unit of energy, making it a more sustainable option.

Table 4. 5 Factors for CO2 measurement per fuel type.

Fuel Type	**Fuel Name**	**Fuel Factor (CO_2)**
LNG	Liquefied Natural Gas	2.750 (kg CO_2/kg Fuel)
VLSFO	Very Low Sulfur Fuel Oil	3.114 (kg CO_2/kg Fuel)
LSMGO	Low Sulfur Marine Gas Oil	3.206 (kg CO_2/kg Fuel)

4.5 Summary

Chapter 4 presents the framework design, featuring AI-based predictive models built on critical vessel performance information, this framework benefits charterers through operational logistics insights and helps shipping companies boost profitability and reputation. It also sets the stage for the next chapter's case studies.

5. Chapter 5 – Case Studies

5.1 Introduction

Chapter 5 applies the research framework described in the previous chapter, using the methodology on three case studies across three LNG vessels under two conditions—laden and ballast—to evaluate the model's effectiveness in diverse operational scenarios using real-world data.

5.2 LNG Operational Context and Utilization Patterns

To ensure a clear understanding of the research framework and the context in which the case studies are applied, this chapter begins with a comprehensive section that outlines the aspects of LNG vessel utilization. Initially, Figure 5.1 shows the front and top of LNG drawing. Also, it is necessary to define the main characteristic of an LNG vessel: it is a type of ship designed to transport energy cargo, specifically, liquefied natural gas (LNG). LNG is a gaseous cargo converted into liquid form by cooling it to approximately -162°C, which reduces its volume by about 600 times, making it much more efficient to transport. (Yin & Ju, 2022). Therefore, LNG cargo must be stored and transported in cryogenic tanks to maintain its liquid state. As LNG is maintained at cryogenic temperatures, the pressure inside LNG cargo tanks must be controlled in accordance with the International Gas Carrier (IGC) Code, which is essential for the safe transport of liquefied gases in bulk (Yin & Ju, 2022; IMO, 2016). Typically, it is maintained in a pressure between 100 to 250 kPa (1 to 2.5 bar) to ensure safe containment. Effective pressure regulation is critical to prevent excessive buildup, which could compromise tank integrity (Yoon et al, 2020). In addition to maintaining optimal pressure, controlling the temperature within the cargo tanks is also crucial to prevent overcooling or overheating, both of which can lead to operational inefficiencies or safety risks.

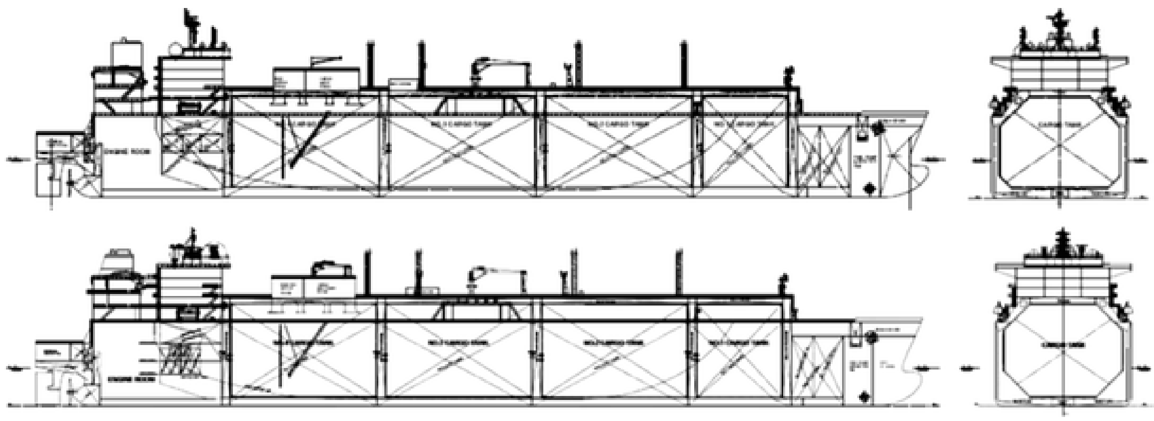

Figure 5.1. LNG vessel – front and top view. Source: Park et el., [2008].

It is important also to first establish the operational vessel conditions definitions. An LNG vessel is considered 'loaded' when it transports cargo from the loading port to the discharging port, a condition referred to as the laden passage. A vessel is typically classified as fully loaded when cargo tank capacity reaches 98.5% which is around 175.400 m³ in a conventional LNG vessel. In contrast, a vessel is considered 'unloaded' when it sails from the discharging port to the loading port with cargo intended for loading. This leg of the voyage is known as the ballast passage.

However, there are restrictions on the volume of cargo that can be transferred in an LNG vessel during both laden and ballast conditions. These limitations are directly related to the safety cargo transportation related to design of the cargo containment system, which, in these case studies, is a membrane-type system with prismatic-shaped tanks. Figure 5.2 shows the prismatic-shaped tank from inner. The allowable cargo quantity on board varies depending on the vessel size and the type of containment system. For a conventional LNG vessel with a maximum loaded capacity of around 175,400 m³, the typical volume restrictions correspond to more than 150,000 m³ when loaded and less than 14,000 m³ when unloaded (heel quantity). A vessel's safe cargo-carrying capability is therefore influenced by limitations related to a phenomenon known as sloshing. Sloshing refers to the movement of LNG within the cargo tanks, which can potentially damage the containment system due to the impact forces generated by the liquid's motion from the vessel's movement. To mitigate this risk, operational restrictions are imposed on the allowable volume of LNG in each cargo tank. Specifically, LNG levels must remain either above 70% or below 10% of the tank height to avoid the harmful effects of sloshing.

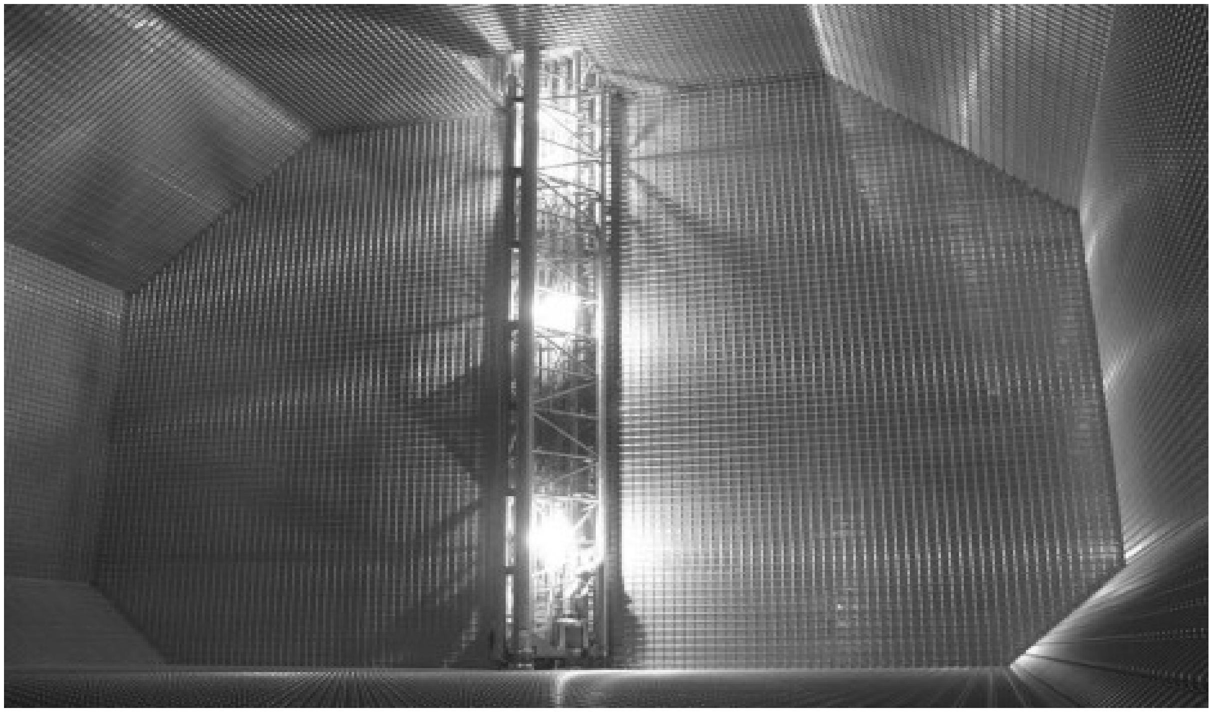

Figure 5.2. Prismatic-shaped tank from inner. Source: Eyres and Bruce [2012].

The next aspect of an LNG vessel relates to cargo evaporation. This is caused mainly by heat ingress from the external environment. Since the cargo is maintained at extremely low temperatures, it tends to revert to its gaseous state. This physical phenomenon is commonly referred to as boil-off gas (BOG). Specifically, external environmental factors such as sea water temperature influence the thermal balance of the LNG containment system. LNG carriers are typically designed with insulation systems and protective barriers to minimize thermal ingress from the external environment (Yoon, et al., 2020; Hoang & Choung, 2021). However, even with such protective systems in place, a portion of heat can still penetrate the insulation, particularly during prolonged exposure to warm sea conditions. (Hoang & Choung, 2021). Its rate depends on the type of LNG containment system installed the vessel tanks used. BOG generation is approximately between 140 m^3 and 180 m^3 per day depends on the type of cargo containment system and size of the vessel. Thus, the vessel is able to take advantage of the cargo's evaporation and use it as fuel for both the main and auxiliary engines. If the vessel requires less fuel than the amount of vapor provided, the excess can be reliquefied in case there is reliquefaction system onboard.

Another significant reason for generation of BOG is due to movements of the vessel, such as rolling (tilting side to side) or pitch (tilting front to back). Adverse weather conditions, such as high waves, strong winds, and rough seas, significantly increase boil-off gas (BOG) generation on LNG carriers. Rough seas cause LNG to slosh in filled tanks, moving the liquid surface and promoting vaporization through heat exchange and mechanical motion. Constant movement also stresses insulation systems, increasing thermal input through tank walls. These dynamic forces combine to elevate BOG rates during rough voyages (Yin & Ju, 2022).

The next aspect is related to LNG vessels specifications. Vessels are primarily categorized based on three key characteristics: size, containment system and also engine types. Each of these factors significantly influences the vessel's efficiency, operational capabilities, and suitability for specific trade routes (Yin & Ju, 2022; Gucma & Gucma, 2019).

The size of an LNG vessel is a crucial factor affecting its cargo-carrying capacity, port compatibility, and economic viability, with capacity typically measured in cubic meters (m^3) (Gucma & Gucma, 2019). Conventional LNG carriers, with a standard capacity of approximately 175,000 m^3 and slight variations from 160,000 m^3 to 180,000 m^3, strike a balance between cargo volume and operational flexibility, enabling access to most LNG terminals worldwide (Gucma & Gucma, 2019). Q-Flex vessels, introduced by QatarEnergy, have a larger capacity of 210,000 m^3 to 217,000 m^3, providing economies of scale for high-volume exports, particularly from Qatar's North Field, though their deeper drafts and size limit port accessibility to specialized terminals (Gucma & Gucma, 2019).Q-Max vessels, the largest in operation, boast a capacity of 260,000 m^3 to 266,000 m^3, designed for carrying nearly 50% more LNG than conventional carriers (around 145.000 m^3 to 175.000 m^3), but their size restricts them to select ports with deep-water terminals and wide navigation channels (Aseel, et al., 2021).

In regard to LNG vessels' containment systems, these systems are engineered to minimize heat ingress, reduce LNG evaporation (boil-off gas or BOG), and maintain structural integrity. The two primary LNG containment systems are: first, membrane systems, which use thin, flexible stainless steel or Invar membranes supported by insulated hull structures to maximize cargo space; and second, Moss spherical systems, which feature robust, self-supporting spherical aluminum tanks that are highly resistant to sloshing but offer lower cargo capacity (Yoon, et al., 2020) (Figure 5.3). Less common designs, like the IHI SPB (Self-supporting Prismatic IMO Type B), offer enhanced stability for specific vessels (Adamczyk, et al., 2020).

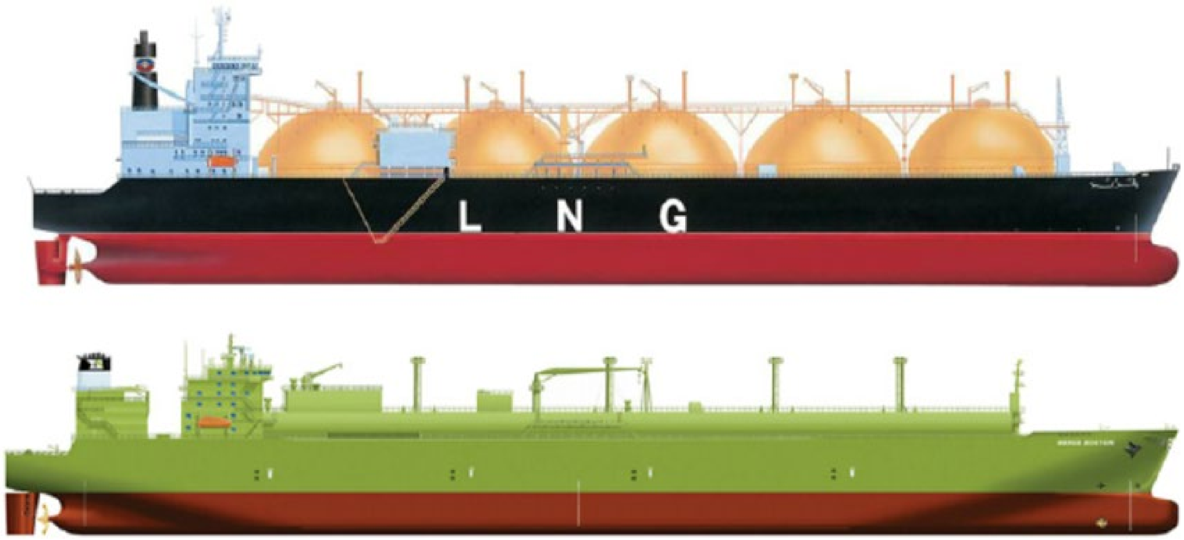

Figure 5.3. Main types of LNG carriers: Moss spherical tankers (top) and membrane tankers (bottom). Source: Vanem et al., 2008 *[Vanem, et al., 2008]*.

Related to the engine type, the main engine is used for propulsion system of an LNG vessel. This plays a pivotal role in determining its fuel efficiency, emissions, and operational costs, with engine type being a key differentiator. Early LNG vessels utilized Steam Turbine Engines, which burn boil-off gas (BOG) to generate steam for propulsion, offering reliability but lower efficiency compared to modern systems (Domić, et al., 2022). Dual-Fuel Diesel Electric (DFDE) engines followed, enhancing efficiency and flexibility by running on LNG or conventional fuels like diesel or heavy fuel oil. Currently, ME-GI (Electronically controlled, M-type engine with high-pressure Gas Injection) engines, high-pressure two-stroke systems, and their evolved version, ME-GA engines(Electronically controlled, M-type engine with low-pressure Gas Admission), which offer improved performance and efficiency, along with XDF (expandable Dual-Fuel) engines, low-pressure dual-fuel systems, dominate modern LNG carriers, delivering superior efficiency and reduced emissions. Engine selection depends on operational requirements, fuel availability, and environmental regulations, such as the IMO's sulfur cap and carbon reduction targets (Xu, et al., 2023).

In addition to the main propulsion system, LNG carriers are equipped with various auxiliary engines and cargo management systems that support the safe and efficient handling of the liquefied natural gas. Auxiliary engines, usually dual-fuel or diesel-powered generators, supply electrical power for all onboard operations, including mainly navigation systems, accommodation services, and cargo-handling equipment. These engines must be capable of adjusting to varying loads, especially during cargo loading and discharging operations when power demand peaks (Martinić-Cezar, et al., 2024).

Moreover, part of the auxiliary components, there is a critical item which is dealing with BOG and also with the temperature and pressure within the cargo tanks. (Yin & Ju, 2022; Wu & Ju, 2021). For efficient cargo management, modern LNG carriers employ a reliquefaction system, which captures the vaporized gas and returns it back into liquid form to the cargo tanks. This method allows for maximum cargo retention and minimal emissions (Yin & Ju, 2022). Moreover, another critical item used on LNG carriers is the Gas Combustion Unit (GCU). The GCU serves as a controlled and safe way to dispose of excess BOG by burning it off in a dedicated combustion chamber. While combustion of BOG does result in some energy loss, the GCU is often used as a backup or during conditions where reliquefaction or engine consumption of BOG is not feasible (Bouman, et al., 2020). Additionally, other critical item under the auxiliary components of an LNG vessels are the compressors, heaters, and vaporizers form an integral part of the cargo management system. Compressors are used to manage pressure within the tanks, while heaters and vaporizers assist in conditioning the LNG for transfer or regasification (Suprapti, et al., 2023).

However, regarding the fuel mode that an LNG can burn. To take advantage of BOG, modern LNG vessels are equipped with dual-fuel engines for propulsion, which means that the engines can consume gas and liquid fuel (Mijailovi, et al., 2024). More specifically, there are three distinct modes, more specifically gas mode, fuel mode, and dual mode, which each influence fuel consumption differently (Martinić-Cezar, et al., 2024). In gas mode, the vessel primarily uses boil-off gas (BOG) from LNG cargo, making it a more fuel-efficient and environmentally friendly option (Romeo, et al., 2020). In fuel mode, the vessel relies on traditional marine fuels, such as diesel or heavy fuel oil, which may be necessary when the boil-off gas supply is insufficient, resulting in higher fuel consumption (Kim & Lee, 2023). Dual mode allows the vessel to switch between LNG and conventional fuels, providing operational flexibility. This mode optimizes fuel consumption by balancing the use of LNG and traditional fuels based on operational needs, fuel availability, and the vessel's condition (Zhang, et al., 2023).

Moreover, based on the author’s database, an analysis of the top five loads per category provides valuable insights into the electrical demand structure of an XDF vessel. The study identifies five key load categories that the generator engines support, supplying power to various onboard equipment for different operational scenarios: continuous loads during sailing, intermittent loads, cargo-related loads during cargo operations, deck machinery loads during port operations, and emergency loads during critical situations. Each category outlines the relevant equipment and its required load capacity, measured in kilowatts (kW). There are two indicative diesel engines, as shown in Table 5.1. Presenting allows the reader to better understand the vessel's requirements across the five categories,

Table 5. 1 Diesel Engines specifications.

	Diesel Engine 1	**Diesel Engine 2**
DG designer	Hyundai Himsen	Hyundai Himsen
DG electrical power at max. Load (kW)	3360	2880
DG rpm at max. load	720	720

The first category, as per Table 5.2, is the continuous load category includes essential equipment that operates constantly during the vessel's voyage and port operations. These systems form the core of the ship's basic functions. The top contributors include the Ballast Pump (558.7 kW) for managing seawater ballast tanks, the Air Lubrication System (ALS) Compressor (548.0 kW) that reduces hull friction, the Main Cooling Seawater Pump (202.1 kW) which supports engine cooling, the Main Air Conditioning Compressor (186.4 kW) serving the accommodation block, and the Engine Room Ventilation Fan (156.5 kW) for thermal regulation. Together, these five represent approximately 78% of the total continuous load.

Table 5. 2 Continuous load analysis providing Power (kW), SFOC No1 (g/kWh) and SFOC No2(g/kWh).

Equipment	**Power (kW)**	**Function**	**SFOC No1 (g/kWh)**	**SFOC No2 (g/kWh)**
Ballast Pump	558.7	Manages seawater ballast tanks	265.5	279.3

ALS Compressor	548	Reduces hull friction	267	280.8
Main Cooling Seawater Pump	202.1	Supports engine cooling	325.9	334.2
Main Air Conditioning Compressor	186.4	Accommodation cooling	329.1	336.9
Engine Room Ventilation Fan	156.5	Thermal regulation	335.2	342.2
Total	1651.7		1522.7	1573.4

Also, another category, the intermittent load group, following Table 5.3, comprises equipment that operates periodically or during specific procedures such as startup, standby, or support. Key systems include the Unit Cooler for the Switchboard Room (121.8 kW) to maintain electrical equipment temperature, the Generator Engine Jacket Preheater (75.0 kW) for efficient cold starts, the Service (74.0 kW) and Main Air Compressors (68.8 kW) for ship wide compressed air supply, and the Galley and Laundry Equipment (57.8 kW) used for crew living support. These top 5 items account for about 87% of the total intermittent load.

Table 5. 3 Intermittent Loads analysis providing Power (kW), SFOC No1 (g/kWh) and SFOC No2(g/kWh).

Equipment	**Power (kW)**	**Function**	**SFOC No1 (g/kWh)**	**SFOC No2 (g/kWh)**
Unit Cooler (Switchboard Room)	121.8	Electrical equipment temperature control	342.5	348.6
Generator Engine Jacket Preheater	75	Efficient cold starts	352.8	357.4

Service Air Compressor	74	Shipwide compressed air	353	357.5
Main Air Compressor	68.8	Compressed air capacity	354.1	358.5
Galley & Laundry Equipment	57.8	Crew living support	356.6	360.7
Total	397.4		1759	1782.7

Subsequently, another category is, Cargo-related electrical loads, based on Table 5.4, are the most energy-intensive, primarily active during LNG loading and unloading operations. The Main Cargo Pump (4,571.4 kW) handles high-capacity discharge of LNG. Supporting it are the High Duty Compressor (1,917.0 kW) and the Low Duty Compressor (708.5 kW), both crucial for LNG reliquefaction and boil-off gas management. The SMR (Single Mixed Refrigerant) Compressor (760.3 kW) manages liquefaction cycles, while the Emergency Cargo Pump (218.3 kW) provides critical backup functionality. Notably, the combined peak of these systems exceeds the total listed cargo load, indicating that these systems operate in non-simultaneous cycles with operational diversity factors applied.

Table 5. 4Cargo-Related Loads analysis providing Power (kW), SFOC No1 (g/kWh) and SFOC No2(g/kWh).

Equipment	**Power (kW)**	**Function**	**SFOC No1 (g/kWh)**	**SFOC No2 (g/kWh)**
Main Cargo Pump	4571.4	High-capacity LNG discharge	68.3	107.5
High Duty Compressor	1917	LNG reliquefaction / boil-off gas mgmt	172.9	176.3
SMR Compressor	760.3	Liquefaction cycle control	239.9	254.4

LD Compressor	708.5	Reliquefaction support	246	260.4
Emergency Cargo Pump	218.3	Critical backup	322.7	331.3
Total	8175.5		1049.8	1130

Moreover, Table 5.5 presents deck machinery loads is another category which pertains to equipment used primarily during mooring and cargo handling at port. The largest consumers are the Aft Mooring Winches (101.3 kW), Forward Winches (60.8 kW), and the Windlass/Mooring Combo Units (40.5 kW) for anchoring and securing the vessel. Auxiliary devices such as the Provision Crane (42.4 kW) and Compressor Room Crane (30.0 kW) support loading operations and machinery maintenance. These systems don't operate simultaneously; hence their combined rated power exceeds the total deck load under typical conditions.

Table 5. 5 Deck Machinery Loads analysis providing Power (kW), SFOC No1(g/kWh) and SFOC No2. (g/kWh)

Equipment	**Power (kW)**	**Function**	**SFOC No1 (g/kWh)**	**SFOC No2 (g/kWh)**
Aft Mooring Winches	101.3	Mooring operations aft	347	352.4
Forward Winches	60.8	Forward mooring operations	355.9	360.1
Windlass/Mooring Combo Units	40.5	Anchoring/ securing vessel	360.6	364
Provision Crane	42.4	Loading provisions	360.1	363.6
Compressor Room Crane	30	Maintenance support	363	366.1
Total	275		1786.6	1806.2

The last category is Emergency loads, as per Table 5.6, represent critical systems that must remain operational during a blackout or fire. The Emergency Fire Pump (150.3 kW) is the highest consumer, essential for fire suppression. The Auxiliary Boiler Unit (44.0 kW) and Boiler Feed Water Pump (26.1 kW) sustain steam operations, while the Generator Preheater (25.0 kW) ensures quick engine start-up in emergencies. The Emergency Lighting System (33.3 kW) maintains visibility and safety across the vessel. These top systems account for roughly 74% of the total emergency load.

Table 5. 6 Emergency Loads analysis providing Power (kW), SFOC No1(g/kWh) and SFOC No2(g/kWh).

Equipment	**Power (kW)**	**Function**	**SFOC No1 (g/kWh)**	**SFOC No2 (g/kWh)**
Emergency Fire Pump	150.3	Fire suppression	336.5	343.4
Emergency Lighting System	33.3	Visibility and safety	362.2	365.4
Auxiliary Boiler Unit	44	Maintains steam supply	359.8	363.3
Boiler Feed Water Pump	26.1	Steam system support	363.9	366.8
Generator Preheater	25	Quick engine start-up	364.1	367
Total	278.7		1786.5	1806

Table 5. 7 The indicative quantities that an LNG vessel consumes in gas or liquid fuel (in laden condition per speed).

presents the quantities used for LNG vessels, including both gas and liquid fuel, providing an overview of vessel’s consumption in a specific sailing speed. It is intended to illustrate the indicative amounts consumed in LNG fuel or VLSFO based on the vessel’s operational instructions from charterer. The decision on which type of fuel to use depends on several factors: optimization of boil-off gas, fuel prices (for example, natural gas and VLSFO, Very Low Sulfur Fuel Oil, a commonly used liquid fuel) the quantity the charterers intend to transfer, and compliance with environmentally friendly practices.

Table 5. 7 The indicative quantities that an LNG vessel consumes in gas or liquid fuel (in laden condition per speed).

Vessel Speed	**LNG Quantity (m^3/day)**	**VLSFO (mt/day) (Very Low Sulphur Fuel Oil)**
12 knots	80	40
15 kntos	110	55
19 knots	190	95

Lastly, it is necessary to be highlighted that the gas fuel consumption of an LNG vessel is significantly influenced by the composition of the LNG cargo being transported (Martinić-Cezar, et al., 2024). LNG is a mixture of hydrocarbons, primarily methane (CH_4), but it may also contain varying levels mainly of ethane (C_2H_6), propane (C_3H_8), butane (C_4H_{10}), and nitrogen (N_2) (Cronshaw, 2021). The specific composition affects the energy content (calorific value), boil-off rate, and combustion characteristics, all which impact fuel efficiency and operational performance. One of the primary factors affecting LNG fuel consumption is the methane content in the cargo. Higher methane content results in higher energy efficiency, as methane has a higher combustion efficiency compared to heavier hydrocarbons (Pavlenko, et al., 2020). In contrast, LNG with higher levels of ethane or propane has a higher calorific value per unit mass, which may alter the vessel's fuel efficiency. Additionally, the nitrogen content in LNG plays a crucial role, as high nitrogen concentrations reduce the energy content, leading to higher fuel consumption to achieve the same propulsion power. Another significant impact of cargo composition on fuel consumption is related to boil-off gas (BOG) production (Yoon, et al., 2020). Different LNG compositions have varying evaporation rates due to differences in vapor pressure and molecular weight. LNG with higher nitrogen or lighter hydrocarbon fractions tends to evaporate more rapidly, increasing BOG generation and influencing the vessel's fuel management strategy (Yoon, et al., 2020; Yao, et al., 2022).

Table 5.8 presents the molar masses, chemical formulas related to LNG, and names of common hydrocarbons. It includes light alkanes such as methane, ethane, and propane, as well as their isomers like iso-butane and n-butane. In addition, it lists nitrogen which is also an important component of the LNG cargo.

This information is especially useful in the context of LNG trading, as charterers are paid based on the MMBtu (Million British Thermal Units), a unit representing the heating value of the cargo. British Thermal Unit is the amount of heat required to raise the temperature of one pound of water by one-degree Fahrenheit. Thus, the chemical composition determines whether the LNG cargo is rich in energy, directly impacting its commercial value. Furthermore, since LNG vessels consume a portion of their own cargo as fuel during transport, knowing the energy content is important, a cargo with a higher heating value allows for more efficient fuel consumption and potentially reduces the amount of LNG used for propulsion.

Table 5. 8 Molar mass per LNG chemical composition.

Molar Mass	**Chemical Composition**	**Molecule Name**
16,04	CH4	Methane
30,06	C2H6	Ethane
44,09	C3H8	Propane
58,12	i-C4H10	Iso-Butane
58,12	n-C4H10	N-Butane
72,14	i-C5H12	Iso-Pentane
72,14	n-C5H12	N-Pentane
86,17	n-C6H14	N-Hexane
28,01	N2	Nitrogen
31,99	O2	Oxygen
44,0095	CO2	Carbon Dioxide

Lastly, it is important to define that Liquefied Natural Gas (LNG) is primarily composed of methane (CH_4), which typically accounts for 85–95% of the volume and has a boiling point of –161.5°C (Table 5.9). The remaining components include small percentages of heavier hydrocarbons such as ethane (C_2H_6, boiling point –88.6°C), propane (C_3H_8, –42.1°C), and butanes (C_4H_{10}, –0.5°C to –11.7°C), along with trace amounts of pentanes and heavier hydrocarbons, which have boiling points above 36°C. Additionally, nitrogen (N_2) may be present in concentrations of 0.5–1.5%, with a much lower boiling point of –195.8°C. The composition of LNG significantly influences its physical and thermal properties, including energy content, density, and vaporization behavior. Since the cargo tanks on LNG vessels are maintained at approximately –161°C, it is primarily methane and nitrogen that evaporate. This evaporated gas, known as boil-off gas (BOG), is then consumed by the ship's engines as fuel, making it a critical factor in both vessel operation and energy efficiency.

Table 5. 9 Component volume (%) and boiling point of LNG components. Source: SIGTTO (2024).

Component	Chemical Formula	Range of Volume %	Boiling Point (°C)
Methane	CH_4	85–95%	–161.5
Ethane	C_2H_6	2–6%	–88.6
Propane	C_3H_8	0.1–2%	–42.1
Butanes	C_4H_{10}	<0.5%	– 0.5 to 11.7
Pentanes+	C_5^+	-	>36
Nitrogen	N_2	0.5–1.5%	–195.8

5.3 Strategic Business Factors Influencing Charterer Satisfaction

This section demonstrates how the models of the CSI align with the practical needs of charterers. These models incorporate both commercial and financial characteristics, balancing cost and revenue considerations with the operational commitments that charterers undertake when arranging LNG cargo transportation through a hired vessel. By doing so, the CSI framework not only supports accurate performance forecasting but also enables charterers to optimize profitability.

Since CSI incorporates models that account for fuel consumption during laden passages, heel amount, estimated LNG discharging quantity, and the vessel's emissions footprint, charterers can leverage these predicted values to support more efficient decision-making for requirements of cargo transportation. As each voyage, charterers must evaluate vessel options carefully to identify the most suitable one, thereby maximizing operational efficiency and profitability.

Therefore, an indicative example is provided below to illustrate how these CSI models interact in the charterer's decision-making process to maximize net income (profit) in a practical and realistic manner. Specifically, vessel specifications, relative fuel consumption, LNG prices, and fixed freight rates are presented as indicative values in the following example, enabling the reader to clearly understand how the models included in the CSI can be applied by charterers

Initially, the example considers two vessels, Vessel 1 and Vessel 2, with different capabilities, operating under two voyage scenarios: a long voyage (Scenario A) with 90 days and a short voyage (Scenario B) with 40 days. Vessel 1 is more modern than Vessel 2 and is equipped with advanced technology, resulting in a higher daily freight cost of \$120,000. In contrast, Vessel 2, being older, has a lower daily freight cost of \$80,000. For this example, the assumptions regarding vessel consumption include an LNG price of \$500 per m^3. Also, the revenue is calculated based on the loaded cargo quantity and for both vessels the cargo capacity is 174,000 m^3.

In Scenario A, the net incomes of Vessel 1 and Vessel 2 are analyzed over a 90-day LNG voyage. Based on the voyage requirements, Vessel 1 consumes 140 m^3 per day (BOG per day) while Vessel 2 consumes 185 m^3 per day (BOG per day). While, in Scenario B, the net incomes of Vessel 1 and Vessel 2 are analyzed over a 40-day LNG voyage. Based on the voyage requirements, Vessel 1 consumes 100 m^3 per day while Vessel 2 consumes 130 m^3 per day.

5.3.1 Scenario A

In Scenario A, which involves a long voyage lasting 90 days, the charterers' profit for Vessels 1 and 2 is determined by the revenue from the loaded quantity delivered, minus the associated costs. These costs include the freight cost, based on the vessel's daily rate, and the fuel cost required for the voyage. The key figures for each vessel are summarized as follows:

i. **Vessel 1**

Step 1: Calculating the Fuel cost which is assumed that the fuel consumption is 140 m^3 per day, resulting in a total fuel usage of 12,600 m^3 over the 90-day voyage. At $500 per ton, the total fuel cost is $6,300,000. Specifically, the fuel cost is determined using the following calculation:

- 140 m^3 * 90 days = 12,600 m^3 total consumption.
- 12,600 m^3 * $500/ton = $6,300,000 fuel cost

Step 2: Calculating the Freight cost which is based on a daily freight rate of $120,000 over 90 days, totals $10,800,000. Specifically, the freight cost is determined using the following calculation:

- $120,000 m^3 * 90 days = $10,800,000 freight cost

Step 3: Calculating Revenue amount which is the net cargo delivered is calculated by subtracting the fuel used from the total cargo, which results in 161,400 m^3. At the given LNG price ($500), this yields a total revenue of $80,700,000. Specifically, the Revenue amount is determined using the following calculation:

- 174,000 m^3 – 12,600 m^3 = 161,400 m^3 is the total volume discharged
- 161,400 m^3 * $500/ ton = $80,700,000 is the revenue amount

Step 4: Calculating the charterer's profit: Vessel A's profit is $63,600,000, calculated by subtracting both the freight and fuel costs from the revenue. Specifically, the charterers profit is determined using the following calculation:

- $80,700,000 – $10,800,000 – $6,300,000= $63,600,000 is charterers' profit

ii. **Vessel 2**

Similarly, the same steps are applied with same 90-day voyage for Vessel 2, as follows;

Step 1: Calculating the Fuel cost of Vessel B having a higher daily fuel consumption of 185 m^3, resulting in a total fuel usage of 16,650 m^3 over the 90-day voyage. At $500 per m^3, the fuel cost amounts to $8,325,000. Specifically, the fuel cost is determined using the following calculation:

- 185 m^3 * 90 days = 16,650 m^3 total consumption.
- 16,6500 m^3 * $500/ton = $8,325,000 fuel cost

Step 2: Calculating the Freight cost which is based on a daily freight rate of $80,000, totaling $7,200,000 over the 90 days. Specifically, the freight is determined using the following calculation:

- $80,000 m³ * 90 days = $7,200,000 freight cost

Step 3: Calculating Revenue amount which is calculated by subtracting the fuel consumed from the total cargo capacity: 157,350 m³. At the LNG price of $500 per ton, the total revenue for Vessel B is $78,675,000. Specifically, the Revenue amount is determined using the following calculation:

- 174,000 m³ – 16,650 m³ = 157,350 m³ is the total volume discharged
- 157,350 m³ * $500/ ton = $78,675,000 is the revenue amount

Step 4: Calculating the charterers profit: it is $63,350,000, calculated as revenue minus freight and fuel costs. Specifically, the charterers profit is determined using the following calculation:

- $78,875,000 – $7,200,000 – $8,325,000= $63,350,000 is charterers' profit

As presented in Table 5.10, Vessel 2 benefits from a lower freight rate; however, its higher fuel consumption slightly reduces overall profitability, making it lower than that of Vessel 1.

Table 5. 10 Vessel's Costs, Income and Profit (Scenario A).

Long Voyage (90 Days)	**Vessel 1**	**Vessel 2**
Revenue amount	$80.700.000,00	$78.8750.000,00
Freight cost	$10.800.000,00	$7.200.000,00
Fuel Cost	$6.300.000,00	$8.325.000,00
Profit	$63.600.000,00	$63.350.000,00

5.3.2 Scenario B

In contrast, in Scenario B the voyage lasts 40 days and the charterers' profit for Vessels 1 and 2 are summarized as follows:

iii. Vessel 1

Step 1 Calculating the Fuel cost for Vessel 1: the fuel consumption is 100 m^3 per day, resulting in a total fuel usage of 4,000 m^3 over the 40-day voyage. At $500 per ton, the total fuel cost amounts to $2,000,000. Specifically, the fuel cost is determined using the following calculation:

- 100 m^3 * 40 days = 4,000 m^3 total consumption.
- 4,000 m^3 * $500/ton = $2,000,000 fuel cost

Step 2: Calculating the Freight cost: it is based on a daily rate of $120,000 over 40 days, totals $4,800,000. Specifically, the freight is determined using the following calculation:

- $120,000 m^3 * 40 days = $4,800,000 is the freight cost

Step 3: Calculating Revenue amount: the cargo delivered is calculated by subtracting the fuel used from the total cargo, which results in 170,000 m^3. At the given LNG price, this yields a total revenue of $85,000,000. Specifically, the Revenue amount is determined using the following calculation:

- 174,000 m^3 – 4,000 m^3 = 170,000 m^3 is the total volume discharged
- 170,000 m^3 * $500/ ton = $85,000,000 is the revenue amount

Step 4: Calculating the charterer's profit: the income for Vessel 1 is $78,200,000, calculated by subtracting both the freight and fuel costs from the revenue. Specifically, the charterers profit is determined using the following calculation:

- $85,000,000 – $4,800,000 – $2,000,000= $78,200,000 is charterers' profit

iv. Vessel 2

Similarly, the same steps are applied with same 40-day voyage for Vessel 2, as follows;

Step 1: Calculating the Fuel cost: Vessel 2 has a higher daily fuel consumption of 130 m^3, resulting in a total fuel usage of 5,200 m^3 over the 40-day voyage. At $500 per m^3, the fuel cost amounts to $2,600,000. Specifically, the fuel cost is determined using the following calculation:

- 130 m^3 * 40 days = 5,200 m^3 total consumption
- 5,200 m^3 * $500/ton = $2,600,000 fuel cost

Step 2: Calculating the Freight cost, which is based on a lower daily rate of \$80,000, totaling \$3,200,000 over the 40 days. Specifically, the freight cost is determined using the following calculation:

- \$80,000 m^3 * 40 days = \$3,200,000 is the freight cost

Step 3: Calculating Revenue amount which is based on the delivered cargo is calculated by subtracting the fuel consumed from the total cargo capacity:168,800 m^3. At the LNG price of \$500 per ton, the total revenue for Vessel B is \$84,400,000.

Specifically, the Revenue amount is determined using the following calculation:

- 174,000 m^3 – 5,200 m^3 = 168,800 m^3 is the total volume discharged
- 168,000 m^3 * \$500/ ton = \$84,400,000 is the revenue amount

Step 4: Calculating the charterer's profit: their income for Vessel 2 is \$78,200,000, calculated as revenue minus freight and fuel costs. Specifically, the charterers profit is determined using the following calculation:

- \$84,400,000 – \$3,200,000 – \$2,600,000= \$78,200,000 is charterers' profit

Thus, Table 5.11 shows the calculations and allows for an easy comparison. It demonstrates that Vessel 2 has a higher margin than Vessel 1. Even though Vessel 1 has higher fuel consumption than Vessel 2, the freight rate for Vessel 2 is lower, which results in a better margin for shorter voyages. Therefore, Vessel 2, with its low freight rate and higher fuel consumption, is more suitable for shorter voyages.

Table 5. 11 Vessel's Costs, Income and Profit (Scenario B).

Short Voyage (40 Days)	**Vessel 1**	**Vessel 2**
Revenue amount	\$85.000.000,00	\$84.400.000,00
Freight cost	\$4.800.000,00	\$3.200.000,00
Fuel Cost	\$2.000.000,00	\$2.600.000,00
Profit	\$78.200.000,00	\$79.650.000,00

Based on those two scenarios, it shows that by providing accurate information of the vessel how it is consumed and discharging quantity then the charterers can decide even more efficiently what vessels should be selected for each voyage (as the scenarios this may differ shorter or longer). So, this proves the importance of the models of CSI.

5.4 Thesis Framework implementation

This part of the chapter outlines all the steps involved in implementing the thesis framework, CSI. Initially, it provides the prediction details of fuel consumption based on both pre- and post-machine learning processes, following the research methodology described in Chapter 4. Subsequently, the CSI can be calculated and analyzed separately with respect to fuel, heel, estimated discharging quantities, and emission footprint models. Finally, the results and performance evaluations are presented at the end of the chapter.

5.4.1 CSI implementation

The CSI formula implementation is outlined below. Charterer satisfaction is measured by the deviation between predicted and actual model values; smaller deviations indicate higher satisfaction and support optimal vessel cargo matching.

Therefore, the CSI are calculated using models which a percentage deviation formula by comparing predicted values to actual values, as follows:

CSI = {w1 * [(|Predicted Fuel - Actual Fuel|) / Actual Fuel]} + {w2 *[(|Predicted Heel - Actual Heel|) / Actual Heel]} + {w3 * [(|Predicted EDQ – Actual EDQ|) / Actual DQ]} +

{w4 * [(|Predicted Emission - Actual Emission|) / Actual Emission]}

Where,

W1 = this weight is related to the fuel quantity performance metrics

W2 = this weight is related to the heel quantity performance metrics

W3= this weight is related to the discharging quantity performance metrics

W4 = this weight is related to the emission quantity performance metrics

5.4.2 Case Study Description and Scenario Setup

The case studies have been conducted on three XDF LNG vessels, each operating on different routes based on real-life condition. These vessels are of conventional size, with a full load capacity of 174,500 m³ (reaching the 98.5% of the full capacity of the cargo tanks), and are equipped with a Mark III cargo containment system.

Also, it is necessary to be defined that the case studies focus solely on predicting fuel amount only and does not take into account any voyage optimization concerning the route, speed adjustments, or weather impact mitigation. A short description of the three XDF LNG vessels, based on their specifications, is presented as follows:

Vessel 1: The LNG carrier was built in 2022 and registered under the flag of Malta (port of registry: MTMLA), has a design deadweight of 93,535 t and a gross tonnage of 116,542 t, with a cargo capacity of 170,510 t. The vessel measures 299 m LOA, 291 m LPP, and 46.4 m breadth, and is powered by two Wartsila 2-stroke main engines rated at 12,112 kW each (77 rpm), supported by four auxiliary diesel generators (DG1 & DG4: 3840 kW, DG2 & DG3: 2880 kW). Propulsion is provided by two fixed-pitch propellers with 8.5 m diameter, a mean pitch of 8.9981 m, and a maximum torque of 3004. The cargo system features a Mark III membrane containment with four tanks, each insulated (0.1 m primary, 0.3 m secondary) and fitted with two pumps (1750 m³/h). The natural boil-off rate is 17 m³/day for Tank 1 and 22.6 m³/day for Tanks 2–4, with cooling-down capacities ranging from 43–76 m³ (<2 days) up to 59–100 m³ (<20 days) depending on the tank. The vessel operates at speeds of 10 knots in congested water, 14 knots economic, 16 knots high, and 18 knots full speed, with a defined consumption polynomial.

Vessel 2: The LNG carrier was built in 2021 and flagged under France (port of registry: FRFOS), has a design deadweight of 88,721 t and a gross tonnage of 115,000 t. It measures 293 m LOA, 286 m LPP, and 45.8 m breadth, and is powered by two Wartsila 2-stroke main engines rated at 11,350 kW each (74 rpm), supported by four Wartsila auxiliary generators of 2880 kW each. Propulsion is delivered through two fixed-pitch propellers with a maximum torque of 2930 and a mean pitch of 8.3702 m. The cargo system is based on a Mark III membrane containment with four tanks, each insulated (0.1 m primary, 0.3 m secondary) and fitted with two pumps (1750 m³/h). Each tank records a natural boil-off rate of 30 m³/day and a cooling-down capacity of 60 m³ across all timeframes (2–20 days). Operational speeds include 10 knots at a low speed in congested water, 14 knots economic, 16 knots high, and 18 knots full speed, while the vessel's fuel consumption follows a defined polynomial curve.

Vessel 3: The LNG carrier was built in 2021 and registered in Valletta, Malta (MLVAL), has a design deadweight of 93,098 t and a gross tonnage of 116,284 t, with a design speed of 18.5 knots and a design draft of 12.5 m. The vessel measures 297 m LOA and 46.4 m breadth and is equipped with two Wartsila 2-stroke main engines delivering a combined 24,224 kW at 77 rpm, supported by four Himsen auxiliary generators (DG1 & DG4: 3880 kW, DG2 & DG3: 2960 kW). Propulsion is via two fixed-pitch propellers with three blades each and a mean pitch of 7.6961 m. The cargo containment system is Mark III membrane type, with four tanks featuring 0.1 m primary and 0.3 m secondary insulation, fitted with two pumps per tank (1850 m^3/h capacity). Natural boil-off rates and cooling-down capacities are not specified. The vessel operates at 10 knots (low speed in congested waters), 14 knots (economic), 16 knots (high), and 18 knots (full speed), with a consumption polynomial defined by coefficients.

Descriptive statistics play a crucial role in data exploration by validating the reliability and consistency of a dataset. The following details are presented for three vessels to help the reader understand the case studies more thoroughly and efficiently.

i. Vessel 1

More specifically, vessels statistics have been retrieved from the Ascenz Marorka platform for all vessels (Figure 5.4). Over a span of 732 days, Vessel 1 covered approximately 215,419 nautical miles by GPS, with around 213,397 nautical miles logged at speeds exceeding 5 knots. The vessel maintained an average GPS speed of 14.82 knots and an average log speed of 14.66 knots. Fuel consumption was substantial, with the main engine consuming 25,485.54 metric tons and auxiliary systems consuming 10,607.46 metric tons. Notably, there was no recorded fuel use for the boilers. The vessel's mean draft was 9.91 meters, with a slight negative trim of -0.63 meters, indicating a slightly stern-heavy posture. Environmental conditions encountered included a maximum wave height of 6.22 meters and peak wind speeds of 60.23 knots, with an average current of 0.63 knots.

Distance by GPS	215419.4 nm
Distance by GPS (above 5 kn)	213397.35 nm
Distance by log	211764.31 nm
Duration	732d 0h 0m
Duration (above 5 kn)	600d 4h 0m
ME fuel consumption	25485.54 MT
Aux fuel consumption	10607.46 MT
Boiler fuel consumption	0 MT
Avg. GPS Speed*	14.82 knots
Avg. Log Speed*	14.66 knots
Mean Draft*	9.91 m
Trim*	-0.63 m
Max wave height	6.22 m
Max wind	60.23 knots
Avg. Current	0.63 knots

Figure 5.4. Descriptive statistics for Vessel 1 data. Source: Ascenz Marorka platform, data available as of 06 June 2025.

Next, the dataset is described based on the voyage routes (Figure 5.5). The voyage trading of vessel 1 routes shown on the map primarily connect major global regions by sea. Routes are in East Asia, especially Japan, and pass through Southeast Asia, the Indian subcontinent, and the Middle East, continuing across the Indian Ocean. From there, routes either move northward through the Red Sea into the Mediterranean and Europe, or proceed southward around the Cape of Good Hope, following the coastlines of East and Southern Africa. These paths extend westward across the Atlantic Ocean, linking with West and Central Africa and reaching the Caribbean, particularly Cuba. Additional routes stretch down the east coast of South America and loop back toward Cuba, forming a wide-reaching maritime network that ties together ports across Asia, Africa, Europe, and the Americas.

Figure 5.5. Vessel 1 voyage trade routes. Source: Ascenz Marorka platform, data available as of 06 June 2025.

In addition, the "Trade area", chart Figure 5.6, illustrates the vessel's operating time across various ocean regions. The Atlantic Ocean overwhelmingly dominates with around 10,000 hours, significantly more than any other region. The Indian Ocean follows with just under 3,000 hours, and the Mediterranean Sea shows a slightly lower figure, while the Pacific Ocean has under 1,500 hours. In contrast, regions like the North Sea, Baltic Sea, and other account for negligible operational time.

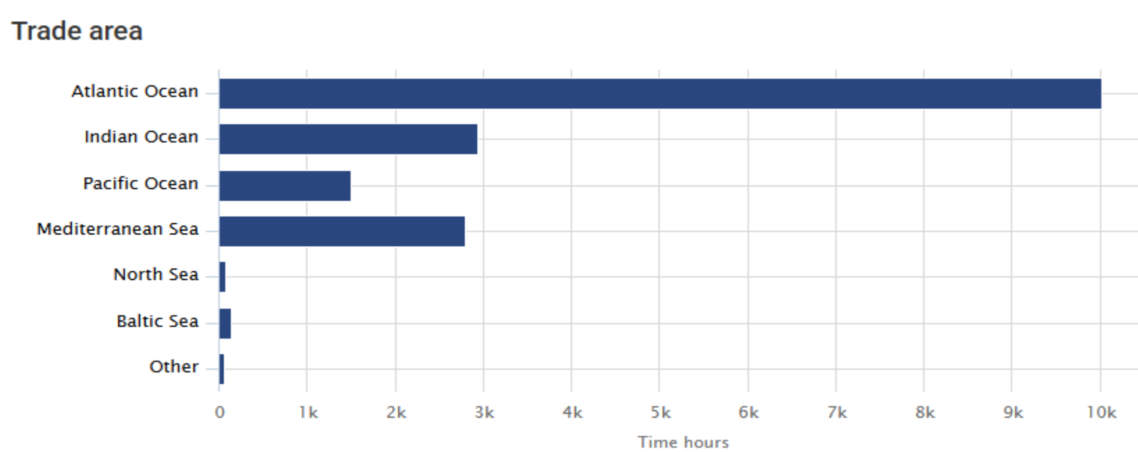

Figure 5.6. Vessel 1 voyage trade area. Source: GTT platform, data available as of 06 June 2025.

Also, the "Main engine load" graph (Figure 5.7) compares the load percentages of two main engines (ME1 and ME2) across different ranges. The engines spent a large amount of time at 56.1% and 61.2% load, with ME1 slightly exceeding ME2 at these levels. A considerable number of hours were also recorded at 0% load, indicating periods of inactivity or idling. Engine loads above 66% occurred less frequently, suggesting that high-load operations were less common during the observed period.

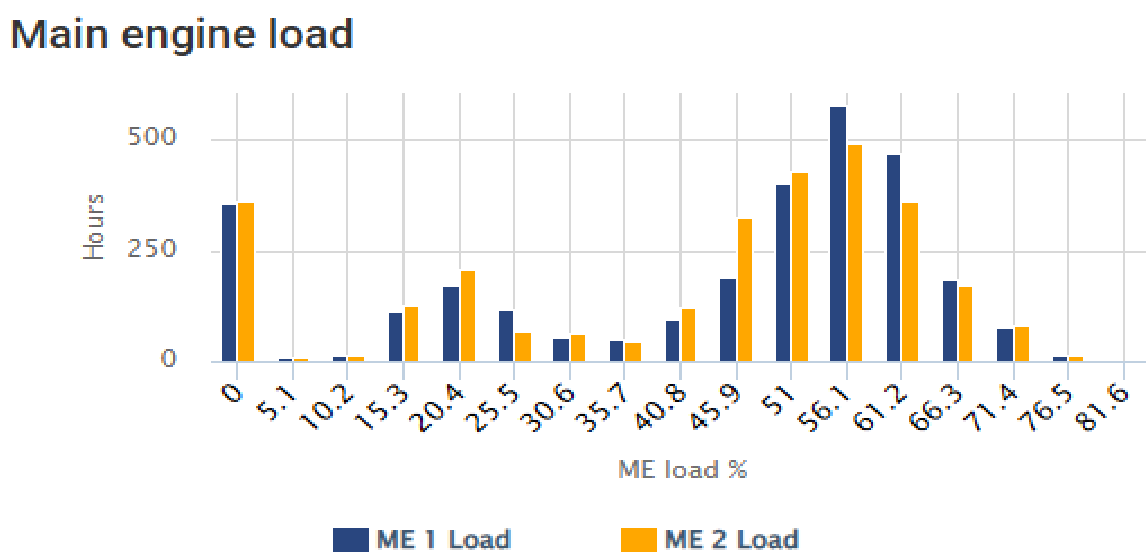

Figure 5.7. Vessel 1 Main engine load. Source: Ascenz Marorka platform, data available as of 06 June 2025.

The "Shaft RPM" chart (Figure 5.8) provides insight into the rotational speed of the main engines' shafts. Both ME1 and ME2 exhibit the highest operating time in the 55–65 RPM range, with a peak around 60–65 RPM. A notable number of hours were also logged at 0 RPM, pointing again to idle times or port stays. Very low or very high RPM ranges were rarely used, showing that the engines operated predominantly within an efficient mid-range band.

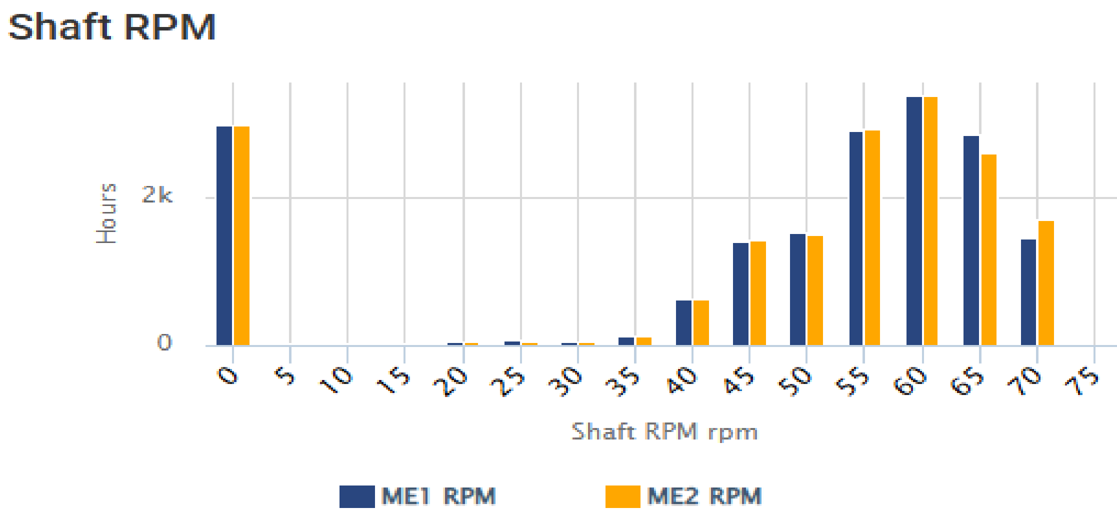

Figure 5.8. Vessel 1 Shaft RPM. Source: Ascenz Marorka platform, data available as of 06 June 2025.

What is more, in the "Consumption by consumer" chart (Figure 5.9), fuel usage is broken down by system. Main engines (MEs) are the largest consumers, burning nearly 35 metric tons per day, while diesel generators (DGs) consume around 14–15 MT/day. Boiler usage is minimal, and the Gas Combustion Unit (GCU) registers no visible consumption. This highlights that propulsion-related systems are the primary energy consumers on board.

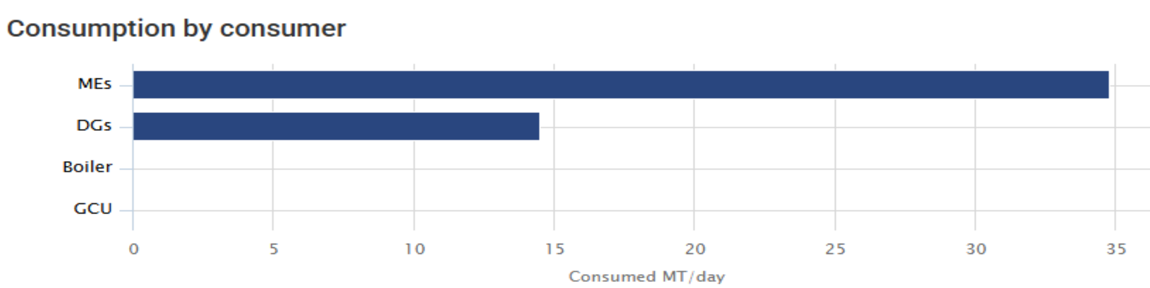

Figure 5.9. Vessel 1 Consumption by consumer. Source: Ascenz Marorka platform, data available as of 06 June 2025.

While the "DG running hours" chart (Figure 5.10) displays the operational time for each diesel generator. DG2, DG3, and DG4 have the highest usage, each running for more than 7,500 hours, while DG1 is slightly behind. DG5 and DG6 are not shown to be in use, possibly held as standby units or inactive during the measured period.

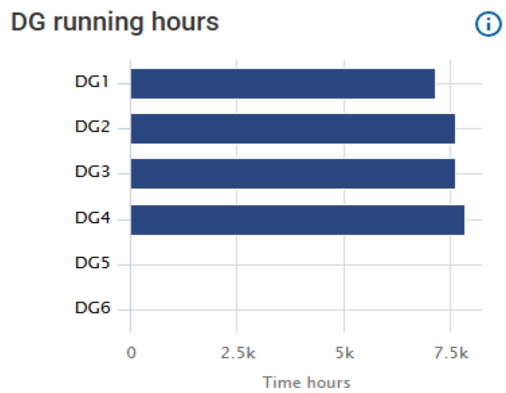

Figure 5.10. Vessel 1 DG running hours. Source: Ascenz Marorka platform, data available as of 06 June 2025.

Lastly, the "DG average load" graph (Figure 5.11) reveals that DG1 and DG4 operated with the highest average loads, close to 60%, followed by DG2 and DG3, both near 55%. These load levels suggest a consistent and efficient use of the generators. As with running hours, DG5 and DG6 show no data, indicating non-utilization.

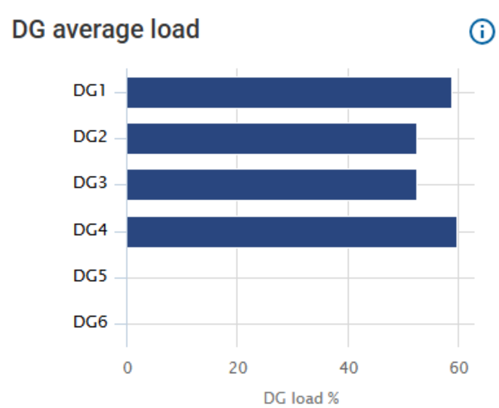

Figure 5.11. Vessel 1 DG average load. Source: Ascenz Marorka platform, data available as of 06 June 2025.

v. Vessel 2

During its 732-day voyage (Figure 5.12), Vessel 2 recorded the greatest overall distance among the three ships, traveling 237,182.69 nautical miles by GPS and maintaining over 621 days above 5 knots. The vessel showed strong performance metrics with an average GPS speed of 15.75 knots and an average log speed of 15.58 knots. It had a main engine fuel consumption of 29,547.19 metric tons, auxiliary consumption of 10,453.83 metric tons, and boiler consumption of 725.09 metric tons, indicating active use of steam systems. The mean draft was 7.28 meters with a pronounced negative trim of -1.49 meters. The vessel encountered wave heights up to 7.33 meters and wind speeds reaching 53.48 knots, with a slightly higher average current of 0.67 knots compared to the others.

Distance by GPS	237182.69 nm
Distance by GPS (above 5 kn)	235094.71 nm
Distance by log	233717.12 nm
Duration	732d 0h 0m
Duration (above 5 kn)	621d 20h 30m
ME fuel consumption	29547.19 MT
Aux fuel consumption	10453.83 MT
Boiler fuel consumption	725.09 MT
Avg. GPS Speed*	15.75 knots
Avg. Log Speed*	15.58 knots
Mean Draft*	7.28 m
Trim*	-1.49 m
Max wave height	7.33 m
Max wind	53.48 knots
Avg. Current	0.67 knots

Figure 5.12. Descriptive statistics for Vessel 2 data. Source: GTT platform, data available as of 06 June 2025.

Also, next voyage trading routes for vessel 2 (Figure 5.13) is from West Africa the routes extend eastward through the Mediterranean, the Middle East, and into South and East Asia, including connections to the Indian subcontinent, Southeast Asia, and China. Some lines pass through the Red Sea and around the Horn of Africa. From Asia, ships continue westward either around the Cape of Good Hope or across the Atlantic Ocean, ultimately reaching Cuba in the Caribbean. Additional branches extend from Europe and West Africa directly to Cuba, while others pass through the Americas. Together, these paths form a circular global trade route that links Africa, Europe, Asia, and the Americas across the Atlantic, Indian, and Pacific Oceans.

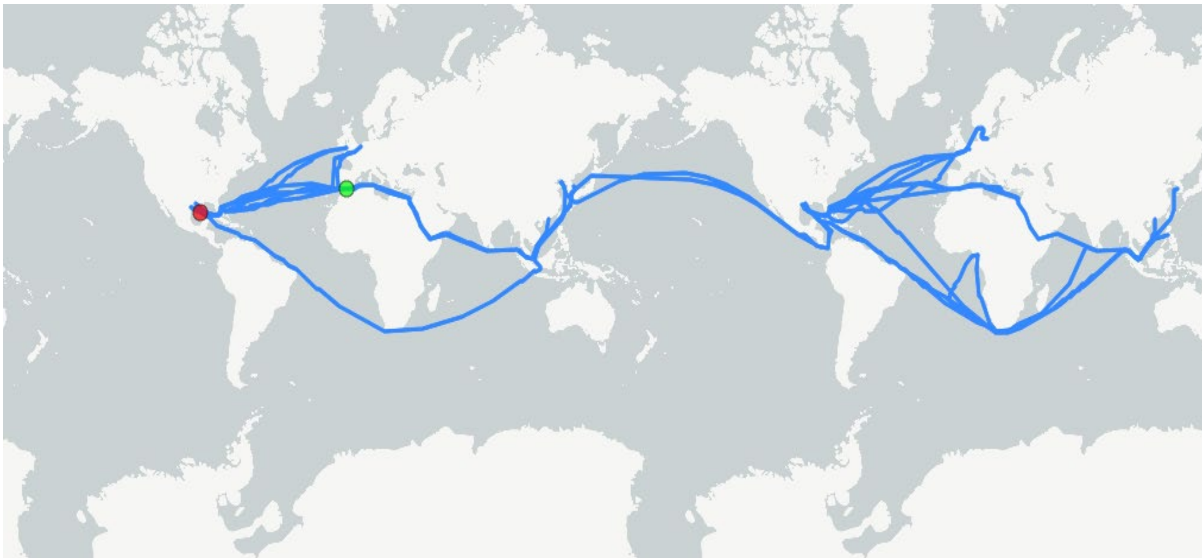

Figure 5.13. Vessel 2 voyage trade routes. Source: Ascenz Marorka platform, data available as of 06 June 2025.

Moreover, Figure 5.14, titled "Trade area," displays the operational time spent in various maritime regions. The Atlantic Ocean stands out with the highest activity, accumulating nearly 9000 hours. This is significantly more than the Indian Ocean and Pacific Ocean, which both register around 3500 to 4000 hours. The Mediterranean Sea follows with a lower figure of about 2000 hours, while the North Sea, Baltic Sea, and other areas show minimal activity, indicating limited operation in those regions.

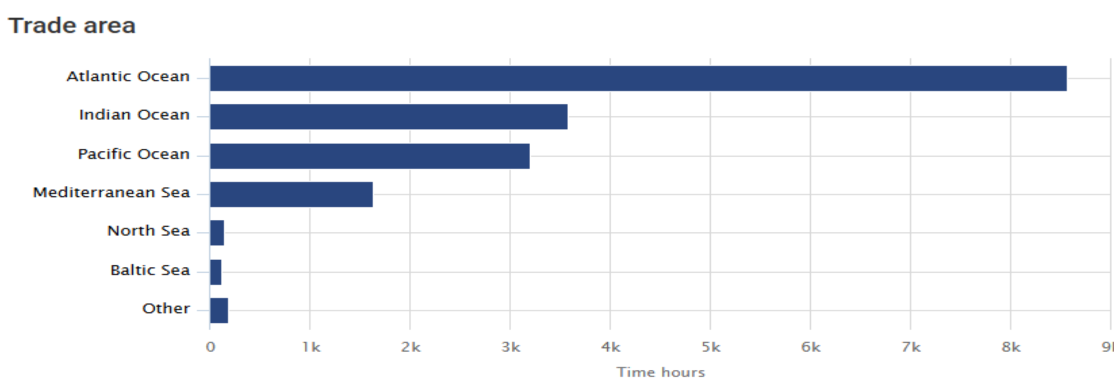

Figure 5.14. Vessel 2 voyage trade area. Source: Ascenz Marorka platform, data available as of 06 June 2025.

Also, the next Figure 5.15, "Shaft RPM," compares the operating hours of two main engines (ME1 and ME2) across different RPM ranges. Both engines have substantial hours logged at higher RPM ranges, particularly between 62.4 and 78 RPM, where the peak operation is observed, especially in the 72.8–78 RPM band. Notably, a large number of hours were also recorded at 0 RPM, suggesting periods of engine idling or shutdown. The data shows a consistent operational pattern between the two engines, with ME2 often slightly exceeding ME1 in usage.

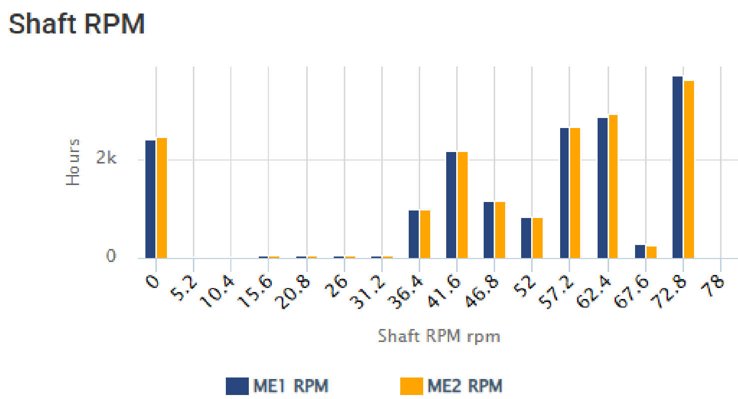

Figure 5.15. Vessel 2 Shaft RPM. Source: Ascenz Marorka platform, data available as of 06 June 2025.

In the following Figure 5.16, "Consumption by consumer," the fuel consumption across different onboard systems is shown. Main Engines (MEs) are by far the largest consumers, using approximately 40 metric tons per day. Diesel Generators (DGs) come next with about 15 MT/day, followed by minimal usage by the Boiler. The Gas Combustion Unit (GCU) shows negligible or no recorded consumption, indicating it's either rarely used or not active during the period.

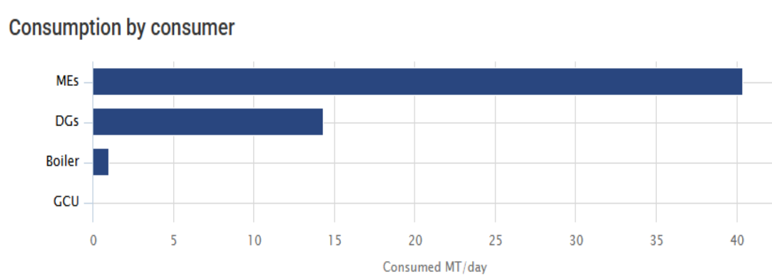

Figure 5.16. Vessel 2 Consumption by consumer. Source: Ascenz Marorka platform, data available as of 06 June 2025.

The next Figure 5.17, "DG running hours," illustrates the operational time of diesel generators. DG1 and DG4 are the most utilized, each with around 7500 to 8000 running hours. DG2 and

DG3 show moderate use, while DG5 and DG6 have no recorded hours, suggesting they were either non-operational or used as standby units during this time frame.

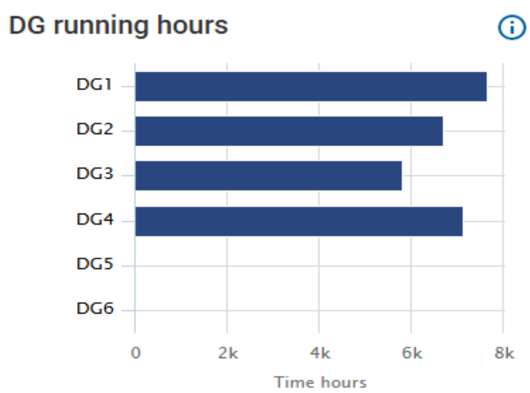

Figure 5.17. Vessel 2 DG running hours. Source: Ascenz Marorka platform, data available as of 06 June 2025.

Therefore, Figure 5.18, "DG average load," displays the average load percentage for each diesel generator. DG1 and DG4 again lead, each operating at close to 60% average load, indicating consistent and possibly efficient use. DG2 and DG3 follow closely behind with slightly lower load percentages. DG5 and DG6 once again show no data, reaffirming their lack of activity.

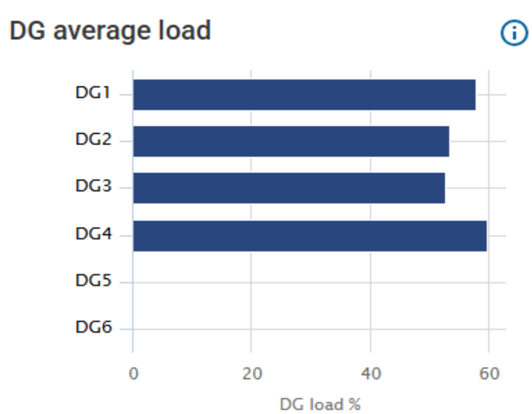

Figure 5.18. Vessel 2 DG average load. Source: Ascenz Marorka platform, data available as of 06 June 2025.

ii. Vessel 3

Lastly, Vessel 3 completed its 732-day voyage with a GPS distance of 217,904.86 nautical miles and 582 days logged at speeds over 5 knots, the shortest high-speed duration of the three vessels (Figure 5.19). The vessel averaged a GPS speed of 15.45 knots and a nearly identical log speed of 15.43 knots, demonstrating consistent propulsion. Main engine fuel use totaled 24,820.41

metric tons, with auxiliary usage at 9,109.43 metric tons and minor boiler fuel use of 27.24 metric tons. The vessel maintained a mean draft of 8.56 meters and the most significant negative trim among the group at -3.35 meters. It faced a maximum wave height of 6.49 meters and maximum wind of 46.53 knots, with an average current matching Abidal at 0.63 knots.

Distance by GPS	217904.86 nm
Distance by GPS (above 5 kn)	215923.57 nm
Distance by log	216390.48 nm
Duration	732d 0h 0m
Duration (above 5 kn)	582d 12h 0m
ME fuel consumption	24820.41 MT
Aux fuel consumption	9109.43 MT
Boiler fuel consumption	27.24 MT
Avg. GPS Speed*	15.45 knots
Avg. Log Speed*	15.43 knots
Mean Draft*	8.56 m
Trim*	-3.35 m
Max wave height	6.49 m
Max wind	46.53 knots
Avg. Current	0.63 knots

Figure 5.19. Descriptive statistics for Vessel 3 data. Source: Ascenz Marorka platform, data available as of 06 June 2025.

In regard to the vessel 3 trading routes, this map (Figure 5.20) shows global maritime trading routes concentrated around key regions. The routes begin in the eastern Pacific near Central America (marked by the green dot) and converge at Cuba (red dot), which functions as a central trading hub. From Cuba, ships travel across the Atlantic Ocean to West Africa and Europe, including destinations in the UK, France, Spain, and the Nordic countries, as well as through the Mediterranean Sea. From Europe and Africa, the routes continue either through the Suez Canal or around the southern tip of Africa, extending into the Middle East, South Asia, and further east to Southeast Asia, Japan, Indonesia, and Australia. Additional lines stretch down the eastern coast of South America and across the Indian Ocean, touching ports in Madagascar, the Maldives, and coastal East Africa. In summary, the trading routes span the Caribbean, Atlantic Ocean, Europe, Africa, the Indian Ocean, and the Asia-Pacific region, forming a vast, interconnected web of global maritime commerce.

Figure 5.20. Vessel 3 voyage trade routes. Source: Ascenz Marorka platform, data available as of 06 June 2025.

Moreover, the "Trade area" chart (Figure 5.21)shows the distribution of operational hours spent by the vessel across different marine regions. The Atlantic Ocean dominates with over 10,000 hours, significantly more than any other region. The Pacific Ocean follows with just under 4,000 hours, while the Indian Ocean records slightly more than 2,000 hours. The Mediterranean Sea, North Sea, and Baltic Sea account for minimal time, with less than 1,000 hours each. Other areas show negligible activity.

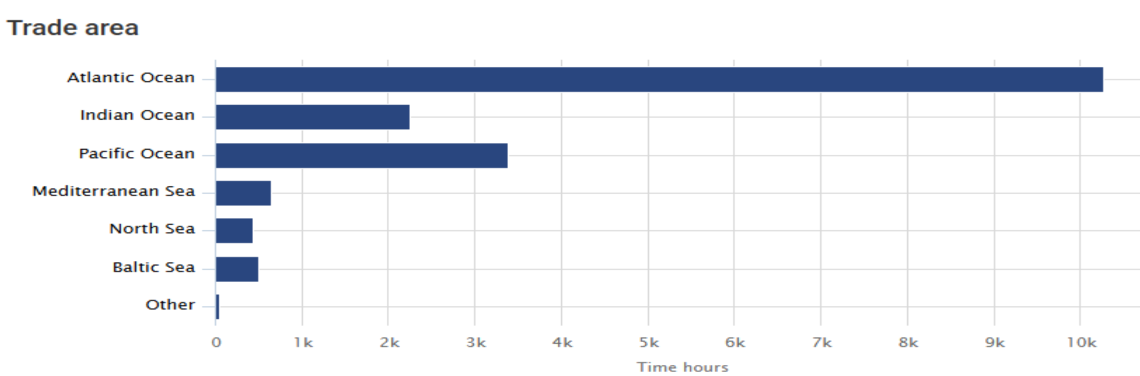

Figure 5.21. Vesel 3 voyage trade area. Source: Ascenz Marorka platform, data available as of 06 June 2025.

Also, the "Main engine load" chart (Figure 5.22) details the number of hours the main engines (ME1 and ME2) operated at various load percentages. Both engines spent the most time around the 30.6% load range, with ME2 recording slightly higher hours. Additionally, there was a significant number of hours at 0% load, indicating idle or non-operational periods. Other load ranges like 20.4%, 61.2%, and 71.4% show moderate usage, while extreme high or low loads occurred less frequently.

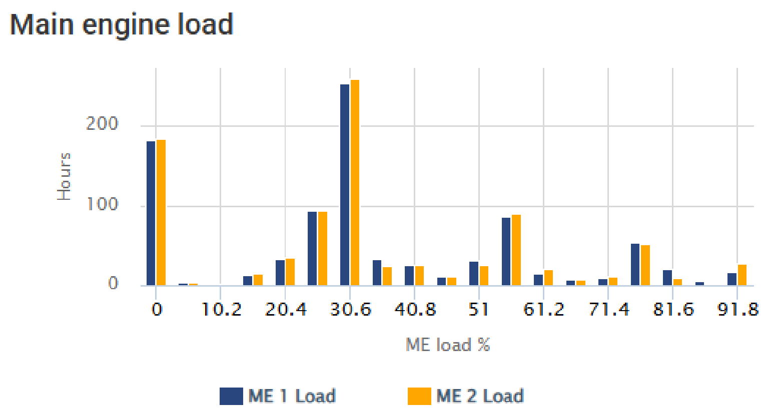

Figure 5.22. Vessel 3 Main engine load. Source: Ascenz Marorka platform, data available as of 06 June 2025.

Equally important, the "Shaft RPM" chart (Figure 5.23) presents the distribution of shaft revolutions per minute (RPM) for both main engines. The highest number of hours occurred between 51 and 61.2 RPM, with ME1 slightly leading. There’s also a large amount of time logged at 0 RPM, reflecting engine stoppages or idle periods. Mid-range RPMs between 45 and 66 RPM were the most commonly used during active operation.

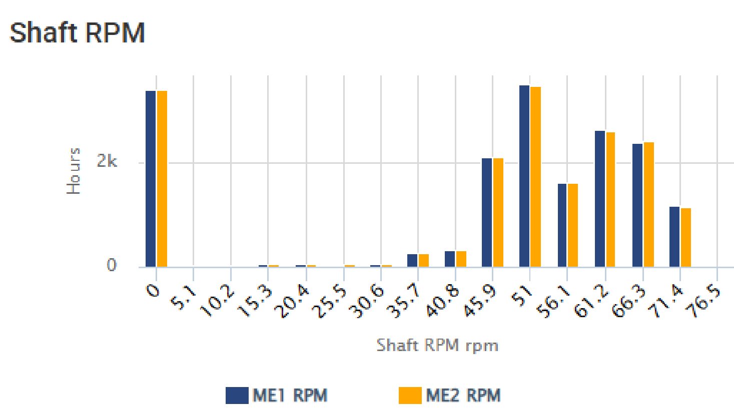

Figure 5.23. Vessel 3 Shaft RPM. Source: Ascenz Marorka platform, data available as of 06 June 2025.

Additionally, the "Consumption by consumer" chart (Figure 5.24), the fuel consumption by different onboard systems is shown. The Main Engines (MEs) are the largest consumers, burning nearly 34 metric tons per day, followed by the Diesel Generators (DGs) with about 13–

14 MT/day. The Boiler shows very low fuel use, and the Gas Combustion Unit (GCU) registers no consumption, implying it was either inactive or not in use during the recorded timeframe.

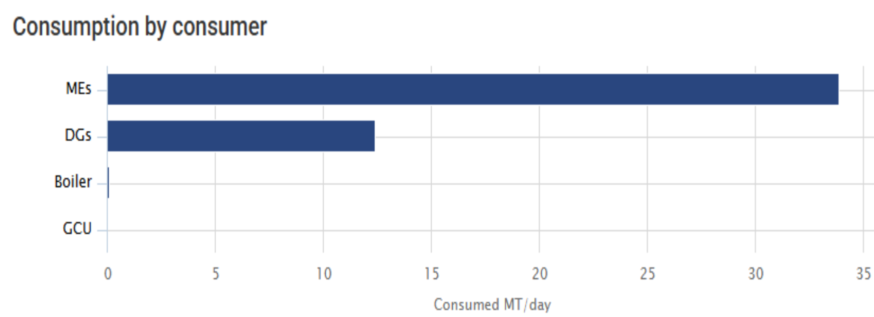

Figure 5.24. Vessel 3 Consumption by consumer. Source: G Ascenz Marorka TT platform, data available as of 06 June 2025.

In addition, the "DG running hours" chart (Figure 5.25) reveals the operating hours for the diesel generators. DG1 and DG4 have the highest runtime, both logging close to 8,000 hours. DG2 and DG3 show significantly less operation, suggesting a partial load distribution or differing roles among the generators. DG5 and DG6 are not shown as active.

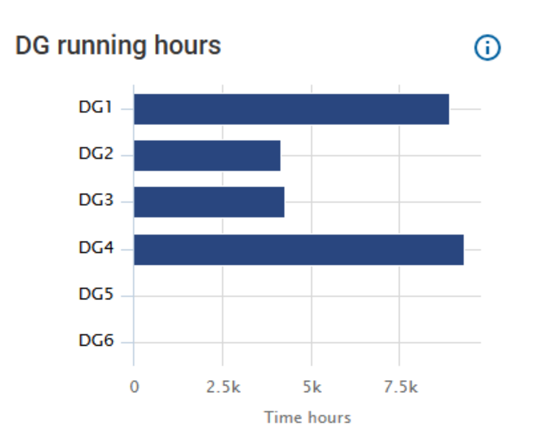

Figure 5.25. Vessel 3 DG running hours. Source: Ascenz Marorka platform, data available as of 06 June 2025.

Finally, the "DG average load" chart (Figure 5.26) illustrates the average operational load for each DG. DG1 and DG4 consistently operated at higher loads, nearing 60%, indicating efficient and sustained use. DG2 and DG3 had lower average loads (between 45%–50%), which aligns with their lower running hours. DG5 and DG6, once again, appear to be inactive during this reporting period.

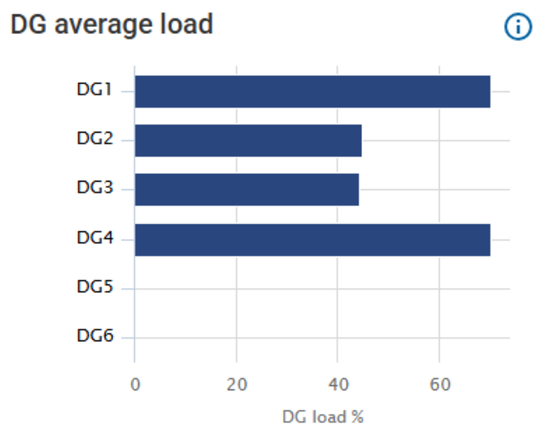

Figure 5.26. Vessel 3 DG average load. Source: Ascenz Marorka platform, data available as of 06 June 2025.

Moreover, it is necessary to be defined as the restriction of the model. Initially, the changes in cargo composition due to evaporation during LNG cargo transportation are not taken into account in this study. At cryogenic temperatures (-162°C), lighter components such as methane and nitrogen tend to vaporize more readily, resulting in daily variations in the density and lower calorific value of the boil-off gas. These changes can influence engine performance and fuel consumption. Ignoring these variations in cargo composition may result in fuel performance deviations in the range of 1–5%, depending on the voyage duration, boil-off gas management strategy, and engine type (Zhao & Guo, 2021). However, for the scope of this research, a simplifying assumption is made that the cargo composition remains static. Future studies may incorporate the dynamic behavior of cargo composition based on the thermodynamic characteristics of the LNG system.

Similarly, temperature variations during voyages from cargo loading to discharging operations, such as those caused by thermal expansion and contraction of the cargo, and so this is excluded from the current model to maintain simplicity and preserve a business-focused scope. Addressing these factors would require a dedicated focus on the thermodynamics of LNG composition, which falls outside the intended objectives of this study.

Additionally, the cooling process during the ballast leg is not included in this study. This process involves preparing the cargo tanks for loading by lowering their internal temperature to the required cryogenic conditions. The cool-down process is crucial for vessels to load new cargo, as the cargo containment tanks must be cooled to below -130°C, as recommended by the maker

(GTT). To achieve this, the ship consumes energy to reach the required temperature in the cargo containment system, enabling it to receive a new LNG cargo. However, this energy consumption is not accounted for in the heel model of the study. The approximate energy required for the cool-down process is roughly 800 m^3 for all cargo tanks, equals about 18,800 MMBtu, based on a typical density of 450 kg/m^3 and a gross calorific value of 55 MJ/kg, from a warm condition around 40 C to colder than -140 C. Future research could incorporate this parameter, which depends on the thermodynamic characteristics of the system. This would require specific data from equipment such as a chromatograph or, alternatively, a gas analyzer. These systems measure the BOG (Boil-off Gas) composition and can more accurately determine the heating value required for each cooling-down process.

5.4.3 Prediction of fuel consumption

The research framework centers on fuel consumption prediction, which directly influences the four key performance metric models, as detailed in the following sections. To assess fuel prediction effectiveness, three studies were conducted on three vessels under both laden and ballast conditions across various real-time operating scenarios.

5.4.3.1 Data Acquisition

This section provides a detailed description of the dataset. Ensuring data quality is a critical step in model development, as the included data must be accurate and reliable.

The data acquisition is based on a vessel type that reflects the latest technological advancements in the LNG industry, XDF vessels. These vessels are known for their superior fuel efficiency, reduced emissions, and reliable performance, making them highly competitive in the freight market.

The datasets covering the period from 01/01/2023 to 01/01/2025 (two years) were obtained from the GTT platform as analyzed in the section “5.4.3.2 Exploratory data analysis & Dara pre-processing”. It is selected as the platform for providing credible datasets due to its rigorous data qualification process, including precise quality testing, making it a suitable source of vessel data for developing this model framework.

The dataset used in this analysis was sourced from the Ascenz Marorka platform, which applies its own rigorous data quality validation processes, as mentioned in Section 4.3 (Research Methodology). Datasets are selected based on this validation process; however, this does not mean that additional pre-processing steps such as data cleaning, feature engineering, imputation, and outlier handling were not performed in the thesis. The benefit of this validation is used only to ensure the selection of the best vessel's dataset within the platform.

Briefly, the platform monitors key vessel parameters, including GPS and log speed, shaft RPM, shaft power, main engine fuel consumption, and draft readings at both the fore and aft. Vessels are selected for analysis based on the relevance and applicability of these parameters. Data quality is assessed through a comprehensive validation process involving several criteria: Out of bounds (values outside realistic or configurable ship-specific thresholds), Frozen values (unchanging data over time where variability is expected), Cross validation (inconsistencies such as the vessel sailing without corresponding consumption or RPM), and Missing data (lack of transmitted values). When all measurements are received without triggering any of these validation filters, the data quality is 100%, which is the optimal and desired condition for reliable analysis.

The following Figure 5.27 presents the XDF vessels along with their respective measurement quality scores and corresponding averages. From this evaluation, the top three vessels have been selected, achieving scores of 94%, 92%, and 86%, respectively. The average score of the other vessels is noticeably lower; therefore, the selection has been limited to three vessels. It is important to note that this limitation is also driven by hardware capacity constraints, which restrict the handling of larger datasets.

Ship	ME consumed (%)	Shaft power (%)	Shaft rpm (%)	Draft fore (%)	Draft aft (%)	GPS speed (%)	Log speed (%)	Boiler consumed (%)	DG consumed (%)	DG electrical power (%)	Average (%)
[redacted]	100	98	100	100	100	100	100	–	75	75	94
[redacted]	94	100	100	100	100	100	99	75	75	75	92
[redacted]	0	0	0	0	0	0	0	–	0	0	0
[redacted]	0	0	–	0	0	0	0	–	0	0	0
[redacted]	0	0	0	0	0	0	0	–	0	0	0
[redacted]	97	77	77	77	77	100	74	75	75	52	78
[redacted]	85	78	87	87	87	87	87	26	75	75	77
[redacted]	99	100	100	100	100	100	100	11	75	75	86
[redacted]	77	79	79	82	82	83	82	3	77	79	72
[redacted]	60	62	79	66	66	62	67	3	61	62	59
[redacted]	–	–	–	–	–	–	–	–	–	–	–
[redacted]	–	69	78	71	71	76	76	45	53	53	66
[redacted]	77	78	79	79	79	79	79	79	78	79	78
[redacted]	57	79	79	66	66	77	78	78	65	78	72

Figure 5.27. Auto-logged data quality table from the Ascenz Marorka platform . Source: GTT platform, data available as of 06 June 2025.

In the Figure 5.28 below, one of the selected vessels is analyzed in detail, providing a more analytical breakdown of the measurement quality scores. Specifically, it illustrates that the selected two-year period, the average data quality score for key parameters, GPS and log speed, shaft RPM, shaft power, main engine fuel consumption, and draft readings (fore and aft), is 94%. This score is derived based on the platform’s validation criteria, including Out of Bounds, Frozen Values, Cross Validation, and Missing Data, ensuring high reliability and consistency in the dataset. The remaining two vessels are presented in Appendix 3 for reference.

Data quality

	Out of bounds (%)	Frozen data (%)	Cross validation (%)	Missing data (%)	Valid data (%)
GPS speed	0	0	0	0	100
Log speed	0	0	0	0	100
ME consumed	0	0	0	0	100
Shaft power	2	0	0	0	98
Shaft rpm	0	0	0	0	100
Draft fore	0	0	0	0	100
Draft aft	0	0	0	0	100
DG consumed	0	0	0	25	75
DG electrical power	0	0	0	25	75
Average (%)	**0**	**0**	**0**	**6**	**94**

Figure 5.28. Data quality of the Vessel 1. Source: Ascenz Marorka platform, data available as of 06 June 2025.

More specifically, Figure 5.29 illustrates the GPS speed measurements for the selected vessel, showing no issues across the four key validation metrics defined by Ascenz Marorka: Out of Bounds, Frozen Values, Cross Validation, and Missing Data. This indicates that the GPS speed data is of consistently high quality throughout the analyzed period.

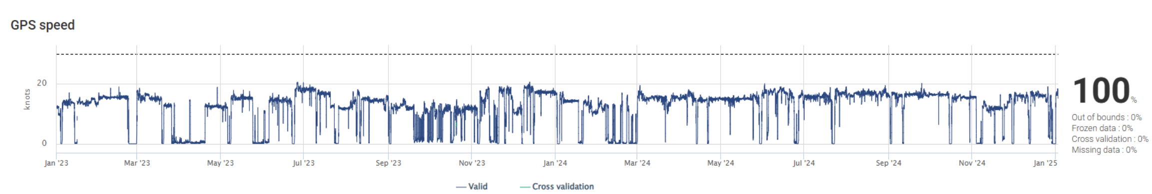

Figure 5.29 GPS data quality results of Vessel 1. Source: Ascenz Marorka platform, data available as of 06 June 2025.

Similarly, in Figure 5.30, Log Speed has been evaluated using the same validation process and achieved a perfect score of 100%.

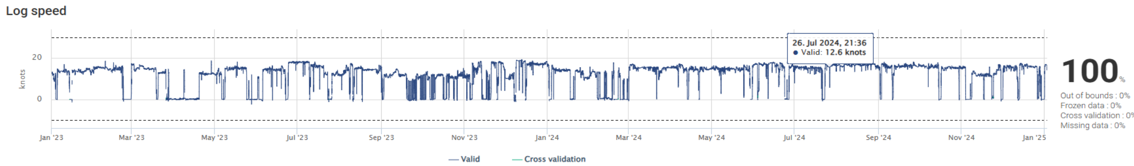

Figure 5.30. LOG Speed data quality results of Vessel 1. Source: Ascenz Marorka platform, data available as of 06 June 2025.

The Main Engine (ME) fuel consumption data also achieved a 100% score (Figure 5.31), indicating no issues detected across all four validation criteria: Out of Bounds, Frozen Values, Cross Validation, and Missing Data. This confirms the high reliability and integrity of the ME consumption measurements throughout the period analyzed.

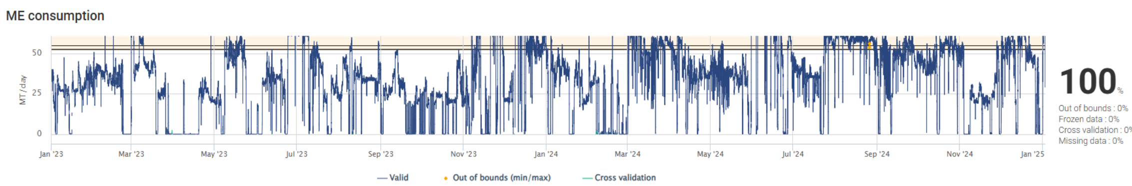

Figure 5.31. ME consumption data quality results of Vessel 1. Source: Ascenz Marorka platform, data available as of 06 June 2025.

The Shaft RPM data likewise received a 100% score (Figure 5.32), with no issues identified during the data validation process. This indicates that the data collected from the platform was consistently accurate and complete, meeting all quality criteria set by Ascenz Marorka.

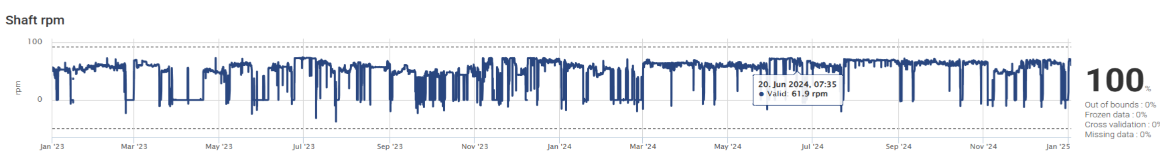

Figure 5.32. Shaft RPM data quality results of Vessel 1. Source: Ascenz Marorka platform, data available as of 06 June 2025.

The Shaft Power data received a score of 98% (Figure 5.33), slightly lower due to the presence of outliers classified under the Out of Bounds validation category. Specifically, these anomalies consist of data points that exceed realistic or configurable ship-specific thresholds, primarily observed during the later period of the dataset. Despite this minor deviation, the overall data quality remains high and reliable for analysis.

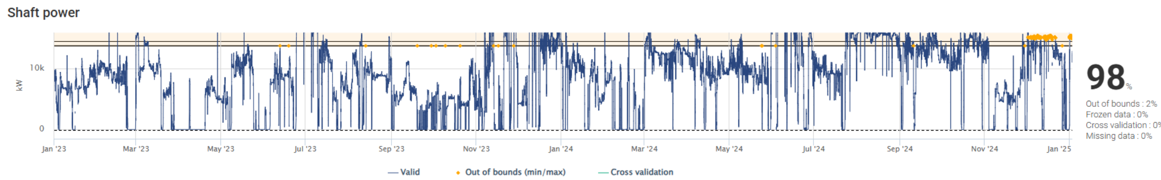

Figure 5.33. Shaft power data quality results of Vessel 1. Source: Ascenz Marorka platform, data available as of 06 June 2025.

The Draft Fore and aft measurement achieved a perfect score of 100% (Figure 5.34 and Figure 5.355), indicating that the data collected by the Ascenz Marorka platform is fully reliable. No issues were detected across any of the validation criteria, confirming the consistency and accuracy of this parameter throughout the analyzed period.

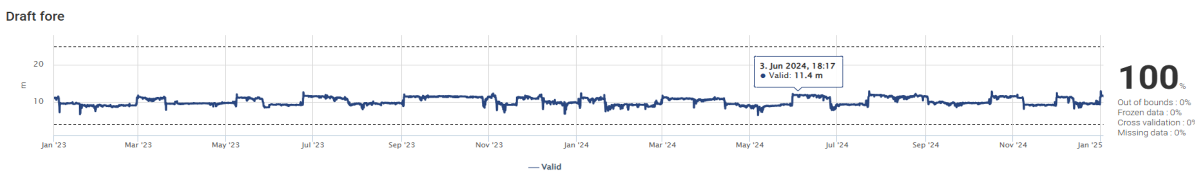

Figure 5.34. Draft force data quality results of Vessel 1. Source: Ascenz Marorka platform, data available as of 06 June 2025.

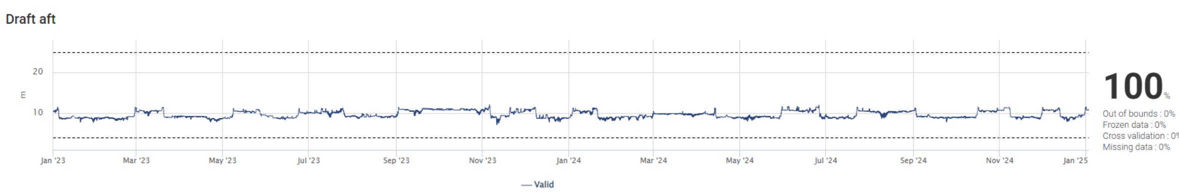

Figure 5.35. Draft aft quality results of Vessel 1. Source: Ascenz Marorka platform, data available as of 06 June 2025.

The DG (Diesel Generator) consumption and power measurements achieved a score of 75%, indicating a generally reliable dataset collected by the Ascenz Marorka platform. However, the remaining 25% of the data is classified as missing, which highlights a gap (Figure 5.36). As a result, special attention and appropriate handling will be required during the pre-processing phase to address this missing data and ensure the integrity of any subsequent analysis.

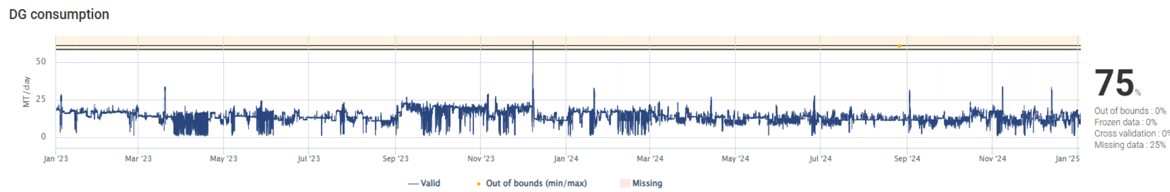

Figure 5.36. DG consumption data quality results of Vessel 1. Source: Ascenz Marorka platform, data available as of 06 June 2025.

This plot (Figure 5.37) illustrates the power output of the Diesel Generators (DG) over the observed period, measured in kilowatts (kW). The data displays a stable base load pattern with intermittent peaks, indicating periodic increases in auxiliary power demand. These spikes are typical during equipment start-up or higher onboard energy usage. Despite the valid segments being clear and consistent, there is a noticeable amount of missing data, approximately 25%, as indicated in the metrics. This gap reduces the overall data quality score to 75, even though there are no out-of-bound, frozen, or cross-validation issues detected. The pattern is otherwise typical for shipboard auxiliary systems.

Figure 5.37. DG power data quality results of Vessel 1. Source: GTT platform, data available as of 06 June 2025.

5.4.3.2 Exploratory data analysis & data preprocessing

This section presents a comprehensive overview of the dataset handling process, encompassing key preprocessing stages outlined in Chapter 4. Specifically, it covers Data Collection, Exploration, Cleaning, Transformation, Reduction, and Splitting as applied in the case studies.

The first step in the process is data collection. The dataset is diverse and robust, consisting of 894 features, and spans a period of two years (01/01/2023 to 01/01/2025) with a sampling frequency of every 15 minutes. This interval was chosen based on the observation that neither weather conditions nor vessel states typically change significantly in less than 15 minutes. The dataset includes data from three vessels operating in two modes: laden and ballast. While the goal is to maximize the number of vessels with long-term data records, hardware limitations (Central Processing Unit (CPU) / Graphics Processing Unit (GPU) capacity) restricted the dataset to three vessels. To build an effective model, it is crucial to assess which features are relevant, which can be directly used, and which require imputation or further preprocessing.

i. Handling of variables (features)

First part of preprocessing is the handling of variables as explained in the Chapter 4, section "4.4.3.2 Exploratory data analysis & data preprocessing".

Firstly, the data exploration step which is related to features is conducted. It is identifying data types, numeric, categorical, date, etc. to ensure proper handling in later stages. Once done, the focus shifts to Exploratory Data Analysis (EDA), which reveals patterns, outliers, and relationships, guiding hypothesis generation and model selection. Then, to ensure safe, efficient, and regulatory-compliant operations aboard an LNG carrier, ship data (894 features) is systematically categorized based on functionality and system association. These categories span identification, propulsion, cargo handling, and safety systems, each playing a crucial role in daily marine operations as summarized below by category. However, a list with full data is included in the Appendix 4.

Vessel Identification and General Information encompass key identifiers like the Company, Ship Name, and IMO No. These elements establish the vessel's unique identity, serving essential roles in documentation, compliance, and global tracking systems.

Navigation and Positioning include parameters such as Date Time, Latitude, Longitude, State, COG (Course Over Ground) heading, and Under keel clearance. These values allow for real-time monitoring of the ship's location, direction, and speed, critical for voyage planning, route optimization, and hazard avoidance in constrained waterways.

Vessel Dynamics and Stability data such as Draft measurements, Roll, Pitch, and Yaw, including Sloshed metrics, inform the crew about the vessel's movement and stability. For LNG ships, this is especially important to assess how the liquid cargo behaves under motion, reducing risks related to tank stress or imbalance.

Environmental Conditions like wind speed, air pressure, humidity, and seawater temperature help crews adapt operations to external changes. These factors influence routing, engine performance, and even fuel consumption under varying atmospheric and sea states.

Propulsion and Power Systems are monitored through metrics like Shaft Power, RPM, and Torque of the main engines (ME1, ME2). These readings provide insights into the propulsion system's performance and detect inefficiencies or potential issues affecting vessel mobility.

Fuel Consumption data covers all engine and boiler-related usage, including BOG, HFO, and MGO/MDO across different systems. Understanding this consumption is vital for fuel efficiency, emissions control and managing boil-off gas.

Diesel Generators (DG) Performance tracks electricity production and operational status of DG1–DG4. As diesel generators supply power for most shipboard systems, maintaining visibility into their performance ensures operational continuity and redundancy.

Rudder and Steering functionality is covered via Rudder Angle measurements. Accurate steering data is fundamental for navigational control, especially during tight manoeuvres or docking procedures.

LNG Tank Conditions (General), including RHO LNG and LNG volume, help monitor cargo behaviours and integrity. Boil-Off Rate (BOR) tracking is essential for ensuring evaporating gas is either consumed or reliquefied safely, preventing overpressure or cargo loss.

Tank-Specific Measurements (Tanks 1–4) go into fine detail, covering everything from liquid/vapour temperatures and pressure control to pump operation and gas composition. These parameters ensure LNG is stored under stable conditions and that tanks operate safely under varying loads.

Tank Impact and Sloshing data, such as impact frequency, tank-specific alarms, and Sloshed thresholds, serve to detect excessive liquid movement within tanks. Early detection of sloshing can prevent mechanical stress or even structural failure of containment systems.

Gas Management Systems monitor processes like BOG to GCU, Vaporizer outputs, Reliquefaction, and Sub-Cooling. These systems manage excess gas, stabilize tank pressure and temperature, and ensure gas is conditioned properly for reuse or reinjection.

Compressor Systems (Low and High-Pressure) provide pressure, temperature, and flow data for managing vapour. These compressors are integral to gas handling and propulsion supply, ensuring the engines and boilers receive fuel under the right conditions.

Gas and Liquid Lines track flow, temperature, and pressure in systems such as Cross-Over, Spray, Bunkering, and MAIN lines. Proper functioning of these lines is critical for LNG loading/unloading and internal distribution.

Mist Separators, including NBO and FBO units, monitor condensate levels and temperatures. These components remove liquid from gas streams, protecting downstream equipment from damage due to moisture or freezing.

Fuel Gas Control Systems such as valves on X-DF, GCU, GE, and the NG buffer tanks regulate gas supply to propulsion and auxiliary systems. These controls ensure steady combustion and operational efficiency.

Gas Heaters, including those for NG, LNG, and Fuel Gas, manage the thermal conditioning of gas streams. Heating gas to optimal temperatures is vital for complete combustion and preventing engine or pipeline issues.

Bilge and Water Levels track liquid accumulation in bilge wells, serving as early indicators of flooding or leakage. These readings help maintain vessel safety and structural integrity, especially in the engine room and cargo spaces.

Cooling Systems data, particularly sea water inlet temperatures, ensures main engines and auxiliary systems are adequately cooled. Overheating prevention is essential for maintaining uptime and avoiding costly repairs.

Cofferdam Temperatures (Tanks 1–5) measure insulation performance by recording ambient temperatures around LNG tanks. Any abnormal readings may indicate insulation compromise, requiring inspection to avoid potential hazards.

Nitrogen System metrics monitor pressure levels, valve operation, and generator conditions (e.g., O_2 content and dew point). Nitrogen is used to create inert environments in LNG tanks, reducing the risk of combustion or explosion.

Gas Composition (General) data includes hydrocarbon makeup (C1–C6), N_2, CO_2, HHV, LHV, and Methane Number. These values define fuel quality, calorific value, and combustion characteristics.

Inventory and Remaining Fuel values track quantities of LNG, MGO, HFO, LO, and FW onboard. These metrics support voyage planning and ensure adequate fuel and consumables are available for the entire journey.

Lastly, Miscellaneous parameters, such as Main Engine FO supply temperature, though fewer, still contribute to engine performance optimization and operational safety when closely monitored.

Following the research methodology, the next step in the pipeline is data cleaning. In some cases, entire fields related to sensor-based measurements may be missing, likely due to data never being recorded. Such fields can be excluded from modelling if they do not provide meaningful information. So, features with more than 60% of missing values are removed (Table 5.12). There is full analysis of the dataset which contains the deleted data due to missing of more than 60% of columns in the Appendix 5,6 and 7 respectively.

Table 5. 12 Deleted features due to 60% of missing value.

	Deleted features due to 60% of missing value
Vessel 1	546
Vessel 2	498
Vessel 3	582

When missing data occurs at random, is minimal in proportion, and does not follow a systematic pattern, simple imputation methods can be applied. For instance, missing values may be replaced with the mean if the distribution of the feature is approximately systematic, or with the median if the feature is skewed. This decision is typically guided by the skewness report of the dataset. Specifically, when the skewness value is close to zero (between -0.5 and +0.5), the data is approximately normally distributed, and the mean can be safely used for imputation. If the skewness is moderate (between -1 and -0.5, or between +0.5 and +1), the data is slightly asymmetric, and in such cases, the median is generally more robust than the mean. For highly skewed distributions (less than -1 or greater than +1), where the data shows a strong long-tail effect, the median is the preferred imputation method. In Appendices 10, 11, and 12, there are lists of vessels showing the percentage of data imputation. In Appendices 13, 14, and 15, there are reports indicating whether the imputations were completed using the mean or median, depending on the skewness.

Moreover, related to duplication checks, they are performed to confirm that the dataset contains no redundant rows. Final validation steps include consistency checks and re-analysis to ensure that data quality is maintained after cleaning.

The next step involves removing features that are irrelevant to fuel prediction. The results of the drop of features in the dataset are that as it contains a very large number of vessel and cargo tank measurements, many of which are highly detailed engineering diagnostics rather than fuel consumption drivers which are deleted (Appendix 8). A significant portion of the variables are internal tank temperature readings (bottom, middle, upper, ceiling, side walls, and hull walls across all four tanks). These provide insight into structural and cargo condition monitoring but have negligible impact on overall vessel consumption. Similarly, there are numerous cofferdam temperature measurements across compartments (forward, aft, port, starboard, upper, middle, lower) that serve as structural safety references but are not relevant to consumption analysis.

Another large group consists of pump-related operational data, including current, discharge pressures, and valve positions for spray pumps and cargo pumps in each tank. While important for equipment diagnostics, they do not directly affect fuel or boil-off gas (BOG) consumption. The same applies to internal valve settings and tank pressurization details (supply/exhaust valves, IS pressure, N_2 differential), which are technical control parameters. Compressor diagnostics (filter differential pressures, IGV positions, inlet/outlet temperatures, orifice pressures) and vaporizer input/output readings fall into the same category: useful for maintenance monitoring but not linked to vessel consumption.

The dataset also includes fault flags (binary indicators such as N_2 generator system faults), which are valuable for event tracking but not consumption metrics. There are some duplicate or redundant measurements of fuel and BOG consumption (e.g., ME1/ME2 and DG-specific breakdowns), which are less useful since totals are already provided. More meaningful are the consolidated figures such as Total BOG consumption, NBOG, LBOG, forced boil-off, and BOG split to main engines, auxiliaries, or diesel generators. These totals, alongside environmental conditions (wind speed/direction, ambient air pressure and temperature, seawater temperature), provide direct relevance to vessel fuel performance and energy efficiency.

In addition, there are impact sensors and alarms that track structural vibrations or shocks per tank, again safety-oriented rather than consumption-related. Cargo condition monitoring is further supported by stratified liquid temperature readings (top, 95%, 60%, 30%, bottom for each tank), as well as trunk deck, pipe duct, and Inboard Sensor (IBS) pressure readings, which provide detailed cargo environment monitoring. Expanded sets of pump and compressor readings, plus spray inlet temperatures for each tank, add to the operational detail without strong consumption relevance. Finally, additional cofferdam temperatures and N_2 generator dew points readings appear as engineering quality checks.

Following 5.13, a feature-dropping process takes place, as many features are irrelevant. As described below, Vessel 1,2 amd 3 have 237 features with Appendix 9 to provide the dataset with remaining features.

Table 5. 13 Dropping features irrelevant to fuel consumption.

	Dropping features irrelevant to fuel consumption.
Vessel 1	237
Vessel 2	237
Vessel 3	237

As a completion of preparation in regards the features, a correlation matrix is made so that a dataset full to be presented as per Appendix 16, which concludes with the same features across three vessels.

Finally, a feature-merging process was applied, where pairs of similar features were combined into one. For example, GPS speed and LOG speed were merged, with GPS speed retained since it accounts for weather effects, unlike LOG speed. In addition, averages and totals of certain features were calculated to further reduce dimensionality and improve dataset efficiency. For instance, features such as drafts, shaft power, shaft RPM, DG power, ME torque, ME shaft power, ME RPM, and liquid volumes of tanks were aggregated. Ratios were also created, such as swell steepness (derived from swell height and frequency) and wave steepness. Similarly, total fuel consumption was consolidated into a single feature representing the combined.

Table 5.14 refers to 21 variables (columns) which was consistently applied across the datasets of all three vessels. The 21 variables are presented below:

- Ship Name – vessel identifier.
- Date Time – timestamp of each observation.
- Average Draft Mid [m] – average vessel draft used to represent loading and displacement condition.
- GPS Speed [knots] – vessel speed over ground.
- Shaft Power [kW] – propulsion shaft power.
- Shaft RPM [rpm] – shaft rotational speed.
- Total DG Power [kW] – combined electrical power generated by the diesel generators.
- Total ME Torque [kNm] – combined main-engine torque.
- Total ME Shaft Power [kW] – combined shaft power produced by the main engines.
- Average ME RPM [rpm] – average main-engine rotational speed.
- Wind Speed – prevailing wind-speed measurement.
- Current Speed – prevailing ocean-current speed.
- Water Temperature – sea-water temperature.
- BOG to GCU [kg/h] – boil-off gas directed to the Gas Combustion Unit.
- Reliquefaction Electrical Consumption [kW] – electrical power consumed by the reliquefaction system.
- Swell Steepness [m/s] – derived indicator representing swell characteristics.
- Maximum Starboard Roll [°] – maximum starboard rolling angle, representing vessel motion and possible sloshing.
- Wave Steepness – engineered feature calculated from wind-wave height divided by wind-wave period.
- Total Liquid Volume – engineered feature calculated as the sum of the LNG volume in cargo tanks 1–4.

- Vessel Condition – engineered categorical variable defined as *ballast* when total liquid volume is below 15,000 m^3 and *laden* when it is equal to or above 15,000 m^3.
- Total Consumption – total vessel fuel consumption and the target variable predicted by the machine-learning models.

Table 5. 14 Features of dataset for model generation.

1	Ship Name
2	Date Time
3	Average Draft Mid [m]
4	GPS speed [knots]
5	Shaft power [kW]
6	Shaft rpm [rpm]
7	Total DG Power [kW]
8	Total ME Torque [knm]
9	Total ME Shaft Power [kW]
10	Average ME RPM [rpm]
11	Wind Speed
12	Current Speed
13	Water Temperature
14	BOG to GCU [kg/h]
15	Reliquefaction - Electrical consumption [kW]",
16	Swell Steepness [m/s]
17	Roll max starboard (Sloshed) [°]",
18	Wave Steepness # Engineered: WindWaveHeight / Wind Wave Period (period median used for 0)
19	Total Liquid Volume # Engineered: sum of tanks 1 to 4 volume

20	Vessel Condition # Engineered: 'Ballast' if Total Liquid Volume < 15000 else 'Laden'
21	Total consumption

In summary, each of the three vessels began with 894 features as per Table 5.15. Feature reduction was performed in multiple stages. Features with over 60% missing values were first removed (546, 498, and 582 features deleted, respectively). Then, irrelevant or non-informative features were dropped (237 features, respectively). In the next step, redundant or highly correlated features were merged, retaining only the most representative ones. The resulting datasets each contained 21 final features for subsequent modeling and analysis.

Table 5. 15 Features handling.

	Vessel 1 (feature numbers)	**Vessel 2 (feature numbers)**	**Vessel 3 (feature numbers)**
Initial number of the Features	894	894	894
Deleted features due to 60% of missing value	546	498	582
Dropping the features due to irrelevance	237	237	237
Remaining data	108	159	75
Final number of features in the dataset	**21**	**21**	**21**

ii. Handling of Rows

Following the handling of features, the rows are subsequently processed. For fuel consumption modelling, categorical indicators such as operational modes (At Sea vs. In Port) help capture system variations, while data from docking, manoeuvring, cargo operations, anchoring, or drifting has been excluded for consistency. the model is focused solely on sailing periods, with the dataset filtered to retain only instances where GPS speed exceeds 5 knots, the minimum operational speed for LNG vessels. All rows with speed values below this threshold were removed to ensure alignment with the modelling objective.

For Vessel 1, the dataset in Table 5.16 shows a clear reduction in rows once entries with speeds below five are removed. In the laden condition, the full dataset originally contained 31,628 rows, out of which 7,228 rows were deleted. Similarly, in the ballast condition, the dataset had 38,543 rows in total, and 5,443 of these were eliminated. This indicates that both laden and ballast datasets had a significant portion of data points filtered out during the transformation process, though the laden dataset experienced a slightly larger proportion of deletions compared to ballast.

Table 5. 16 Vessel 1 - Data Transformation per vessel (Deleted rows). .

	Number full dataset (rows)	**Deleted rows due to speed less than 5 knots (rows)**	
Laden	31628	7228	
Ballast	38543	5443	

For Vessel 2, the data transformation in Table 5.17 also involved removing rows that did not meet the required speed threshold. In the laden case, the dataset consisted of 34,668 rows initially, with 6,131 rows deleted. For the ballast condition, the full dataset contained 35,377 rows, and 8,117 rows were eliminated. Compared to Vessel 1, Vessel 2 had fewer deletions in the laden condition but a slightly higher number of removed rows in the ballast dataset. This demonstrates that the speed filter influenced both operational modes differently across vessels, though the scale of deletions remains significant.

Table 5. 17 Vessel 2 - Data Transformation per vessel (Deleted rows).

	Number full dataset (rows)	**Deleted rows due to speed less than 5 knots (rows)**
Laden	34668	6131
Ballast	35377	8117

For Vessel 3, the process resulted, as shown Table 5.18 in an even higher level of data reduction in comparison to the other vessels. In the laden condition, the dataset originally included 32,191rows, and 5,004 of these were removed. The ballast dataset contained 37,968 rows in total, and as many as 5,379 rows were deleted. This shows that Vessel 3 had the largest number of deletions overall, particularly in the ballast condition. The results suggest that this vessel had more instances of low-speed operations, making it more affected by the data transformation rule than Vessels 1 and 2.

Table 5. 18 Vessel 3 - Data Transformation per vessel (Deleted rows).

	Number full dataset (rows)	**Deleted rows due to speed less than 5 knots (rows)**
Laden	32191	5004
Ballast	37968	5379

Table 5.19 presents Each vessel dataset initially consisted of approximately 70,000 unique data points (70,171 for Vessel 1, 70,045 for Vessel 2, and 70,159 for Vessel 3). Data cleaning involved removing instances where vessel speed was below 5 knots, reducing the datasets by 12,671, 14,248, and 10,383 observations, respectively. The cleaned data were subsequently divided into subsets: 10% reserved as unseen validation data and the remaining 90% partitioned into training (80%) and testing (20%) datasets. The resulting training sets contained 41,400, 40,174, and 43,040 records, while the testing sets contained 10,350, 10,045, and 10,760 records for Vessels 1, 2, and 3, respectively.

Table 5. 19 Columns handling.

	Vessel 1 (rows)	**Vessel 2 (rows)**	**Vessel 3 (rows)**
Initial number of column (unique data points)	70171	70045	70159
Deleted due speed less than 5 knots	12671	14248	10383
10% unseen dataset	5752	5581	5978
80% training of dataset	41400	40174	43040
20% testing of dataset	10350	10045	10760

In conclusion, after handling both features and rows, the total number of data points included in the model generation (80% training + 20% testing) was computed by multiplying the final 21 features with the combined training and testing records, yielding 3,271,107 (Table 5.20). For Vessel 1, this is calculated as 21 × (41,400 + 10,350) = 1,086,750. For Vessel 2, the calculation is 21 × (40,174 + 10,045) = 1,054,557. For Vessel 3, it is 21 × (43,040 + 10,760) = 1,129,800.

Table 5. 20 Total data included in each dataset.

	Vessel 1 (dataset)	**Vessel 2 (dataset)**	**Vessel 3 ((rows)**
Total number of data included in the model generation (80% training + 20% testing)	21 * (41400+10350) = = 1.086.750	21 * (40174+10.045)= 1.054.599	21 *(43040+10760) = = 1.129.800

In conclusion, the handling of dataset related to columns and features have been processed properly following the research methodology in the Chapter 4. Therefore, there is a table below which summarizes the results of the datasets handling.

5.4.3.3 Learning algorithms

Following the research methodology, the next step involves developing the prediction model. Artificial Intelligence (AI) models, particularly supervised learning techniques, play a crucial role in forecasting maritime vessel fuel consumption (Melo et al., 2024. Specifically, the models applied are Linear Regression, Lasso Regression, Random Forest, Gradient Boosting, AdaBoost, XGBoost, Histogram-based Gradient Boosting, and LightGBM following the codes provided in the Appendix 17 - Coding for the fuel prediction.

5.4.3.4 Evaluation metrics

After running the models, the results of each case study based on the evaluation metrics are presented. The best-performing model is assessed using R^2, Mean Absolute Error (MAE), and Root Mean Square Error (RMSE), with the final selection determined by MAE for its direct interpretation of average prediction error in the testing process.

Overall, the best-performing model for Vessel 1 is the Random Forest, with MAE = 0.003, RMSE = 0.007, and R^2 = 0.998 during training, and MAE = 0.009, RMSE = 0.018, and R^2 = 0.985 during testing (Table 5.21).

Table 5. 21 Vessel 1 - Evaluation of metrics per machine learning model.

Training (80%)	**Model**	**MAE**	**RMSE**	**R^2**
	Linear	0.027	0.041	0.924
	Lasso	0.03	0.043	0.918
	Random forest	0.003	0.007	0.998
	Gradient Boosting	0.019	0.03	0.961
	AdaBoost	0.038	0.05	0.887
	XGBoost	0.009	0.014	0.991

	Hist Gradient Boosting	0.012	0.02	0.981
	Light GBM	0.013	0.02	0.981
Testing (20%)	**Model**	**MAE**	**RMSE**	**R^2**
	Linear	0.028	0.041	0.923
	Lasso	0.03	0.043	0.917
	Random forest	0.009	0.018	0.985
	Gradient Boosting	0.02	0.03	0.959
	AdaBoost	0.039	0.051	0.885
	XGBoost	0.012	0.02	0.982
	Hist Gradient Boosting	0.013	0.022	0.978
	Light GBM	0.013	0.022	0.978

However, for Vessel 2, the best-performing model is again the Random Forest, with MAE = 0.003, RMSE = 0.007, and R^2 = 0.999 during training, and MAE = 0.007, RMSE = 0.019, and R^2 = 0.992 during testing (Table 5.22).

Table 5. 22 Fuel consumption results of the Vessel 2.

Training (80%)	**Model**	**MAE**	**RMSE**	**R^2**
	Linear	0.03	0.044	0.0955
	Lasso	0.037	0.051	0.939
	Random forest	0.003	0.007	0.999

	Gradient Boosting	0.02	0.033	0.976
	AdaBoost	0.042	0.055	0.931
	XGBoost	0.009	0.016	0.994
	Hist Gradient Boosting	0.012	0.021	0.99
	Light GBM	0.012	0.021	0.99
Testing (20%)	**Model**	**MAE**	**RMSE**	**R^2**
	Linear	0.03	0.043	0.956
	Lasso	0.036	0.05	0.941
	Random forest	0.007	0.019	0.992
	Gradient Boosting	0.02	0.033	0.974
	AdaBoost	0.042	0.055	0.93
	XGBoost	0.01	0.02	0.991
	Hist Gradient Boosting	0.013	0.022	0.989
	Light GBM	0.013	0.022	0.989

Lastly, vessel 3 results, the best-performing model is again the Random Forest, with MAE = 0.002, RMSE = 0.004, and R^2 = 0.999 during training, and MAE = 0.005, RMSE = 0.009, and R^2 = 0.997 during testing (Table 5.23).

Table 5. 23 Fuel consumption results of the Vessel 3.

Training (80%)	Model	MAE	RMSE	R²
	Linear	0.023	0.035	0.962
	Lasso	0.025	0.038	0.954
	Random forest	0.002	0.004	0.999
	Gradient Boosting	0.013	0.018	0.989
	AdaBoost	0.038	0.045	0.934
	XGBoost	0.005	0.008	0.998
	HistGradient Boosting	0.007	0.011	0.996
	Light GBM	0.007	0.011	0.996
Testing (20%)	**Model**	**MAE**	**RMSE**	**R²**
	Linear	0.023	0.035	0.961
	Lasso	0.025	0.037	0.955
	Random forest	0.005	0.009	0.997
	Gradient Boosting	0.013	0.019	0.989
	AdaBoost	0.038	0.045	0.934
	XGBoost	0.006	0.01	0.997
	Hist Gradient Boosting	0.008	0.012	0.995
	Light GBM	0.008	0.012	0.995

5.4.3.5 Fuel consumption results

In the three case studies using Random Forest as the predictive model, the results show a very close alignment between actual and predicted fuel consumption across both laden and ballast conditions. For Vessel 1, the actual fuel consumption is 1255.84 metric tons (mt) (laden) and 2130.26 mt (ballast), while the prediction is 1258.67 mt and 2133.87 mt respectively, showing only minor deviations of about 2.8 and 3.6 tonnes (Table 5.24)

Table 5. 24 Fuel consumption results of the vessel 1.

Vessel 1	**Laden (mt)**	**Ballast(mt)**
Actual Fuel consumption	1255.84	2130.26
Predicted Fuel consumption	1258.67	2133.87

Similarly, for Vessel 2, the actual values are 2133.23 mt (laden) and 1693.15 mt (ballast), compared to predictions of 2126.35 mt and 1698.17 mt, with small differences of –6.9 and +5.0 tonnes (Table 5.25)

Table 5. 25 Fuel consumption results of the vessel 2.

Vessel 2	**Laden(mt)**	**Ballast(mt)**
Actual Fuel consumption	2133.23	1693.15
Predicted Fuel consumption	2126.35	1698.17

For Vessel 3, the accuracy is a slightly higher, with actual values of 1678.22 mt (laden) and 1500.69 mt (ballast) compared to predictions of 1677.48 tonnes and 1500.10 mt, showing negligible differences of –0.74 and –0.59 mt (Table 5.26).

Table 5. 26 Fuel consumption results of the vessel 3.

Vessel 3	**Laden(mt)**	**Ballast(mt)**
Actual Fuel consumption	1678.22	1500.69
Predicted Fuel consumption	1677.48	1500.10

These results confirm that the Random Forest model provides highly reliable and accurate predictions of fuel consumption, with deviations consistently within only a few units when comparing predicted to actual values. This demonstrates its robustness and suitability as the best-performing model for fuel consumption prediction in both laden and ballast operations.

In conclusion, all three vessels are LNG carriers of the same type, equipped with the same propulsion technology and sail worldwide. However, there are differences which reflect variations in voyage execution, operating conditions and weather conditions.

The observed variations in performance were mainly associated with route- and operational-level factors, including differences in weather conditions such as wind, waves, and ocean currents, trading routes and voyage distances, speed optimisation and engine loading strategies, and operational decisions related to boil-off gas (BOG) management, reliquefaction, and propulsion mode. Port waiting times and cargo-handling practices also introduced additional variability into the vessels' operational profiles.

Vessel 2 recorded the highest prediction deviations because its operational profile exhibited greater variability. More frequent speed changes, exposure to diverse environmental conditions, and less consistent operating patterns. Vessels 1 and 3 demonstrated lower prediction deviations, as their voyages were generally characterised by more stable operating conditions, more consistent sailing speeds, and smoother voyage execution, allowing the predictive models to estimate their operational performance more accurately.

A similar pattern was identified when comparing laden and ballast voyages. Laden voyages generally produced smaller prediction errors, as vessel displacement, draft, and propulsion conditions tended to remain relatively stable throughout the voyage. Conversely, ballast voyages exhibited greater operational variability due to changes in LNG heel quantity, BOG utilisation, ballast condition, and propulsion management, making vessel performance more challenging to predict accurately.

Overall, the results indicate that vessels operating under more stable and consistent operational profiles achieved lower prediction deviations across multiple performance indicators. This suggests that fuel prediction is influenced not only by vessel characteristics but also by the consistency of voyage execution and operational management. The findings therefore demonstrate the ability of the CSI framework to capture differences in operational reliability across vessels operating under varying trading and environmental conditions.

5.4.4 Fuel in laden model

The results of the fuel in laden model are based on three LNG vessels, as per section "5.4.3.5 Fuel consumption results" and consider the results of fuel consumption only in laden passage. This shows that the predicted values generated by the Random Forest model are very close to the actual recorded consumption, with only minimal differences. For Vessel 1, the actual fuel consumption was 1255.84 mt, while the predicted amount was 1258.67 mt, resulting in a small difference of 2.83 mt. In the case of Vessel 2, the actual consumption was 2133.23 tons, compared with a prediction of 2126.35 mt, giving a difference of 6.88 mt. For Vessel 3, the accuracy was particularly high, with actual consumption of 1678.22 mt and a prediction of 1677.48 mt, leaving only a 0.74-ton difference (Table 5.27).

In Conclusion, the results demonstrate that the model achieves remarkably accurate predictions, with discrepancies between actual and predicted consumption kept consistently low. The largest deviation was just 6.88 mt (Vessel 2), while the smallest was 0.74 mt (Vessel 3), confirming that the Random Forest model provides highly reliable estimates of fuel consumption across different vessels.

Table 5. 27 Fuel consumption results.

Fuel in laden model				
Vessel Name	**Step 1: The total actual consumption (mt) is defined.**	**Step 2: The total predicted consumption (mt) is defined (mt) is defined**	**Step 3: The difference between actual and predicted amount (mt) is defined**	**Results of the actual and predicted amount in %**
Vessel 1	1255.84	1258.67	2.83	0.23%
Vessel 2	2133.23	2126.35	6.88	0.32%
Vessel 3	1678.22	1677.48	0.74	0.04%

5.4.5 Heel amount results

Heel modelling generated by the thesis study is based on the LNG fuel required for operational purposes and vessel needs for any other reason as mainly for preparation of a loading operation by cooling down the cargo tanks. However, the prediction of the LNG heel amount required for cargo tank cooling is excluded from this model, as it was explained in the Chapter 4 with the research methodology, as specific data needed for calculating the amount needed for the cooling down. Therefore, the prediction of the LNG heel amount is based on the vessel's fuel consumption model developed for ballast conditions.

The analysis of heel amounts based on the section "5.4.3.5 Fuel Consumption results" across the three vessels shows that the predicted values are very close to the actual recorded values, with only small differences observed (Table 5.28). For Vessel 1, the actual heel amount was 2130.26 mt, while the model predicted 2133.87 mt, resulting in a difference of 3.61 mt. For Vessel 2, the actual heel was 1693.15 mt compared to a predicted value of 1698.17 mt, with a deviation of 5.02 tons. Finally, Vessel 3 showed the smallest discrepancy, with an actual heel of 1500.69 tons and a predicted value of 1500.10 tons, leaving a difference of only 0.59 tons.

In Conclusion, the results in Table 5.28 highlight the high accuracy of the prediction model for heel amounts, with deviations consistently within just a few tons. The largest observed difference was 5.02 mt (Vessel 2), while the smallest was 0.59 mt (Vessel 3). This confirms that the model provides robust and reliable estimates of heel amounts across different vessels.

Table 5. 28 Heel results.

Vessel Name	**Step 1: The total heel amount (mt) is defined.**	**Step 2: The total predicted heel amount (mt) is defined**	**Step 3: The difference between actual and predicted heel amount (mt) is defined**	**Results of the actual and predicted amount in %**
Vessel 1	2130.26	2133.87	3.61	0.17
Vessel 2	1693.15	1698.17	5.02	0.30
Vessel 3	1500.69	1500.1	0.59	0.04

5.4.6 Estimated Discharging Quantity model results

The Estimated Discharging Quantities (EDQ) is another key performance metric and so a relative model is generated. EDQ model is based on the loaded cargo quantity minus the LNG fuel consumed during the laden voyage to the discharging port, as well as the fuel required for the ballast passage back to the loading port. However, as it is outlined in the section 4.4.6 “Estimated Discharging quantities” factors such as Quantity Expansion or Shrinkage (QES) and GCU amount are excluded from the formula.

For practical reasons, the loaded cargo quantity is considered a fixed value of 174,000 cubic meters or 74,820 tonnes (considering 0.43 m3/tonnes for the density) per vessel, with fuel consumption playing a significant role in determining the final discharging quantity. The analysis of Estimated Discharging Quantities (EDQ) demonstrates that the predicted values are almost identical to the actual recorded figures, with only minimal differences across all three vessels. More specifically, the results are as follows:

For Vessel 1, the actual discharging quantity was 71,434 tons of LNG, while the model predicted 71,427 tonnes, resulting in a very small difference of 6.44 m^3. Specifically, calculations are as follows:

- 74,820 mt – 1,255.84 mt – 2,130.26 mt = 71,434 mt are the actual discharging quantity
- 74,820 mt -1,258.67 mt – 2,133.87 mt = 71,427 mt are the predicted discharging quantity

For Vessel 2, the actual amount was 70,994 tons compared to a predicted value of 70,995 mt giving a difference of just 1.86 mt. Specifically, calculations are as follows:

- 74,820 mt - 2,133.23 mt – 1,693.15 tonnes = 70,994 mt are the actual discharging quantity
- 74,820 mt - 2.126,35 mt -1698,17 mt = 70,995 mt are the predicted discharging quantity

Finally, Vessel 3 showed the highest precision, with an actual discharging quantity of 71,641 mt and a predicted value of 71,642 mt, leading to a difference of only 1.33 mt. Specifically, calculations are as follows:

Table 5. 29 Estimated Discharging Quantities results. .

Estimated Discharging Quantities				
Vessel Name	**Step 1: The total actual consumption (mt) is defined.**	**Step 2: The total predicted consumption (mt) is defined**	**Step 3: The difference between actual and predicted amount (mt) is defined**	**Results of the actual and predicted amount in %**
Vessel 1	71,434	71,427	6.44	0.004
Vessel 2	70,994	70,995	1.86	0.001
Vessel 3	71,641	71,642	1.33	0.001

5.4.7 Emission footprint model results

The emission footprint model of the vessel is calculated based on the fuel consumption which is predicted in the section "5.4.3.5 Fuel Consumption results" considering both passages, laden and ballast. More specifically, the actual values refer to the total amount of the fuel consumption in both passages compared to the respective predicted values predicted and are multiplied with the emission factor of the LNG fuel which is 2.75 (Table 4.30).

For Vessel 1, the total actual emissions were 9,311.77 tonnes CO_2 compared with a predicted value of 9,329.49 tonnes CO_2, resulting in a difference of 17.71 tonnes of CO_2. Specifically, calculations are as follows:

- ➢ 1,255.84 mt + 2,130.26 mt = 3,386.1 mt and so 3,3861 tonnes * 2.75 = 9,311.77 tonnes CO_2 is the actual emission amount
- ➢ 1,258,67 mt + 2,133,87 mt = 3,392.54 tonnes and so 3,392.54 tonnes * 2.75 = 9,329.49 tonnes CO_2 is the predicted emission amount

Vessel 2 recorded an actual footprint of 10,522.55 tonnes CO_2 while the predicted amount was 10,517.43 tonnes CO_2 leaving a deviation of just 5.12 tonnes CO_2. Specifically, calculations are as follows:

- ➢ 2,133.23 mt + 1,693 mt = 3,826.23 mt and so 3,826.23 tonnes * 2.75 = 10,522.55 tonnes CO_2 is the actual emission amount

- 2,126.35 mt + 1,698.17 mt = 3,824.52 mt and so 3,824.52 tonnes * 2.75 = 10,517.43 tonnes CO_2 is the predicted emission amount

Finally, Vessel 3 showed the highest accuracy, with an actual emission footprint of 8,742 tonnes CO_2 versus a predicted amount of 8,738.34 tonnes CO_2 producing an almost negligible difference of 3.65 tons CO_2. Specifically, calculations are as follows:

- 1,678.22 mt + 1,500.69 mt = 3,178.91 mt and so 3,178.91 tonnes * 2.75 = 8,742 tonnes CO_2 is the actual emission amount
- 1,677.48 mt + 1,500.69 mt = 3,178.17 mt considering and so 3,178.17 tonnes * 2.75 = 8,738.34 tonnes CO_2 is the predicted emission amount

In conclusion, the results in Table 5.30 confirm that the model provides highly accurate predictions of emission footprint and carbon emissions, with discrepancies consistently below 2 tons across all vessels. The very small deviations, less than 0.2% of actual values, demonstrate the robustness of the predictive approach and highlight its potential to support effective carbon emission strategies and monitoring efforts in maritime operations.

Table 5. 30 Emission Footprint results. .

Emission footprint				
Vessel Name	**Step 1:** **The total amount of Emission footprint & Carbon Emission Strategy (tonnes CO_2) is defined.**	**Step 2:** **The total predicted amount of Emission footprint & Carbon Emission footprint (tonnes CO_2) is defined.**	**Step 3:** **The difference between the total amount and predicted amount of Carbon Emission footprint (tonnes CO_2) is defined.**	**Results of the actual and predicted amount in %**
Vessel 1	9,311.77	9,329.48	17.71	0.19
Vessel 2	10,522.54	10,517.43	5.12	0.05
Vessel 3	8,742.00	8,738.34	3.65	0.04

5.4.8 Results and Performance Evaluation of the research framework

This section presents the comprehensive results of the research framework, conducted using the methodology outlined in Chapter 4 and applied to three XDF vessels as case studies. For clarity, the formula for the Charterer Satisfaction Index (CSI) is presented below as follows:

Therefore, it is provided the results of Charterer Satisfaction Index (CSI) of the three case studies based on the following: Fuel in laden Consumption model, Heel model, Estimated Discharging Quantities model, and Emission Footprint model. Related to the weights of the model importance, AHP method has been applied following the methodology and relative calculation is presented in detail in Appendix 1 and 2.

Following Table 5.31, the evaluation of Vessel 1's performance metrics shows that the Random Forest model provides highly accurate predictions with only small deviations from the actual values. Fuel consumption shows a small deviation of 2.83, contributing 0.29 after weighting, while heel amount records a deviation of 3.61 with a weighted contribution of 0.83. Estimated discharging quantities have the largest influence, with a deviation of 6.44 and a weighted contribution of 3.79 due to their higher importance. Emission footprint shows a deviation of 17.71 but contributes only 1.40 because of its lower weight. Overall, these results lead to an average deviation in predicted performance metrics of 6.31, reflecting good operational consistency for Vessel 1.

Table 5. 31 Vessel 1: Performance Deviation Analysis.

Vessel 1			
Key Performance Metrics	**Step 1: using the formula Σ ((Predicted$_i$ − Actual$_i$) ÷ Predicted$_i$)**	**Step 3: weighted the formula. Σ [((Predicted$_i$ − Actual$_i$) ÷ Predicted$_i$) × w$_i$]**	
		weight	
Fuel consumption results	**2.83**	**10.2%**	**0.29**
Heel amount	**3.61**	**23.1%**	**0.83**
Estimated Discharging quantities	**6.44**	**58.8%**	**3.79**
Emission footprint	**17.71**	**7.9%**	**1.40**
Average deviation in predicted performance metrics		**6.31**	

Table 5.32 for Vessel 2's performance metrics shows that fuel consumption has a deviation of 6.88, which contributes 0.70 after weighting, while heel amount shows a deviation of 5.02 with a weighted contribution of 1.16. Estimated discharging quantities record a very small deviation

of 1.33 and, despite having the highest weight, contributed only 0.78. Emission footprint has a deviation of 5.11 and contributes 0.40 due to its lower weight. Overall, these weighted results lead to an average deviation in predicted performance metrics of 3.05, indicating high prediction accuracy and consistent operational performance for Vessel 2.

Table 5. 32 Vessel 2: Performance Deviation Index Analysis.

Vessel 2			
Key Performance Metrics	**Step 1: using the formula Σ ((Predicted$_i$ − Actual$_i$) ÷ Predicted$_i$)**	**Step 3: weighted the formula. Σ [((Predicted$_i$ − Actual$_i$) ÷ Predicted$_i$) × w$_i$]**	
		weight	
Fuel consumption results	**6.88**	**10.2%**	**0.70**
Heel amount	**5.02**	**23.1%**	**1.16**
Estimated Discharging quantities	**1.33**	**58.8%**	**0.78**
Emission footprint	**5.11**	**7.9%**	**0.40**
Average deviation in predicted performance metrics		**3.05**	

The results in Table 5.33 show results of Vessel 3 performance metrics, which indicates excellent agreement between predicted and actual performance metrics, with very small deviations across all categories. Fuel consumption shows a minimal deviation of 0.74, contributing only 0.08 after weighting, while heel amount has a deviation of 0.59 with a weighted contribution of 0.14. Estimated discharging quantities, despite having the highest weight, record a low deviation of 1.33 and contribute 0.78. Emission footprint shows a deviation of 3.66 and contributes 0.29 due to its lower weight. Overall, the average deviation in predicted performance metrics is 1.28, demonstrating the highest prediction accuracy and best operational consistency among the vessels.

Table 5. 33 Vessel 3: Performance Deviation Index Analysis.

Vessel 3			
Key Performance Metrics	**Step 1: using the formula Σ ((Predicted$_i$ − Actual$_i$) ÷ Predicted$_i$)**	**Step 3: weighted the formula. Σ [((Predicted$_i$ − Actual$_i$) ÷ Predicted$_i$) × w$_i$]**	
		weight	
Fuel consumption results	**0.74**	**10.2%**	**0.08**
Heel amount	**0.59**	**23.1%**	**0.14**
Estimated Discharging quantities	**1.33**	**58.8%**	**0.78**
Emission footprint	**3.66**	**7.9%**	**0.29**
Average deviation in predicted performance metrics		**1.28**	

In conclusion, the Charterer Satisfaction Index (CSI) results in The Charterer Satisfaction Index (CSI) case study compares the overall performance of three vessels based on their weighted deviations in predicted performance metrics. The Charterer Satisfaction Index (CSI) results show that Vessel 3 achieves the highest level of charterer satisfaction with the lowest CSI value (1.28), indicating very close alignment between predicted and actual performance. Vessel 2 follows with a CSI of 3.05, while Vessel 1 records a slightly higher CSI of 6.31, reflecting larger performance deviations. Overall, all Vessels perform very efficiently as the results are very close to zero.

4 highlight varying levels of performance across the three vessels. The Charterer Satisfaction Index (CSI) case study compares the overall performance of three vessels based on their weighted deviations in predicted performance metrics. The Charterer Satisfaction Index (CSI) results show that Vessel 3 achieves the highest level of charterer satisfaction with the lowest CSI value (1.28), indicating very close alignment between predicted and actual performance. Vessel 2 follows with a CSI of 3.05, while Vessel 1 records a slightly higher CSI of 6.31, reflecting larger performance deviations. Overall, all Vessels perform very efficiently as the results are very close to zero.

Table 5. 34 Summary of Charterer Satisfaction Index per vessel.

Case study No.	**Charterer Satisfaction Index (CSI)**
Vessel 1	6.31
Vessel 2	3.05
Vessel 3	1.28

5.4.9 Sensitivity analysis of CSI

This section of Chapter 5 presents the sensitivity analysis of the Charterer Satisfaction Index (CSI). Following the results obtained from the proposed research framework, a sensitivity analysis is conducted to evaluate how variations in prediction accuracy affect CSI. The analysis incorporates insights from interviews with industry experts, as detailed in Appendix 18, with the corresponding results summarized in Appendix 19.

The interview participants possess extensive practical experience within the shipping industry. The majority have served as ship captains and have held both onboard and shore-based operational roles. A smaller proportion of participants come from commercial and managerial backgrounds, contributing valuable perspectives on market-oriented and business decision-making. Overall, the interview sample represents a well-balanced and highly experienced group, ensuring the reliability of the qualitative input used in the sensitivity analysis.

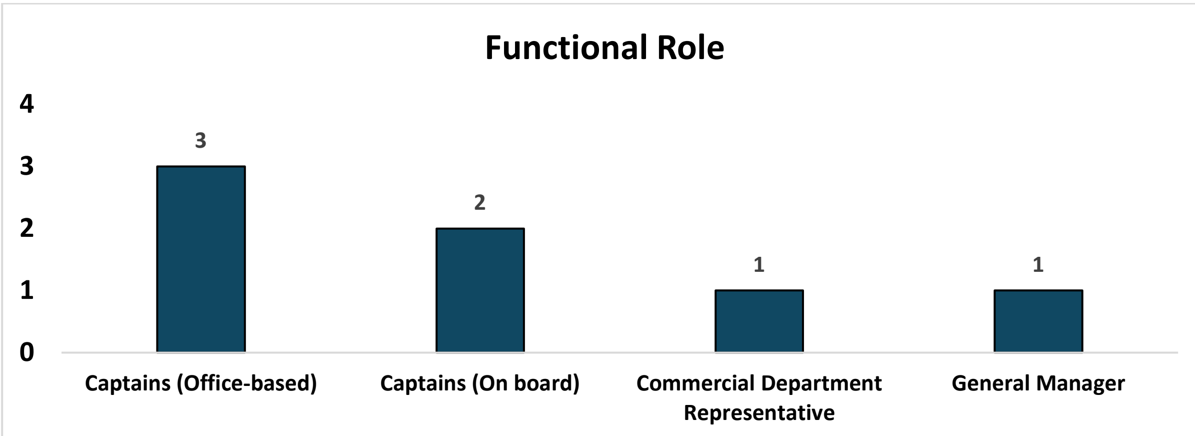

Figure 5.38. Functional Role for Interview for CSI Sensitivity analysis.

Based on expert input and analytical results, CSI values are categorized into five satisfaction levels according to predefined score ranges. Importantly, lower CSI values correspond to higher charterer satisfaction, as they reflect smaller deviations between predicted and actual vessel performance. CSI scores between 0 and 100 indicate Very High Satisfaction, representing excellent predictive accuracy and strong alignment with charterer expectations. Scores in the range of 100 to 200 correspond to High Satisfaction, reflecting generally positive performance with minor discrepancies. A CSI range of 200 to 300 indicates Moderate Satisfaction, where operational outcomes meet expectations but allow room for improvement. Scores between 300 and 400 represent Low Satisfaction, suggesting noticeable deviations that may affect charterer confidence. Finally, CSI values above 400 indicate Very Low Satisfaction, highlighting significant performance inconsistencies that require immediate corrective actions (Table 5.35).

Table 5. 35 CSI Score range.

CSI Score Range	Very Low Satisfaction	Low Satisfaction	Moderate Satisfaction	High Satisfaction	Very High Satisfaction
0–100					X
100–200				X	
200–300			X		
300–400		X			
400+	X				

Considering that Fuel consumption prediction accuracy is categorized into four levels Fuel consumption prediction accuracy is similarly classified into four levels based on the magnitude of prediction error. An error range of 0%–3% is defined as Highly Accurate, indicating strong predictive reliability. Errors between 3% and 6% are considered Acceptable Accuracy, reflecting minor deviations with limited operational impact. Prediction errors in the range of 6%–10% are categorized as Low Accuracy, where discrepancies become noticeable and may influence charterer trust. Errors above 10% are classified as Poor Accuracy, indicating unreliable predictions with a substantial negative effect on satisfaction (Table 5.36)

Table 5. 36 Prediction Error Range.

Prediction Error Range	Highly Accurate	Acceptable Accuracy	Low Accuracy	Poor Accuracy
0%–3%	X			
3%–6%		X		
6%–10%			X	
Above 10%				X

The sensitivity analysis of CSI is based on the relationship between prediction accuracy and CSI values across the three vessels. In the thesis research study, all vessels record very low CSI values, with Vessel 3 consistently outperforming Vessels 2 and 1, indicating the highest level of charterer satisfaction. As prediction error increases from the 0–3% range to above 10%, CSI values rise significantly for all vessels, reflecting a corresponding decline in satisfaction.

Therefore, applying this categorization to the CSI results from the sensitivity analysis:

- Thesis research study (CSI ≈ 1–7): Falls within 0–100, indicating Very High Satisfaction for all vessels.
- 0–3% deviation range (CSI ≈ 92–100): Also, within 0–100, representing Very High Satisfaction.
- 3–6% deviation range (CSI ≈ 185–201): Lies in 100–200, corresponding to High Satisfaction.
- 6–10% deviation range (CSI ≈ 307–335): Falls in 300–400, indicating Low Satisfaction.
- Above 10% deviation range (CSI ≈ 339–368): Remains in 300–400, reflecting Low Satisfaction.

This categorization shows that charterer satisfaction decreases steadily as deviation levels increase, with very high satisfaction achieved only when performance deviations are minimal.

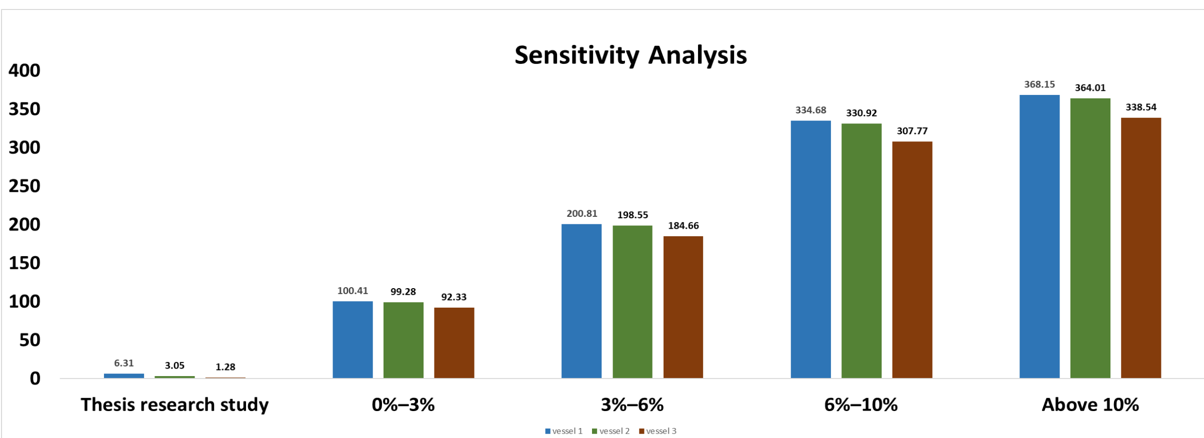

Figure 5.39. CSI Sensitivity analysis.

In conclusion, applying the CSI satisfaction categorization to the sensitivity analysis results confirms that Very High Satisfaction is achieved only when prediction deviations are minimal. As error levels increase, satisfaction declines progressively from High to Low Satisfaction, reinforcing the importance of predictive accuracy in maintaining charterer confidence. Overall, the findings validate the robustness of the proposed CSI framework and highlight its effectiveness in capturing the impact of operational deviations on charterer satisfaction.

5.4.10 Conclusion

This study developed and applied a structured research framework to evaluate LNG vessel performance in relation to charterer satisfaction. The framework is demonstrated through case studies, showcasing its practical application. Based on these outcomes, the following chapter presents a detailed discussion and interpretation of the findings.

6. Chapter 6 - Conclusion

6.1 Introduction

This chapter concludes the research by summarising the key findings and discussing their implications for both academic knowledge and industry practice. It presents the main contributions of the research, acknowledges its limitations and challenges, and identifies opportunities for future work.

6.2 Findings and conclusions

This section of the chapter presents the findings and conclusions derived from the research framework, which is designed to address the need for a structured, data-driven approach to measuring charterer satisfaction in the LNG shipping industry.

Therefore, this research demonstrates that machine learning techniques can be successfully applied to predict key operational performance indicators for LNG carriers and that these predictions can be integrated into a practical framework for evaluating charterer satisfaction. The proposed Charterer Satisfaction Index (CSI) combines predictions of fuel consumption, heel quantity, estimated discharging quantity, and emission footprint into a single performance measure, providing an objective assessment of vessel commercial performance from the charterer's perspective.

The results indicate that the proposed framework is capable of accurately estimating operational performance across the three case-study vessels. Among the machine learning algorithms evaluated, the Random Forest model consistently provided the most reliable predictions and therefore formed the basis of the Charterer Satisfaction Index. Rather than relying on a single operational parameter, the framework demonstrates that combining multiple performance indicators produces a more comprehensive assessment of commercial performance.

The predictive performance across the three vessel datasets was compared to assess the consistency and robustness of the developed models.The Random Forest model demonstrated consistently high predictive performance across all three datasets, with R^2 values exceeding 0.98. Vessel 3 achieved the highest accuracy, followed by Vessel 2 and Vessel 1, although the differences were marginal. Overall, the results indicate that the selected features effectively captured the vessels' operational behaviour.The small variations in predictive performance are mainly attributed to differences in dataset size and operational conditions, including voyage profiles, environmental conditions, vessel speed, engine loading, BOG management, reliquefaction operation, and cargo characteristics. Since the same features, preprocessing procedures, data splitting, and modelling methodology were applied to all three datasets, these differences primarily reflect dataset and operational variability rather than vessel design or modelling approach.

Also, the findings demonstrate that expert judgement can be effectively integrated with predictive analytics through the Analytic Hierarchy Process (AHP). By assigning different levels of importance to the operational performance criteria, the framework reflects the priorities of LNG charterers and provides a transparent method for evaluating vessel performance beyond purely technical measures.

Overall, the research confirms that smaller deviations between predicted and actual operational performance are associated with higher levels of charterer satisfaction. Consequently, the proposed Charterer Satisfaction Index provides shipping companies and charterers with a practical decision-support tool that can assist vessel performance evaluation, vessel selection, and operational planning.

Also, the research further demonstrates that objective operational data can complement traditional customer satisfaction approaches. Unlike perception-based models that rely primarily on customer opinions or surveys, the proposed framework measures satisfaction using measurable operational performance, thereby introducing a data-driven perspective to service-performance evaluation in LNG shipping.

Finally, the study highlights the growing role of artificial intelligence and data analytics in maritime management. By integrating predictive modelling with commercial performance assessment, the proposed framework contributes to the digital transformation of LNG shipping and provides a foundation for future decision-support applications within maritime logistics.

6.3 Contribution of the research

The main contributions of this research are categorized into practical, methodological, and academic contributions. These contributions collectively address operational challenges in LNG shipping, advance predictive and decision-making methodologies, and extend existing literature on service-performance evaluation.

i. Practical Contribution to LNG Shipping Management

From a practical perspective, this research develops a Charterer Satisfaction Index (CSI) that provides shipping companies and charterers with an objective and data-driven tool for evaluating the commercial performance of LNG vessels. The framework uses AI-based predictive models to estimate fuel consumption, heel quantity, estimated discharging quantity, and emission footprint, which represent key operational and commercial performance criteria. By comparing predicted and actual vessel performance, shipping companies can benchmark vessel performance, identify operational deviations, and improve transparency in their relationships with charterers. At the same time, the CSI can support charterers in evaluating vessels whose expected operational performance is closely aligned with contractual and commercial requirements, thereby reducing commercial uncertainty and supporting more informed decision-making.

ii. Methodological Contribution

From a methodological perspective, the research proposes a novel integrated framework combining machine learning predictive models with an expert-based multi-criteria decision-making approach. Four independently developed predictive models—covering fuel consumption, heel quantity, estimated discharging quantity, and emission footprint—are integrated into a single Charterer Satisfaction Index (CSI). The Analytic Hierarchy Process (AHP) is used to derive expert-based weights for these criteria, ensuring that their relative contribution to the CSI reflects their commercial importance from the charterer's perspective. This approach demonstrates how predictive analytics and expert judgement can be systematically combined within a transparent, objective, and reproducible framework for LNG vessel performance evaluation.

iii. Academic Contribution to Satisfaction and Service-Performance Research

From an academic perspective, the research extends the literature on customer satisfaction and service-performance measurement by introducing an objective, data-driven approach to assessing charterer satisfaction in LNG shipping. It complements established satisfaction frameworks, including SERVQUAL, Expectancy-Disconfirmation Theory, and the Kano Model, which predominantly rely on subjective perceptions, by incorporating objectively measured operational performance. Furthermore, the research demonstrates how machine learning and predictive analytics can be integrated into satisfaction assessment, particularly through the development and application of predictive models for LNG carrier operational performance. This provides a bridge between traditional satisfaction theory and data-driven vessel performance evaluation.

6.4 Limitarion of the research

This research is subject to several limitations that should be considered when interpreting the findings and assessing their broader applicability. The main limitations are summarised below:

- Limited empirical validation
  - The proposed Charterer Satisfaction Index (CSI) framework was developed and validated using operational data from three LNG carriers.
- External validity
  - The findings cannot be assumed to be directly generalisable across different LNG fleets, shipping companies, chartering arrangements, or operating contexts.
  - Consequently, the external validity of the proposed framework remains uncertain and requires further validation using larger datasets and multiple operators for other LNG vessels.
- LNG cargo composition
  - The framework does not account for changes in LNG cargo composition during the voyage, such as the preferential evaporation of methane and nitrogen.
  - These changes can influence cargo density, calorific value, engine efficiency, and fuel consumption but were excluded due to the limited availability of detailed thermodynamic data.
- Ballast-leg tank cooling
  - The heel model excludes the LNG consumed during the ballast-leg tank cooling process prior to cargo loading.
  - Although this operation has a measurable impact on LNG consumption and heel management, incorporating it would require detailed thermodynamic modelling and specialised operational data beyond the scope of this research.
- Cargo temperature variations
  - Temperature-induced cargo expansion and contraction during transportation are not incorporated into the proposed framework.

    - While these phenomena may influence loading and discharging quantities, they were intentionally excluded to maintain the business-oriented focus of the study.
- Expert-derived weighting
    - The relative importance of the CSI criteria was determined using the Analytic Hierarchy Process (AHP) based on expert judgement.
    - Although AHP provides a transparent and systematic weighting methodology, different experts, organisations, or commercial environments may assign different priorities to the evaluation criteria.
- Scope of the research
    - The objective of this research was to develop a practical, data-driven decision-support framework rather than a comprehensive thermodynamic model of LNG behaviour.

6.5 Future work

The optimization of maritime transportation continues to evolve, presenting significant opportunities for innovation. Building on the research presented in this thesis, this section highlights key areas where future studies can enhance the efficiency and sustainability of cargo and vessel management in maritime logistics, benefiting both shipping companies and charterers.

The proposed Charterer Satisfaction Index (CSI) provides a foundation for future research into data-driven decision support for LNG shipping. Future work can be divided into short-term validation priorities and longer-term research directions.

1. Short-term validation priorities

The immediate priority is to further validate and strengthen the proposed framework through broader empirical testing. Future research should focus on:

- Validating the framework using additional LNG fleets to evaluate its robustness across different commercial and operational environments.
- Applying the framework to different vessel classes, including MEGI-powered LNG carriers, Moss-type vessels, and other LNG carrier designs, in order to assess its applicability beyond the XDF vessels examined in this study.
- Investigating alternative weighting methodologies, such as Best-Worst Method (BWM), DEMATEL, or entropy-based weighting, to compare with the expert-based Analytic Hierarchy Process (AHP) and assess the sensitivity of the Charterer Satisfaction Index.

- Collecting behavioural and survey-based evidence of charterer satisfaction to validate whether the proposed CSI accurately reflects charterers' perceptions of service quality and commercial performance.
- Improving the predictive models by incorporating additional operational variables, including LNG cargo composition, cargo shrinkage and expansion, ballast-leg cooling requirements, and detailed thermodynamic data that influence fuel consumption, heel quantity, and estimated discharging quantity.

2. Long-term research directions

Beyond framework validation, future research should explore the evolution of the CSI into an integrated decision-support system for LNG shipping.

- Developing real-time decision-support systems that continuously monitor vessel performance and automatically update Charterer Satisfaction Index values using live operational and environmental data.
- Integrating weather-based route optimisation with the predictive framework to optimise fuel consumption, voyage duration, emissions, and operational efficiency simultaneously.
- Extending the framework to support vessel–cargo matching, enabling charterers to identify the most suitable vessel for a specific cargo based on predicted commercial performance.
- Incorporating advanced thermodynamic models that account for LNG composition changes, methane and nitrogen evaporation, cargo temperature variation, and cargo shrinkage throughout the transportation cycle.
- Expanding the framework beyond LNG shipping by investigating its applicability to other shipping sectors and vessel types, thereby assessing whether objective, data-driven satisfaction measurement can be adopted more widely within maritime logistics.

6.6 Conclusion

This chapter has provided a summary of the research findings, and the conclusions highlight the practical relevance of the study. Opportunities for future research have also been identified, aiming to build upon the current model and address emerging challenges in maritime logistics. Finally, this thesis has made a meaningful contribution to academia by bridging academic research with real-world industry applications.

Appendix 1 - Interview for research framework development

Section 1: Respondent Background

Full Name: ___________________________

Position/Title: ________________________

Sector/Industry: ______________________

Section 2: Key vessel performance models for Customer Satisfaction

"Which of the following models of CSI are formally tracked by your organization to measure customer satisfaction?

a) Fuel consumption
b) Heel amount (define e.g., residual cargo after discharge)
c) Discharging quantity
d) Emission footprint
e) Other (please specify): ___________________________

Section 3: Pairwise Factor Comparison (AHP Method)

"For each pair below, select the factor that has a greater influence on customer satisfaction in your experience:"

Fuel consumption vs. Heel amount

a) ○ Fuel consumption
b) ○ Heel amount
c) ○ Equally important

Fuel consumption vs. Discharging quantity

a) ○ Fuel consumption
b) ○ Discharging quantity
c) ○ Equally important

Fuel consumption vs. Emission footprint

a) ○ Fuel consumption
b) ○ Emission footprint

c) ○ Equally important

Heel amount vs. Discharging quantity

a) ○ Heel amount
b) ○ Discharging quantity
c) ○ Equally important

Heel amount vs. Emission footprint

a) ○ Heel amount
b) ○ Emission footprint
c) ○ Equally important

Discharging quantity vs. Emission footprint

a) ○ Discharging quantity
b) ○ Emission footprint
c) ○ Equally important

Section 4: Deviation Analysis

"How does your organization handle deviations in the following scenarios?"

When actual results deviate from customer expectations:

a) ○ Accepted (within tolerance)
b) ○ Not accepted (requires corrective action)
c) ○ Other: ___________________________

Maximum allowable deviation for discharging quantity:

a) ○ ≤ [___]% (specify threshold)
b) ○ > [___]% (specify threshold)

Section 5: Freight Rate Impact Analysis

"What percentage of freight factors are affected when:"

The vessel fixed rate exceeds the market rate:

a) ○ <10%
b) ○ 10–25%

c) ○ 26–50%

d) ○ >50%

The vessel fixed rate is lower than the market rate:

a) ○ <10%

b) ○ 10–25%

c) ○ 26–50%

d) ○ >50%

Interview results

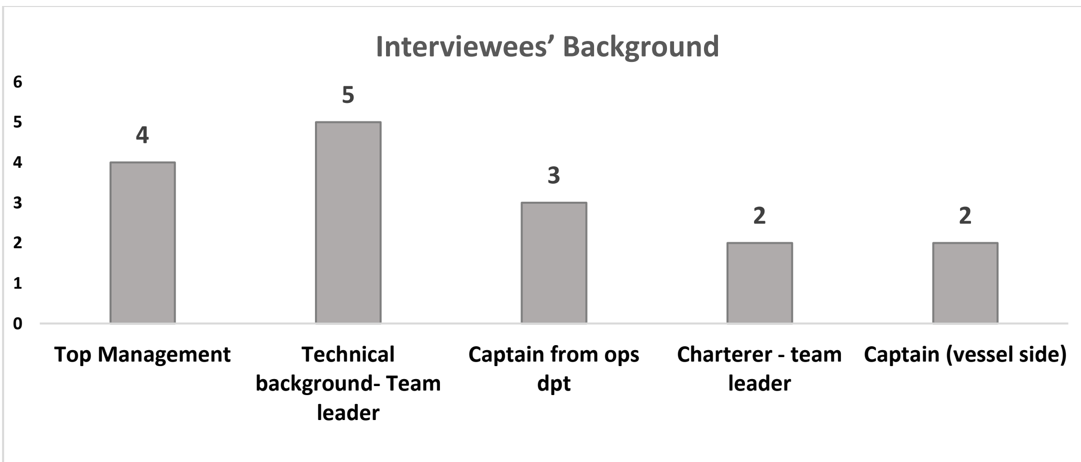

Appendix 2 - Interview for research framework development results

Factors Compared

- Fuel Consumption
- Heel Amount
- Discharging Quantity
- Emission Footprint

Pairwise Comparison Summary

Comparison	Preferred Factor(s)	Ratio (approx.)
Fuel vs. Heel	Heel (11), Fuel (3)	1:4
Fuel vs. Discharging qnt	Discharging (12), Fuel (0)	1:9
Fuel vs. Emission	Fuel (7), Emission (6)	1:1
Heel vs. Discharging qnt	Discharging (12), Heel (0)	1:9
Heel vs. Emission	Heel (7), Emission (6)	2:1
Discharging qnt vs. Emission	Discharging (4), Emission (0)	9:1

Pairwise Comparison Matrix

	Fuel	Heel	Discharging	Emission
Fuel	1	1/4	1/9	1
Heel	4	1	1/9	2
Discharging qnt	9	9	1	9
Emission	1	1/2	1/9	1

Priority Weights (Normalized Matrix)

Factor	Priority Weight
Discharging quantity	0.588 (58.8%)
Heel	0.231 (23.1%)
Fuel	0.102 (10.2%)
Emission	0.079 (7.9%)

Consistency Check

- λmax = 4.35
- CI = (λmax - n) / (n - 1) = (4.35 - 4) / 3 = 0.12
- RI (for n=4) = 0.90
- CR = CI / RI = 0.13

⚠ Note: CR > 0.10 suggests marginal inconsistency, especially around emission comparisons.

Final Ranking

1. Discharging Quantity – 58.8% (Most important)
2. Heel Amount – 23.1%
3. Fuel Consumption – 10.2%
4. Emission Footprint – 7.9% (Least important)

Appendix 3 - Data quality & Descriptive Analysis

A comprehensive analysis of Vessel 2 is conducted, covering key parameters such as SOG (Speed Over Ground), STW (Speed Through Water), ME (Main Engine) Consumption, Shaft RPM, Shaft Power, Draft Fore, Draft Aft, DG (Diesel Generator) Consumption, Boiler Consumption, and DG Power, as retrieved from the GTT Platform (Ascenz Marorka). These parameters are evaluated based on the platform’s data quality assessment process as follows:

SOG (Speed Over Ground): This plot represents the vessel's speed over ground throughout the year. The data appears mostly valid with occasional gaps (indicating short-term inactivity or signal loss), particularly around April and again in March–April the following year. The plot shows active periods where speeds hover around 15–20 knots, which suggests regular operation, and a quality score of 100, indicating complete data integrity with no out-of-bound, frozen, or missing data.

STW (Speed Through Water): The STW data is visually similar to the SOG plot with consistent readings around 15–20 knots during active periods. Small disruptions are visible throughout the year, and there is a notable gap in April where the data is missing. The overall quality score is 99, with 1% missing data and no frozen or out-of-bound readings, implying high data reliability.

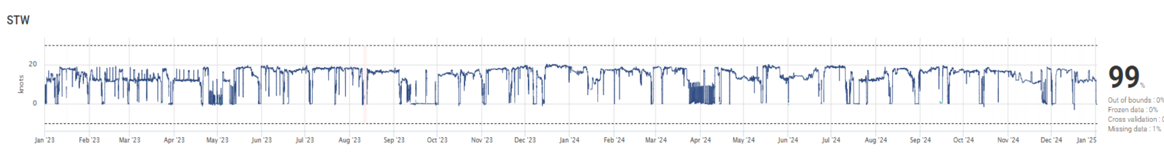

ME (Main Engine) Consumption: This chart reflects engine fuel consumption over time. Peaks in activity coincide with operational periods, and the data shows higher variability than the speed charts. Some values hit the upper limit of the graph, likely indicating maximum consumption during high load. Despite its complexity, the data has a quality score of 94, with 1% missing data and no frozen or out-of-bound values, suggesting strong but slightly degraded data reliability.

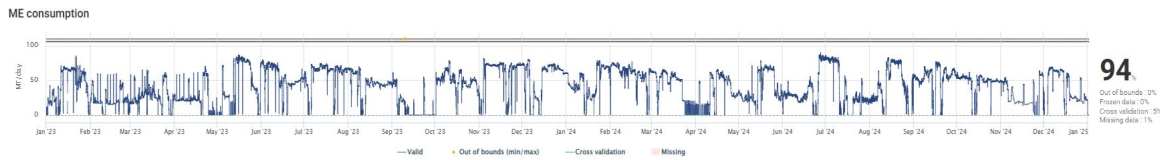

Shaft RPM: This figure shows the revolutions per minute of the propulsion shaft. Like the speed charts, data is consistent during voyages and drops to zero during idle periods. Gaps align with known inactive intervals. The quality score is 100, meaning complete and accurate data without any anomalies.

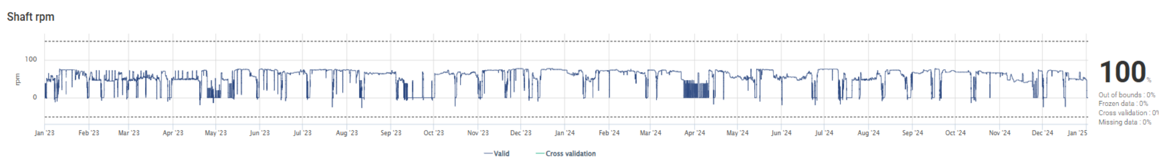

Shaft Power: This graph shows the power delivered through the shaft in kilowatts. It is consistently lower than the maximum, indicating typical operational loads. No apparent anomalies or interruptions are present. The data quality is perfect, reflected by a 100 score, with no out-of-bound, frozen, or missing data.

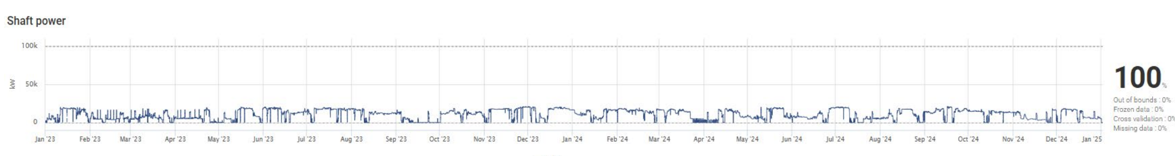

Draft Fore: The fore draft (front part of the vessel's draft) remains mostly stable throughout the year, with some minor fluctuations. There's a single instance where the value slightly exceeds the defined bounds, marked by a small orange dot. Still, the overall data quality remains 100, showing high confidence with minimal outlier issues.

Draft Aft: The aft draft (rear draft) shows stable and steady values over time, with very few changes. No missing or abnormal data is detected. This plot, like the fore draft, has a quality score of 100, reflecting excellent data integrity and consistency.

DG (Diesel Generator) Consumption: This chart tracks auxiliary engine fuel use. Unlike the propulsion-related plots, this data shows continuous operation, even during idle vessel periods, likely for hotel loads. However, there's a significant 25% missing data (marked in gray), bringing the overall score down to 75 despite having no frozen or out-of-bound data.

DG Power: The power output of the diesel generators fluctuates regularly, reflecting operational load changes. Spikes likely correspond to high power demand periods. However, the plot shows around 25% missing data, similar to the other auxiliary systems, and the quality score is also 75, indicating the need for attention in auxiliary power system monitoring.

Also, a comprehensive analysis of Vessel 3 is conducted as well, covering same key parameters. These parameters are evaluated based on the platform's data quality assessment process as follows:

SOG (Speed Over Ground): The SOG plot shows a regular sailing pattern with speeds mostly ranging between 0 and 20 knots. Clear cycles of operation and idle periods are visible throughout the year. There is one minor out-of-bounds data point (marked in orange), but it doesn't affect the overall integrity, which remains high with a 100 quality score and no missing data.

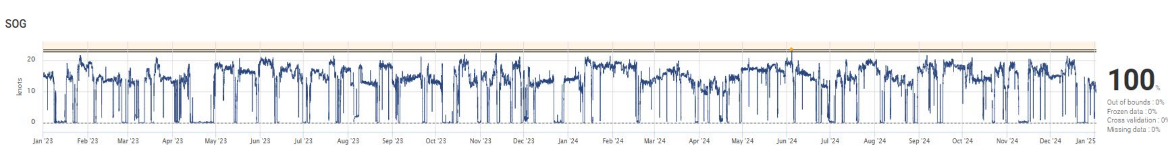

STW (Speed Through Water): This plot closely mirrors the SOG trend, with consistent operational behavior and pauses during non-sailing intervals. The data appears uninterrupted and clean, with no anomalies such as frozen or missing data. It scores a perfect 100, confirming complete reliability.

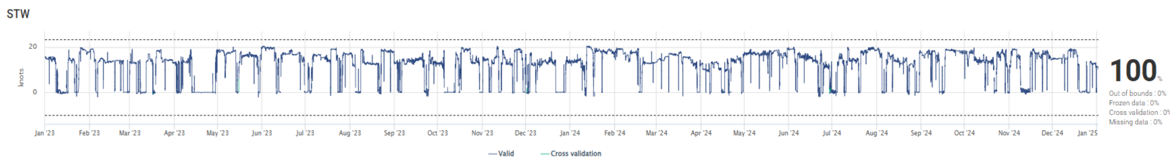

ME (Main Engine) Consumption: The ME consumption data reflects dynamic fuel usage during sailing operations. The pattern aligns well with the sailing periods seen in SOG/STW. Several out-of-bounds points are highlighted, and a small portion of the data is flagged for cross-validation. These lead to a slightly reduced quality score of 99, though data reliability remains very high.

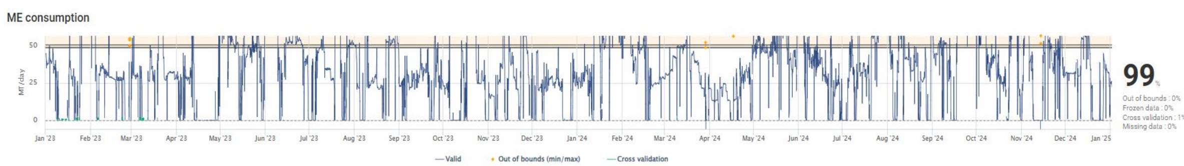

Shaft RPM: This figure displays a cyclical pattern in RPM values, rising during operational phases and falling to zero during idle periods. The data is smooth and consistent, with no visible errors or anomalies. It holds a quality score of 100, indicating perfect integrity.

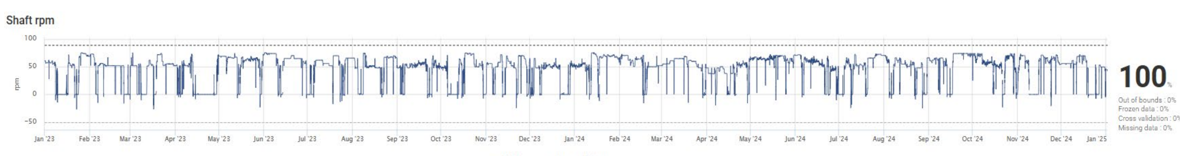

Shaft Power: Shaft power shows a varied and dynamic range of values during operation, with spikes representing increased propulsion demands. The transitions are natural and consistent with other propulsion-related signals. The data is clean with no issues, reflected in a 100 quality score.

Draft Fore: This draft measurement remains stable throughout the timeline, with gradual fluctuations likely tied to changes in cargo or ballast. The data is smooth and uninterrupted, with a 100 score confirming its reliability and completeness.

Draft Aft: Similar to the fore draft, the aft draft values show slight long-term variations but remain within expected operational ranges. The time series is consistent and free of noise, achieving a 100 quality score, indicating no data loss or anomalies.

DG (Diesel Generator) Consumption: DG consumption data shows continuous but subtle fluctuations typical of auxiliary engine usage. However, around 25% of the data is missing, lowering the quality score to 75. Despite this, the available data looks valid and consistent with auxiliary load patterns

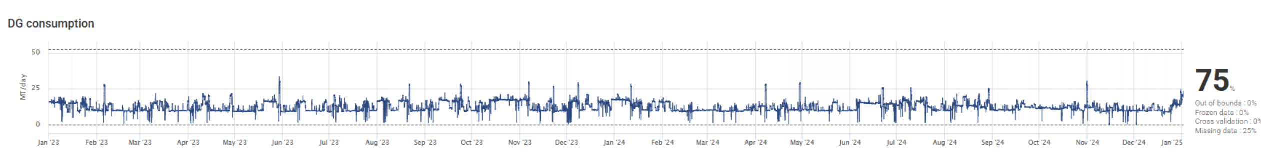

DG Power: The DG power output shows fluctuating patterns that align with expected auxiliary load demands. Peaks suggest high load periods, and the base load is relatively stable. However, similar to DG consumption, 25% of the data is missing, resulting in a 75 quality score, despite having no invalid or out-of-bound readings.


DG power
7.5k
5k
2.5k
0
kW
Jan '23
Feb '23
Mar '23
Apr '23
May '23
Jun '23
Jul '23
Aug '23
Sep '23
Oct '23
Nov '23
Dec '23
Jan '24
Feb '24
Mar '24
Apr '24
May '24
Jun '24
Jul '24
Aug '24
Sep '24
Oct '24
Nov '24
Dec '24
Jan '25
75%
Out of bounds : 0%
Frozen data : 0%
Cross validation : 0%
Missing data : 25%
Valid
Missing

Appendix 4 - Full dataset

	Column 1		Column 2		Column 3
1	Company	295	Tank 3 - N2 differential IBS/IS [mbar]	590	NG Fuel Heaters to NG Main buffer tank - Temp [B°C]
2	ShipName	296	Tank 3 - N2 IBS inlet control valve opening [%]	591	LNG Heater - GAS INLET PRESS [bar]
3	IMONo	297	Tank 3 - N2 IBS exhaust control valve opening [%]	592	LNG Heater - GAS OUTLET PRESS [bar]
4	DateTime	298	Tank 3 - N2 IS inlet control valve opening [%]	593	LNG Heater - GAS INLET TEMP [B°C]
5	Latitude	299	Tank 3 - N2 IS exhaust control valve opening [%]	594	LNG Heater - GAS OUTLET TEMP [B°C]
6	Longitude	300	Tank 4 - IBS AFT P BTM TEMP (MAIN) [B°C]	595	Fuel Gas Heater - GAS INLET PRESS [bar]
7	State	301	Tank 4 - IBS AFT P BTM TEMP (ST-BY) [B°C]	596	Fuel Gas Heater - GAS OUTLET PRESS [bar]
8	Boiler consumed [MT]	302	Tank 4 - IBS AFT MID BTM TEMP (MAIN) [B°C]	597	Fuel Gas Heater - GAS INLET TEMP [B°C]

9	DG consumed [MT]	303	Tank 4 - IBS AFT MID BTM TEMP (ST-BY) [B°C]	598	Fuel Gas Heater - GAS OUTLET TEMP [B°C]
10	ME consumed [MT]	304	Tank 4 - IBS AFT S BTM TEMP (MAIN) [B°C]	599	No.1 Water level AFT bilge well [mm]
11	DG electrical power [kW]	305	Tank 4 - IBS AFT S BTM TEMP (ST-BY) [B°C]	600	No.2 Water level AFT bilge well [mm]
12	Shaft power [kW]	306	Tank 4 - IS BTM AFT MID TEMP(MAIN) [B°C]	601	No.1 Water level FORE bilge well [mm]
13	Shaft rpm [rpm]	307	Tank 4 - IS BTM AFT MID TEMP(ST-BY) [B°C]	602	No.2 Water level FORE bilge well [mm]
14	Draft fore [m]	308	Tank 4 - IS BTM MIDDLE TEMP(MAIN) [B°C]	603	Total BOG consumption [MT/day]
15	Draft aft [m]	309	Tank 4 - IS BTM MIDDLE TEMP(ST-BY) [B°C]	604	Total NBOG [MT/day]
16	Relative wind speed [m/s]	310	Tank 4 - IS PORT LOW CHAM TEMP(MAIN) [B°C]	605	Forced boil-off [MT/day]
17	Relative wind direction [B°]	311	Tank 4 - IS PORT LOW CHAM TEMP(ST-BY) [B°C]	606	BOG to ME [MT/day]
18	COG heading [B°]	312	Tank 4 - IS PORT SIDE WALL TEMP(MAIN) [B°C]	607	BOG to AUX [MT/day]
19	GPS speed [knots]	313	Tank 4 - IS PORT SIDE WALL TEMP(ST-BY) [B°C]	608	LBOG [MT/day]

20	Log speed [knots]	314	Tank 4 - IS PORT UPP CHAM TEMP(MAIN) [B°C]	609	1 COFFERDAM FWD UPPER TEMP [B°C]
21	Under keel clearance [m]	315	Tank 4 - IS PORT UPP CHAM TEMP(ST-BY) [B°C]	610	1 COFFERDAM FWD MIDDLE TEMP [B°C]
22	DG1 Power [kW]	316	Tank 4 - IS CEIL TEMP(MAIN) [B°C]	611	1 COFFERDAM FWD LOWER TEMP [B°C]
23	DG2 Power [kW]	317	Tank 4 - IS CEIL TEMP(ST-BY) [B°C]	612	1 COFFERDAM FWD STBD UPPER TEMP [B°C]
24	DG3 Power [kW]	318	Tank 4 - IS AFT TRAN WALL TEMP(MAIN) [B°C]	613	1 COFFERDAM FWD PORT LOWER TEMP [B°C]
25	DG4 Power [kW]	319	Tank 4 - IS AFT TRAN WALL TEMP(ST-BY) [B°C]	614	1 COFFERDAM FWD PORT UPPER TEMP [B°C]
26	Ambient air pressure [mbar]	320	Tank 4 - IS FWD TRAN WALL TEMP(MAIN) [B°C]	615	1 COFFERDAM

					FWD STBD LOWER TEMP [B°C]
27	Ambient air temperature [B°C]	321	Tank 4 - IS FWD TRAN WALL TEMP(ST-BY) [B°C]	616	1 COFFERDAM AFT UPPER TEMP [B°C]
28	Ambient air relative humidity [%]	322	Tank 4 - IS PORT SIDE WALL TEMP(MAIN) - (HULL) [B°C]	617	1 COFFERDAM AFT MIDDLE TEMP [B°C]
29	Seawater temperature [B°C]	323	Tank 4 - IS PORT SIDE WALL TEMP(ST-BY) - (HULL) [B°C]	618	1 COFFERDAM AFT LOWER TEMP [B°C]
30	Roll average [B°]	324	Tank 4 - TK TRUNK DK AFT TEMP [B°C]	619	1 COFFERDAM AFT STBD UPPER TEMP [B°C]
31	Pitch average [B°]	325	Tank 4 - TK TRUNK DK MIDDLE TEMP [B°C]	620	1 COFFERDAM AFT PORT LOWER TEMP [B°C]
32	Yaw average [B°]	326	Tank 4 - TK PIPE DUCT AFT TEMP [B°C]	621	1 COFFERDAM AFT PORT

					UPPER TEMP [B°C]
33	Shaft Torque [kNm]	327	Tank 4 - TK PIPE DUCT MIDDLE TEMP [B°C]	622	1 COFFERDAM AFT STBD LOWER TEMP [B°C]
34	Rudder Angle [B°]	328	Tank 4 - TK PIPE DUCT FWD TEMP [B°C]	623	2 COFFERDAM FWD UPPER TEMP [B°C]
35	Boiler HFO consumed [MT]	329	Tank 4 - BHD PORT TOP TEMP [B°C]	624	2 COFFERDAM FWD MIDDLE TEMP [B°C]
36	Boiler MGO/MDO consumed [MT]	330	Tank 4 - BHD PORT MID TEMP [B°C]	625	2 COFFERDAM FWD LOWER TEMP [B°C]
37	ME1 RPM [rpm]	331	Tank 4 - BHD PORT LOW TEMP [B°C]	626	2 COFFERDAM FWD STBD UPPER TEMP [B°C]
38	ME1 Shaft Power [kW]	332	Tank 4 - BHD STBD TOP TEMP [B°C]	627	2 COFFERDAM FWD PORT LOWER TEMP [B°C]

39	ME1 Torque [knm]	333	Tank 4 - BHD STBD MID TEMP [B°C]	628	2 COFFERDAM FWD PORT UPPER TEMP [B°C]
40	ME2 RPM [rpm]	334	Tank 4 - BHD STBD LOW TEMP [B°C]	629	2 COFFERDAM FWD STBD LOWER TEMP [B°C]
41	ME2 Shaft Power [kW]	335	Tank 4 - IBS PRESSURE [mbar]	630	2 COFFERDAM AFT UPPER TEMP [B°C]
42	ME2 Torque [knm]	336	Tank 4 - IBS inlet PRESSURE [mbar]	631	2 COFFERDAM AFT MIDDLE TEMP [B°C]
43	Rudder Angle min (B°) [deg]	337	Tank 4 - IBS exhaust PRESSURE [%]	632	2 COFFERDAM AFT LOWER TEMP [B°C]
44	Rudder Angle max (B°) [deg]	338	Tank 4 - IBS SUPPLY V/V [%]	633	2 COFFERDAM AFT STBD UPPER TEMP [B°C]
45	Shaft 1 RPM [rpm]	339	Tank 4 - IBS EXHAUST V/V [%]	634	2 COFFERDAM

					AFT PORT LOWER TEMP [B°C]
46	Shaft 2 RPM [rpm]	340	Tank 4 - HC content in IBS [%]	635	2 COFFERDAM AFT PORT UPPER TEMP [B°C]
47	Shaft 1 Power [kW]	341	Tank 4 - Liquid Dome IS inlet pressure [mbar]	636	2 COFFERDAM AFT STBD LOWER TEMP [B°C]
48	Shaft 2 Power [kW]	342	Tank 4 - IS PRESSURE [mbar]	637	3 COFFERDAM FWD UPPER TEMP [B°C]
49	Shaft 1 Torque [kNm]	343	Tank 4 - IS inlet PRESSURE [mbar]	638	3 COFFERDAM FWD MIDDLE TEMP [B°C]
50	Shaft 2 Torque [kNm]	344	Tank 4 - IS exhaust PRESSURE [mbarg]	639	3 COFFERDAM FWD LOWER TEMP [B°C]
51	ME BOG [MT]	345	Tank 4 - IS SUPPLY V/V [%]	640	3 COFFERDAM FWD STBD

					UPPER TEMP [B°C]
52	ME HFO [MT]	346	Tank 4 - IS EXHAUST V/V [%]	641	3 COFFERDAM FWD PORT LOWER TEMP [B°C]
53	ME MGO/MDO [MT]	347	Tank 4 - HC content in IS [%]	642	3 COFFERDAM FWD PORT UPPER TEMP [B°C]
54	ME1 BOG [MT/day]	348	Tank 4 - N2 differential IBS/IS [mbar]	643	3 COFFERDAM FWD STBD LOWER TEMP [B°C]
55	ME1 HFO [MT/d]	349	Tank 4 - N2 IBS inlet control valve opening [%]	644	3 COFFERDAM AFT UPPER TEMP [B°C]
56	ME1 MGO/MDO [MT/d]	350	Tank 4 - N2 IBS exhaust control valve opening [%]	645	3 COFFERDAM AFT MIDDLE TEMP [B°C]
57	ME2 BOG [MT/day]	351	Tank 4 - N2 IS inlet control valve opening [%]	646	3 COFFERDAM AFT LOWER TEMP [B°C]

58	ME2 HFO [MT/d]	352	Tank 4 - N2 IS exhaust control valve opening [%]	647	3 COFFERDAM AFT STBD UPPER TEMP [B°C]
59	ME2 MGO/MDO [MT/d]	353	Tank 1 - Cargo Pump 1 - CURRENT [A]	648	3 COFFERDAM AFT PORT LOWER TEMP [B°C]
60	DG Total BOG [MT]	354	Tank 1 - Cargo Pump 1 - DISCH PRESS [barg]	649	3 COFFERDAM AFT PORT UPPER TEMP [B°C]
61	DG Total HFO [MT]	355	Tank 1 - Cargo Pump 1 - DISCH V/V [%]	650	3 COFFERDAM AFT STBD LOWER TEMP [B°C]
62	DG Total MGO/MDO [MT]	356	Tank 1 - Cargo Pump 2 - CURRENT [A]	651	4 COFFERDAM FWD UPPER TEMP [B°C]
63	DG Port HFO [MT/day]	357	Tank 1 - Cargo Pump 2 - DISCH PRESS [barg]	652	4 COFFERDAM FWD MIDDLE TEMP [B°C]

64	DG Port MGO/MDO [MT/day]	358	Tank 1 - Cargo Pump 2 - DISCH V/V [%]	653	4 COFFERDAM FWD LOWER TEMP [B°C]
65	DG STBD HFO [MT/day]	359	Tank 1 - Spraying Pump - CURRENT [A]	654	4 COFFERDAM FWD STBD UPPER TEMP [B°C]
66	DG STBD MGO/MDO [MT/day]	360	Tank 1 - Spraying Pump - DISCH PRESS [barg]	655	4 COFFERDAM FWD PORT LOWER TEMP [B°C]
67	DG1 BOG [MT/day]	361	Tank 1 - Spraying Pump - DISCH V/V [%]	656	4 COFFERDAM FWD PORT UPPER TEMP [B°C]
68	DG2 BOG [MT/day]	362	Tank 1 - Fuel Gas Pump 1 - CURRENT [A]	657	4 COFFERDAM FWD STBD LOWER TEMP [B°C]
69	DG3 BOG [MT/day]	363	Tank 1 - Fuel Gas Pump 1 - DISCH PRESS [barg]	658	4 COFFERDAM AFT UPPER TEMP [B°C]

70	DG4 BOG [MT/day]	364	Tank 1 - Fuel Gas Pump 1 - DISCH V/V [%]	659	4 COFFERDAM AFT MIDDLE TEMP [B°C]
71	Total impacts all tanks []	365	Tank 1 - Fuel Gas Pump 1 - Recycle [%]	660	4 COFFERDAM AFT LOWER TEMP [B°C]
72	Impacts tank 1 []	366	Tank 1 - Fuel Gas Pump 2 - CURRENT [A]	661	4 COFFERDAM AFT STBD UPPER TEMP [B°C]
73	Impacts tank 2 []	367	Tank 1 - Fuel Gas Pump 2 - DISCH PRESS [barg]	662	4 COFFERDAM AFT PORT LOWER TEMP [B°C]
74	Impacts tank 3 []	368	Tank 1 - Fuel Gas Pump 2 - DISCH V/V [%]	663	4 COFFERDAM AFT PORT UPPER TEMP [B°C]
75	Impacts tank 4 []	369	Tank 1 - Fuel Gas Pump 2 - Recycle [%]	664	4 COFFERDAM AFT STBD LOWER TEMP [B°C]

76	Impacts tank 5 []	370	Tank 1 - Fuel Gas Pump 3 - CURRENT [A]	665	5 COFFERDAM FWD UPPER TEMP [B°C]
77	Impacts tank 6 []	371	Tank 1 - Fuel Gas Pump 3 - DISCH PRESS [barg]	666	5 COFFERDAM FWD MIDDLE TEMP [B°C]
78	Roll max starboard (Sloshield) [B°]	372	Tank 1 - Fuel Gas Pump 3 - DISCH V/V [%]	667	5 COFFERDAM FWD LOWER TEMP [B°C]
79	Pitch max fore (Sloshield) [B°]	373	Tank 1 - Fuel Gas Pump 3 - Recycle [%]	668	5 COFFERDAM FWD STBD UPPER TEMP [B°C]
80	Roll avarage (Sloshield) [B°]	374	Tank 1 - Fuel Gas Pump 4 - CURRENT [A]	669	5 COFFERDAM FWD PORT LOWER TEMP [B°C]
81	Pitch avarage (Sloshield) [B°]	375	Tank 1 - Fuel Gas Pump 4 - DISCH PRESS [barg]	670	5 COFFERDAM FWD PORT UPPER TEMP [B°C]
82	Impact alarm critical	376	Tank 1 - Fuel Gas Pump 4 - DISCH V/V [%]	671	5 COFFERDAM

	threshold [Impact/min]				FWD STBD LOWER TEMP [B°C]
83	Impact alarm warning threshold [Impact/min]	377	Tank 1 - Fuel Gas Pump 4 - Recycle [%]	672	5 COFFERDAM AFT UPPER TEMP [B°C]
84	Impacts per minute overall [Impact/min]	378	Tank 2 - Cargo Pump 1 - CURRENT [A]	673	5 COFFERDAM AFT MIDDLE TEMP [B°C]
85	Impact alarm overall []	379	Tank 2 - Cargo Pump 1 - DISCH PRESS [barg]	674	5 COFFERDAM AFT LOWER TEMP [B°C]
86	Impacts per minute tank 1 [Impact/min]	380	Tank 2 - Cargo Pump 1 - DISCH V/V [%]	675	5 COFFERDAM AFT STBD UPPER TEMP [B°C]
87	Impact alarm tank 1 []	381	Tank 2 - Cargo Pump 2 - CURRENT [A]	676	5 COFFERDAM AFT PORT LOWER TEMP [B°C]
88	Impacts per minute tank 2 [Impact/min]	382	Tank 2 - Cargo Pump 2 - DISCH PRESS [barg]	677	5 COFFERDAM AFT PORT

					UPPER TEMP [B°C]
89	Impact alarm tank 2 []	383	Tank 2 - Cargo Pump 2 - DISCH V/V [%]	678	5 COFFERDAM AFT STBD LOWER TEMP [B°C]
90	Impacts per minute tank 3 [Impact/min]	384	Tank 2 - Spraying Pump - CURRENT [A]	679	Nitrogen system - Bleeding pressure [bar]
91	Impact alarm tank 3 []	385	Tank 2 - Spraying Pump - DISCH PRESS [barg]	680	Nitrogen system - Buffer tank pressure [bar]
92	Impacts per minute tank 4 [Impact/min]	386	Tank 2 - Spraying Pump - DISCH V/V [%]	681	Nitrogen system - Header pressure [mbarg]
93	Impact alarm tank 4 []	387	Tank 2 - Fuel Gas Pump 1 - CURRENT [A]	682	Nitrogen system - Header control valve [%]
94	RHO LNG [Kg/m^3]	388	Tank 2 - Fuel Gas Pump 1 - DISCH PRESS [barg]	683	NO.1 N2 GEN SYSTEM FAULT [True/False]
95	LNG tank volume [m^3]	389	Tank 2 - Fuel Gas Pump 1 - DISCH V/V [%]	684	NO.1 N2 GENERATOR PRODUCT OXYGEN CONTENT [%]

96	BOR alarm low [%]	390	Tank 2 - Fuel Gas Pump 1 - Recycle [%]	685	NO.1 N2 GENERATOR PRODUCT DEW POINT [B°C]
97	BOR alarm high [%]	391	Tank 2 - Fuel Gas Pump 2 - CURRENT [A]	686	NO.1 N2 GENERATOR Outlet temperature [B°C]
98	Daily BOR (Sloshield) [MT/Day]	392	Tank 2 - Fuel Gas Pump 2 - DISCH PRESS [barg]	687	NO.1 N2 GENERATOR O2 Percentage [%]
99	Daily BOR alarm []	393	Tank 2 - Fuel Gas Pump 2 - DISCH V/V [%]	688	NO.1 N2 GENERATOR SYSTEM RUNNING [True/False]
100	BOR rate running average (Sloshield) [MT/Day]	394	Tank 2 - Fuel Gas Pump 2 - Recycle [%]	689	NO.2 N2 GEN SYSTEM FAULT [True/False]
101	Tank 1 - Liquid temp TOP [B°C]	395	Tank 2 - Fuel Gas Pump 3 - CURRENT [A]	690	NO.2 N2 GENERATOR PRODUCT OXYGEN CONTENT [%]

102	Tank 1 - Liquid temp 95% [B°C]	396	Tank 2 - Fuel Gas Pump 3 - DISCH PRESS [barg]	691	NO.2 N2 GENERATOR PRODUCT DEW POINT [B°C]
103	Tank 1 - Liquid temp 60% [B°C]	397	Tank 2 - Fuel Gas Pump 3 - DISCH V/V [%]	692	NO.2 N2 GENERATOR Outlet temperature [B°C]
104	Tank 1 - Liquid temp 30% [B°C]	398	Tank 2 - Fuel Gas Pump 3 - Recycle [%]	693	NO.2 N2 GENERATOR O2 Percentage [%]
105	Tank 1 - Liquid temp BTM [B°C]	399	Tank 2 - Fuel Gas Pump 4 - CURRENT [A]	694	NO.2 N2 GENERATOR SYSTEM RUNNING [True/False]
106	Tank 1 - Average Liquid temp [B°C]	400	Tank 2 - Fuel Gas Pump 4 - DISCH PRESS [barg]	695	Liquid - C1 [%]
107	Tank 2 - Liquid temp TOP [B°C]	401	Tank 2 - Fuel Gas Pump 4 - DISCH V/V [%]	696	Liquid - C2 [%]
108	Tank 2 - Liquid temp 95% [B°C]	402	Tank 2 - Fuel Gas Pump 4 - Recycle [%]	697	Liquid - C3 [%]

109	Tank 2 - Liquid temp 60% [B°C]	403	Tank 3 - Cargo Pump 1 - CURRENT [A]	698	Liquid - nC4 [%]
110	Tank 2 - Liquid temp 30% [B°C]	404	Tank 3 - Cargo Pump 1 - DISCH PRESS [barg]	699	Liquid - iC4 [%]
111	Tank 2 - Liquid temp BTM [B°C]	405	Tank 3 - Cargo Pump 1 - DISCH V/V [%]	700	Liquid - nC5 [%]
112	Tank 2 - Average Liquid temp [B°C]	406	Tank 3 - Cargo Pump 2 - CURRENT [A]	701	Liquid - iC5 [%]
113	Tank 3 - Liquid temp TOP [B°C]	407	Tank 3 - Cargo Pump 2 - DISCH PRESS [barg]	702	Liquid - C6 [%]
114	Tank 3 - Liquid temp 95% [B°C]	408	Tank 3 - Cargo Pump 2 - DISCH V/V [%]	703	Liquid - N2 [%]
115	Tank 3 - Liquid temp 60% [B°C]	409	Tank 3 - Spraying Pump - CURRENT [A]	704	Liquid - CO2 [%]
116	Tank 3 - Liquid temp 30% [B°C]	410	Tank 3 - Spraying Pump - DISCH PRESS [barg]	705	Liquid - 02 [%]
117	Tank 3 - Liquid temp BTM [B°C]	411	Tank 3 - Spraying Pump - DISCH V/V [%]	706	Liquid - HHV [MW]

118	Tank 3 - Average Liquid temp [B°C]	412	Tank 3 - Fuel Gas Pump 1 - CURRENT [A]	707	Liquid - LHV [MW]
119	Tank 4 - Liquid temp TOP [B°C]	413	Tank 3 - Fuel Gas Pump 1 - DISCH PRESS [barg]	708	Liquid - Density [kg/m^3]
120	Tank 4 - Liquid temp 95% [B°C]	414	Tank 3 - Fuel Gas Pump 1 - DISCH V/V [%]	709	Liquid - MN []
121	Tank 4 - Liquid temp 60% [B°C]	415	Tank 3 - Fuel Gas Pump 1 - Recycle [%]	710	Vapour - C1 [%]
122	Tank 4 - Liquid temp 30% [B°C]	416	Tank 3 - Fuel Gas Pump 2 - CURRENT [A]	711	Vapour - C2 [%]
123	Tank 4 - Liquid temp BTM [B°C]	417	Tank 3 - Fuel Gas Pump 2 - DISCH PRESS [barg]	712	Vapour - C3 [%]
124	Tank 4 - Average Liquid temp [B°C]	418	Tank 3 - Fuel Gas Pump 2 - DISCH V/V [%]	713	Vapour - nC4 [%]
125	Tank 1 - Liquid level corrected [m]	419	Tank 3 - Fuel Gas Pump 2 - Recycle [%]	714	Vapour - iC4 [%]
126	Tank 1 - Liquid Volume [m^3]	420	Tank 3 - Fuel Gas Pump 3 - CURRENT [A]	715	Vapour - nC5 [%]

127	Tank 2 - Liquid level corrected [m]	421	Tank 3 - Fuel Gas Pump 3 - DISCH PRESS [barg]	716	Vapour - iC5 [%]
128	Tank 2 - Liquid Volume [m^3]	422	Tank 3 - Fuel Gas Pump 3 - DISCH V/V [%]	717	Vapour - C6 [%]
129	Tank 3 - Liquid level corrected [m]	423	Tank 3 - Fuel Gas Pump 3 - Recycle [%]	718	Vapour - N2 [%]
130	Tank 3 - Liquid Volume [m^3]	424	Tank 3 - Fuel Gas Pump 4 - CURRENT [A]	719	Vapour - CO2 [%]
131	Tank 4 - Liquid level corrected [m]	425	Tank 3 - Fuel Gas Pump 4 - DISCH PRESS [barg]	720	Vapour - 02 [%]
132	Tank 4 - Liquid Volume [m^3]	426	Tank 3 - Fuel Gas Pump 4 - DISCH V/V [%]	721	Vapour - HHV [MW]
133	Tank 1 - Vapour pressure [mbarg]	427	Tank 3 - Fuel Gas Pump 4 - Recycle [%]	722	Vapour - LHV [MW]
134	Tank 1 - Vapour temperature [B°C]	428	Tank 4 - Cargo Pump 1 - CURRENT [A]	723	Vapour - Density [kg/m^3]
135	Tank 2 - Vapour pressure [mbarg]	429	Tank 4 - Cargo Pump 1 - DISCH PRESS [barg]	724	Vapour - MN []

136	Tank 2 - Vapour temperature [B°C]	430	Tank 4 - Cargo Pump 1 - DISCH V/V [%]	725	Mixed Gas - C1 [%]
137	Tank 3 - Vapour pressure [mbarg]	431	Tank 4 - Cargo Pump 2 - CURRENT [A]	726	Mixed Gas - C2 [%]
138	Tank 3 - Vapour temperature [B°C]	432	Tank 4 - Cargo Pump 2 - DISCH PRESS [barg]	727	Mixed Gas - C3 [%]
139	Tank 4 - Vapour pressure [mbarg]	433	Tank 4 - Cargo Pump 2 - DISCH V/V [%]	728	Mixed Gas - nC4 [%]
140	Tank 4 - Vapour temperature [B°C]	434	Tank 4 - Spraying Pump - CURRENT [A]	729	Mixed Gas - iC4 [%]
141	Tank 1 - IBS AFT P BTM TEMP (MAIN) [B°C]	435	Tank 4 - Spraying Pump - DISCH PRESS [barg]	730	Mixed Gas - nC5 [%]
142	Tank 1 - IBS AFT P BTM TEMP (ST-BY) [B°C]	436	Tank 4 - Spraying Pump - DISCH V/V [%]	731	Mixed Gas - iC5 [%]

143	Tank 1 - IBS AFT MID BTM TEMP (MAIN) [B°C]	437	Tank 4 - Fuel Gas Pump 1 - CURRENT [A]	732	Mixed Gas - C6 [%]
144	Tank 1 - IBS AFT MID BTM TEMP (ST-BY) [B°C]	438	Tank 4 - Fuel Gas Pump 1 - DISCH PRESS [barg]	733	Mixed Gas - N2 [%]
145	Tank 1 - IBS AFT S BTM TEMP (MAIN) [B°C]	439	Tank 4 - Fuel Gas Pump 1 - DISCH V/V [%]	734	Mixed Gas - CO2 [%]
146	Tank 1 - IBS AFT S BTM TEMP (ST-BY) [B°C]	440	Tank 4 - Fuel Gas Pump 1 - Recycle [%]	735	Mixed Gas - 02 [%]
147	Tank 1 - IS BTM AFT MID TEMP(MAIN) [B°C]	441	Tank 4 - Fuel Gas Pump 2 - CURRENT [A]	736	Mixed Gas - HHV [MW]
148	Tank 1 - IS BTM AFT MID TEMP(ST-BY) [B°C]	442	Tank 4 - Fuel Gas Pump 2 - DISCH PRESS [barg]	737	Mixed Gas - LHV [MW]
149	Tank 1 - IS BTM MIDDLE	443	Tank 4 - Fuel Gas Pump 2 - DISCH V/V [%]	738	Mixed Gas - Density [kg/m^3]

	TEMP(MAIN) [B°C]				
150	Tank 1 - IS BTM MIDDLE TEMP(ST-BY) [B°C]	444	Tank 4 - Fuel Gas Pump 2 - Recycle [%]	739	Mixed Gas - MN []
151	Tank 1 - IS PORT LOW CHAM TEMP(MAIN) [B°C]	445	Tank 4 - Fuel Gas Pump 3 - CURRENT [A]	740	Tank 1 - Liquid - C1 [%]
152	Tank 1 - IS PORT LOW CHAM TEMP(ST-BY) [B°C]	446	Tank 4 - Fuel Gas Pump 3 - DISCH PRESS [barg]	741	Tank 1 - Liquid - C2 [%]
153	Tank 1 - IS PORT SIDE WALL TEMP(MAIN) [B°C]	447	Tank 4 - Fuel Gas Pump 3 - DISCH V/V [%]	742	Tank 1 - Liquid - C3 [%]
154	Tank 1 - IS PORT SIDE WALL TEMP(ST-BY) [B°C]	448	Tank 4 - Fuel Gas Pump 3 - Recycle [%]	743	Tank 1 - Liquid - nC4 [%]
155	Tank 1 - IS PORT UPP CHAM	449	Tank 4 - Fuel Gas Pump 4 - CURRENT [A]	744	Tank 1 - Liquid - iC4 [%]

	TEMP(MAIN) [B°C]				
156	Tank 1 - IS PORT UPP CHAM TEMP(ST-BY) [B°C]	450	Tank 4 - Fuel Gas Pump 4 - DISCH PRESS [barg]	745	Tank 1 - Liquid - nC5 [%]
157	Tank 1 - IS CEIL TEMP(MAIN) [B°C]	451	Tank 4 - Fuel Gas Pump 4 - DISCH V/V [%]	746	Tank 1 - Liquid - iC5 [%]
158	Tank 1 - IS CEIL TEMP(ST-BY) [B°C]	452	Tank 4 - Fuel Gas Pump 4 - Recycle [%]	747	Tank 1 - Liquid - C6 [%]
159	Tank 1 - IS AFT TRAN WALL TEMP(MAIN) [B°C]	453	BOG to GCU [kg/h]	748	Tank 1 - Liquid - N2 [%]
160	Tank 1 - IS AFT TRAN WALL TEMP(ST-BY) [B°C]	454	BOG to GCU V/V [%]	749	Tank 1 - Liquid - CO2 [%]
161	Tank 1 - IS FWD TRAN WALL	455	FUEL GAS to GCU - Pressure [bar]	750	Tank 1 - Liquid - 02 [%]

	TEMP(MAIN) [B°C]				
162	Tank 1 - IS FWD TRAN WALL TEMP(ST-BY) [B°C]	456	FUEL GAS TEMP to GCU - Temperature [B°C]	751	Tank 1 - Liquid - HHV [MW]
163	Tank 1 - IS PORT SIDE WALL TEMP(MAIN) - (HULL) [B°C]	457	FUEL GAS TO GCU V/V [0-1-2]	752	Tank 1 - Liquid - LHV [MW]
164	Tank 1 - IS PORT SIDE WALL TEMP(ST-BY) - (HULL) [B°C]	458	LNG Vaporizer - DISCH FLOW [kg/h]	753	Tank 1 - Liquid - Density [kg/m^3]
165	Tank 1 - TK TRUNK DK AFT TEMP [B°C]	459	LNG Vaporizer - INLET PRESS [bar]	754	Tank 1 - Liquid - MN []
166	Tank 1 - TK TRUNK DK MIDDLE TEMP [B°C]	460	LNG Vaporizer - OUTLET PRESS [bar]	755	Tank 1 - Vapour - C1 [%]
167	Tank 1 - TK PIPE DUCT	461	LNG Vaporizer - INLET TEMP [B°C]	756	Tank 1 - Vapour - C2 [%]

	AFT TEMP [B°C]				
168	Tank 1 - TK PIPE DUCT MIDDLE TEMP [B°C]	462	LNG Vaporizer - OUTLET TEMP [B°C]	757	Tank 1 - Vapour - C3 [%]
169	Tank 1 - TK PIPE DUCT FWD TEMP [B°C]	463	LNG Vaporizer 2 - DISCH FLOW [kg/h]	758	Tank 1 - Vapour - nC4 [%]
170	Tank 1 - BHD PORT TOP TEMP [B°C]	464	LNG Vaporizer 2 - INLET PRESS [bara]	759	Tank 1 - Vapour - iC4 [%]
171	Tank 1 - BHD PORT MID TEMP [B°C]	465	LNG Vaporizer 2 - OUTLET PRESS [bara]	760	Tank 1 - Vapour - nC5 [%]
172	Tank 1 - BHD PORT LOW TEMP [B°C]	466	LNG Vaporizer 2 - INLET TEMP [B°C]	761	Tank 1 - Vapour - iC5 [%]
173	Tank 1 - BHD STBD TOP TEMP [B°C]	467	LNG Vaporizer 2 - OUTLET TEMP [B°C]	762	Tank 1 - Vapour - C6 [%]
174	Tank 1 - BHD STBD MID TEMP [B°C]	468	FORCING Vaporizer - DISCH FLOW [kg/h]	763	Tank 1 - Vapour - N2 [%]
175	Tank 1 - BHD STBD LOW TEMP [B°C]	469	FORCING Vaporizer - INLET PRESS [barg*100]	764	Tank 1 - Vapour - CO2 [%]

176	Tank 1 - IBS PRESSURE [mbar]	470	FORCING Vaporizer - OUTLET PRESS [barg*100]	765	Tank 1 - Vapour - 02 [%]
177	Tank 1 - IBS inlet PRESSURE [mbar]	471	FORCING Vaporizer - INLET TEMP [B°C]	766	Tank 1 - Vapour - HHV [MW]
178	Tank 1 - IBS exhaust PRESSURE [mbarg]	472	FORCING Vaporizer - OUTLET TEMP [B°C]	767	Tank 1 - Vapour - LHV [MW]
179	Tank 1 - IBS SUPPLY V/V [%]	473	Reliquefaction - Outlet flow [kg/h]	768	Tank 1 - Vapour - Density [kg/m^3]
180	Tank 1 - IBS EXHAUST V/V [%]	474	Reliquefaction - Outlet temperature [B°C]	769	Tank 1 - Vapour - MN []
181	Tank 1 - HC content in IBS [%]	475	Reliquefaction - Outlet pressure [mbara]	770	Tank 2 - Liquid - C1 [%]
182	Tank 1 - Liquid Dome IS inlet pressure [mbar]	476	Reliquefaction - Inlet flow [kg/h]	771	Tank 2 - Liquid - C2 [%]
183	Tank 1 - IS PRESSURE [mbar]	477	Reliquefaction - Inlet temperature [B°C]	772	Tank 2 - Liquid - C3 [%]
184	Tank 1 - IS inlet PRESSURE [mbar]	478	Reliquefaction - Inlet pressure [mbara]	773	Tank 2 - Liquid - nC4 [%]

185	Tank 1 - IS exhaust PRESSURE [mbarg]	479	Reliquefaction - Electrical consumption [kW]	774	Tank 2 - Liquid - iC4 [%]
186	Tank 1 - IS SUPPLY V/V [%]	480	Sub-Cooler - Inlet flow [kg/h]	775	Tank 2 - Liquid - nC5 [%]
187	Tank 1 - IS EXHAUST V/V [%]	481	Sub-Cooler - Outlet flow [kg/h]	776	Tank 2 - Liquid - iC5 [%]
188	Tank 1 - HC content in IS [%]	482	Sub-Cooler - Inlet pressure [bara]	777	Tank 2 - Liquid - C6 [%]
189	Tank 1 - N2 differential IBS/IS [mbar]	483	Sub-Cooler - Outlet pressure [bara]	778	Tank 2 - Liquid - N2 [%]
190	Tank 1 - N2 IBS inlet control valve opening [%]	484	Sub-Cooler - Diffrential Pressure [mbar]	779	Tank 2 - Liquid - CO2 [%]
191	Tank 1 - N2 IBS exhaust control valve opening [%]	485	Sub-Cooler - Inlet temperature [B°C]	780	Tank 2 - Liquid - 02 [%]
192	Tank 1 - N2 IS inlet control valve opening [%]	486	Sub-Cooler - Outlet temperature [B°C]	781	Tank 2 - Liquid - HHV [MW]

193	Tank 1 - N2 IS exhaust control valve opening [%]	487	Sub-Cooler - Cold power [%]	782	Tank 2 - Liquid - LHV [MW]
194	Tank 2 - IBS AFT P BTM TEMP (MAIN) [B°C]	488	Sub-Cooler - MTC1.POWER [kW]	783	Tank 2 - Liquid - Density [kg/m^3]
195	Tank 2 - IBS AFT P BTM TEMP (ST-BY) [B°C]	489	Sub-Cooler - MC1.POWER [kW]	784	Tank 2 - Liquid - MN []
196	Tank 2 - IBS AFT MID BTM TEMP (MAIN) [B°C]	490	Sub-Cooler - MC2.POWER [kW]	785	Tank 2 - Vapour - C1 [%]
197	Tank 2 - IBS AFT MID BTM TEMP (ST-BY) [B°C]	491	Sub-Cooler - MTC2.POWER [kW]	786	Tank 2 - Vapour - C2 [%]
198	Tank 2 - IBS AFT S BTM TEMP (MAIN) [B°C]	492	Sub-Cooler - MC3.POWER [kW]	787	Tank 2 - Vapour - C3 [%]
199	Tank 2 - IBS AFT S BTM TEMP (ST-BY) [B°C]	493	Sub-Cooler - MTC3.POWER [kW]	788	Tank 2 - Vapour - nC4 [%]

200	Tank 2 - IS BTM AFT MID TEMP(MAIN) [B°C]	494	Sub-Cooler - MC4.POWER [kW]	789	Tank 2 - Vapour - iC4 [%]
201	Tank 2 - IS BTM AFT MID TEMP(ST-BY) [B°C]	495	Tank 1 Spray Line Portside Valve [0-1-2]	790	Tank 2 - Vapour - nC5 [%]
202	Tank 2 - IS BTM MIDDLE TEMP(MAIN) [B°C]	496	Tank 1 Spray Line Starboard Valve [0-1-2]	791	Tank 2 - Vapour - iC5 [%]
203	Tank 2 - IS BTM MIDDLE TEMP(ST-BY) [B°C]	497	Tank 1 Mixing Nozzle Valve [0-1-2]	792	Tank 2 - Vapour - C6 [%]
204	Tank 2 - IS PORT LOW CHAM TEMP(MAIN) [B°C]	498	Tank 2 Spray Line Portside Valve [0-1-2]	793	Tank 2 - Vapour - N2 [%]
205	Tank 2 - IS PORT LOW CHAM TEMP(ST-BY) [B°C]	499	Tank 2 Spray Line Starboard Valve [0-1-2]	794	Tank 2 - Vapour - CO2 [%]

206	Tank 2 - IS PORT SIDE WALL TEMP(MAIN) [B°C]	500	Tank 2 Mixing Nozzle Valve [0-1-2]	795	Tank 2 - Vapour - 02 [%]
207	Tank 2 - IS PORT SIDE WALL TEMP(ST-BY) [B°C]	501	Tank 3 Spray Line Portside Valve [0-1-2]	796	Tank 2 - Vapour - HHV [MW]
208	Tank 2 - IS PORT UPP CHAM TEMP(MAIN) [B°C]	502	Tank 3 Spray Line Starboard Valve [0-1-2]	797	Tank 2 - Vapour - LHV [MW]
209	Tank 2 - IS PORT UPP CHAM TEMP(ST-BY) [B°C]	503	Tank 3 Mixing Nozzle Valve [0-1-2]	798	Tank 2 - Vapour - Density [kg/m^3]
210	Tank 2 - IS CEIL TEMP(MAIN) [B°C]	504	Tank 4 Spray Line Portside Valve [0-1-2]	799	Tank 2 - Vapour - MN []
211	Tank 2 - IS CEIL TEMP(ST-BY) [B°C]	505	Tank 4 Spray Line Starboard Valve [0-1-2]	800	Tank 3 - Liquid - C1 [%]

212	Tank 2 - IS AFT TRAN WALL TEMP(MAIN) [B°C]	506	Tank 4 Mixing Nozzle Valve [0-1-2]	801	Tank 3 - Liquid - C2 [%]
213	Tank 2 - IS AFT TRAN WALL TEMP(ST-BY) [B°C]	507	LD compressor 1 - INLET PRESS [bara]	802	Tank 3 - Liquid - C3 [%]
214	Tank 2 - IS FWD TRAN WALL TEMP(MAIN) [B°C]	508	LD compressor 1 - OUTLET PRESS [barg]	803	Tank 3 - Liquid - nC4 [%]
215	Tank 2 - IS FWD TRAN WALL TEMP(ST-BY) [B°C]	509	LD compressor 1 - INLET TEMP [B°C]	804	Tank 3 - Liquid - iC4 [%]
216	Tank 2 - IS PORT SIDE WALL TEMP(MAIN) - (HULL) [B°C]	510	LD compressor 1 - OUTLET TEMP A [B°C]	805	Tank 3 - Liquid - nC5 [%]
217	Tank 2 - IS PORT SIDE WALL TEMP(ST-BY)	511	LD compressor 1 - OUTLET TEMP B [B°C]	806	Tank 3 - Liquid - iC5 [%]

	- (HULL) [B°C]				
218	Tank 2 - TK TRUNK DK AFT TEMP [B°C]	512	LD compressor 1 - DISCH FLOW [kg/h]	807	Tank 3 - Liquid - C6 [%]
219	Tank 2 - TK TRUNK DK MIDDLE TEMP [B°C]	513	LD compressor 1 - L.O FILTER DIFF PRESS [bar]	808	Tank 3 - Liquid - N2 [%]
220	Tank 2 - TK PIPE DUCT AFT TEMP [B°C]	514	LD compressor 1 - SPRAY AFT. CLR. TEMP VV POS. [%]	809	Tank 3 - Liquid - CO2 [%]
221	Tank 2 - TK PIPE DUCT MIDDLE TEMP [B°C]	515	LD compressor 2 - INLET PRESS [bara]	810	Tank 3 - Liquid - 02 [%]
222	Tank 2 - TK PIPE DUCT FWD TEMP [B°C]	516	LD compressor 2 - OUTLET PRESS [barg]	811	Tank 3 - Liquid - HHV [MW]
223	Tank 2 - BHD PORT TOP TEMP [B°C]	517	LD compressor 2 - INLET TEMP [B°C]	812	Tank 3 - Liquid - LHV [MW]
224	Tank 2 - BHD PORT MID TEMP [B°C]	518	LD compressor 2 - OUTLET TEMP A [B°C]	813	Tank 3 - Liquid - Density [kg/m^3]

225	Tank 2 - BHD PORT LOW TEMP [B°C]	519	LD compressor 2 - OUTLET TEMP B [B°C]	814	Tank 3 - Liquid - MN []
226	Tank 2 - BHD STBD TOP TEMP [B°C]	520	LD compressor 2 - DISCH FLOW [kg/h]	815	Tank 3 - Vapour - C1 [%]
227	Tank 2 - BHD STBD MID TEMP [B°C]	521	LD compressor 2 - L.O FILTER DIFF PRESS [bar]	816	Tank 3 - Vapour - C2 [%]
228	Tank 2 - BHD STBD LOW TEMP [B°C]	522	LD compressor 2 - SPRAY AFT. CLR. TEMP VV POS. [%]	817	Tank 3 - Vapour - C3 [%]
229	Tank 2 - IBS PRESSURE [mbar]	523	HD compressor 1 - INLET PRESS [bar]	818	Tank 3 - Vapour - nC4 [%]
230	Tank 2 - IBS inlet PRESSURE [mbar]	524	HD compressor 1 - OUTLET PRESS [bar]	819	Tank 3 - Vapour - iC4 [%]
231	Tank 2 - IBS exhaust PRESSURE [%]	525	HD compressor 1 - INLET TEMP [B°C]	820	Tank 3 - Vapour - nC5 [%]
232	Tank 2 - IBS SUPPLY V/V [%]	526	HD compressor 1 - OUTLET TEMP A [B°C]	821	Tank 3 - Vapour - iC5 [%]
233	Tank 2 - IBS EXHAUST V/V [%]	527	HD compressor 1 - OUTLET TEMP B [B°C]	822	Tank 3 - Vapour - C6 [%]

234	Tank 2 - HC content in IBS [%]	528	HD compressor 1 - GAS SUC FLOW [kg/h]	823	Tank 3 - Vapour - N2 [%]
235	Tank 2 - Liquid Dome IS inlet pressure [mbar]	529	HD compressor 1 - L.O FILTER DIFF PRESS [bar]	824	Tank 3 - Vapour - CO2 [%]
236	Tank 2 - IS PRESSURE [mbar]	530	HD compressor 1 - IGV POSITION [%]	825	Tank 3 - Vapour - 02 [%]
237	Tank 2 - IS inlet PRESSURE [mbar]	531	HD compressor 1 - Orifice Plate Diffrencial Press [mbar]	826	Tank 3 - Vapour - HHV [MW]
238	Tank 2 - IS exhaust PRESSURE [mbarg]	532	HD compressor 2 - INLET PRESS [bar]	827	Tank 3 - Vapour - LHV [MW]
239	Tank 2 - IS SUPPLY V/V [%]	533	HD compressor 2 - OUTLET PRESS [bar]	828	Tank 3 - Vapour - Density [kg/m^3]
240	Tank 2 - IS EXHAUST V/V [%]	534	HD compressor 2 - INLET TEMP [B°C]	829	Tank 3 - Vapour - MN []
241	Tank 2 - HC content in IS [%]	535	HD compressor 2 - OUTLET TEMP A [B°C]	830	Tank 4 - Liquid - C1 [%]
242	Tank 2 - N2 differential IBS/IS [mbar]	536	HD compressor 2 - OUTLET TEMP B [B°C]	831	Tank 4 - Liquid - C2 [%]

243	Tank 2 - N2 IBS inlet control valve opening [%]	537	HD compressor 2 - GAS SUC FLOW [B°C]	832	Tank 4 - Liquid - C3 [%]
244	Tank 2 - N2 IBS exhaust control valve opening [%]	538	HD compressor 2 - L.O FILTER DIFF PRESS [bar]	833	Tank 4 - Liquid - nC4 [%]
245	Tank 2 - N2 IS inlet control valve opening [%]	539	HD compressor 2 - IGV POSITION [%]	834	Tank 4 - Liquid - iC4 [%]
246	Tank 2 - N2 IS exhaust control valve opening [%]	540	HD compressor 2 - Orifice Plate Diffrencial Press [mbar]	835	Tank 4 - Liquid - nC5 [%]
247	Tank 3 - IBS AFT P BTM TEMP (MAIN) [B°C]	541	Liquid MAIN - FWD temperature [B°C]	836	Tank 4 - Liquid - iC5 [%]
248	Tank 3 - IBS AFT P BTM TEMP (ST-BY) [B°C]	542	Liquid MAIN - AFT temperature [B°C]	837	Tank 4 - Liquid - C6 [%]
249	Tank 3 - IBS AFT MID BTM TEMP (MAIN) [B°C]	543	Liquid Cross-Over - FWD pressure [mbar]	838	Tank 4 - Liquid - N2 [%]

250	Tank 3 - IBS AFT MID BTM TEMP (ST-BY) [B°C]	544	Liquid Cross-Over - AFT pressure [mbarg]	839	Tank 4 - Liquid - CO2 [%]
251	Tank 3 - IBS AFT S BTM TEMP (MAIN) [B°C]	545	Liquid Cross-Over - FWD temperature [B°C]	840	Tank 4 - Liquid - 02 [%]
252	Tank 3 - IBS AFT S BTM TEMP (ST-BY) [B°C]	546	Liquid Cross-Over - AFT temperature [B°C]	841	Tank 4 - Liquid - HHV [MW]
253	Tank 3 - IS BTM AFT MID TEMP(MAIN) [B°C]	547	Vapour MAIN - Gauge pressure [mbarg]	842	Tank 4 - Liquid - LHV [MW]
254	Tank 3 - IS BTM AFT MID TEMP(ST-BY) [B°C]	548	Vapour MAIN - FWD temperature [B°C]	843	Tank 4 - Liquid - Density [kg/m^3]
255	Tank 3 - IS BTM MIDDLE TEMP(MAIN) [B°C]	549	Vapour MAIN - AFT temperature [B°C]	844	Tank 4 - Liquid - MN []
256	Tank 3 - IS BTM MIDDLE	550	Vapour Cross-Over - Pressure [barG]	845	Tank 4 - Vapour - C1 [%]

	TEMP(ST-BY) [B°C]				
257	Tank 3 - IS PORT LOW CHAM TEMP(MAIN) [B°C]	551	Vapour Cross-Over - Temperature [B°C]	846	Tank 4 - Vapour - C2 [%]
258	Tank 3 - IS PORT LOW CHAM TEMP(ST-BY) [B°C]	552	VAPOR RETURN TO SHORE TEMP [B°C]	847	Tank 4 - Vapour - C3 [%]
259	Tank 3 - IS PORT SIDE WALL TEMP(MAIN) [B°C]	553	Vapour Flow To Shore [kg/h]	848	Tank 4 - Vapour - nC4 [%]
260	Tank 3 - IS PORT SIDE WALL TEMP(ST-BY) [B°C]	554	Vapour Flow From Shore [kg/h]	849	Tank 4 - Vapour - iC4 [%]
261	Tank 3 - IS PORT UPP CHAM TEMP(MAIN) [B°C]	555	Spray MAIN - FWD temperature [B°C]	850	Tank 4 - Vapour - nC5 [%]
262	Tank 3 - IS PORT UPP	556	Spray MAIN - AFT temperature [B°C]	851	Tank 4 - Vapour - iC5 [%]

	CHAM TEMP(ST-BY) [B°C]				
263	Tank 3 - IS CEIL TEMP(MAIN) [B°C]	557	Tank 1 - Spray return pressure [barg]	852	Tank 4 - Vapour - C6 [%]
264	Tank 3 - IS CEIL TEMP(ST-BY) [B°C]	558	Tank 2 - Spray return pressure [barg]	853	Tank 4 - Vapour - N2 [%]
265	Tank 3 - IS AFT TRAN WALL TEMP(MAIN) [B°C]	559	Tank 3 - Spray return pressure [barg]	854	Tank 4 - Vapour - CO2 [%]
266	Tank 3 - IS AFT TRAN WALL TEMP(ST-BY) [B°C]	560	Tank 4 - Spray return pressure [barg]	855	Tank 4 - Vapour - 02 [%]
267	Tank 3 - IS FWD TRAN WALL TEMP(MAIN) [B°C]	561	Tank 1 - Spray Inlet temperature [B°C]	856	Tank 4 - Vapour - HHV [MW]
268	Tank 3 - IS FWD TRAN WALL	562	Tank 2 - Spray Inlet temperature [B°C]	857	Tank 4 - Vapour - LHV [MW]

	TEMP(ST-BY) [B°C]				
269	Tank 3 - IS PORT SIDE WALL TEMP(MAIN) - (HULL) [B°C]	563	Tank 3 - Spray Inlet temperature [B°C]	858	Tank 4 - Vapour - Density [kg/m^3]
270	Tank 3 - IS PORT SIDE WALL TEMP(ST-BY) - (HULL) [B°C]	564	Tank 4 - Spray Inlet temperature [B°C]	859	Tank 4 - Vapour - MN [ ]
271	Tank 3 - TK TRUNK DK AFT TEMP [B°C]	565	Bunkering Liquid Line - Flow [kg/h]	860	Draft mid portside [m]
272	Tank 3 - TK TRUNK DK MIDDLE TEMP [B°C]	566	Bunker Vapour Line Pressure [bara]	861	Draft mid starboard [m]
273	Tank 3 - TK PIPE DUCT AFT TEMP [B°C]	567	LNG supply HDR - Temperature [B°C]	862	DG1 energy production [kWh]
274	Tank 3 - TK PIPE DUCT	568	LNG supply HDR - Pressure [mbarg]	863	DG1 running hours [h]

	MIDDLE TEMP [B°C]				
275	Tank 3 - BHD PORT TOP TEMP [B°C]	569	NBO mist separator - Condensate temperature [B°C]	864	DG2 energy production [kWh]
276	Tank 3 TK PIPE DUCT FWD TEMP [B°C]	570	NBO mist separator - Level [mm]	865	DG2 running hours [h]
277	Tank 3 - BHD PORT MID TEMP [B°C]	571	FBO mist separator - Condensate temperature [B°C]	866	DG3 energy production [kWh]
278	Tank 3 - BHD PORT LOW TEMP [B°C]	572	FBO mist separator - Level [mm]	867	DG3 running hours [h]
279	Tank 3 - BHD STBD TOP TEMP [B°C]	573	X-DF - DFDE FUEL GAS PRESS CONTROL V/V [%]	868	DG4 energy production [kWh]
280	Tank 3 - BHD STBD MID TEMP [B°C]	574	GCU - FUEL GAS PRESS CONTROL V/V [%]	869	DG4 running hours [h]
281	Tank 3 - BHD STBD LOW TEMP [B°C]	575	GE(STBD) FUEL GAS CONTROL VALVE [%]	870	ME FO supply temperature [B°C]
282	Tank 3 - IBS PRESSURE [mbar]	576	GE(PORT) FUEL GAS CONTROL VALVE [%]	871	ME running hours [h]

283	Tank 3 - IBS inlet PRESSURE [mbar]	577	NG Main Buffer Tank - Pressure [bara]	872	ME1 Shaft RPM [rpm]
284	Tank 3 - IBS exhaust PRESSURE [%]	578	NG Main Buffer Tank - Disc.Temp. [B°C]	873	ME2 Shaft RPM [rpm]
285	Tank 3 - IBS SUPPLY V/V [%]	579	NG Aux. Buffer Tank - Pressure [bara]	874	Main Cooling Sea Water Port Temp [B°C]
286	Tank 3 - IBS EXHAUST V/V [%]	580	NG Aux. Buffer Tank - Disc.Temp. [B°C]	875	Main Cooling Sea Water Stbd Temp [B°C]
287	Tank 3 - HC content in IBS [%]	581	NG Aux.buffer to DF Boiler - Pressure [mbarg]	876	ME1 Power [kW]
288	Tank 3 - Liquid Dome IS inlet pressure [mbar]	582	NG Heater - GAS INLET PRESS [bara]	877	ME2 Power [kW]
289	Tank 3 - IS PRESSURE [mbar]	583	NG Heater - GAS OUTLET PRESS [bara]	878	ME LNG consumed [MT]
290	Tank 3 - IS inlet PRESSURE [mbar]	584	NG Heater - GAS INLET TEMP [B°C]	879	LO Remaining on Board [MT]
291	Tank 3 - IS exhaust	585	NG Heater - GAS OUTLET TEMP [B°C]	880	FW Remaining on Board [MT]

	PRESSURE [mbarg]				
292	Tank 3 - IS SUPPLY V/V [%]	586	NG Heater II - GAS INLET PRESS [bara]	881	MGO Remaining on Board [MT]
293	Tank 3 - IS EXHAUST V/V [%]	587	NG Heater II - GAS OUTLET PRESS [bara]	882	LNG Remaining on Board [MT]
294	Tank 3 - HC content in IS [%]	588	NG Heater II - GAS INLET TEMP [B°C]	883	HFO Remaining on Board [MT]

Appendix 5 - Missing values Vessel 1

	Column 1		Column 2		Column 3
1	- State: 100.00% NaNs	183	- Tank 2 - Fuel Gas Pump 3 - CURRENT [A]: 100.00% NaNs	365	- NO.1 N2 GENERATOR O2 Percentage [%]: 100.00% NaNs
2	- Boiler consumed [MT]: 100.00% NaNs	184	- Tank 2 - Fuel Gas Pump 3 - DISCH PRESS [bar]: 100.00% NaNs	366	- NO.1 N2 GENERATOR SYSTEM RUNNING [True/False]: 100.00% NaNs
3	- Under keel clearance [m]: 100.00% NaNs	185	- Tank 2 - Fuel Gas Pump 3 - DISCH V/V [%]: 100.00% NaNs	367	- NO.2 N2 GENERATOR PRODUCT OXYGEN CONTENT [%]: 100.00% NaNs
4	- Ambient air relative humidity [%]: 100.00% NaNs	186	- Tank 2 - Fuel Gas Pump 3 - Recycle [%]: 100.00% NaNs	368	- NO.2 N2 GENERATOR Outlet temperature [°C]: 100.00% NaNs
5	- Shaft Torque [kNm]:	187	- Tank 2 - Fuel Gas Pump 4 - CURRENT [A]: 100.00% NaNs	369	- NO.2 N2 GENERATOR O2 Percentage

	100.00% NaNs				[%]: 100.00% NaNs
6	- Rudder Angle [°]: 100.00% NaNs	188	- Tank 2 - Fuel Gas Pump 4 - DISCH PRESS [bar]: 100.00% NaNs	370	- NO.2 N2 GENERATOR SYSTEM RUNNING [True/False]: 100.00% NaNs
7	- Boiler HFO consumed [MT]: 100.00% NaNs	189	- Tank 2 - Fuel Gas Pump 4 - DISCH V/V [%]: 100.00% NaNs	371	- Liquid - C1 [%]: 100.00% NaNs
8	- Boiler MGO/MDO consumed [MT]: 100.00% NaNs	190	- Tank 2 - Fuel Gas Pump 4 - Recycle [%]: 100.00% NaNs	372	- Liquid - C2 [%]: 100.00% NaNs
9	- Heave Average [m]: 100.00% NaNs	191	- Tank 3 - Fuel Gas Pump 1 - CURRENT [A]: 100.00% NaNs	373	- Liquid - C3 [%]: 100.00% NaNs
10	- Sway Average [m]: 100.00% NaNs	192	- Tank 3 - Fuel Gas Pump 1 - DISCH PRESS [bar]: 100.00% NaNs	374	- Liquid - nC4 [%]: 100.00% NaNs

11	- Surge Average [m]: 100.00% NaNs	193	- Tank 3 - Fuel Gas Pump 1 - DISCH V/V [%]: 100.00% NaNs	375	- Liquid - iC4 [%]: 100.00% NaNs
12	- Rudder Angle min (°) [deg]: 100.00% NaNs	194	- Tank 3 - Fuel Gas Pump 1 - Recycle [%]: 100.00% NaNs	376	- Liquid - nC5 [%]: 100.00% NaNs
13	- Rudder Angle max (°) [deg]: 100.00% NaNs	195	- Tank 3 - Fuel Gas Pump 2 - CURRENT [A]: 100.00% NaNs	377	- Liquid - iC5 [%]: 100.00% NaNs
14	- Shaft 1 RPM [rpm]: 100.00% NaNs	196	- Tank 3 - Fuel Gas Pump 2 - DISCH PRESS [bar]: 100.00% NaNs	378	- Liquid - C6 [%]: 100.00% NaNs
15	- Shaft 2 RPM [rpm]: 100.00% NaNs	197	- Tank 3 - Fuel Gas Pump 2 - DISCH V/V [%]: 100.00% NaNs	379	- Liquid - N2 [%]: 100.00% NaNs
16	- Shaft 1 Power [kW]: 100.00% NaNs	198	- Tank 3 - Fuel Gas Pump 2 - Recycle [%]: 100.00% NaNs	380	- Liquid - CO2 [%]: 100.00% NaNs
17	- Shaft 2 Power [kW]:	199	- Tank 3 - Fuel Gas Pump 3 - CURRENT [A]: 100.00% NaNs	381	- Liquid - 02 [%]: 100.00% NaNs

	100.00% NaNs				
18	- Shaft 1 Torque [kNm]: 100.00% NaNs	200	- Tank 3 - Fuel Gas Pump 3 - DISCH PRESS [bar]: 100.00% NaNs	382	- Liquid - HHV [MW]: 100.00% NaNs
19	- Shaft 2 Torque [kNm]: 100.00% NaNs	201	- Tank 3 - Fuel Gas Pump 3 - DISCH V/V [%]: 100.00% NaNs	383	- Liquid - LHV [MW]: 100.00% NaNs
20	- Daily BOR (Sloshield) [MT/Day]: 100.00% NaNs	202	- Tank 3 - Fuel Gas Pump 3 - Recycle [%]: 100.00% NaNs	384	- Liquid - Density [kg/m^3]: 100.00% NaNs
21	- Daily BOR alarm []: 100.00% NaNs	203	- Tank 3 - Fuel Gas Pump 4 - CURRENT [A]: 100.00% NaNs	385	- Liquid - MN []: 100.00% NaNs
22	- BOR rate running average (Sloshield) [MT/Day]: 100.00% NaNs	204	- Tank 3 - Fuel Gas Pump 4 - DISCH PRESS [bar]: 100.00% NaNs	386	- Vapour - C1 [%]: 100.00% NaNs

23	- Tank 1 - Liquid temp 75% [°C]: 100.00% NaNs	205	- Tank 3 - Fuel Gas Pump 4 - DISCH V/V [%]: 100.00% NaNs	387	- Vapour - C2 [%]: 100.00% NaNs
24	- Tank 2 - Liquid temp 75% [°C]: 100.00% NaNs	206	- Tank 3 - Fuel Gas Pump 4 - Recycle [%]: 100.00% NaNs	388	- Vapour - C3 [%]: 100.00% NaNs
25	- Tank 3 - Liquid temp 75% [°C]: 100.00% NaNs	207	- Tank 4 - Fuel Gas Pump 1 - CURRENT [A]: 100.00% NaNs	389	- Vapour - nC4 [%]: 100.00% NaNs
26	- Tank 4 - Liquid temp 75% [°C]: 100.00% NaNs	208	- Tank 4 - Fuel Gas Pump 1 - DISCH PRESS [bar]: 100.00% NaNs	390	- Vapour - iC4 [%]: 100.00% NaNs
27	- Tank 1 - IBS AFT P BTM TEMP (MAIN) [°C]: 100.00% NaNs	209	- Tank 4 - Fuel Gas Pump 1 - DISCH V/V [%]: 100.00% NaNs	391	- Vapour - nC5 [%]: 100.00% NaNs

28	- Tank 1 - IBS AFT P BTM TEMP (ST-BY) [°C]: 100.00% NaNs	210	- Tank 4 - Fuel Gas Pump 1 - Recycle [%]: 100.00% NaNs	392	- Vapour - iC5 [%]: 100.00% NaNs
29	- Tank 1 - IBS AFT MID BTM TEMP (MAIN) [°C]: 100.00% NaNs	211	- Tank 4 - Fuel Gas Pump 2 - CURRENT [A]: 100.00% NaNs	393	- Vapour - C6 [%]: 100.00% NaNs
30	- Tank 1 - IBS AFT MID BTM TEMP (ST-BY) [°C]: 100.00% NaNs	212	- Tank 4 - Fuel Gas Pump 2 - DISCH PRESS [bar]: 100.00% NaNs	394	- Vapour - N2 [%]: 100.00% NaNs
31	- Tank 1 - IBS AFT S BTM TEMP (MAIN) [°C]: 100.00% NaNs	213	- Tank 4 - Fuel Gas Pump 2 - DISCH V/V [%]: 100.00% NaNs	395	- Vapour - CO2 [%]: 100.00% NaNs

32	- Tank 1 - IBS AFT S BTM TEMP (ST-BY) [°C]: 100.00% NaNs	214	- Tank 4 - Fuel Gas Pump 2 - Recycle [%]: 100.00% NaNs	396	- Vapour - 02 [%]: 100.00% NaNs
33	- Tank 1 - IS BTM AFT MID TEMP(ST-BY) [°C]: 100.00% NaNs	215	- Tank 4 - Fuel Gas Pump 3 - CURRENT [A]: 100.00% NaNs	397	- Vapour - HHV [MW]: 100.00% NaNs
34	- Tank 1 - IS BTM MIDDLE TEMP(ST-BY) [°C]: 100.00% NaNs	216	- Tank 4 - Fuel Gas Pump 3 - DISCH PRESS [bar]: 100.00% NaNs	398	- Vapour - LHV [MW]: 100.00% NaNs
35	- Tank 1 - IS PORT LOW CHAM TEMP(ST-BY) [°C]: 100.00% NaNs	217	- Tank 4 - Fuel Gas Pump 3 - DISCH V/V [%]: 100.00% NaNs	399	- Vapour - Density [kg/m^3]: 100.00% NaNs

36	- Tank 1 - IS PORT SIDE WALL TEMP(ST-BY) [°C]: 100.00% NaNs	218	- Tank 4 - Fuel Gas Pump 3 - Recycle [%]: 100.00% NaNs	400	- Vapour - MN []: 100.00% NaNs
37	- Tank 1 - IS PORT UPP CHAM TEMP(ST-BY) [°C]: 100.00% NaNs	219	- Tank 4 - Fuel Gas Pump 4 - CURRENT [A]: 100.00% NaNs	401	- Mixed Gas - C1 [%]: 100.00% NaNs
38	- Tank 1 - IS CEIL TEMP(ST-BY) [°C]: 100.00% NaNs	220	- Tank 4 - Fuel Gas Pump 4 - DISCH PRESS [bar]: 100.00% NaNs	402	- Mixed Gas - C2 [%]: 100.00% NaNs
39	- Tank 1 - IS AFT TRAN WALL TEMP(ST-BY) [°C]: 100.00% NaNs	221	- Tank 4 - Fuel Gas Pump 4 - DISCH V/V [%]: 100.00% NaNs	403	- Mixed Gas - C3 [%]: 100.00% NaNs

40	- Tank 1 - IS FWD TRAN WALL TEMP(ST-BY) [°C]: 100.00% NaNs	222	- Tank 4 - Fuel Gas Pump 4 - Recycle [%]: 100.00% NaNs	404	- Mixed Gas - nC4 [%]: 100.00% NaNs
41	- Tank 1 - IS PORT SIDE WALL TEMP(ST-BY) - (HULL) [°C]: 100.00% NaNs	223	- BOG to GCU V/V [%]: 100.00% NaNs	405	- Mixed Gas - iC4 [%]: 100.00% NaNs
42	- Tank 1 - TK PIPE DUCT FWD TEMP [°C]: 100.00% NaNs	224	- FUEL GAS to GCU - Pressure [bar]: 100.00% NaNs	406	- Mixed Gas - nC5 [%]: 100.00% NaNs
43	- Tank 1 - BHD PORT TOP TEMP [°C]: 100.00% NaNs	225	- FUEL GAS TEMP to GCU - Temperature [°C]: 100.00% NaNs	407	- Mixed Gas - iC5 [%]: 100.00% NaNs

44	- Tank 1 - BHD PORT MID TEMP [°C]: 100.00% NaNs	226	- FUEL GAS TO GCU V/V [0-1-2]: 100.00% NaNs	408	- Mixed Gas - C6 [%]: 100.00% NaNs
45	- Tank 1 - BHD PORT LOW TEMP [°C]: 100.00% NaNs	227	- LNG Vaporizer 2 - DISCH FLOW [kg/h]: 100.00% NaNs	409	- Mixed Gas - N2 [%]: 100.00% NaNs
46	- Tank 1 - BHD STBD TOP TEMP [°C]: 100.00% NaNs	228	- LNG Vaporizer 2 - INLET PRESS [bara]: 100.00% NaNs	410	- Mixed Gas - CO2 [%]: 100.00% NaNs
47	- Tank 1 - BHD STBD MID TEMP [°C]: 100.00% NaNs	229	- LNG Vaporizer 2 - OUTLET PRESS [bara]: 100.00% NaNs	411	- Mixed Gas - 02 [%]: 100.00% NaNs
48	- Tank 1 - BHD STBD LOW TEMP [°C]: 100.00% NaNs	230	- LNG Vaporizer 2 - INLET TEMP [°C]: 100.00% NaNs	412	- Mixed Gas - HHV [MW]: 100.00% NaNs

49	- Tank 1 - IBS inlet PRESSURE [mbar]: 100.00% NaNs	231	- LNG Vaporizer 2 - OUTLET TEMP [°C]: 100.00% NaNs	413	- Mixed Gas - LHV [MW]: 100.00% NaNs
50	- Tank 1 - IBS exhaust PRESSURE [mbarg]: 100.00% NaNs	232	- Reliquefaction - Outlet flow [kg/h]: 100.00% NaNs	414	- Mixed Gas - Density [kg/m^3]: 100.00% NaNs
51	- Tank 1 - HC content in IBS [%]: 100.00% NaNs	233	- Reliquefaction - Outlet temperature [°C]: 83.63% NaNs	415	- Mixed Gas - MN []: 100.00% NaNs
52	- Tank 1 - Liquid Dome IS inlet pressure [mbar]: 100.00% NaNs	234	- Reliquefaction - Outlet pressure [mbara]: 100.00% NaNs	416	- Tank 1 - Liquid - C1 [%]: 100.00% NaNs
53	- Tank 1 - IS inlet PRESSURE [mbar]: 100.00% NaNs	235	- Sub-Cooler - Inlet flow [kg/h]: 100.00% NaNs	417	- Tank 1 - Liquid - C2 [%]: 100.00% NaNs

54	- Tank 1 - IS exhaust PRESSURE [mbarg]: 100.00% NaNs	236	- Sub-Cooler - Outlet flow [kg/h]: 100.00% NaNs	418	- Tank 1 - Liquid - C3 [%]: 100.00% NaNs
55	- Tank 1 - HC content in IS [%]: 100.00% NaNs	237	- Sub-Cooler - Inlet pressure [bara]: 100.00% NaNs	419	- Tank 1 - Liquid - nC4 [%]: 100.00% NaNs
56	- Tank 1 - N2 IBS inlet control valve opening [%]: 100.00% NaNs	238	- Sub-Cooler - Outlet pressure [bara]: 100.00% NaNs	420	- Tank 1 - Liquid - iC4 [%]: 100.00% NaNs
57	- Tank 1 - N2 IBS exhaust control valve opening [%]: 100.00% NaNs	239	- Sub-Cooler - Diffrential Pressure [mbar]: 100.00% NaNs	421	- Tank 1 - Liquid - nC5 [%]: 100.00% NaNs
58	- Tank 1 - N2 IS inlet control valve opening [%]: 100.00% NaNs	240	- Sub-Cooler - Inlet temperature [°C]: 100.00% NaNs	422	- Tank 1 - Liquid - iC5 [%]: 100.00% NaNs

59	- Tank 1 - N2 IS exhaust control valve opening [%]: 100.00% NaNs	241	- Sub-Cooler - Outlet temperature [°C]: 100.00% NaNs	423	- Tank 1 - Liquid - C6 [%]: 100.00% NaNs
60	- Tank 2 - IBS AFT P BTM TEMP (MAIN) [°C]: 100.00% NaNs	242	- Sub-Cooler - Cold power [%]: 100.00% NaNs	424	- Tank 1 - Liquid - N2 [%]: 100.00% NaNs
61	- Tank 2 - IBS AFT P BTM TEMP (ST-BY) [°C]: 100.00% NaNs	243	- Sub-Cooler - MTC1.POWER [kW]: 100.00% NaNs	425	- Tank 1 - Liquid - CO2 [%]: 100.00% NaNs
62	- Tank 2 - IBS AFT MID BTM TEMP (MAIN) [°C]: 100.00% NaNs	244	- Sub-Cooler - MC1.POWER [kW]: 100.00% NaNs	426	- Tank 1 - Liquid - 02 [%]: 100.00% NaNs

63	- Tank 2 - IBS AFT MID BTM TEMP (ST-BY) [°C]: 100.00% NaNs	245	- Sub-Cooler - MC2.POWER [kW]: 100.00% NaNs	427	- Tank 1 - Liquid - HHV [MW]: 100.00% NaNs
64	- Tank 2 - IBS AFT S BTM TEMP (MAIN) [°C]: 100.00% NaNs	246	- Sub-Cooler - MTC2.POWER [kW]: 100.00% NaNs	428	- Tank 1 - Liquid - LHV [MW]: 100.00% NaNs
65	- Tank 2 - IBS AFT S BTM TEMP (ST-BY) [°C]: 100.00% NaNs	247	- Sub-Cooler - MC3.POWER [kW]: 100.00% NaNs	429	- Tank 1 - Liquid - Density [kg/m^3]: 100.00% NaNs
66	- Tank 2 - IS BTM AFT MID TEMP(ST-BY) [°C]: 100.00% NaNs	248	- Sub-Cooler - MTC3.POWER [kW]: 100.00% NaNs	430	- Tank 1 - Liquid - MN []: 100.00% NaNs

67	- Tank 2 - IS BTM MIDDLE TEMP(ST-BY) [°C]: 100.00% NaNs	249	- Sub-Cooler - MC4.POWER [kW]: 100.00% NaNs	431	- Tank 1 - Vapour - C1 [%]: 100.00% NaNs
68	- Tank 2 - IS PORT LOW CHAM TEMP(ST-BY) [°C]: 100.00% NaNs	250	- Tank 1 Spray Line Portside Valve [0-1-2]: 100.00% NaNs	432	- Tank 1 - Vapour - C2 [%]: 100.00% NaNs
69	- Tank 2 - IS PORT SIDE WALL TEMP(ST-BY) [°C]: 100.00% NaNs	251	- Tank 1 Spray Line Starboard Valve [0-1-2]: 100.00% NaNs	433	- Tank 1 - Vapour - C3 [%]: 100.00% NaNs
70	- Tank 2 - IS PORT UPP CHAM TEMP(ST-BY) [°C]: 100.00% NaNs	252	- Tank 1 Mixing Nozzle Valve [0-1-2]: 100.00% NaNs	434	- Tank 1 - Vapour - nC4 [%]: 100.00% NaNs
71	- Tank 2 - IS CEIL	253	- Tank 2 Spray Line Portside Valve [0-1-2]: 100.00% NaNs	435	- Tank 1 - Vapour - iC4

	TEMP(ST-BY) [°C]: 100.00% NaNs				[%]: 100.00% NaNs
72	- Tank 2 - IS AFT TRAN WALL TEMP(ST-BY) [°C]: 100.00% NaNs	254	- Tank 2 Spray Line Starboard Valve [0-1-2]: 100.00% NaNs	436	- Tank 1 - Vapour - nC5 [%]: 100.00% NaNs
73	- Tank 2 - IS FWD TRAN WALL TEMP(ST-BY) [°C]: 100.00% NaNs	255	- Tank 2 Mixing Nozzle Valve [0-1-2]: 100.00% NaNs	437	- Tank 1 - Vapour - iC5 [%]: 100.00% NaNs
74	- Tank 2 - IS PORT SIDE WALL TEMP(ST-BY) - (HULL) [°C]: 100.00% NaNs	256	- Tank 3 Spray Line Portside Valve [0-1-2]: 100.00% NaNs	438	- Tank 1 - Vapour - C6 [%]: 100.00% NaNs

75	- Tank 2 - TK PIPE DUCT FWD TEMP [°C]: 100.00% NaNs	257	- Tank 3 Spray Line Starboard Valve [0-1-2]: 100.00% NaNs	439	- Tank 1 - Vapour - N2 [%]: 100.00% NaNs
76	- Tank 2 - BHD PORT TOP TEMP [°C]: 100.00% NaNs	258	- Tank 3 Mixing Nozzle Valve [0-1-2]: 100.00% NaNs	440	- Tank 1 - Vapour - CO2 [%]: 100.00% NaNs
77	- Tank 2 - BHD PORT MID TEMP [°C]: 100.00% NaNs	259	- Tank 4 Spray Line Portside Valve [0-1-2]: 100.00% NaNs	441	- Tank 1 - Vapour - 02 [%]: 100.00% NaNs
78	- Tank 2 - BHD PORT LOW TEMP [°C]: 100.00% NaNs	260	- Tank 4 Spray Line Starboard Valve [0-1-2]: 100.00% NaNs	442	- Tank 1 - Vapour - HHV [MW]: 100.00% NaNs
79	- Tank 2 - BHD STBD TOP TEMP [°C]: 100.00% NaNs	261	- Tank 4 Mixing Nozzle Valve [0-1-2]: 100.00% NaNs	443	- Tank 1 - Vapour - LHV [MW]: 100.00% NaNs

80	- Tank 2 - BHD STBD MID TEMP [°C]: 100.00% NaNs	262	- LD compressor 1 - SPRAY AFT. CLR. TEMP VV POS. [%]: 100.00% NaNs	444	- Tank 1 - Vapour - Density [kg/m^3]: 100.00% NaNs
81	- Tank 2 - BHD STBD LOW TEMP [°C]: 100.00% NaNs	263	- LD compressor 2 - DISCH FLOW [kg/h]: 100.00% NaNs	445	- Tank 1 - Vapour - MN []: 100.00% NaNs
82	- Tank 2 - IBS inlet PRESSURE [mbar]: 100.00% NaNs	264	- LD compressor 2 - SPRAY AFT. CLR. TEMP VV POS. [%]: 100.00% NaNs	446	- Tank 2 - Liquid - C1 [%]: 100.00% NaNs
83	- Tank 2 - IBS exhaust PRESSURE [%]: 100.00% NaNs	265	- HD compressor 1 - GAS SUC FLOW [kg/h]: 100.00% NaNs	447	- Tank 2 - Liquid - C2 [%]: 100.00% NaNs
84	- Tank 2 - HC content in IBS [%]: 100.00% NaNs	266	- HD compressor 2 - OUTLET PRESS [mbara]: 100.00% NaNs	448	- Tank 2 - Liquid - C3 [%]: 100.00% NaNs

85	- Tank 2 - Liquid Dome IS inlet pressure [mbar]: 100.00% NaNs	267	- HD compressor 2 - INLET TEMP [°C]: 100.00% NaNs	449	- Tank 2 - Liquid - nC4 [%]: 100.00% NaNs
86	- Tank 2 - IS inlet PRESSURE [mbar]: 100.00% NaNs	268	- HD compressor 2 - OUTLET TEMP A [°C]: 100.00% NaNs	450	- Tank 2 - Liquid - iC4 [%]: 100.00% NaNs
87	- Tank 2 - IS exhaust PRESSURE [mbarg]: 100.00% NaNs	269	- HD compressor 2 - GAS SUC FLOW [°C]: 100.00% NaNs	451	- Tank 2 - Liquid - nC5 [%]: 100.00% NaNs
88	- Tank 2 - HC content in IS [%]: 100.00% NaNs	270	- Vapour Cross-Over - Temperature [°C]: 100.00% NaNs	452	- Tank 2 - Liquid - iC5 [%]: 100.00% NaNs
89	- Tank 2 - N2 IBS inlet control valve opening [%]: 100.00% NaNs	271	- VAPOR RETURN TO SHORE TEMP [°C]: 100.00% NaNs	453	- Tank 2 - Liquid - C6 [%]: 100.00% NaNs

90	- Tank 2 - N2 IBS exhaust control valve opening [%]: 100.00% NaNs	272	- Vapour Flow To Shore [kg/h]: 100.00% NaNs	454	- Tank 2 - Liquid - N2 [%]: 100.00% NaNs
91	- Tank 2 - N2 IS inlet control valve opening [%]: 100.00% NaNs	273	- Vapour Flow From Shore [kg/h]: 100.00% NaNs	455	- Tank 2 - Liquid - CO2 [%]: 100.00% NaNs
92	- Tank 2 - N2 IS exhaust control valve opening [%]: 100.00% NaNs	274	- Tank 1 - Spray return pressure [barg]: 100.00% NaNs	456	- Tank 2 - Liquid - 02 [%]: 100.00% NaNs
93	- Tank 3 - IBS AFT P BTM TEMP (MAIN) [°C]: 100.00% NaNs	275	- Tank 2 - Spray return pressure [barg]: 100.00% NaNs	457	- Tank 2 - Liquid - HHV [MW]: 100.00% NaNs
94	- Tank 3 - IBS AFT P BTM TEMP	276	- Tank 3 - Spray return pressure [barg]: 100.00% NaNs	458	- Tank 2 - Liquid - LHV

	(ST-BY) [°C]: 100.00% NaNs				[MW]: 100.00% NaNs
95	- Tank 3 - IBS AFT MID BTM TEMP (MAIN) [°C]: 100.00% NaNs	277	- Tank 4 - Spray return pressure [barg]: 100.00% NaNs	459	- Tank 2 - Liquid - Density [kg/m^3]: 100.00% NaNs
96	- Tank 3 - IBS AFT MID BTM TEMP (ST-BY) [°C]: 100.00% NaNs	278	- Bunkering Liquid Line - Flow [kg/h]: 100.00% NaNs	460	- Tank 2 - Liquid - MN []: 100.00% NaNs
97	- Tank 3 - IBS AFT S BTM TEMP (MAIN) [°C]: 100.00% NaNs	279	- Bunker Vapour Line Pressure [bara]: 100.00% NaNs	461	- Tank 2 - Vapour - C1 [%]: 100.00% NaNs
98	- Tank 3 - IBS AFT S BTM TEMP (ST-BY)	280	- LNG supply HDR - Temperature [°C]: 100.00% NaNs	462	- Tank 2 - Vapour - C2 [%]: 100.00% NaNs

	[°C]: 100.00% NaNs				
99	- Tank 3 - IS BTM AFT MID TEMP(ST-BY) [°C]: 100.00% NaNs	281	- NBO mist separator - Condensate temperature [°C]: 100.00% NaNs	463	- Tank 2 - Vapour - C3 [%]: 100.00% NaNs
100	- Tank 3 - IS BTM MIDDLE TEMP(ST-BY) [°C]: 100.00% NaNs	282	- NBO mist separator - Level [mm]: 100.00% NaNs	464	- Tank 2 - Vapour - nC4 [%]: 100.00% NaNs
101	- Tank 3 - IS PORT LOW CHAM TEMP(ST-BY) [°C]: 100.00% NaNs	283	- FBO mist separator - Condensate temperature [°C]: 100.00% NaNs	465	- Tank 2 - Vapour - iC4 [%]: 100.00% NaNs
102	- Tank 3 - IS PORT SIDE WALL TEMP(ST-BY) [°C]:	284	- FBO mist separator - Level [mm]: 100.00% NaNs	466	- Tank 2 - Vapour - nC5 [%]: 100.00% NaNs

	100.00% NaNs				
103	- Tank 3 - IS PORT UPP CHAM TEMP(ST-BY) [°C]: 100.00% NaNs	285	- X-DF - DFDE FUEL GAS PRESS CONTROL V/V [%]: 100.00% NaNs	467	- Tank 2 - Vapour - iC5 [%]: 100.00% NaNs
104	- Tank 3 - IS CEIL TEMP(ST-BY) [°C]: 100.00% NaNs	286	- GCU - FUEL GAS PRESS CONTROL V/V [%]: 100.00% NaNs	468	- Tank 2 - Vapour - C6 [%]: 100.00% NaNs
105	- Tank 3 - IS AFT TRAN WALL TEMP(ST-BY) [°C]: 100.00% NaNs	287	- GE(STBD) FUEL GAS CONTROL VALVE [%]: 100.00% NaNs	469	- Tank 2 - Vapour - N2 [%]: 100.00% NaNs
106	- Tank 3 - IS FWD TRAN WALL TEMP(ST-BY) [°C]:	288	- GE(PORT) FUEL GAS CONTROL VALVE [%]: 100.00% NaNs	470	- Tank 2 - Vapour - CO2 [%]: 100.00% NaNs

	100.00% NaNs				
107	- Tank 3 - IS PORT SIDE WALL TEMP(ST-BY) - (HULL) [°C]: 100.00% NaNs	289	- NG Main Buffer Tank - Pressure [bara]: 100.00% NaNs	471	- Tank 2 - Vapour - 02 [%]: 100.00% NaNs
108	- Tank 3 - BHD PORT TOP TEMP [°C]: 100.00% NaNs	290	- NG Main Buffer Tank - Disc.Temp. [°C]: 100.00% NaNs	472	- Tank 2 - Vapour - HHV [MW]: 100.00% NaNs
109	- Tank 3 TK PIPE DUCT FWD TEMP [°C]: 100.00% NaNs	291	- NG Aux. Buffer Tank - Pressure [bara]: 100.00% NaNs	473	- Tank 2 - Vapour - LHV [MW]: 100.00% NaNs
110	- Tank 3 - BHD PORT MID TEMP [°C]: 100.00% NaNs	292	- NG Aux. Buffer Tank - Disc.Temp. [°C]: 100.00% NaNs	474	- Tank 2 - Vapour - Density [kg/m^3]: 100.00% NaNs

111	- Tank 3 - BHD PORT LOW TEMP [°C]: 100.00% NaNs	293	- NG Aux.buffer to DF Boiler - Pressure [mbarg]: 100.00% NaNs	475	- Tank 2 - Vapour - MN []: 100.00% NaNs
112	- Tank 3 - BHD STBD TOP TEMP [°C]: 100.00% NaNs	294	- NG Heater - GAS INLET PRESS [bara]: 100.00% NaNs	476	- Tank 3 - Liquid - C1 [%]: 100.00% NaNs
113	- Tank 3 - BHD STBD MID TEMP [°C]: 100.00% NaNs	295	- NG Heater - GAS OUTLET PRESS [bara]: 100.00% NaNs	477	- Tank 3 - Liquid - C2 [%]: 100.00% NaNs
114	- Tank 3 - BHD STBD LOW TEMP [°C]: 100.00% NaNs	296	- NG Heater - GAS INLET TEMP [°C]: 100.00% NaNs	478	- Tank 3 - Liquid - C3 [%]: 100.00% NaNs
115	- Tank 3 - IBS inlet PRESSURE [mbar]: 100.00% NaNs	297	- NG Heater - GAS OUTLET TEMP [°C]: 100.00% NaNs	479	- Tank 3 - Liquid - nC4 [%]: 100.00% NaNs

116	- Tank 3 - IBS exhaust PRESSURE [%]: 100.00% NaNs	298	- NG Heater II - GAS INLET PRESS [bara]: 100.00% NaNs	480	- Tank 3 - Liquid - iC4 [%]: 100.00% NaNs
117	- Tank 3 - HC content in IBS [%]: 100.00% NaNs	299	- NG Heater II - GAS OUTLET PRESS [bara]: 100.00% NaNs	481	- Tank 3 - Liquid - nC5 [%]: 100.00% NaNs
118	- Tank 3 - Liquid Dome IS inlet pressure [mbar]: 100.00% NaNs	300	- NG Heater II - GAS INLET TEMP [°C]: 100.00% NaNs	482	- Tank 3 - Liquid - iC5 [%]: 100.00% NaNs
119	- Tank 3 - IS inlet PRESSURE [mbar]: 100.00% NaNs	301	- NG Heater II - GAS OUTLET TEMP [°C]: 100.00% NaNs	483	- Tank 3 - Liquid - C6 [%]: 100.00% NaNs
120	- Tank 3 - IS exhaust PRESSURE [mbarg]: 100.00% NaNs	302	- NG Fuel Heaters to NG Main buffer tank - Temp [°C]: 100.00% NaNs	484	- Tank 3 - Liquid - N2 [%]: 100.00% NaNs

121	- Tank 3 - HC content in IS [%]: 100.00% NaNs	303	- LNG Heater - GAS INLET PRESS [bar]: 100.00% NaNs	485	- Tank 3 - Liquid - CO2 [%]: 100.00% NaNs
122	- Tank 3 - N2 IBS inlet control valve opening [%]: 100.00% NaNs	304	- LNG Heater - GAS OUTLET PRESS [bar]: 100.00% NaNs	486	- Tank 3 - Liquid - 02 [%]: 100.00% NaNs
123	- Tank 3 - N2 IBS exhaust control valve opening [%]: 100.00% NaNs	305	- LNG Heater - GAS INLET TEMP [°C]: 100.00% NaNs	487	- Tank 3 - Liquid - HHV [MW]: 100.00% NaNs
124	- Tank 3 - N2 IS inlet control valve opening [%]: 100.00% NaNs	306	- LNG Heater - GAS OUTLET TEMP [°C]: 100.00% NaNs	488	- Tank 3 - Liquid - LHV [MW]: 100.00% NaNs
125	- Tank 3 - N2 IS exhaust control valve opening [%]:	307	- Fuel Gas Heater - GAS INLET PRESS [bar]: 100.00% NaNs	489	- Tank 3 - Liquid - Density [kg/m^3]: 100.00% NaNs

	100.00% NaNs				
126	- Tank 4 - IBS AFT P BTM TEMP (MAIN) [°C]: 100.00% NaNs	308	- Fuel Gas Heater - GAS OUTLET PRESS [bar]: 100.00% NaNs	490	- Tank 3 - Liquid - MN []: 100.00% NaNs
127	- Tank 4 - IBS AFT P BTM TEMP (ST-BY) [°C]: 100.00% NaNs	309	- Fuel Gas Heater - GAS INLET TEMP [°C]: 100.00% NaNs	491	- Tank 3 - Vapour - C1 [%]: 100.00% NaNs
128	- Tank 4 - IBS AFT MID BTM TEMP (MAIN) [°C]: 100.00% NaNs	310	- Fuel Gas Heater - GAS OUTLET TEMP [°C]: 100.00% NaNs	492	- Tank 3 - Vapour - C2 [%]: 100.00% NaNs
129	- Tank 4 - IBS AFT MID BTM TEMP (ST-BY) [°C]:	311	- No.1 Water level AFT bilge well [mm]: 100.00% NaNs	493	- Tank 3 - Vapour - C3 [%]: 100.00% NaNs

	100.00% NaNs				
130	- Tank 4 - IBS AFT S BTM TEMP (MAIN) [°C]: 100.00% NaNs	312	- No.2 Water level AFT bilge well [mm]: 100.00% NaNs	494	- Tank 3 - Vapour - nC4 [%]: 100.00% NaNs
131	- Tank 4 - IBS AFT S BTM TEMP (ST-BY) [°C]: 100.00% NaNs	313	- No.1 Water level FORE bilge well [mm]: 100.00% NaNs	495	- Tank 3 - Vapour - iC4 [%]: 100.00% NaNs
132	- Tank 4 - IS BTM AFT MID TEMP(ST-BY) [°C]: 100.00% NaNs	314	- No.2 Water level FORE bilge well [mm]: 100.00% NaNs	496	- Tank 3 - Vapour - nC5 [%]: 100.00% NaNs
133	- Tank 4 - IS BTM MIDDLE TEMP(ST-BY) [°C]: 100.00% NaNs	315	- Total BOG consumption [MT/day]: 100.00% NaNs	497	- Tank 3 - Vapour - iC5 [%]: 100.00% NaNs

134	- Tank 4 - IS PORT LOW CHAM TEMP(ST-BY) [°C]: 100.00% NaNs	316	- Total NBOG [MT/day]: 100.00% NaNs	498	- Tank 3 - Vapour - C6 [%]: 100.00% NaNs
135	- Tank 4 - IS PORT SIDE WALL TEMP(ST-BY) [°C]: 100.00% NaNs	317	- 1 COFFERDAM FWD UPPER TEMP [°C]: 100.00% NaNs	499	- Tank 3 - Vapour - N2 [%]: 100.00% NaNs
136	- Tank 4 - IS PORT UPP CHAM TEMP(ST-BY) [°C]: 100.00% NaNs	318	- 1 COFFERDAM FWD MIDDLE TEMP [°C]: 100.00% NaNs	500	- Tank 3 - Vapour - CO2 [%]: 100.00% NaNs
137	- Tank 4 - IS CEIL TEMP(ST-BY) [°C]: 100.00% NaNs	319	- 1 COFFERDAM FWD LOWER TEMP [°C]: 100.00% NaNs	501	- Tank 3 - Vapour - 02 [%]: 100.00% NaNs
138	- Tank 4 - IS AFT TRAN	320	- 1 COFFERDAM FWD STBD UPPER TEMP [°C]: 100.00% NaNs	502	- Tank 3 - Vapour - HHV

	WALL TEMP(ST-BY) [°C]: 100.00% NaNs				[MW]: 100.00% NaNs
139	- Tank 4 - IS FWD TRAN WALL TEMP(ST-BY) [°C]: 100.00% NaNs	321	- 1 COFFERDAM FWD PORT LOWER TEMP [°C]: 100.00% NaNs	503	- Tank 3 - Vapour - LHV [MW]: 100.00% NaNs
140	- Tank 4 - IS PORT SIDE WALL TEMP(ST-BY) - (HULL) [°C]: 100.00% NaNs	322	- 1 COFFERDAM FWD PORT UPPER TEMP [°C]: 100.00% NaNs	504	- Tank 3 - Vapour - Density [kg/m^3]: 100.00% NaNs
141	- Tank 4 - TK PIPE DUCT FWD TEMP [°C]: 100.00% NaNs	323	- 1 COFFERDAM FWD STBD LOWER TEMP [°C]: 100.00% NaNs	505	- Tank 3 - Vapour - MN []: 100.00% NaNs

142	- Tank 4 - BHD PORT TOP TEMP [°C]: 100.00% NaNs	324	- 1 COFFERDAM AFT UPPER TEMP [°C]: 100.00% NaNs	506	- Tank 4 - Liquid - C1 [%]: 100.00% NaNs
143	- Tank 4 - BHD PORT MID TEMP [°C]: 100.00% NaNs	325	- 1 COFFERDAM AFT LOWER TEMP [°C]: 100.00% NaNs	507	- Tank 4 - Liquid - C2 [%]: 100.00% NaNs
144	- Tank 4 - BHD PORT LOW TEMP [°C]: 100.00% NaNs	326	- 2 COFFERDAM FWD STBD UPPER TEMP [°C]: 100.00% NaNs	508	- Tank 4 - Liquid - C3 [%]: 100.00% NaNs
145	- Tank 4 - BHD STBD TOP TEMP [°C]: 100.00% NaNs	327	- 2 COFFERDAM FWD PORT LOWER TEMP [°C]: 100.00% NaNs	509	- Tank 4 - Liquid - nC4 [%]: 100.00% NaNs
146	- Tank 4 - BHD STBD MID TEMP [°C]: 100.00% NaNs	328	- 2 COFFERDAM FWD PORT UPPER TEMP [°C]: 100.00% NaNs	510	- Tank 4 - Liquid - iC4 [%]: 100.00% NaNs

147	- Tank 4 - BHD STBD LOW TEMP [°C]: 100.00% NaNs	329	- 2 COFFERDAM FWD STBD LOWER TEMP [°C]: 100.00% NaNs	511	- Tank 4 - Liquid - nC5 [%]: 100.00% NaNs
148	- Tank 4 - IBS inlet PRESSURE [mbar]: 100.00% NaNs	330	- 2 COFFERDAM AFT STBD UPPER TEMP [°C]: 100.00% NaNs	512	- Tank 4 - Liquid - iC5 [%]: 100.00% NaNs
149	- Tank 4 - IBS exhaust PRESSURE [%]: 100.00% NaNs	331	- 2 COFFERDAM AFT PORT LOWER TEMP [°C]: 100.00% NaNs	513	- Tank 4 - Liquid - C6 [%]: 100.00% NaNs
150	- Tank 4 - HC content in IBS [%]: 100.00% NaNs	332	- 2 COFFERDAM AFT PORT UPPER TEMP [°C]: 100.00% NaNs	514	- Tank 4 - Liquid - N2 [%]: 100.00% NaNs
151	- Tank 4 - Liquid Dome IS inlet pressure [mbar]: 100.00% NaNs	333	- 2 COFFERDAM AFT STBD LOWER TEMP [°C]: 100.00% NaNs	515	- Tank 4 - Liquid - CO2 [%]: 100.00% NaNs

152	- Tank 4 - IS inlet PRESSURE [mbar]: 100.00% NaNs	334	- 3 COFFERDAM FWD STBD UPPER TEMP [°C]: 100.00% NaNs	516	- Tank 4 - Liquid - 02 [%]: 100.00% NaNs
153	- Tank 4 - IS exhaust PRESSURE [mbarg]: 100.00% NaNs	335	- 3 COFFERDAM FWD PORT LOWER TEMP [°C]: 100.00% NaNs	517	- Tank 4 - Liquid - HHV [MW]: 100.00% NaNs
154	- Tank 4 - HC content in IS [%]: 100.00% NaNs	336	- 3 COFFERDAM FWD PORT UPPER TEMP [°C]: 100.00% NaNs	518	- Tank 4 - Liquid - LHV [MW]: 100.00% NaNs
155	- Tank 4 - N2 IBS inlet control valve opening [%]: 100.00% NaNs	337	- 3 COFFERDAM FWD STBD LOWER TEMP [°C]: 100.00% NaNs	519	- Tank 4 - Liquid - Density [kg/m^3]: 100.00% NaNs
156	- Tank 4 - N2 IBS exhaust control valve opening [%]: 100.00% NaNs	338	- 3 COFFERDAM AFT STBD UPPER TEMP [°C]: 100.00% NaNs	520	- Tank 4 - Liquid - MN []: 100.00% NaNs

157	- Tank 4 - N2 IS inlet control valve opening [%]: 100.00% NaNs	339	- 3 COFFERDAM AFT PORT LOWER TEMP [°C]: 100.00% NaNs	521	- Tank 4 - Vapour - C1 [%]: 100.00% NaNs
158	- Tank 4 - N2 IS exhaust control valve opening [%]: 100.00% NaNs	340	- 3 COFFERDAM AFT PORT UPPER TEMP [°C]: 100.00% NaNs	522	- Tank 4 - Vapour - C2 [%]: 100.00% NaNs
159	- Tank 1 - Fuel Gas Pump 1 - CURRENT [A]: 100.00% NaNs	341	- 3 COFFERDAM AFT STBD LOWER TEMP [°C]: 100.00% NaNs	523	- Tank 4 - Vapour - C3 [%]: 100.00% NaNs
160	- Tank 1 - Fuel Gas Pump 1 - DISCH PRESS [bar]: 100.00% NaNs	342	- 4 COFFERDAM FWD STBD UPPER TEMP [°C]: 100.00% NaNs	524	- Tank 4 - Vapour - nC4 [%]: 100.00% NaNs
161	- Tank 1 - Fuel Gas Pump 1 - DISCH V/V	343	- 4 COFFERDAM FWD PORT LOWER TEMP [°C]: 100.00% NaNs	525	- Tank 4 - Vapour - iC4 [%]: 100.00% NaNs

	[%]: 100.00% NaNs				
162	- Tank 1 - Fuel Gas Pump 1 - Recycle [%]: 100.00% NaNs	344	- 4 COFFERDAM FWD PORT UPPER TEMP [°C]: 100.00% NaNs	526	- Tank 4 - Vapour - nC5 [%]: 100.00% NaNs
163	- Tank 1 - Fuel Gas Pump 2 - CURRENT [A]: 100.00% NaNs	345	- 4 COFFERDAM FWD STBD LOWER TEMP [°C]: 100.00% NaNs	527	- Tank 4 - Vapour - iC5 [%]: 100.00% NaNs
164	- Tank 1 - Fuel Gas Pump 2 - DISCH PRESS [bar]: 100.00% NaNs	346	- 4 COFFERDAM AFT STBD UPPER TEMP [°C]: 100.00% NaNs	528	- Tank 4 - Vapour - C6 [%]: 100.00% NaNs
165	- Tank 1 - Fuel Gas Pump 2 - DISCH V/V [%]: 100.00% NaNs	347	- 4 COFFERDAM AFT PORT LOWER TEMP [°C]: 100.00% NaNs	529	- Tank 4 - Vapour - N2 [%]: 100.00% NaNs

166	- Tank 1 - Fuel Gas Pump 2 - Recycle [%]: 100.00% NaNs	348	- 4 COFFERDAM AFT PORT UPPER TEMP [°C]: 100.00% NaNs	530	- Tank 4 - Vapour - CO2 [%]: 100.00% NaNs
167	- Tank 1 - Fuel Gas Pump 3 - CURRENT [A]: 100.00% NaNs	349	- 4 COFFERDAM AFT STBD LOWER TEMP [°C]: 100.00% NaNs	531	- Tank 4 - Vapour - 02 [%]: 100.00% NaNs
168	- Tank 1 - Fuel Gas Pump 3 - DISCH PRESS [bar]: 100.00% NaNs	350	- 5 COFFERDAM FWD UPPER TEMP [°C]: 100.00% NaNs	532	- Tank 4 - Vapour - HHV [MW]: 100.00% NaNs
169	- Tank 1 - Fuel Gas Pump 3 - DISCH V/V [%]: 100.00% NaNs	351	- 5 COFFERDAM FWD LOWER TEMP [°C]: 100.00% NaNs	533	- Tank 4 - Vapour - LHV [MW]: 100.00% NaNs
170	- Tank 1 - Fuel Gas Pump 3 - Recycle [%]:	352	- 5 COFFERDAM AFT UPPER TEMP [°C]: 100.00% NaNs	534	- Tank 4 - Vapour - Density [kg/m^3]: 100.00% NaNs

	100.00% NaNs				
171	- Tank 1 - Fuel Gas Pump 4 - CURRENT [A]: 100.00% NaNs	353	- 5 COFFERDAM AFT MIDDLE TEMP [°C]: 100.00% NaNs	535	- Tank 4 - Vapour - MN [ ]: 100.00% NaNs
172	- Tank 1 - Fuel Gas Pump 4 - DISCH PRESS [bar]: 100.00% NaNs	354	- 5 COFFERDAM AFT LOWER TEMP [°C]: 100.00% NaNs	536	- ME1 Shaft RPM [rpm]: 100.00% NaNs
173	- Tank 1 - Fuel Gas Pump 4 - DISCH V/V [%]: 100.00% NaNs	355	- 5 COFFERDAM AFT STBD UPPER TEMP [°C]: 100.00% NaNs	537	- ME2 Shaft RPM [rpm]: 100.00% NaNs
174	- Tank 1 - Fuel Gas Pump 4 - Recycle [%]: 100.00% NaNs	356	- 5 COFFERDAM AFT PORT LOWER TEMP [°C]: 100.00% NaNs	538	- Main Cooling Sea Water Port Temp [°C]: 100.00% NaNs

175	- Tank 2 - Fuel Gas Pump 1 - CURRENT [A]: 100.00% NaNs	357	- 5 COFFERDAM AFT PORT UPPER TEMP [°C]: 100.00% NaNs	539	- Main Cooling Sea Water Stbd Temp [°C]: 100.00% NaNs
176	- Tank 2 - Fuel Gas Pump 1 - DISCH PRESS [bar]: 100.00% NaNs	358	- 5 COFFERDAM AFT STBD LOWER TEMP [°C]: 100.00% NaNs	540	- ME1 Power [kW]: 83.63% NaNs
177	- Tank 2 - Fuel Gas Pump 1 - DISCH V/V [%]: 100.00% NaNs	359	- Nitrogen system - Bleeding pressure [bar]: 100.00% NaNs	541	- ME2 Power [kW]: 83.63% NaNs
178	- Tank 2 - Fuel Gas Pump 1 - Recycle [%]: 100.00% NaNs	360	- Nitrogen system - Buffer tank pressure [bar]: 100.00% NaNs	542	- ME LNG consumed [MT]: 100.00% NaNs
179	- Tank 2 - Fuel Gas Pump 2 - CURRENT	361	- Nitrogen system - Header pressure [mbarg]: 100.00% NaNs	543	- LO Remaining on Board [MT]: 100.00% NaNs

	[A]: 100.00% NaNs				
180	- Tank 2 - Fuel Gas Pump 2 - DISCH PRESS [bar]: 100.00% NaNs	362	- Nitrogen system - Header control valve [%]: 100.00% NaNs	544	- FW Remaining on Board [MT]: 100.00% NaNs
181	- Tank 2 - Fuel Gas Pump 2 - DISCH V/V [%]: 100.00% NaNs	363	- NO.1 N2 GENERATOR PRODUCT OXYGEN CONTENT [%]: 100.00% NaNs	545	- MGO Remaining on Board [MT]: 100.00% NaNs
182	- Tank 2 - Fuel Gas Pump 2 - Recycle [%]: 100.00% NaNs	364	- NO.1 N2 GENERATOR Outlet temperature [°C]: 100.00% NaNs	546	- LNG Remaining on Board [MT]: 100.00% NaNs

Appendix 6 - Missing values Vessel 2

	Column 1		Column 2
1	- Under keel clearance [m]: 100.00% NaNs	250	- GE(PORT) FUEL GAS CONTROL VALVE [%]: 100.00% NaNs
2	- Ambient air relative humidity [%]: 100.00% NaNs	251	- NG Main Buffer Tank - Pressure [bara]: 100.00% NaNs
3	- Shaft Torque [kNm]: 100.00% NaNs	252	- NG Main Buffer Tank - Disc.Temp. [°C]: 100.00% NaNs
4	- Rudder Angle [°]: 100.00% NaNs	253	- NG Aux. Buffer Tank - Pressure [bara]: 100.00% NaNs
5	- Boiler HFO consumed [MT]: 100.00% NaNs	254	- NG Aux. Buffer Tank - Disc.Temp. [°C]: 100.00% NaNs
6	- Boiler MGO/MDO consumed [MT]: 100.00% NaNs	255	- NG Aux.buffer to DF Boiler - Pressure [mbarg]: 100.00% NaNs
7	- Rudder Angle min (°) [deg]: 100.00% NaNs	256	- NG Heater - GAS INLET PRESS [bara]: 100.00% NaNs
8	- Rudder Angle max (°) [deg]: 100.00% NaNs	257	- NG Heater - GAS OUTLET PRESS [bara]: 100.00% NaNs
9	- Shaft 1 RPM [rpm]: 100.00% NaNs	258	- NG Heater - GAS INLET TEMP [°C]: 100.00% NaNs
10	- Shaft 2 RPM [rpm]: 100.00% NaNs	259	- NG Heater - GAS OUTLET TEMP [°C]: 100.00% NaNs
11	- Shaft 1 Power [kW]: 100.00% NaNs	260	- NG Heater II - GAS INLET PRESS [bara]: 100.00% NaNs
12	- Shaft 2 Power [kW]: 100.00% NaNs	261	- NG Heater II - GAS OUTLET PRESS [bara]: 100.00% NaNs

13	- Shaft 1 Torque [kNm]: 100.00% NaNs	262	- NG Heater II - GAS INLET TEMP [°C]: 100.00% NaNs
14	- Shaft 2 Torque [kNm]: 100.00% NaNs	263	- NG Heater II - GAS OUTLET TEMP [°C]: 100.00% NaNs
15	- Impacts tank 5 []: 100.00% NaNs	264	- NG Fuel Heaters to NG Main buffer tank - Temp [°C]: 100.00% NaNs
16	- Impacts tank 6 []: 100.00% NaNs	265	- No.1 Water level AFT bilge well [mm]: 100.00% NaNs
17	- Tank 1 - Liquid temp 95% [°C]: 100.00% NaNs	266	- No.2 Water level AFT bilge well [mm]: 100.00% NaNs
18	- Tank 2 - Liquid temp 95% [°C]: 100.00% NaNs	267	- No.1 Water level FORE bilge well [mm]: 100.00% NaNs
19	- Tank 3 - Liquid temp 95% [°C]: 100.00% NaNs	268	- No.2 Water level FORE bilge well [mm]: 100.00% NaNs
20	- Tank 4 - Liquid temp 95% [°C]: 100.00% NaNs	269	- 1 COFFERDAM FWD UPPER TEMP [°C]: 100.00% NaNs
21	- Tank 1 - IBS AFT P BTM TEMP (MAIN) [°C]: 100.00% NaNs	270	- 1 COFFERDAM FWD MIDDLE TEMP [°C]: 100.00% NaNs
22	- Tank 1 - IBS AFT P BTM TEMP (ST-BY) [°C]: 100.00% NaNs	271	- 1 COFFERDAM FWD LOWER TEMP [°C]: 100.00% NaNs
23	- Tank 1 - IBS AFT MID BTM TEMP (MAIN) [°C]: 100.00% NaNs	272	- 1 COFFERDAM FWD STBD UPPER TEMP [°C]: 100.00% NaNs
24	- Tank 1 - IBS AFT MID BTM TEMP (ST-BY) [°C]: 100.00% NaNs	273	- 1 COFFERDAM FWD PORT LOWER TEMP [°C]: 100.00% NaNs
25	- Tank 1 - IBS AFT S BTM TEMP (MAIN) [°C]: 100.00% NaNs	274	- 1 COFFERDAM FWD PORT UPPER TEMP [°C]: 100.00% NaNs

26	- Tank 1 - IBS AFT S BTM TEMP (ST-BY) [°C]: 100.00% NaNs	275	- 1 COFFERDAM FWD STBD LOWER TEMP [°C]: 100.00% NaNs
27	- Tank 1 - TK PIPE DUCT FWD TEMP [°C]: 100.00% NaNs	276	- 1 COFFERDAM AFT UPPER TEMP [°C]: 100.00% NaNs
28	- Tank 1 - BHD PORT TOP TEMP [°C]: 100.00% NaNs	277	- 1 COFFERDAM AFT LOWER TEMP [°C]: 100.00% NaNs
29	- Tank 1 - BHD PORT MID TEMP [°C]: 100.00% NaNs	278	- 2 COFFERDAM FWD STBD UPPER TEMP [°C]: 100.00% NaNs
30	- Tank 1 - BHD PORT LOW TEMP [°C]: 100.00% NaNs	279	- 2 COFFERDAM FWD PORT LOWER TEMP [°C]: 100.00% NaNs
31	- Tank 1 - BHD STBD TOP TEMP [°C]: 100.00% NaNs	280	- 2 COFFERDAM FWD PORT UPPER TEMP [°C]: 100.00% NaNs
32	- Tank 1 - BHD STBD MID TEMP [°C]: 100.00% NaNs	281	- 2 COFFERDAM FWD STBD LOWER TEMP [°C]: 100.00% NaNs
33	- Tank 1 - BHD STBD LOW TEMP [°C]: 100.00% NaNs	282	- 2 COFFERDAM AFT STBD UPPER TEMP [°C]: 100.00% NaNs
34	- Tank 1 - IBS inlet PRESSURE [mbar]: 100.00% NaNs	283	- 2 COFFERDAM AFT PORT LOWER TEMP [°C]: 100.00% NaNs
35	- Tank 1 - IBS exhaust PRESSURE [mbarg]: 100.00% NaNs	284	- 2 COFFERDAM AFT PORT UPPER TEMP [°C]: 100.00% NaNs
36	- Tank 1 - HC content in IBS [%]: 100.00% NaNs	285	- 2 COFFERDAM AFT STBD LOWER TEMP [°C]: 100.00% NaNs
37	- Tank 1 - IS inlet PRESSURE [mbar]: 100.00% NaNs	286	- 3 COFFERDAM FWD STBD UPPER TEMP [°C]: 100.00% NaNs
38	- Tank 1 - IS exhaust PRESSURE [mbarg]: 100.00% NaNs	287	- 3 COFFERDAM FWD PORT LOWER TEMP [°C]: 100.00% NaNs

39	- Tank 1 - HC content in IS [%]: 100.00% NaNs	288	- 3 COFFERDAM FWD PORT UPPER TEMP [°C]: 100.00% NaNs
40	- Tank 1 - N2 differential IBS/IS [mbar]: 100.00% NaNs	289	- 3 COFFERDAM FWD STBD LOWER TEMP [°C]: 100.00% NaNs
41	- Tank 1 - N2 IBS inlet control valve opening [%]: 100.00% NaNs	290	- 3 COFFERDAM AFT STBD UPPER TEMP [°C]: 100.00% NaNs
42	- Tank 1 - N2 IBS exhaust control valve opening [%]: 100.00% NaNs	291	- 3 COFFERDAM AFT PORT LOWER TEMP [°C]: 100.00% NaNs
43	- Tank 1 - N2 IS inlet control valve opening [%]: 100.00% NaNs	292	- 3 COFFERDAM AFT PORT UPPER TEMP [°C]: 100.00% NaNs
44	- Tank 1 - N2 IS exhaust control valve opening [%]: 100.00% NaNs	293	- 3 COFFERDAM AFT STBD LOWER TEMP [°C]: 100.00% NaNs
45	- Tank 2 - IBS AFT P BTM TEMP (MAIN) [°C]: 100.00% NaNs	294	- 4 COFFERDAM FWD STBD UPPER TEMP [°C]: 100.00% NaNs
46	- Tank 2 - IBS AFT P BTM TEMP (ST-BY) [°C]: 100.00% NaNs	295	- 4 COFFERDAM FWD PORT LOWER TEMP [°C]: 100.00% NaNs
47	- Tank 2 - IBS AFT MID BTM TEMP (MAIN) [°C]: 100.00% NaNs	296	- 4 COFFERDAM FWD PORT UPPER TEMP [°C]: 100.00% NaNs
48	- Tank 2 - IBS AFT MID BTM TEMP (ST-BY) [°C]: 100.00% NaNs	297	- 4 COFFERDAM FWD STBD LOWER TEMP [°C]: 100.00% NaNs
49	- Tank 2 - IBS AFT S BTM TEMP (MAIN) [°C]: 100.00% NaNs	298	- 4 COFFERDAM AFT STBD UPPER TEMP [°C]: 100.00% NaNs
50	- Tank 2 - IBS AFT S BTM TEMP (ST-BY) [°C]: 100.00% NaNs	299	- 4 COFFERDAM AFT PORT LOWER TEMP [°C]: 100.00% NaNs
51	- Tank 2 - TK PIPE DUCT FWD TEMP [°C]: 100.00% NaNs	300	- 4 COFFERDAM AFT PORT UPPER TEMP [°C]: 100.00% NaNs

52	- Tank 2 - BHD PORT TOP TEMP [°C]: 100.00% NaNs	301	- 4 COFFERDAM AFT STBD LOWER TEMP [°C]: 100.00% NaNs
53	- Tank 2 - BHD PORT MID TEMP [°C]: 100.00% NaNs	302	- 5 COFFERDAM FWD UPPER TEMP [°C]: 100.00% NaNs
54	- Tank 2 - BHD PORT LOW TEMP [°C]: 100.00% NaNs	303	- 5 COFFERDAM FWD LOWER TEMP [°C]: 100.00% NaNs
55	- Tank 2 - BHD STBD TOP TEMP [°C]: 100.00% NaNs	304	- 5 COFFERDAM AFT UPPER TEMP [°C]: 100.00% NaNs
56	- Tank 2 - BHD STBD MID TEMP [°C]: 100.00% NaNs	305	- 5 COFFERDAM AFT MIDDLE TEMP [°C]: 100.00% NaNs
57	- Tank 2 - BHD STBD LOW TEMP [°C]: 100.00% NaNs	306	- 5 COFFERDAM AFT LOWER TEMP [°C]: 100.00% NaNs
58	- Tank 2 - IBS inlet PRESSURE [mbar]: 100.00% NaNs	307	- 5 COFFERDAM AFT STBD UPPER TEMP [°C]: 100.00% NaNs
59	- Tank 2 - IBS exhaust PRESSURE [%]: 100.00% NaNs	308	- 5 COFFERDAM AFT PORT LOWER TEMP [°C]: 100.00% NaNs
60	- Tank 2 - HC content in IBS [%]: 100.00% NaNs	309	- 5 COFFERDAM AFT PORT UPPER TEMP [°C]: 100.00% NaNs
61	- Tank 2 - IS inlet PRESSURE [mbar]: 100.00% NaNs	310	- 5 COFFERDAM AFT STBD LOWER TEMP [°C]: 100.00% NaNs
62	- Tank 2 - IS exhaust PRESSURE [mbarg]: 100.00% NaNs	311	- Nitrogen system - Buffer tank pressure [bar]: 100.00% NaNs
63	- Tank 2 - HC content in IS [%]: 100.00% NaNs	312	- Nitrogen system - Header pressure [mbarg]: 100.00% NaNs
64	- Tank 2 - N2 differential IBS/IS [mbar]: 100.00% NaNs	313	- Nitrogen system - Header control valve [%]: 100.00% NaNs

65	- Tank 2 - N2 IBS inlet control valve opening [%]: 100.00% NaNs	314	- NO.1 N2 GENERATOR Outlet temperature [°C]: 100.00% NaNs
66	- Tank 2 - N2 IBS exhaust control valve opening [%]: 100.00% NaNs	315	- NO.1 N2 GENERATOR O2 Percentage [%]: 100.00% NaNs
67	- Tank 2 - N2 IS inlet control valve opening [%]: 100.00% NaNs	316	- NO.1 N2 GENERATOR SYSTEM RUNNING [True/False]: 100.00% NaNs
68	- Tank 2 - N2 IS exhaust control valve opening [%]: 100.00% NaNs	317	- NO.2 N2 GENERATOR Outlet temperature [°C]: 100.00% NaNs
69	- Tank 3 - IBS AFT P BTM TEMP (MAIN) [°C]: 100.00% NaNs	318	- NO.2 N2 GENERATOR O2 Percentage [%]: 100.00% NaNs
70	- Tank 3 - IBS AFT P BTM TEMP (ST-BY) [°C]: 100.00% NaNs	319	- NO.2 N2 GENERATOR SYSTEM RUNNING [True/False]: 100.00% NaNs
71	- Tank 3 - IBS AFT MID BTM TEMP (MAIN) [°C]: 100.00% NaNs	320	- Liquid - C1 [%]: 100.00% NaNs
72	- Tank 3 - IBS AFT MID BTM TEMP (ST-BY) [°C]: 100.00% NaNs	321	- Liquid - C2 [%]: 100.00% NaNs
73	- Tank 3 - IBS AFT S BTM TEMP (MAIN) [°C]: 100.00% NaNs	322	- Liquid - C3 [%]: 100.00% NaNs
74	- Tank 3 - IBS AFT S BTM TEMP (ST-BY) [°C]: 100.00% NaNs	323	- Liquid - nC4 [%]: 100.00% NaNs
75	- Tank 3 - BHD PORT TOP TEMP [°C]: 100.00% NaNs	324	- Liquid - iC4 [%]: 100.00% NaNs
76	- Tank 3 TK PIPE DUCT FWD TEMP [°C]: 100.00% NaNs	325	- Liquid - nC5 [%]: 100.00% NaNs

77	- Tank 3 - BHD PORT MID TEMP [°C]: 100.00% NaNs	326	- Liquid - iC5 [%]: 100.00% NaNs
78	- Tank 3 - BHD PORT LOW TEMP [°C]: 100.00% NaNs	327	- Liquid - C6 [%]: 100.00% NaNs
79	- Tank 3 - BHD STBD TOP TEMP [°C]: 100.00% NaNs	328	- Liquid - N2 [%]: 100.00% NaNs
80	- Tank 3 - BHD STBD MID TEMP [°C]: 100.00% NaNs	329	- Liquid - CO2 [%]: 100.00% NaNs
81	- Tank 3 - BHD STBD LOW TEMP [°C]: 100.00% NaNs	330	- Liquid - 02 [%]: 100.00% NaNs
82	- Tank 3 - IBS inlet PRESSURE [mbar]: 100.00% NaNs	331	- Liquid - HHV [MW]: 100.00% NaNs
83	- Tank 3 - IBS exhaust PRESSURE [%]: 100.00% NaNs	332	- Liquid - LHV [MW]: 100.00% NaNs
84	- Tank 3 - HC content in IBS [%]: 100.00% NaNs	333	- Liquid - Density [kg/m^3]: 100.00% NaNs
85	- Tank 3 - IS inlet PRESSURE [mbar]: 100.00% NaNs	334	- Liquid - MN []: 100.00% NaNs
86	- Tank 3 - IS exhaust PRESSURE [mbarg]: 100.00% NaNs	335	- Vapour - C1 [%]: 100.00% NaNs
87	- Tank 3 - HC content in IS [%]: 100.00% NaNs	336	- Vapour - C2 [%]: 100.00% NaNs
88	- Tank 3 - N2 differential IBS/IS [mbar]: 100.00% NaNs	337	- Vapour - C3 [%]: 100.00% NaNs
89	- Tank 3 - N2 IBS inlet control valve opening [%]: 100.00% NaNs	338	- Vapour - nC4 [%]: 100.00% NaNs

90	- Tank 3 - N2 IBS exhaust control valve opening [%]: 100.00% NaNs	339	- Vapour - iC4 [%]: 100.00% NaNs
91	- Tank 3 - N2 IS inlet control valve opening [%]: 100.00% NaNs	340	- Vapour - nC5 [%]: 100.00% NaNs
92	- Tank 3 - N2 IS exhaust control valve opening [%]: 100.00% NaNs	341	- Vapour - iC5 [%]: 100.00% NaNs
93	- Tank 4 - IBS AFT P BTM TEMP (MAIN) [°C]: 100.00% NaNs	342	- Vapour - C6 [%]: 100.00% NaNs
94	- Tank 4 - IBS AFT P BTM TEMP (ST-BY) [°C]: 100.00% NaNs	343	- Vapour - N2 [%]: 100.00% NaNs
95	- Tank 4 - IBS AFT MID BTM TEMP (MAIN) [°C]: 100.00% NaNs	344	- Vapour - CO2 [%]: 100.00% NaNs
96	- Tank 4 - IBS AFT MID BTM TEMP (ST-BY) [°C]: 100.00% NaNs	345	- Vapour - 02 [%]: 100.00% NaNs
97	- Tank 4 - IBS AFT S BTM TEMP (MAIN) [°C]: 100.00% NaNs	346	- Vapour - HHV [MW]: 100.00% NaNs
98	- Tank 4 - IBS AFT S BTM TEMP (ST-BY) [°C]: 100.00% NaNs	347	- Vapour - LHV [MW]: 100.00% NaNs
99	- Tank 4 - TK PIPE DUCT FWD TEMP [°C]: 100.00% NaNs	348	- Vapour - Density [kg/m^3]: 100.00% NaNs
100	- Tank 4 - BHD PORT TOP TEMP [°C]: 100.00% NaNs	349	- Vapour - MN []: 100.00% NaNs
101	- Tank 4 - BHD PORT MID TEMP [°C]: 100.00% NaNs	350	- Mixed Gas - C1 [%]: 100.00% NaNs
102	- Tank 4 - BHD PORT LOW TEMP [°C]: 100.00% NaNs	351	- Mixed Gas - C2 [%]: 100.00% NaNs

103	- Tank 4 - BHD STBD TOP TEMP [°C]: 100.00% NaNs	352	- Mixed Gas - C3 [%]: 100.00% NaNs
104	- Tank 4 - BHD STBD MID TEMP [°C]: 100.00% NaNs	353	- Mixed Gas - nC4 [%]: 100.00% NaNs
105	- Tank 4 - BHD STBD LOW TEMP [°C]: 100.00% NaNs	354	- Mixed Gas - iC4 [%]: 100.00% NaNs
106	- Tank 4 - IBS inlet PRESSURE [mbar]: 100.00% NaNs	355	- Mixed Gas - nC5 [%]: 100.00% NaNs
107	- Tank 4 - IBS exhaust PRESSURE [%]: 100.00% NaNs	356	- Mixed Gas - iC5 [%]: 100.00% NaNs
108	- Tank 4 - HC content in IBS [%]: 100.00% NaNs	357	- Mixed Gas - C6 [%]: 100.00% NaNs
109	- Tank 4 - IS inlet PRESSURE [mbar]: 100.00% NaNs	358	- Mixed Gas - N2 [%]: 100.00% NaNs
110	- Tank 4 - IS exhaust PRESSURE [mbarg]: 100.00% NaNs	359	- Mixed Gas - CO2 [%]: 100.00% NaNs
111	- Tank 4 - HC content in IS [%]: 100.00% NaNs	360	- Mixed Gas - 02 [%]: 100.00% NaNs
112	- Tank 4 - N2 differential IBS/IS [mbar]: 100.00% NaNs	361	- Mixed Gas - HHV [MW]: 100.00% NaNs
113	- Tank 4 - N2 IBS inlet control valve opening [%]: 100.00% NaNs	362	- Mixed Gas - LHV [MW]: 100.00% NaNs
114	- Tank 4 - N2 IBS exhaust control valve opening [%]: 100.00% NaNs	363	- Mixed Gas - Density [kg/m^3]: 100.00% NaNs
115	- Tank 4 - N2 IS inlet control valve opening [%]: 100.00% NaNs	364	- Mixed Gas - MN []: 100.00% NaNs

116	- Tank 4 - N2 IS exhaust control valve opening [%]: 100.00% NaNs	365	- Tank 1 - Liquid - C1 [%]: 100.00% NaNs
117	- Tank 1 - Fuel Gas Pump 1 - CURRENT [A]: 100.00% NaNs	366	- Tank 1 - Liquid - C2 [%]: 100.00% NaNs
118	- Tank 1 - Fuel Gas Pump 1 - DISCH PRESS [bar]: 100.00% NaNs	367	- Tank 1 - Liquid - C3 [%]: 100.00% NaNs
119	- Tank 1 - Fuel Gas Pump 1 - DISCH V/V [%]: 100.00% NaNs	368	- Tank 1 - Liquid - nC4 [%]: 100.00% NaNs
120	- Tank 1 - Fuel Gas Pump 1 - Recycle [%]: 100.00% NaNs	369	- Tank 1 - Liquid - iC4 [%]: 100.00% NaNs
121	- Tank 1 - Fuel Gas Pump 2 - CURRENT [A]: 100.00% NaNs	370	- Tank 1 - Liquid - nC5 [%]: 100.00% NaNs
122	- Tank 1 - Fuel Gas Pump 2 - DISCH PRESS [bar]: 100.00% NaNs	371	- Tank 1 - Liquid - iC5 [%]: 100.00% NaNs
123	- Tank 1 - Fuel Gas Pump 2 - DISCH V/V [%]: 100.00% NaNs	372	- Tank 1 - Liquid - C6 [%]: 100.00% NaNs
124	- Tank 1 - Fuel Gas Pump 2 - Recycle [%]: 100.00% NaNs	373	- Tank 1 - Liquid - N2 [%]: 100.00% NaNs
125	- Tank 1 - Fuel Gas Pump 3 - CURRENT [A]: 100.00% NaNs	374	- Tank 1 - Liquid - CO2 [%]: 100.00% NaNs
126	- Tank 1 - Fuel Gas Pump 3 - DISCH PRESS [bar]: 100.00% NaNs	375	- Tank 1 - Liquid - 02 [%]: 100.00% NaNs
127	- Tank 1 - Fuel Gas Pump 3 - DISCH V/V [%]: 100.00% NaNs	376	- Tank 1 - Liquid - HHV [MW]: 100.00% NaNs
128	- Tank 1 - Fuel Gas Pump 3 - Recycle [%]: 100.00% NaNs	377	- Tank 1 - Liquid - LHV [MW]: 100.00% NaNs

129	- Tank 1 - Fuel Gas Pump 4 - CURRENT [A]: 100.00% NaNs	378	- Tank 1 - Liquid - Density [kg/m^3]: 100.00% NaNs
130	- Tank 1 - Fuel Gas Pump 4 - DISCH PRESS [bar]: 100.00% NaNs	379	- Tank 1 - Liquid - MN []: 100.00% NaNs
131	- Tank 1 - Fuel Gas Pump 4 - DISCH V/V [%]: 100.00% NaNs	380	- Tank 1 - Vapour - C1 [%]: 100.00% NaNs
132	- Tank 1 - Fuel Gas Pump 4 - Recycle [%]: 100.00% NaNs	381	- Tank 1 - Vapour - C2 [%]: 100.00% NaNs
133	- Tank 2 - Fuel Gas Pump 1 - CURRENT [A]: 100.00% NaNs	382	- Tank 1 - Vapour - C3 [%]: 100.00% NaNs
134	- Tank 2 - Fuel Gas Pump 1 - DISCH PRESS [bar]: 100.00% NaNs	383	- Tank 1 - Vapour - nC4 [%]: 100.00% NaNs
135	- Tank 2 - Fuel Gas Pump 1 - DISCH V/V [%]: 100.00% NaNs	384	- Tank 1 - Vapour - iC4 [%]: 100.00% NaNs
136	- Tank 2 - Fuel Gas Pump 1 - Recycle [%]: 100.00% NaNs	385	- Tank 1 - Vapour - nC5 [%]: 100.00% NaNs
137	- Tank 2 - Fuel Gas Pump 2 - CURRENT [A]: 100.00% NaNs	386	- Tank 1 - Vapour - iC5 [%]: 100.00% NaNs
138	- Tank 2 - Fuel Gas Pump 2 - DISCH PRESS [bar]: 100.00% NaNs	387	- Tank 1 - Vapour - C6 [%]: 100.00% NaNs
139	- Tank 2 - Fuel Gas Pump 2 - DISCH V/V [%]: 100.00% NaNs	388	- Tank 1 - Vapour - N2 [%]: 100.00% NaNs
140	- Tank 2 - Fuel Gas Pump 2 - Recycle [%]: 100.00% NaNs	389	- Tank 1 - Vapour - CO2 [%]: 100.00% NaNs
141	- Tank 2 - Fuel Gas Pump 3 - CURRENT [A]: 100.00% NaNs	390	- Tank 1 - Vapour - 02 [%]: 100.00% NaNs

142	- Tank 2 - Fuel Gas Pump 3 - DISCH PRESS [bar]: 100.00% NaNs	391	- Tank 1 - Vapour - HHV [MW]: 100.00% NaNs
143	- Tank 2 - Fuel Gas Pump 3 - DISCH V/V [%]: 100.00% NaNs	392	- Tank 1 - Vapour - LHV [MW]: 100.00% NaNs
144	- Tank 2 - Fuel Gas Pump 3 - Recycle [%]: 100.00% NaNs	393	- Tank 1 - Vapour - Density [kg/m^3]: 100.00% NaNs
145	- Tank 2 - Fuel Gas Pump 4 - CURRENT [A]: 100.00% NaNs	394	- Tank 1 - Vapour - MN []: 100.00% NaNs
146	- Tank 2 - Fuel Gas Pump 4 - DISCH PRESS [bar]: 100.00% NaNs	395	- Tank 2 - Liquid - C1 [%]: 100.00% NaNs
147	- Tank 2 - Fuel Gas Pump 4 - DISCH V/V [%]: 100.00% NaNs	396	- Tank 2 - Liquid - C2 [%]: 100.00% NaNs
148	- Tank 2 - Fuel Gas Pump 4 - Recycle [%]: 100.00% NaNs	397	- Tank 2 - Liquid - C3 [%]: 100.00% NaNs
149	- Tank 3 - Fuel Gas Pump 1 - CURRENT [A]: 100.00% NaNs	398	- Tank 2 - Liquid - nC4 [%]: 100.00% NaNs
150	- Tank 3 - Fuel Gas Pump 1 - DISCH PRESS [bar]: 100.00% NaNs	399	- Tank 2 - Liquid - iC4 [%]: 100.00% NaNs
151	- Tank 3 - Fuel Gas Pump 1 - DISCH V/V [%]: 100.00% NaNs	400	- Tank 2 - Liquid - nC5 [%]: 100.00% NaNs
152	- Tank 3 - Fuel Gas Pump 1 - Recycle [%]: 100.00% NaNs	401	- Tank 2 - Liquid - iC5 [%]: 100.00% NaNs
153	- Tank 3 - Fuel Gas Pump 2 - CURRENT [A]: 100.00% NaNs	402	- Tank 2 - Liquid - C6 [%]: 100.00% NaNs
154	- Tank 3 - Fuel Gas Pump 2 - DISCH PRESS [bar]: 100.00% NaNs	403	- Tank 2 - Liquid - N2 [%]: 100.00% NaNs

155	- Tank 3 - Fuel Gas Pump 2 - DISCH V/V [%]: 100.00% NaNs	404	- Tank 2 - Liquid - CO2 [%]: 100.00% NaNs
156	- Tank 3 - Fuel Gas Pump 2 - Recycle [%]: 100.00% NaNs	405	- Tank 2 - Liquid - 02 [%]: 100.00% NaNs
157	- Tank 3 - Fuel Gas Pump 3 - CURRENT [A]: 100.00% NaNs	406	- Tank 2 - Liquid - HHV [MW]: 100.00% NaNs
158	- Tank 3 - Fuel Gas Pump 3 - DISCH PRESS [bar]: 100.00% NaNs	407	- Tank 2 - Liquid - LHV [MW]: 100.00% NaNs
159	- Tank 3 - Fuel Gas Pump 3 - DISCH V/V [%]: 100.00% NaNs	408	- Tank 2 - Liquid - Density [kg/m^3]: 100.00% NaNs
160	- Tank 3 - Fuel Gas Pump 3 - Recycle [%]: 100.00% NaNs	409	- Tank 2 - Liquid - MN []: 100.00% NaNs
161	- Tank 3 - Fuel Gas Pump 4 - CURRENT [A]: 100.00% NaNs	410	- Tank 2 - Vapour - C1 [%]: 100.00% NaNs
162	- Tank 3 - Fuel Gas Pump 4 - DISCH PRESS [bar]: 100.00% NaNs	411	- Tank 2 - Vapour - C2 [%]: 100.00% NaNs
163	- Tank 3 - Fuel Gas Pump 4 - DISCH V/V [%]: 100.00% NaNs	412	- Tank 2 - Vapour - C3 [%]: 100.00% NaNs
164	- Tank 3 - Fuel Gas Pump 4 - Recycle [%]: 100.00% NaNs	413	- Tank 2 - Vapour - nC4 [%]: 100.00% NaNs
165	- Tank 4 - Fuel Gas Pump 1 - CURRENT [A]: 100.00% NaNs	414	- Tank 2 - Vapour - iC4 [%]: 100.00% NaNs
166	- Tank 4 - Fuel Gas Pump 1 - DISCH PRESS [bar]: 100.00% NaNs	415	- Tank 2 - Vapour - nC5 [%]: 100.00% NaNs
167	- Tank 4 - Fuel Gas Pump 1 - DISCH V/V [%]: 100.00% NaNs	416	- Tank 2 - Vapour - iC5 [%]: 100.00% NaNs

168	- Tank 4 - Fuel Gas Pump 1 - Recycle [%]: 100.00% NaNs	417	- Tank 2 - Vapour - C6 [%]: 100.00% NaNs
169	- Tank 4 - Fuel Gas Pump 2 - CURRENT [A]: 100.00% NaNs	418	- Tank 2 - Vapour - N2 [%]: 100.00% NaNs
170	- Tank 4 - Fuel Gas Pump 2 - DISCH PRESS [bar]: 100.00% NaNs	419	- Tank 2 - Vapour - CO2 [%]: 100.00% NaNs
171	- Tank 4 - Fuel Gas Pump 2 - DISCH V/V [%]: 100.00% NaNs	420	- Tank 2 - Vapour - 02 [%]: 100.00% NaNs
172	- Tank 4 - Fuel Gas Pump 2 - Recycle [%]: 100.00% NaNs	421	- Tank 2 - Vapour - HHV [MW]: 100.00% NaNs
173	- Tank 4 - Fuel Gas Pump 3 - CURRENT [A]: 100.00% NaNs	422	- Tank 2 - Vapour - LHV [MW]: 100.00% NaNs
174	- Tank 4 - Fuel Gas Pump 3 - DISCH PRESS [bar]: 100.00% NaNs	423	- Tank 2 - Vapour - Density [kg/m^3]: 100.00% NaNs
175	- Tank 4 - Fuel Gas Pump 3 - DISCH V/V [%]: 100.00% NaNs	424	- Tank 2 - Vapour - MN []: 100.00% NaNs
176	- Tank 4 - Fuel Gas Pump 3 - Recycle [%]: 100.00% NaNs	425	- Tank 3 - Liquid - C1 [%]: 100.00% NaNs
177	- Tank 4 - Fuel Gas Pump 4 - CURRENT [A]: 100.00% NaNs	426	- Tank 3 - Liquid - C2 [%]: 100.00% NaNs
178	- Tank 4 - Fuel Gas Pump 4 - DISCH PRESS [bar]: 100.00% NaNs	427	- Tank 3 - Liquid - C3 [%]: 100.00% NaNs
179	- Tank 4 - Fuel Gas Pump 4 - DISCH V/V [%]: 100.00% NaNs	428	- Tank 3 - Liquid - nC4 [%]: 100.00% NaNs
180	- Tank 4 - Fuel Gas Pump 4 - Recycle [%]: 100.00% NaNs	429	- Tank 3 - Liquid - iC4 [%]: 100.00% NaNs

181	- BOG to GCU V/V [%]: 100.00% NaNs	430	- Tank 3 - Liquid - nC5 [%]: 100.00% NaNs
182	- FUEL GAS to GCU - Pressure [bar]: 100.00% NaNs	431	- Tank 3 - Liquid - iC5 [%]: 100.00% NaNs
183	- FUEL GAS TEMP to GCU - Temperature [°C]: 100.00% NaNs	432	- Tank 3 - Liquid - C6 [%]: 100.00% NaNs
184	- FUEL GAS TO GCU V/V [0-1-2]: 100.00% NaNs	433	- Tank 3 - Liquid - N2 [%]: 100.00% NaNs
185	- LNG Vaporizer 2 - DISCH FLOW [kg/h]: 100.00% NaNs	434	- Tank 3 - Liquid - CO2 [%]: 100.00% NaNs
186	- LNG Vaporizer 2 - INLET PRESS [bara]: 100.00% NaNs	435	- Tank 3 - Liquid - 02 [%]: 100.00% NaNs
187	- LNG Vaporizer 2 - OUTLET PRESS [bara]: 100.00% NaNs	436	- Tank 3 - Liquid - HHV [MW]: 100.00% NaNs
188	- LNG Vaporizer 2 - INLET TEMP [°C]: 100.00% NaNs	437	- Tank 3 - Liquid - LHV [MW]: 100.00% NaNs
189	- LNG Vaporizer 2 - OUTLET TEMP [°C]: 100.00% NaNs	438	- Tank 3 - Liquid - Density [kg/m^3]: 100.00% NaNs
190	- FORCING Vaporizer - OUTLET TEMP [°C]: 100.00% NaNs	439	- Tank 3 - Liquid - MN []: 100.00% NaNs
191	- Reliquefaction - Outlet flow [kg/h]: 100.00% NaNs	440	- Tank 3 - Vapour - C1 [%]: 100.00% NaNs
192	- Reliquefaction - Outlet pressure [mbara]: 100.00% NaNs	441	- Tank 3 - Vapour - C2 [%]: 100.00% NaNs
193	- Sub-Cooler - Inlet flow [kg/h]: 100.00% NaNs	442	- Tank 3 - Vapour - C3 [%]: 100.00% NaNs

194	- Sub-Cooler - Outlet flow [kg/h]: 100.00% NaNs	443	- Tank 3 - Vapour - nC4 [%]: 100.00% NaNs
195	- Sub-Cooler - Inlet pressure [bara]: 100.00% NaNs	444	- Tank 3 - Vapour - iC4 [%]: 100.00% NaNs
196	- Sub-Cooler - Outlet pressure [bara]: 100.00% NaNs	445	- Tank 3 - Vapour - nC5 [%]: 100.00% NaNs
197	- Sub-Cooler - Diffrential Pressure [mbar]: 100.00% NaNs	446	- Tank 3 - Vapour - iC5 [%]: 100.00% NaNs
198	- Sub-Cooler - Inlet temperature [°C]: 100.00% NaNs	447	- Tank 3 - Vapour - C6 [%]: 100.00% NaNs
199	- Sub-Cooler - Outlet temperature [°C]: 100.00% NaNs	448	- Tank 3 - Vapour - N2 [%]: 100.00% NaNs
200	- Sub-Cooler - Cold power [%]: 100.00% NaNs	449	- Tank 3 - Vapour - CO2 [%]: 100.00% NaNs
201	- Sub-Cooler - MTC1.POWER [kW]: 100.00% NaNs	450	- Tank 3 - Vapour - 02 [%]: 100.00% NaNs
202	- Sub-Cooler - MC1.POWER [kW]: 100.00% NaNs	451	- Tank 3 - Vapour - HHV [MW]: 100.00% NaNs
203	- Sub-Cooler - MC2.POWER [kW]: 100.00% NaNs	452	- Tank 3 - Vapour - LHV [MW]: 100.00% NaNs
204	- Sub-Cooler - MTC2.POWER [kW]: 100.00% NaNs	453	- Tank 3 - Vapour - Density [kg/m^3]: 100.00% NaNs
205	- Sub-Cooler - MC3.POWER [kW]: 100.00% NaNs	454	- Tank 3 - Vapour - MN []: 100.00% NaNs
206	- Sub-Cooler - MTC3.POWER [kW]: 100.00% NaNs	455	- Tank 4 - Liquid - C1 [%]: 100.00% NaNs

207	- Sub-Cooler - MC4.POWER [kW]: 100.00% NaNs	456	- Tank 4 - Liquid - C2 [%]: 100.00% NaNs
208	- Tank 1 Spray Line Portside Valve [0-1-2]: 100.00% NaNs	457	- Tank 4 - Liquid - C3 [%]: 100.00% NaNs
209	- Tank 1 Spray Line Starboard Valve [0-1-2]: 100.00% NaNs	458	- Tank 4 - Liquid - nC4 [%]: 100.00% NaNs
210	- Tank 1 Mixing Nozzle Valve [0-1-2]: 100.00% NaNs	459	- Tank 4 - Liquid - iC4 [%]: 100.00% NaNs
211	- Tank 2 Spray Line Portside Valve [0-1-2]: 100.00% NaNs	460	- Tank 4 - Liquid - nC5 [%]: 100.00% NaNs
212	- Tank 2 Spray Line Starboard Valve [0-1-2]: 100.00% NaNs	461	- Tank 4 - Liquid - iC5 [%]: 100.00% NaNs
213	- Tank 2 Mixing Nozzle Valve [0-1-2]: 100.00% NaNs	462	- Tank 4 - Liquid - C6 [%]: 100.00% NaNs
214	- Tank 3 Spray Line Portside Valve [0-1-2]: 100.00% NaNs	463	- Tank 4 - Liquid - N2 [%]: 100.00% NaNs
215	- Tank 3 Spray Line Starboard Valve [0-1-2]: 100.00% NaNs	464	- Tank 4 - Liquid - CO2 [%]: 100.00% NaNs
216	- Tank 3 Mixing Nozzle Valve [0-1-2]: 100.00% NaNs	465	- Tank 4 - Liquid - 02 [%]: 100.00% NaNs
217	- Tank 4 Spray Line Portside Valve [0-1-2]: 100.00% NaNs	466	- Tank 4 - Liquid - HHV [MW]: 100.00% NaNs
218	- Tank 4 Spray Line Starboard Valve [0-1-2]: 100.00% NaNs	467	- Tank 4 - Liquid - LHV [MW]: 100.00% NaNs
219	- Tank 4 Mixing Nozzle Valve [0-1-2]: 100.00% NaNs	468	- Tank 4 - Liquid - Density [kg/m^3]: 100.00% NaNs

220	- LD compressor 1 - INLET PRESS [bara]: 100.00% NaNs	469	- Tank 4 - Liquid - MN []: 100.00% NaNs
221	- LD compressor 1 - OUTLET PRESS [barg]: 100.00% NaNs	470	- Tank 4 - Vapour - C1 [%]: 100.00% NaNs
222	- LD compressor 1 - INLET TEMP [°C]: 100.00% NaNs	471	- Tank 4 - Vapour - C2 [%]: 100.00% NaNs
223	- LD compressor 1 - OUTLET TEMP A [°C]: 100.00% NaNs	472	- Tank 4 - Vapour - C3 [%]: 100.00% NaNs
224	- LD compressor 1 - DISCH FLOW [kg/h]: 100.00% NaNs	473	- Tank 4 - Vapour - nC4 [%]: 100.00% NaNs
225	- LD compressor 2 - INLET PRESS [bara]: 100.00% NaNs	474	- Tank 4 - Vapour - iC4 [%]: 100.00% NaNs
226	- LD compressor 2 - OUTLET PRESS [barg]: 100.00% NaNs	475	- Tank 4 - Vapour - nC5 [%]: 100.00% NaNs
227	- LD compressor 2 - INLET TEMP [°C]: 100.00% NaNs	476	- Tank 4 - Vapour - iC5 [%]: 100.00% NaNs
228	- LD compressor 2 - OUTLET TEMP B [°C]: 100.00% NaNs	477	- Tank 4 - Vapour - C6 [%]: 100.00% NaNs
229	- LD compressor 2 - DISCH FLOW [kg/h]: 100.00% NaNs	478	- Tank 4 - Vapour - N2 [%]: 100.00% NaNs
230	- HD compressor 1 - GAS SUC FLOW [kg/h]: 100.00% NaNs	479	- Tank 4 - Vapour - CO2 [%]: 100.00% NaNs
231	- HD compressor 2 - OUTLET PRESS [mbara]: 100.00% NaNs	480	- Tank 4 - Vapour - 02 [%]: 100.00% NaNs
232	- HD compressor 2 - INLET TEMP [°C]: 100.00% NaNs	481	- Tank 4 - Vapour - HHV [MW]: 100.00% NaNs

233	- HD compressor 2 - OUTLET TEMP A [°C]: 100.00% NaNs	482	- Tank 4 - Vapour - LHV [MW]: 100.00% NaNs
234	- HD compressor 2 - GAS SUC FLOW [°C]: 100.00% NaNs	483	- Tank 4 - Vapour - Density [kg/m^3]: 100.00% NaNs
235	- Vapour MAIN - Gauge pressure [mbarg]: 100.00% NaNs	484	- Tank 4 - Vapour - MN [ ]: 100.00% NaNs
236	- Vapour Cross-Over - Temperature [°C]: 100.00% NaNs	485	- ME FO supply temperature [°C]: 100.00% NaNs
237	- VAPOR RETURN TO SHORE TEMP [°C]: 100.00% NaNs	486	- ME1 Shaft RPM [rpm]: 100.00% NaNs
238	- Vapour Flow To Shore [kg/h]: 100.00% NaNs	487	- ME2 Shaft RPM [rpm]: 100.00% NaNs
239	- Vapour Flow From Shore [kg/h]: 100.00% NaNs	488	- Main Cooling Sea Water Port Temp [°C]: 100.00% NaNs
240	- Bunkering Liquid Line - Flow [kg/h]: 100.00% NaNs	489	- Main Cooling Sea Water Stbd Temp [°C]: 100.00% NaNs
241	- Bunker Vapour Line Pressure [bara]: 100.00% NaNs	490	- ME1 Power [kW]: 100.00% NaNs
242	- LNG supply HDR - Temperature [°C]: 100.00% NaNs	491	- ME2 Power [kW]: 100.00% NaNs
243	- NBO mist separator - Condensate temperature [°C]: 100.00% NaNs	492	- ME LNG consumed [MT]: 100.00% NaNs
244	- NBO mist separator - Level [mm]: 100.00% NaNs	493	- LO Remaining on Board [MT]: 100.00% NaNs
245	- FBO mist separator - Condensate temperature [°C]: 100.00% NaNs	494	- FW Remaining on Board [MT]: 100.00% NaNs

246	- FBO mist separator - Level [mm]: 100.00% NaNs	495	- MGO Remaining on Board [MT]: 100.00% NaNs
247	- X-DF - DFDE FUEL GAS PRESS CONTROL V/V [%]: 100.00% NaNs	496	- LNG Remaining on Board [MT]: 100.00% NaNs
248	- GCU - FUEL GAS PRESS CONTROL V/V [%]: 100.00% NaNs	497	- HFO Remaining on Board [MT]: 100.00% NaNs
249	- GE(STBD) FUEL GAS CONTROL VALVE [%]: 100.00% NaNs	498	- MDO Remaining on Board [MT]: 100.00% NaNs

Appendix 7 - Missing values Vessel 3

	Column 1		Column 2		Column 3
1	- Boiler consumed [MT]: 89.22% NaNs	195	- Tank 2 - Fuel Gas Pump 2 - Recycle [%]: 100.00% NaNs	389	- 5 COFFERDAM AFT PORT UPPER TEMP [°C]: 100.00% NaNs
2	- Ambient air pressure [mbar]: 76.93% NaNs	196	- Tank 2 - Fuel Gas Pump 3 - CURRENT [A]: 100.00% NaNs	390	- 5 COFFERDAM AFT STBD LOWER TEMP [°C]: 100.00% NaNs
3	- Ambient air relative humidity [%]: 100.00% NaNs	197	- Tank 2 - Fuel Gas Pump 3 - DISCH PRESS [bar]: 100.00% NaNs	391	- Nitrogen system - Bleeding pressure [bar]: 100.00% NaNs
4	- Shaft Torque [kNm]: 95.90% NaNs	198	- Tank 2 - Fuel Gas Pump 3 - DISCH V/V [%]: 100.00% NaNs	392	- Nitrogen system - Buffer tank pressure [bar]: 100.00% NaNs
5	- Rudder Angle [°]: 100.00% NaNs	199	- Tank 2 - Fuel Gas Pump 3 - Recycle [%]: 100.00% NaNs	393	- Nitrogen system - Header pressure [mbarg]: 100.00% NaNs

6	- Boiler HFO consumed [MT]: 74.05% NaNs	200	- Tank 2 - Fuel Gas Pump 4 - CURRENT [A]: 100.00% NaNs	394	- Nitrogen system - Header control valve [%]: 100.00% NaNs
7	- Boiler MGO/MDO consumed [MT]: 74.05% NaNs	201	- Tank 2 - Fuel Gas Pump 4 - DISCH PRESS [bar]: 100.00% NaNs	395	- NO.1 N2 GEN SYSTEM FAULT [True/False]: 100.00% NaNs
8	- Heave Average [m]: 100.00% NaNs	202	- Tank 2 - Fuel Gas Pump 4 - DISCH V/V [%]: 100.00% NaNs	396	- NO.1 N2 GENERATOR PRODUCT OXYGEN CONTENT [%]: 100.00% NaNs
9	- Sway Average [m]: 100.00% NaNs	203	- Tank 2 - Fuel Gas Pump 4 - Recycle [%]: 100.00% NaNs	397	- NO.1 N2 GENERATOR Outlet temperature [°C]: 100.00% NaNs
10	- Surge Average [m]: 100.00% NaNs	204	- Tank 3 - Fuel Gas Pump 1 - CURRENT [A]: 100.00% NaNs	398	- NO.1 N2 GENERATOR O2 Percentage [%]: 100.00% NaNs
11	- Rudder Angle min (°) [deg]: 100.00% NaNs	205	- Tank 3 - Fuel Gas Pump 1 - DISCH PRESS [bar]: 100.00% NaNs	399	- NO.1 N2 GENERATOR SYSTEM RUNNING

					[True/False]: 100.00% NaNs
12	- Rudder Angle max (°) [deg]: 100.00% NaNs	206	- Tank 3 - Fuel Gas Pump 1 - DISCH V/V [%]: 100.00% NaNs	400	- NO.2 N2 GEN SYSTEM FAULT [True/False]: 100.00% NaNs
13	- Shaft 1 RPM [rpm]: 94.95% NaNs	207	- Tank 3 - Fuel Gas Pump 1 - Recycle [%]: 100.00% NaNs	401	- NO.2 N2 GENERATOR PRODUCT OXYGEN CONTENT [%]: 100.00% NaNs
14	- Shaft 2 RPM [rpm]: 94.95% NaNs	208	- Tank 3 - Fuel Gas Pump 2 - CURRENT [A]: 100.00% NaNs	402	- NO.2 N2 GENERATOR Outlet temperature [°C]: 100.00% NaNs
15	- Shaft 1 Power [kW]: 94.95% NaNs	209	- Tank 3 - Fuel Gas Pump 2 - DISCH PRESS [bar]: 100.00% NaNs	403	- NO.2 N2 GENERATOR O2 Percentage [%]: 100.00% NaNs
16	- Shaft 2 Power [kW]: 94.95% NaNs	210	- Tank 3 - Fuel Gas Pump 2 - DISCH V/V [%]: 100.00% NaNs	404	- NO.2 N2 GENERATOR SYSTEM RUNNING [True/False]: 100.00% NaNs

17	- Shaft 1 Torque [kNm]: 95.20% NaNs	211	- Tank 3 - Fuel Gas Pump 2 - Recycle [%]: 100.00% NaNs	405	- Liquid - C1 [%]: 100.00% NaNs
18	- Shaft 2 Torque [kNm]: 95.20% NaNs	212	- Tank 3 - Fuel Gas Pump 3 - CURRENT [A]: 100.00% NaNs	406	- Liquid - C2 [%]: 100.00% NaNs
19	- ME1 BOG [MT/day]: 95.22% NaNs	213	- Tank 3 - Fuel Gas Pump 3 - DISCH PRESS [bar]: 100.00% NaNs	407	- Liquid - C3 [%]: 100.00% NaNs
20	- Total impacts all tanks []: 66.13% NaNs	214	- Tank 3 - Fuel Gas Pump 3 - DISCH V/V [%]: 100.00% NaNs	408	- Liquid - nC4 [%]: 100.00% NaNs
21	- Impacts tank 5 []: 100.00% NaNs	215	- Tank 3 - Fuel Gas Pump 3 - Recycle [%]: 100.00% NaNs	409	- Liquid - iC4 [%]: 100.00% NaNs
22	- Impacts tank 6 []: 100.00% NaNs	216	- Tank 3 - Fuel Gas Pump 4 - CURRENT [A]: 100.00% NaNs	410	- Liquid - nC5 [%]: 100.00% NaNs
23	- Tank 1 - Liquid temp 75% [°C]: 100.00% NaNs	217	- Tank 3 - Fuel Gas Pump 4 - DISCH PRESS [bar]: 100.00% NaNs	411	- Liquid - iC5 [%]: 100.00% NaNs
24	- Tank 2 - Liquid temp 75% [°C]: 100.00% NaNs	218	- Tank 3 - Fuel Gas Pump 4 - DISCH V/V [%]: 100.00% NaNs	412	- Liquid - C6 [%]: 100.00% NaNs
25	- Tank 3 - Liquid temp 75% [°C]: 100.00% NaNs	219	- Tank 3 - Fuel Gas Pump 4 - Recycle [%]: 100.00% NaNs	413	- Liquid - N2 [%]: 100.00% NaNs

26	- Tank 4 - Liquid temp 75% [°C]: 100.00% NaNs	220	- Tank 4 - Fuel Gas Pump 1 - CURRENT [A]: 100.00% NaNs	414	- Liquid - CO2 [%]: 100.00% NaNs
27	- Tank 1 - IBS AFT P BTM TEMP (MAIN) [°C]: 100.00% NaNs	221	- Tank 4 - Fuel Gas Pump 1 - DISCH PRESS [bar]: 100.00% NaNs	415	- Liquid - 02 [%]: 100.00% NaNs
28	- Tank 1 - IBS AFT P BTM TEMP (ST-BY) [°C]: 100.00% NaNs	222	- Tank 4 - Fuel Gas Pump 1 - DISCH V/V [%]: 100.00% NaNs	416	- Liquid - HHV [MW]: 100.00% NaNs
29	- Tank 1 - IBS AFT MID BTM TEMP (MAIN) [°C]: 100.00% NaNs	223	- Tank 4 - Fuel Gas Pump 1 - Recycle [%]: 100.00% NaNs	417	- Liquid - LHV [MW]: 100.00% NaNs
30	- Tank 1 - IBS AFT MID BTM TEMP (ST-BY) [°C]: 100.00% NaNs	224	- Tank 4 - Fuel Gas Pump 2 - CURRENT [A]: 100.00% NaNs	418	- Liquid - Density [kg/m^3]: 100.00% NaNs
31	- Tank 1 - IBS AFT S BTM TEMP (MAIN) [°C]: 100.00% NaNs	225	- Tank 4 - Fuel Gas Pump 2 - DISCH PRESS [bar]: 100.00% NaNs	419	- Liquid - MN []: 100.00% NaNs
32	- Tank 1 - IBS AFT S BTM TEMP (ST-BY) [°C]: 100.00% NaNs	226	- Tank 4 - Fuel Gas Pump 2 - DISCH V/V [%]: 100.00% NaNs	420	- Vapour - C1 [%]: 100.00% NaNs
33	- Tank 1 - IS BTM AFT MID TEMP(MAIN) [°C]: 100.00% NaNs	227	- Tank 4 - Fuel Gas Pump 2 - Recycle [%]: 100.00% NaNs	421	- Vapour - C2 [%]: 100.00% NaNs
34	- Tank 1 - IS BTM AFT MID TEMP(ST-BY) [°C]: 100.00% NaNs	228	- Tank 4 - Fuel Gas Pump 3 - CURRENT [A]: 100.00% NaNs	422	- Vapour - C3 [%]: 100.00% NaNs

35	- Tank 1 - IS BTM MIDDLE TEMP(ST-BY) [°C]: 100.00% NaNs	229	- Tank 4 - Fuel Gas Pump 3 - DISCH PRESS [bar]: 100.00% NaNs	423	- Vapour - nC4 [%]: 100.00% NaNs
36	- Tank 1 - IS PORT LOW CHAM TEMP(ST-BY) [°C]: 100.00% NaNs	230	- Tank 4 - Fuel Gas Pump 3 - DISCH V/V [%]: 100.00% NaNs	424	- Vapour - iC4 [%]: 100.00% NaNs
37	- Tank 1 - IS PORT SIDE WALL TEMP(ST-BY) [°C]: 100.00% NaNs	231	- Tank 4 - Fuel Gas Pump 3 - Recycle [%]: 100.00% NaNs	425	- Vapour - nC5 [%]: 100.00% NaNs
38	- Tank 1 - IS PORT UPP CHAM TEMP(ST-BY) [°C]: 100.00% NaNs	232	- Tank 4 - Fuel Gas Pump 4 - CURRENT [A]: 100.00% NaNs	426	- Vapour - iC5 [%]: 100.00% NaNs
39	- Tank 1 - IS CEIL TEMP(ST-BY) [°C]: 100.00% NaNs	233	- Tank 4 - Fuel Gas Pump 4 - DISCH PRESS [bar]: 100.00% NaNs	427	- Vapour - C6 [%]: 100.00% NaNs
40	- Tank 1 - IS AFT TRAN WALL TEMP(ST-BY) [°C]: 100.00% NaNs	234	- Tank 4 - Fuel Gas Pump 4 - DISCH V/V [%]: 100.00% NaNs	428	- Vapour - N2 [%]: 100.00% NaNs
41	- Tank 1 - IS FWD TRAN WALL TEMP(ST-BY) [°C]: 100.00% NaNs	235	- Tank 4 - Fuel Gas Pump 4 - Recycle [%]: 100.00% NaNs	429	- Vapour - CO2 [%]: 100.00% NaNs
42	- Tank 1 - IS PORT SIDE WALL TEMP(ST-BY) - (HULL) [°C]: 100.00% NaNs	236	- BOG to GCU V/V [%]: 100.00% NaNs	430	- Vapour - 02 [%]: 100.00% NaNs
43	- Tank 1 - TK PIPE DUCT FWD TEMP [°C]: 100.00% NaNs	237	- FUEL GAS to GCU - Pressure [bar]: 100.00% NaNs	431	- Vapour - HHV [MW]: 100.00% NaNs

44	- Tank 1 - BHD PORT TOP TEMP [°C]: 100.00% NaNs	238	- FUEL GAS TEMP to GCU - Temperature [°C]: 100.00% NaNs	432	- Vapour - LHV [MW]: 100.00% NaNs
45	- Tank 1 - BHD PORT MID TEMP [°C]: 100.00% NaNs	239	- FUEL GAS TO GCU V/V [0-1-2]: 100.00% NaNs	433	- Vapour - Density [kg/m^3]: 100.00% NaNs
46	- Tank 1 - BHD PORT LOW TEMP [°C]: 100.00% NaNs	240	- LNG Vaporizer 2 - DISCH FLOW [kg/h]: 100.00% NaNs	434	- Vapour - MN []: 100.00% NaNs
47	- Tank 1 - BHD STBD TOP TEMP [°C]: 100.00% NaNs	241	- LNG Vaporizer 2 - INLET PRESS [bara]: 100.00% NaNs	435	- Mixed Gas - C1 [%]: 100.00% NaNs
48	- Tank 1 - BHD STBD MID TEMP [°C]: 100.00% NaNs	242	- LNG Vaporizer 2 - OUTLET PRESS [bara]: 100.00% NaNs	436	- Mixed Gas - C2 [%]: 100.00% NaNs
49	- Tank 1 - BHD STBD LOW TEMP [°C]: 100.00% NaNs	243	- LNG Vaporizer 2 - INLET TEMP [°C]: 100.00% NaNs	437	- Mixed Gas - C3 [%]: 100.00% NaNs
50	- Tank 1 - IBS PRESSURE [mbar]: 100.00% NaNs	244	- LNG Vaporizer 2 - OUTLET TEMP [°C]: 100.00% NaNs	438	- Mixed Gas - nC4 [%]: 100.00% NaNs
51	- Tank 1 - IBS inlet PRESSURE [mbar]: 100.00% NaNs	245	- Reliquefaction - Outlet flow [kg/h]: 100.00% NaNs	439	- Mixed Gas - iC4 [%]: 100.00% NaNs
52	- Tank 1 - IBS exhaust PRESSURE [mbarg]: 100.00% NaNs	246	- Reliquefaction - Outlet temperature [°C]: 100.00% NaNs	440	- Mixed Gas - nC5 [%]: 100.00% NaNs

53	- Tank 1 - HC content in IBS [%]: 100.00% NaNs	247	- Reliquefaction - Outlet pressure [mbara]: 100.00% NaNs	441	- Mixed Gas - iC5 [%]: 100.00% NaNs
54	- Tank 1 - Liquid Dome IS inlet pressure [mbar]: 100.00% NaNs	248	- Reliquefaction - Inlet flow [kg/h]: 100.00% NaNs	442	- Mixed Gas - C6 [%]: 100.00% NaNs
55	- Tank 1 - IS PRESSURE [mbar]: 100.00% NaNs	249	- Reliquefaction - Inlet temperature [°C]: 100.00% NaNs	443	- Mixed Gas - N2 [%]: 100.00% NaNs
56	- Tank 1 - IS inlet PRESSURE [mbar]: 100.00% NaNs	250	- Reliquefaction - Inlet pressure [mbara]: 100.00% NaNs	444	- Mixed Gas - CO2 [%]: 100.00% NaNs
57	- Tank 1 - IS exhaust PRESSURE [mbarg]: 100.00% NaNs	251	- Reliquefaction - Electrical consumption [kW]: 100.00% NaNs	445	- Mixed Gas - 02 [%]: 100.00% NaNs
58	- Tank 1 - HC content in IS [%]: 100.00% NaNs	252	- Sub-Cooler - Inlet flow [kg/h]: 100.00% NaNs	446	- Mixed Gas - HHV [MW]: 100.00% NaNs
59	- Tank 1 - N2 IBS inlet control valve opening [%]: 100.00% NaNs	253	- Sub-Cooler - Outlet flow [kg/h]: 100.00% NaNs	447	- Mixed Gas - LHV [MW]: 100.00% NaNs
60	- Tank 1 - N2 IBS exhaust control valve opening [%]: 100.00% NaNs	254	- Sub-Cooler - Inlet pressure [bara]: 100.00% NaNs	448	- Mixed Gas - Density [kg/m^3]: 100.00% NaNs
61	- Tank 1 - N2 IS inlet control valve opening [%]: 100.00% NaNs	255	- Sub-Cooler - Outlet pressure [bara]: 100.00% NaNs	449	- Mixed Gas - MN []: 100.00% NaNs

62	- Tank 1 - N2 IS exhaust control valve opening [%]: 100.00% NaNs	256	- Sub-Cooler - Diffrential Pressure [mbar]: 100.00% NaNs	450	- Tank 1 - Liquid - C1 [%]: 100.00% NaNs
63	- Tank 2 - IBS AFT P BTM TEMP (MAIN) [°C]: 100.00% NaNs	257	- Sub-Cooler - Inlet temperature [°C]: 100.00% NaNs	451	- Tank 1 - Liquid - C2 [%]: 100.00% NaNs
64	- Tank 2 - IBS AFT P BTM TEMP (ST-BY) [°C]: 100.00% NaNs	258	- Sub-Cooler - Outlet temperature [°C]: 100.00% NaNs	452	- Tank 1 - Liquid - C3 [%]: 100.00% NaNs
65	- Tank 2 - IBS AFT MID BTM TEMP (MAIN) [°C]: 100.00% NaNs	259	- Tank 1 Spray Line Portside Valve [0-1-2]: 100.00% NaNs	453	- Tank 1 - Liquid - nC4 [%]: 100.00% NaNs
66	- Tank 2 - IBS AFT MID BTM TEMP (ST-BY) [°C]: 100.00% NaNs	260	- Tank 1 Spray Line Starboard Valve [0-1-2]: 100.00% NaNs	454	- Tank 1 - Liquid - iC4 [%]: 100.00% NaNs
67	- Tank 2 - IBS AFT S BTM TEMP (MAIN) [°C]: 100.00% NaNs	261	- Tank 1 Mixing Nozzle Valve [0-1-2]: 100.00% NaNs	455	- Tank 1 - Liquid - nC5 [%]: 100.00% NaNs
68	- Tank 2 - IBS AFT S BTM TEMP (ST-BY) [°C]: 100.00% NaNs	262	- Tank 2 Spray Line Portside Valve [0-1-2]: 100.00% NaNs	456	- Tank 1 - Liquid - iC5 [%]: 100.00% NaNs
69	- Tank 2 - IS BTM AFT MID TEMP(MAIN) [°C]: 100.00% NaNs	263	- Tank 2 Spray Line Starboard Valve [0-1-2]: 100.00% NaNs	457	- Tank 1 - Liquid - C6 [%]: 100.00% NaNs
70	- Tank 2 - IS BTM AFT MID TEMP(ST-BY) [°C]: 100.00% NaNs	264	- Tank 2 Mixing Nozzle Valve [0-1-2]: 100.00% NaNs	458	- Tank 1 - Liquid - N2 [%]: 100.00% NaNs

71	- Tank 2 - IS BTM MIDDLE TEMP(ST-BY) [°C]: 100.00% NaNs	265	- Tank 3 Spray Line Portside Valve [0-1-2]: 100.00% NaNs	459	- Tank 1 - Liquid - CO2 [%]: 100.00% NaNs
72	- Tank 2 - IS PORT LOW CHAM TEMP(ST-BY) [°C]: 100.00% NaNs	266	- Tank 3 Spray Line Starboard Valve [0-1-2]: 100.00% NaNs	460	- Tank 1 - Liquid - 02 [%]: 100.00% NaNs
73	- Tank 2 - IS PORT SIDE WALL TEMP(MAIN) [°C]: 100.00% NaNs	267	- Tank 3 Mixing Nozzle Valve [0-1-2]: 100.00% NaNs	461	- Tank 1 - Liquid - HHV [MW]: 100.00% NaNs
74	- Tank 2 - IS PORT SIDE WALL TEMP(ST-BY) [°C]: 100.00% NaNs	268	- Tank 4 Spray Line Portside Valve [0-1-2]: 100.00% NaNs	462	- Tank 1 - Liquid - LHV [MW]: 100.00% NaNs
75	- Tank 2 - IS PORT UPP CHAM TEMP(ST-BY) [°C]: 100.00% NaNs	269	- Tank 4 Spray Line Starboard Valve [0-1-2]: 100.00% NaNs	463	- Tank 1 - Liquid - Density [kg/m^3]: 100.00% NaNs
76	- Tank 2 - IS CEIL TEMP(ST-BY) [°C]: 100.00% NaNs	270	- Tank 4 Mixing Nozzle Valve [0-1-2]: 100.00% NaNs	464	- Tank 1 - Liquid - MN []: 100.00% NaNs
77	- Tank 2 - IS AFT TRAN WALL TEMP(ST-BY) [°C]: 100.00% NaNs	271	- LD compressor 1 - OUTLET TEMP B [°C]: 100.00% NaNs	465	- Tank 1 - Vapour - C1 [%]: 100.00% NaNs
78	- Tank 2 - IS FWD TRAN WALL TEMP(ST-BY) [°C]: 100.00% NaNs	272	- LD compressor 1 - SPRAY AFT. CLR. TEMP VV POS. [%]: 100.00% NaNs	466	- Tank 1 - Vapour - C2 [%]: 100.00% NaNs

79	- Tank 2 - IS PORT SIDE WALL TEMP(ST-BY) - (HULL) [°C]: 100.00% NaNs	273	- LD compressor 2 - OUTLET TEMP B [°C]: 100.00% NaNs	467	- Tank 1 - Vapour - C3 [%]: 100.00% NaNs
80	- Tank 2 - TK PIPE DUCT FWD TEMP [°C]: 100.00% NaNs	274	- LD compressor 2 - DISCH FLOW [kg/h]: 100.00% NaNs	468	- Tank 1 - Vapour - nC4 [%]: 100.00% NaNs
81	- Tank 2 - BHD PORT TOP TEMP [°C]: 100.00% NaNs	275	- LD compressor 2 - SPRAY AFT. CLR. TEMP VV POS. [%]: 100.00% NaNs	469	- Tank 1 - Vapour - iC4 [%]: 100.00% NaNs
82	- Tank 2 - BHD PORT MID TEMP [°C]: 100.00% NaNs	276	- HD compressor 1 - GAS SUC FLOW [kg/h]: 100.00% NaNs	470	- Tank 1 - Vapour - nC5 [%]: 100.00% NaNs
83	- Tank 2 - BHD PORT LOW TEMP [°C]: 100.00% NaNs	277	- HD compressor 1 - Orifice Plate Diffrencial Press [mbar]: 100.00% NaNs	471	- Tank 1 - Vapour - iC5 [%]: 100.00% NaNs
84	- Tank 2 - BHD STBD TOP TEMP [°C]: 100.00% NaNs	278	- HD compressor 2 - OUTLET PRESS [mbara]: 100.00% NaNs	472	- Tank 1 - Vapour - C6 [%]: 100.00% NaNs
85	- Tank 2 - BHD STBD MID TEMP [°C]: 100.00% NaNs	279	- HD compressor 2 - INLET TEMP [°C]: 100.00% NaNs	473	- Tank 1 - Vapour - N2 [%]: 100.00% NaNs
86	- Tank 2 - BHD STBD LOW TEMP [°C]: 100.00% NaNs	280	- HD compressor 2 - OUTLET TEMP A [°C]: 100.00% NaNs	474	- Tank 1 - Vapour - CO2

					[%]: 100.00% NaNs
87	- Tank 2 - IBS PRESSURE [mbar]: 100.00% NaNs	281	- HD compressor 2 - GAS SUC FLOW [°C]: 100.00% NaNs	475	- Tank 1 - Vapour - 02 [%]: 100.00% NaNs
88	- Tank 2 - IBS inlet PRESSURE [mbar]: 100.00% NaNs	282	- HD compressor 2 - Orifice Plate Diffrencial Press [mbar]: 100.00% NaNs	476	- Tank 1 - Vapour - HHV [MW]: 100.00% NaNs
89	- Tank 2 - IBS exhaust PRESSURE [%]: 100.00% NaNs	283	- Liquid MAIN - FWD temperature [°C]: 100.00% NaNs	477	- Tank 1 - Vapour - LHV [MW]: 100.00% NaNs
90	- Tank 2 - HC content in IBS [%]: 100.00% NaNs	284	- Liquid MAIN - AFT temperature [°C]: 100.00% NaNs	478	- Tank 1 - Vapour - Density [kg/m^3]: 100.00% NaNs
91	- Tank 2 - Liquid Dome IS inlet pressure [mbar]: 100.00% NaNs	285	- Vapour MAIN - Gauge pressure [mbarg]: 100.00% NaNs	479	- Tank 1 - Vapour - MN []: 100.00% NaNs
92	- Tank 2 - IS PRESSURE [mbar]: 100.00% NaNs	286	- Vapour MAIN - FWD temperature [°C]: 100.00% NaNs	480	- Tank 2 - Liquid - C1 [%]: 100.00% NaNs
93	- Tank 2 - IS inlet PRESSURE [mbar]: 100.00% NaNs	287	- Vapour MAIN - AFT temperature [°C]: 100.00% NaNs	481	- Tank 2 - Liquid - C2 [%]: 100.00% NaNs
94	- Tank 2 - IS exhaust PRESSURE [mbarg]: 100.00% NaNs	288	- Vapour Cross-Over - Temperature [°C]: 100.00% NaNs	482	- Tank 2 - Liquid - C3 [%]: 100.00% NaNs

95	- Tank 2 - HC content in IS [%]: 100.00% NaNs	289	- VAPOR RETURN TO SHORE TEMP [°C]: 100.00% NaNs	483	- Tank 2 - Liquid - nC4 [%]: 100.00% NaNs
96	- Tank 2 - N2 IBS inlet control valve opening [%]: 100.00% NaNs	290	- Vapour Flow To Shore [kg/h]: 100.00% NaNs	484	- Tank 2 - Liquid - iC4 [%]: 100.00% NaNs
97	- Tank 2 - N2 IBS exhaust control valve opening [%]: 100.00% NaNs	291	- Vapour Flow From Shore [kg/h]: 100.00% NaNs	485	- Tank 2 - Liquid - nC5 [%]: 100.00% NaNs
98	- Tank 2 - N2 IS inlet control valve opening [%]: 100.00% NaNs	292	- Spray MAIN - FWD temperature [°C]: 100.00% NaNs	486	- Tank 2 - Liquid - iC5 [%]: 100.00% NaNs
99	- Tank 2 - N2 IS exhaust control valve opening [%]: 100.00% NaNs	293	- Spray MAIN - AFT temperature [°C]: 100.00% NaNs	487	- Tank 2 - Liquid - C6 [%]: 100.00% NaNs
100	- Tank 3 - IBS AFT P BTM TEMP (MAIN) [°C]: 100.00% NaNs	294	- Tank 1 - Spray return pressure [barg]: 100.00% NaNs	488	- Tank 2 - Liquid - N2 [%]: 100.00% NaNs
101	- Tank 3 - IBS AFT P BTM TEMP (ST-BY) [°C]: 100.00% NaNs	295	- Tank 2 - Spray return pressure [barg]: 100.00% NaNs	489	- Tank 2 - Liquid - CO2 [%]: 100.00% NaNs
102	- Tank 3 - IBS AFT MID BTM TEMP (MAIN) [°C]: 100.00% NaNs	296	- Tank 3 - Spray return pressure [barg]: 100.00% NaNs	490	- Tank 2 - Liquid - 02 [%]: 100.00% NaNs
103	- Tank 3 - IBS AFT MID BTM TEMP (ST-BY) [°C]: 100.00% NaNs	297	- Tank 4 - Spray return pressure [barg]: 100.00% NaNs	491	- Tank 2 - Liquid - HHV

					[MW]: 100.00% NaNs
104	- Tank 3 - IBS AFT S BTM TEMP (MAIN) [°C]: 100.00% NaNs	298	- Bunkering Liquid Line - Flow [kg/h]: 100.00% NaNs	492	- Tank 2 - Liquid - LHV [MW]: 100.00% NaNs
105	- Tank 3 - IBS AFT S BTM TEMP (ST-BY) [°C]: 100.00% NaNs	299	- Bunker Vapour Line Pressure [bara]: 100.00% NaNs	493	- Tank 2 - Liquid - Density [kg/m^3]: 100.00% NaNs
106	- Tank 3 - IS BTM AFT MID TEMP(MAIN) [°C]: 100.00% NaNs	300	- LNG supply HDR - Temperature [°C]: 100.00% NaNs	494	- Tank 2 - Liquid - MN []: 100.00% NaNs
107	- Tank 3 - IS BTM AFT MID TEMP(ST-BY) [°C]: 100.00% NaNs	301	- NBO mist separator - Condensate temperature [°C]: 100.00% NaNs	495	- Tank 2 - Vapour - C1 [%]: 100.00% NaNs
108	- Tank 3 - IS BTM MIDDLE TEMP(ST-BY) [°C]: 100.00% NaNs	302	- NBO mist separator - Level [mm]: 100.00% NaNs	496	- Tank 2 - Vapour - C2 [%]: 100.00% NaNs
109	- Tank 3 - IS PORT LOW CHAM TEMP(ST-BY) [°C]: 100.00% NaNs	303	- FBO mist separator - Condensate temperature [°C]: 100.00% NaNs	497	- Tank 2 - Vapour - C3 [%]: 100.00% NaNs
110	- Tank 3 - IS PORT SIDE WALL TEMP(ST-BY) [°C]: 100.00% NaNs	304	- FBO mist separator - Level [mm]: 100.00% NaNs	498	- Tank 2 - Vapour - nC4 [%]: 100.00% NaNs
111	- Tank 3 - IS PORT UPP CHAM TEMP(ST-BY) [°C]: 100.00% NaNs	305	- X-DF - DFDE FUEL GAS PRESS CONTROL V/V [%]: 100.00% NaNs	499	- Tank 2 - Vapour - iC4 [%]: 100.00% NaNs

112	- Tank 3 - IS CEIL TEMP(ST-BY) [°C]: 100.00% NaNs	306	- GCU - FUEL GAS PRESS CONTROL V/V [%]: 100.00% NaNs	500	- Tank 2 - Vapour - nC5 [%]: 100.00% NaNs
113	- Tank 3 - IS AFT TRAN WALL TEMP(ST-BY) [°C]: 100.00% NaNs	307	- GE(STBD) FUEL GAS CONTROL VALVE [%]: 100.00% NaNs	501	- Tank 2 - Vapour - iC5 [%]: 100.00% NaNs
114	- Tank 3 - IS FWD TRAN WALL TEMP(ST-BY) [°C]: 100.00% NaNs	308	- GE(PORT) FUEL GAS CONTROL VALVE [%]: 100.00% NaNs	502	- Tank 2 - Vapour - C6 [%]: 100.00% NaNs
115	- Tank 3 - IS PORT SIDE WALL TEMP(ST-BY) - (HULL) [°C]: 100.00% NaNs	309	- NG Main Buffer Tank - Pressure [bara]: 100.00% NaNs	503	- Tank 2 - Vapour - N2 [%]: 100.00% NaNs
116	- Tank 3 - BHD PORT TOP TEMP [°C]: 100.00% NaNs	310	- NG Main Buffer Tank - Disc.Temp. [°C]: 100.00% NaNs	504	- Tank 2 - Vapour - CO2 [%]: 100.00% NaNs
117	- Tank 3 TK PIPE DUCT FWD TEMP [°C]: 100.00% NaNs	311	- NG Aux. Buffer Tank - Pressure [bara]: 100.00% NaNs	505	- Tank 2 - Vapour - 02 [%]: 100.00% NaNs
118	- Tank 3 - BHD PORT MID TEMP [°C]: 100.00% NaNs	312	- NG Aux. Buffer Tank - Disc.Temp. [°C]: 100.00% NaNs	506	- Tank 2 - Vapour - HHV [MW]: 100.00% NaNs
119	- Tank 3 - BHD PORT LOW TEMP [°C]: 100.00% NaNs	313	- NG Aux.buffer to DF Boiler - Pressure [mbarg]: 100.00% NaNs	507	- Tank 2 - Vapour - LHV [MW]: 100.00% NaNs

120	- Tank 3 - BHD STBD TOP TEMP [°C]: 100.00% NaNs	314	- NG Heater - GAS INLET PRESS [bara]: 100.00% NaNs	508	- Tank 2 - Vapour - Density [kg/m^3]: 100.00% NaNs
121	- Tank 3 - BHD STBD MID TEMP [°C]: 100.00% NaNs	315	- NG Heater - GAS OUTLET PRESS [bara]: 100.00% NaNs	509	- Tank 2 - Vapour - MN []: 100.00% NaNs
122	- Tank 3 - BHD STBD LOW TEMP [°C]: 100.00% NaNs	316	- NG Heater - GAS INLET TEMP [°C]: 100.00% NaNs	510	- Tank 3 - Liquid - C1 [%]: 100.00% NaNs
123	- Tank 3 - IBS PRESSURE [mbar]: 100.00% NaNs	317	- NG Heater - GAS OUTLET TEMP [°C]: 100.00% NaNs	511	- Tank 3 - Liquid - C2 [%]: 100.00% NaNs
124	- Tank 3 - IBS inlet PRESSURE [mbar]: 100.00% NaNs	318	- NG Heater II - GAS INLET PRESS [bara]: 100.00% NaNs	512	- Tank 3 - Liquid - C3 [%]: 100.00% NaNs
125	- Tank 3 - IBS exhaust PRESSURE [%]: 100.00% NaNs	319	- NG Heater II - GAS OUTLET PRESS [bara]: 100.00% NaNs	513	- Tank 3 - Liquid - nC4 [%]: 100.00% NaNs
126	- Tank 3 - HC content in IBS [%]: 100.00% NaNs	320	- NG Heater II - GAS INLET TEMP [°C]: 100.00% NaNs	514	- Tank 3 - Liquid - iC4 [%]: 100.00% NaNs
127	- Tank 3 - Liquid Dome IS inlet pressure [mbar]: 100.00% NaNs	321	- NG Heater II - GAS OUTLET TEMP [°C]: 100.00% NaNs	515	- Tank 3 - Liquid - nC5 [%]: 100.00% NaNs
128	- Tank 3 - IS PRESSURE [mbar]: 100.00% NaNs	322	- NG Fuel Heaters to NG Main buffer tank - Temp [°C]: 100.00% NaNs	516	- Tank 3 - Liquid - iC5 [%]: 100.00% NaNs

129	- Tank 3 - IS inlet PRESSURE [mbar]: 100.00% NaNs	323	- LNG Heater - GAS INLET PRESS [bar]: 100.00% NaNs	517	- Tank 3 - Liquid - C6 [%]: 100.00% NaNs
130	- Tank 3 - IS exhaust PRESSURE [mbarg]: 100.00% NaNs	324	- LNG Heater - GAS OUTLET PRESS [bar]: 100.00% NaNs	518	- Tank 3 - Liquid - N2 [%]: 100.00% NaNs
131	- Tank 3 - HC content in IS [%]: 100.00% NaNs	325	- LNG Heater - GAS INLET TEMP [°C]: 100.00% NaNs	519	- Tank 3 - Liquid - CO2 [%]: 100.00% NaNs
132	- Tank 3 - N2 IBS inlet control valve opening [%]: 100.00% NaNs	326	- LNG Heater - GAS OUTLET TEMP [°C]: 100.00% NaNs	520	- Tank 3 - Liquid - 02 [%]: 100.00% NaNs
133	- Tank 3 - N2 IBS exhaust control valve opening [%]: 100.00% NaNs	327	- Fuel Gas Heater - GAS INLET PRESS [bar]: 100.00% NaNs	521	- Tank 3 - Liquid - HHV [MW]: 100.00% NaNs
134	- Tank 3 - N2 IS inlet control valve opening [%]: 100.00% NaNs	328	- Fuel Gas Heater - GAS OUTLET PRESS [bar]: 100.00% NaNs	522	- Tank 3 - Liquid - LHV [MW]: 100.00% NaNs
135	- Tank 3 - N2 IS exhaust control valve opening [%]: 100.00% NaNs	329	- Fuel Gas Heater - GAS INLET TEMP [°C]: 100.00% NaNs	523	- Tank 3 - Liquid - Density [kg/m^3]: 100.00% NaNs
136	- Tank 4 - IBS AFT P BTM TEMP (MAIN) [°C]: 100.00% NaNs	330	- Fuel Gas Heater - GAS OUTLET TEMP [°C]: 100.00% NaNs	524	- Tank 3 - Liquid - MN []: 100.00% NaNs

137	- Tank 4 - IBS AFT P BTM TEMP (ST-BY) [°C]: 100.00% NaNs	331	- No.1 Water level AFT bilge well [mm]: 100.00% NaNs	525	- Tank 3 - Vapour - C1 [%]: 100.00% NaNs
138	- Tank 4 - IBS AFT MID BTM TEMP (MAIN) [°C]: 100.00% NaNs	332	- No.2 Water level AFT bilge well [mm]: 100.00% NaNs	526	- Tank 3 - Vapour - C2 [%]: 100.00% NaNs
139	- Tank 4 - IBS AFT MID BTM TEMP (ST-BY) [°C]: 100.00% NaNs	333	- No.1 Water level FORE bilge well [mm]: 100.00% NaNs	527	- Tank 3 - Vapour - C3 [%]: 100.00% NaNs
140	- Tank 4 - IBS AFT S BTM TEMP (MAIN) [°C]: 100.00% NaNs	334	- No.2 Water level FORE bilge well [mm]: 100.00% NaNs	528	- Tank 3 - Vapour - nC4 [%]: 100.00% NaNs
141	- Tank 4 - IBS AFT S BTM TEMP (ST-BY) [°C]: 100.00% NaNs	335	- 1 COFFERDAM FWD UPPER TEMP [°C]: 100.00% NaNs	529	- Tank 3 - Vapour - iC4 [%]: 100.00% NaNs
142	- Tank 4 - IS BTM AFT MID TEMP(MAIN) [°C]: 100.00% NaNs	336	- 1 COFFERDAM FWD MIDDLE TEMP [°C]: 100.00% NaNs	530	- Tank 3 - Vapour - nC5 [%]: 100.00% NaNs
143	- Tank 4 - IS BTM AFT MID TEMP(ST-BY) [°C]: 100.00% NaNs	337	- 1 COFFERDAM FWD LOWER TEMP [°C]: 100.00% NaNs	531	- Tank 3 - Vapour - iC5 [%]: 100.00% NaNs
144	- Tank 4 - IS BTM MIDDLE TEMP(ST-BY) [°C]: 100.00% NaNs	338	- 1 COFFERDAM FWD STBD UPPER TEMP [°C]: 100.00% NaNs	532	- Tank 3 - Vapour - C6 [%]: 100.00% NaNs
145	- Tank 4 - IS PORT LOW CHAM TEMP(ST-BY) [°C]: 100.00% NaNs	339	- 1 COFFERDAM FWD PORT LOWER	533	- Tank 3 - Vapour - N2 [%]: 100.00% NaNs

			TEMP [°C]: 100.00% NaNs		
146	- Tank 4 - IS PORT SIDE WALL TEMP(ST-BY) [°C]: 100.00% NaNs	340	- 1 COFFERDAM FWD PORT UPPER TEMP [°C]: 100.00% NaNs	534	- Tank 3 - Vapour - CO2 [%]: 100.00% NaNs
147	- Tank 4 - IS PORT UPP CHAM TEMP(ST-BY) [°C]: 100.00% NaNs	341	- 1 COFFERDAM FWD STBD LOWER TEMP [°C]: 100.00% NaNs	535	- Tank 3 - Vapour - 02 [%]: 100.00% NaNs
148	- Tank 4 - IS CEIL TEMP(ST-BY) [°C]: 100.00% NaNs	342	- 1 COFFERDAM AFT UPPER TEMP [°C]: 100.00% NaNs	536	- Tank 3 - Vapour - HHV [MW]: 100.00% NaNs
149	- Tank 4 - IS AFT TRAN WALL TEMP(ST-BY) [°C]: 100.00% NaNs	343	- 1 COFFERDAM AFT LOWER TEMP [°C]: 100.00% NaNs	537	- Tank 3 - Vapour - LHV [MW]: 100.00% NaNs
150	- Tank 4 - IS FWD TRAN WALL TEMP(ST-BY) [°C]: 100.00% NaNs	344	- 1 COFFERDAM AFT STBD UPPER TEMP [°C]: 100.00% NaNs	538	- Tank 3 - Vapour - Density [kg/m^3]: 100.00% NaNs
151	- Tank 4 - IS PORT SIDE WALL TEMP(ST-BY) - (HULL) [°C]: 100.00% NaNs	345	- 1 COFFERDAM AFT PORT LOWER TEMP [°C]: 100.00% NaNs	539	- Tank 3 - Vapour - MN []: 100.00% NaNs
152	- Tank 4 - TK PIPE DUCT FWD TEMP [°C]: 100.00% NaNs	346	- 1 COFFERDAM AFT PORT UPPER TEMP [°C]: 100.00% NaNs	540	- Tank 4 - Liquid - C1 [%]: 100.00% NaNs

153	- Tank 4 - BHD PORT TOP TEMP [°C]: 100.00% NaNs	347	- 1 COFFERDAM AFT STBD LOWER TEMP [°C]: 100.00% NaNs	541	- Tank 4 - Liquid - C2 [%]: 100.00% NaNs
154	- Tank 4 - BHD PORT MID TEMP [°C]: 100.00% NaNs	348	- 2 COFFERDAM FWD UPPER TEMP [°C]: 100.00% NaNs	542	- Tank 4 - Liquid - C3 [%]: 100.00% NaNs
155	- Tank 4 - BHD PORT LOW TEMP [°C]: 100.00% NaNs	349	- 2 COFFERDAM FWD LOWER TEMP [°C]: 100.00% NaNs	543	- Tank 4 - Liquid - nC4 [%]: 100.00% NaNs
156	- Tank 4 - BHD STBD TOP TEMP [°C]: 100.00% NaNs	350	- 2 COFFERDAM FWD STBD UPPER TEMP [°C]: 100.00% NaNs	544	- Tank 4 - Liquid - iC4 [%]: 100.00% NaNs
157	- Tank 4 - BHD STBD MID TEMP [°C]: 100.00% NaNs	351	- 2 COFFERDAM FWD PORT LOWER TEMP [°C]: 100.00% NaNs	545	- Tank 4 - Liquid - nC5 [%]: 100.00% NaNs
158	- Tank 4 - BHD STBD LOW TEMP [°C]: 100.00% NaNs	352	- 2 COFFERDAM FWD PORT UPPER TEMP [°C]: 100.00% NaNs	546	- Tank 4 - Liquid - iC5 [%]: 100.00% NaNs
159	- Tank 4 - IBS PRESSURE [mbar]: 100.00% NaNs	353	- 2 COFFERDAM FWD STBD LOWER TEMP [°C]: 100.00% NaNs	547	- Tank 4 - Liquid - C6 [%]: 100.00% NaNs
160	- Tank 4 - IBS inlet PRESSURE [mbar]: 100.00% NaNs	354	- 2 COFFERDAM AFT UPPER TEMP [°C]: 100.00% NaNs	548	- Tank 4 - Liquid - N2 [%]: 100.00% NaNs
161	- Tank 4 - IBS exhaust PRESSURE [%]: 100.00% NaNs	355	- 2 COFFERDAM AFT STBD UPPER TEMP [°C]: 100.00% NaNs	549	- Tank 4 - Liquid - CO2 [%]: 100.00% NaNs

162	- Tank 4 - HC content in IBS [%]: 100.00% NaNs	356	- 2 COFFERDAM AFT PORT LOWER TEMP [°C]: 100.00% NaNs	550	- Tank 4 - Liquid - 02 [%]: 100.00% NaNs
163	- Tank 4 - Liquid Dome IS inlet pressure [mbar]: 100.00% NaNs	357	- 2 COFFERDAM AFT PORT UPPER TEMP [°C]: 100.00% NaNs	551	- Tank 4 - Liquid - HHV [MW]: 100.00% NaNs
164	- Tank 4 - IS PRESSURE [mbar]: 100.00% NaNs	358	- 2 COFFERDAM AFT STBD LOWER TEMP [°C]: 100.00% NaNs	552	- Tank 4 - Liquid - LHV [MW]: 100.00% NaNs
165	- Tank 4 - IS inlet PRESSURE [mbar]: 100.00% NaNs	359	- 3 COFFERDAM FWD STBD UPPER TEMP [°C]: 100.00% NaNs	553	- Tank 4 - Liquid - Density [kg/m^3]: 100.00% NaNs
166	- Tank 4 - IS exhaust PRESSURE [mbarg]: 100.00% NaNs	360	- 3 COFFERDAM FWD PORT LOWER TEMP [°C]: 100.00% NaNs	554	- Tank 4 - Liquid - MN []: 100.00% NaNs
167	- Tank 4 - HC content in IS [%]: 100.00% NaNs	361	- 3 COFFERDAM FWD PORT UPPER TEMP [°C]: 100.00% NaNs	555	- Tank 4 - Vapour - C1 [%]: 100.00% NaNs
168	- Tank 4 - N2 IBS inlet control valve opening [%]: 100.00% NaNs	362	- 3 COFFERDAM FWD STBD LOWER TEMP [°C]: 100.00% NaNs	556	- Tank 4 - Vapour - C2 [%]: 100.00% NaNs
169	- Tank 4 - N2 IBS exhaust control valve	363	- 3 COFFERDAM AFT STBD UPPER TEMP [°C]: 100.00% NaNs	557	- Tank 4 - Vapour - C3 [%]: 100.00% NaNs

	opening [%]: 100.00% NaNs				
170	- Tank 4 - N2 IS inlet control valve opening [%]: 100.00% NaNs	364	- 3 COFFERDAM AFT PORT LOWER TEMP [°C]: 100.00% NaNs	558	- Tank 4 - Vapour - nC4 [%]: 100.00% NaNs
171	- Tank 4 - N2 IS exhaust control valve opening [%]: 100.00% NaNs	365	- 3 COFFERDAM AFT PORT UPPER TEMP [°C]: 100.00% NaNs	559	- Tank 4 - Vapour - iC4 [%]: 100.00% NaNs
172	- Tank 1 - Fuel Gas Pump 1 - CURRENT [A]: 100.00% NaNs	366	- 3 COFFERDAM AFT STBD LOWER TEMP [°C]: 100.00% NaNs	560	- Tank 4 - Vapour - nC5 [%]: 100.00% NaNs
173	- Tank 1 - Fuel Gas Pump 1 - DISCH PRESS [bar]: 100.00% NaNs	367	- 4 COFFERDAM FWD STBD UPPER TEMP [°C]: 100.00% NaNs	561	- Tank 4 - Vapour - iC5 [%]: 100.00% NaNs
174	- Tank 1 - Fuel Gas Pump 1 - DISCH V/V [%]: 100.00% NaNs	368	- 4 COFFERDAM FWD PORT LOWER TEMP [°C]: 100.00% NaNs	562	- Tank 4 - Vapour - C6 [%]: 100.00% NaNs
175	- Tank 1 - Fuel Gas Pump 1 - Recycle [%]: 100.00% NaNs	369	- 4 COFFERDAM FWD PORT UPPER TEMP [°C]: 100.00% NaNs	563	- Tank 4 - Vapour - N2 [%]: 100.00% NaNs
176	- Tank 1 - Fuel Gas Pump 2 - CURRENT [A]: 100.00% NaNs	370	- 4 COFFERDAM FWD STBD LOWER TEMP [°C]: 100.00% NaNs	564	- Tank 4 - Vapour - CO2 [%]: 100.00% NaNs

177	- Tank 1 - Fuel Gas Pump 2 - DISCH PRESS [bar]: 100.00% NaNs	371	- 4 COFFERDAM AFT UPPER TEMP [°C]: 100.00% NaNs	565	- Tank 4 - Vapour - 02 [%]: 100.00% NaNs
178	- Tank 1 - Fuel Gas Pump 2 - DISCH V/V [%]: 100.00% NaNs	372	- 4 COFFERDAM AFT LOWER TEMP [°C]: 100.00% NaNs	566	- Tank 4 - Vapour - HHV [MW]: 100.00% NaNs
179	- Tank 1 - Fuel Gas Pump 2 - Recycle [%]: 100.00% NaNs	373	- 4 COFFERDAM AFT STBD UPPER TEMP [°C]: 100.00% NaNs	567	- Tank 4 - Vapour - LHV [MW]: 100.00% NaNs
180	- Tank 1 - Fuel Gas Pump 3 - CURRENT [A]: 100.00% NaNs	374	- 4 COFFERDAM AFT PORT LOWER TEMP [°C]: 100.00% NaNs	568	- Tank 4 - Vapour - Density [kg/m^3]: 100.00% NaNs
181	- Tank 1 - Fuel Gas Pump 3 - DISCH PRESS [bar]: 100.00% NaNs	375	- 4 COFFERDAM AFT PORT UPPER TEMP [°C]: 100.00% NaNs	569	- Tank 4 - Vapour - MN [ ]: 100.00% NaNs
182	- Tank 1 - Fuel Gas Pump 3 - DISCH V/V [%]: 100.00% NaNs	376	- 4 COFFERDAM AFT STBD LOWER TEMP [°C]: 100.00% NaNs	570	- ME FO supply temperature [°C]: 100.00% NaNs
183	- Tank 1 - Fuel Gas Pump 3 - Recycle [%]: 100.00% NaNs	377	- 5 COFFERDAM FWD UPPER TEMP [°C]: 100.00% NaNs	571	- ME1 Shaft RPM [rpm]: 94.95% NaNs
184	- Tank 1 - Fuel Gas Pump 4 - CURRENT [A]: 100.00% NaNs	378	- 5 COFFERDAM FWD MIDDLE TEMP [°C]: 100.00% NaNs	572	- ME2 Shaft RPM [rpm]: 94.95% NaNs

185	- Tank 1 - Fuel Gas Pump 4 - DISCH PRESS [bar]: 100.00% NaNs	379	- 5 COFFERDAM FWD LOWER TEMP [°C]: 100.00% NaNs	573	- Main Cooling Sea Water Port Temp [°C]: 100.00% NaNs
186	- Tank 1 - Fuel Gas Pump 4 - DISCH V/V [%]: 100.00% NaNs	380	- 5 COFFERDAM FWD STBD UPPER TEMP [°C]: 100.00% NaNs	574	- Main Cooling Sea Water Stbd Temp [°C]: 100.00% NaNs
187	- Tank 1 - Fuel Gas Pump 4 - Recycle [%]: 100.00% NaNs	381	- 5 COFFERDAM FWD PORT LOWER TEMP [°C]: 100.00% NaNs	575	- ME1 Power [kW]: 94.95% NaNs
188	- Tank 2 - Fuel Gas Pump 1 - CURRENT [A]: 100.00% NaNs	382	- 5 COFFERDAM FWD PORT UPPER TEMP [°C]: 100.00% NaNs	576	- ME2 Power [kW]: 94.95% NaNs
189	- Tank 2 - Fuel Gas Pump 1 - DISCH PRESS [bar]: 100.00% NaNs	383	- 5 COFFERDAM FWD STBD LOWER TEMP [°C]: 100.00% NaNs	577	- ME LNG consumed [MT]: 100.00% NaNs
190	- Tank 2 - Fuel Gas Pump 1 - DISCH V/V [%]: 100.00% NaNs	384	- 5 COFFERDAM AFT UPPER TEMP [°C]: 100.00% NaNs	578	- LO Remaining on Board [MT]: 87.82% NaNs
191	- Tank 2 - Fuel Gas Pump 1 - Recycle [%]: 100.00% NaNs	385	- 5 COFFERDAM AFT MIDDLE TEMP [°C]: 100.00% NaNs	579	- FW Remaining on Board [MT]: 87.82% NaNs
192	- Tank 2 - Fuel Gas Pump 2 - CURRENT [A]: 100.00% NaNs	386	- 5 COFFERDAM AFT LOWER TEMP [°C]: 100.00% NaNs	580	- MGO Remaining on

					Board [MT]: 87.76% NaNs
193	- Tank 2 - Fuel Gas Pump 2 - DISCH PRESS [bar]: 100.00% NaNs	387	- 5 COFFERDAM AFT STBD UPPER TEMP [°C]: 100.00% NaNs	581	- LNG Remaining on Board [MT]: 87.76% NaNs
194	- Tank 2 - Fuel Gas Pump 2 - DISCH V/V [%]: 100.00% NaNs	388	- 5 COFFERDAM AFT PORT LOWER TEMP [°C]: 100.00% NaNs	582	- HFO Remaining on Board [MT]: 87.76% NaNs

Appendix 8 - Data not related to vessel consumption

	# Highly detailed internal tank temperatures, unlikely to affect overall vessel consumption	118	'Forced boil-off [MT/day]',
1	'Tank 1 - IS BTM AFT MID TEMP(MAIN) [°C]',	119	'BOG to ME [MT/day]',
2	'Tank 1 - IS BTM MIDDLE TEMP(MAIN) [°C]',	120	'BOG to AUX [MT/day]',
3	'Tank 1 - IS PORT LOW CHAM TEMP(MAIN) [°C]',	121	'LBOG [MT/day]',
4	'Tank 1 - IS PORT SIDE WALL TEMP(MAIN) [°C]',	122	'DG1 BOG [MT/day]',
5	'Tank 1 - IS PORT UPP CHAM TEMP(MAIN) [°C]',	123	'DG2 BOG [MT/day]',
6	'Tank 1 - IS CEIL TEMP(MAIN) [°C]',	124	'DG3 BOG [MT/day]',
7	'Tank 1 - IS AFT TRAN WALL TEMP(MAIN) [°C]',	125	'DG4 BOG [MT/day]',
8	'Tank 1 - IS FWD TRAN WALL TEMP(MAIN) [°C]',	126	'Impacts tank 1 []',
9	'Tank 1 - IS PORT SIDE WALL TEMP(MAIN) - (HULL) [°C]',	127	'Impacts tank 2 []',
10	'Tank 2 - IS BTM AFT MID TEMP(MAIN) [°C]',	128	'Impacts tank 3 []',
11	'Tank 2 - IS BTM MIDDLE TEMP(MAIN) [°C]',	129	'Impacts tank 4 []',
12	'Tank 2 - IS PORT LOW CHAM TEMP(MAIN) [°C]',	130	'Impact alarm critical threshold [Impact/min]',

13	'Tank 2 - IS PORT SIDE WALL TEMP(MAIN) [°C]',	131	'Impact alarm warning threshold [Impact/min]',
14	'Tank 2 - IS PORT UPP CHAM TEMP(MAIN) [°C]',	132	'Impacts per minute tank 1 [Impact/min]',
15	'Tank 2 - IS CEIL TEMP(MAIN) [°C]',	133	'Impact alarm tank 1 []',
16	'Tank 2 - IS AFT TRAN WALL TEMP(MAIN) [°C]',	134	'Impacts per minute tank 2 [Impact/min]',
17	'Tank 2 - IS FWD TRAN WALL TEMP(MAIN) [°C]',	135	'Impact alarm tank 2 []',
18	'Tank 2 - IS PORT SIDE WALL TEMP(MAIN) - (HULL) [°C]',	136	'Impacts per minute tank 3 [Impact/min]',
19	'Tank 3 - IS BTM AFT MID TEMP(MAIN) [°C]',	137	'Impact alarm tank 3 []',
20	'Tank 3 - IS BTM MIDDLE TEMP(MAIN) [°C]',	138	'Impacts per minute tank 4 [Impact/min]',
21	'Tank 3 - IS PORT LOW CHAM TEMP(MAIN) [°C]',	139	'Impact alarm tank 4 []',
22	'Tank 3 - IS PORT SIDE WALL TEMP(MAIN) [°C]',	140	'Tank 1 - Liquid temp TOP [°C]',
23	'Tank 3 - IS PORT UPP CHAM TEMP(MAIN) [°C]',	141	'Tank 1 - Liquid temp 95% [°C]',
24	'Tank 3 - IS CEIL TEMP(MAIN) [°C]',	142	'Tank 1 - Liquid temp 60% [°C]',
25	'Tank 3 - IS AFT TRAN WALL TEMP(MAIN) [°C]',	143	'Tank 1 - Liquid temp 30% [°C]',
26	'Tank 3 - IS FWD TRAN WALL TEMP(MAIN) [°C]',	144	'Tank 1 - Liquid temp BTM [°C]',

27	'Tank 3 - IS PORT SIDE WALL TEMP(MAIN) - (HULL) [°C]',	145	'Tank 2 - Liquid temp TOP [°C]',
28	'Tank 4 - IS BTM AFT MID TEMP(MAIN) [°C]',	146	'Tank 2 - Liquid temp 95% [°C]',
29	'Tank 4 - IS BTM MIDDLE TEMP(MAIN) [°C]',	147	'Tank 2 - Liquid temp 60% [°C]',
30	'Tank 4 - IS PORT LOW CHAM TEMP(MAIN) [°C]',	148	'Tank 2 - Liquid temp 30% [°C]',
31	'Tank 4 - IS PORT SIDE WALL TEMP(MAIN) [°C]',	149	'Tank 2 - Liquid temp BTM [°C]',
32	'Tank 4 - IS PORT UPP CHAM TEMP(MAIN) [°C]',	150	'Tank 3 - Liquid temp TOP [°C]',
33	'Tank 4 - IS CEIL TEMP(MAIN) [°C]',	151	'Tank 3 - Liquid temp 95% [°C]',
34	'Tank 4 - IS AFT TRAN WALL TEMP(MAIN) [°C]',	152	'Tank 3 - Liquid temp 60% [°C]',
35	'Tank 4 - IS FWD TRAN WALL TEMP(MAIN) [°C]',	153	'Tank 3 - Liquid temp 30% [°C]',
36	'Tank 4 - IS PORT SIDE WALL TEMP(MAIN) - (HULL) [°C]',	154	'Tank 3 - Liquid temp BTM [°C]',
	# Cofferdam temperatures — highly detailed structural measurements with negligible impact on vessel consumption	155	'Tank 4 - Liquid temp TOP [°C]',
37	'1 COFFERDAM AFT MIDDLE TEMP [°C]',	156	'Tank 4 - Liquid temp 95% [°C]',
38	'1 COFFERDAM AFT STBD UPPER TEMP [°C]',	157	'Tank 4 - Liquid temp 60% [°C]',

39	'1 COFFERDAM AFT PORT LOWER TEMP [°C]',	158	'Tank 4 - Liquid temp 30% [°C]',
40	'2 COFFERDAM FWD UPPER TEMP [°C]',	159	'Tank 4 - Liquid temp BTM [°C]',
41	'3 COFFERDAM AFT LOWER TEMP [°C]',	160	'Tank 1 - TK TRUNK DK AFT TEMP [°C]',
42	'4 COFFERDAM FWD LOWER TEMP [°C]',	161	'Tank 1 - TK TRUNK DK MIDDLE TEMP [°C]',
43	'5 COFFERDAM FWD PORT UPPER TEMP [°C]',	162	'Tank 1 - TK PIPE DUCT AFT TEMP [°C]',
	# Spray and cargo pump sensor readings — very detailed operational metrics that don't directly affect vessel consumption	163	'Tank 1 - TK PIPE DUCT MIDDLE TEMP [°C]',
44	'Tank 1 - Spraying Pump - CURRENT [A]',	164	'Tank 1 - IBS PRESSURE [mbar]',
46	'Tank 1 - Cargo Pump 1 - DISCH PRESS [bar]',	165	'Tank 2 - TK TRUNK DK AFT TEMP [°C]',
47	'Tank 1 - Cargo Pump 2 - DISCH V/V [%]',	166	'Tank 2 - TK TRUNK DK MIDDLE TEMP [°C]',
48	'Tank 2 - Spraying Pump - CURRENT [A]',	167	'Tank 2 - TK PIPE DUCT AFT TEMP [°C]',
49	'Tank 2 - Cargo Pump 1 - DISCH PRESS [bar]',	168	'Tank 2 - TK PIPE DUCT MIDDLE TEMP [°C]',
50	'Tank 2 - Cargo Pump 2 - DISCH V/V [%]',	169	'Tank 2 - IBS PRESSURE [mbar]',
51	'Tank 3 - Spraying Pump - CURRENT [A]',	170	'Tank 3 - TK TRUNK DK AFT TEMP [°C]',

52	'Tank 3 - Cargo Pump 1 - DISCH PRESS [bar]',	171	'Tank 3 - TK TRUNK DK MIDDLE TEMP [°C]',
53	'Tank 3 - Cargo Pump 2 - DISCH V/V [%]',	172	'Tank 3 - TK PIPE DUCT AFT TEMP [°C]',
54	'Tank 4 - Spraying Pump - CURRENT [A]',	173	'Tank 3 - TK PIPE DUCT MIDDLE TEMP [°C]',
55	'Tank 4 - Cargo Pump 1 - DISCH PRESS [bar]',	174	'Tank 3 - IBS PRESSURE [mbar]',
56	'Tank 4 - Cargo Pump 2 - DISCH V/V [%]',	175	'Tank 4 - TK TRUNK DK AFT TEMP [°C]',
	# Internal valve settings and pressures — technical parameters with limited external relevance, not related to vessel consumption	176	'Tank 4 - TK TRUNK DK MIDDLE TEMP [°C]',
57	'Tank 1 - IBS SUPPLY V/V [%]',	177	'Tank 4 - TK PIPE DUCT AFT TEMP [°C]',
58	'Tank 1 - IBS EXHAUST V/V [%]',	178	'Tank 4 - TK PIPE DUCT MIDDLE TEMP [°C]',
59	'Tank 1 - IS PRESSURE [mbar]',	179	'Tank 4 - IBS PRESSURE [mbar]',
60	'Tank 1 - IS SUPPLY V/V [%]',	180	'Tank 1 - Cargo Pump 1 - CURRENT [A]',
61	'Tank 1 - IS EXHAUST V/V [%]',	181	'Tank 1 - Cargo Pump 1 - DISCH V/V [%]',
62	'Tank 1 - N2 differential IBS/IS [mbar]',	182	'Tank 1 - Cargo Pump 2 - CURRENT [A]',
63	'Tank 2 - IBS SUPPLY V/V [%]',	183	'Tank 1 - Cargo Pump 2 - DISCH PRESS [bar]',

64	'Tank 2 - IBS EXHAUST V/V [%]',	184	'Tank 1 - Spraying Pump - DISCH PRESS [bar]',
65	'Tank 2 - IS PRESSURE [mbar]',	185	'Tank 1 - Spraying Pump - DISCH V/V [%]',
66	'Tank 2 - IS SUPPLY V/V [%]',	186	'Tank 2 - Cargo Pump 1 - CURRENT [A]',
67	'Tank 2 - IS EXHAUST V/V [%]',	187	'Tank 2 - Cargo Pump 1 - DISCH V/V [%]',
68	'Tank 2 - N2 differential IBS/IS [mbar]',	188	'Tank 2 - Cargo Pump 2 - CURRENT [A]',
69	'Tank 3 - IBS SUPPLY V/V [%]',	189	'Tank 2 - Cargo Pump 2 - DISCH PRESS [bar]',
70	'Tank 3 - IBS EXHAUST V/V [%]',	190	'Tank 2 - Spraying Pump - DISCH PRESS [bar]',
71	'Tank 3 - IS PRESSURE [mbar]',	191	'Tank 2 - Spraying Pump - DISCH V/V [%]',
72	'Tank 3 - IS SUPPLY V/V [%]',	192	'Tank 3 - Cargo Pump 1 - CURRENT [A]',
73	'Tank 3 - IS EXHAUST V/V [%]',	193	'Tank 3 - Cargo Pump 1 - DISCH V/V [%]',
74	'Tank 3 - N2 differential IBS/IS [mbar]',	194	'Tank 3 - Cargo Pump 2 - CURRENT [A]',
75	'Tank 4 - IBS SUPPLY V/V [%]',	195	'Tank 3 - Cargo Pump 2 - DISCH PRESS [bar]',
76	'Tank 4 - IBS EXHAUST V/V [%]',	196	'Tank 3 - Spraying Pump - DISCH PRESS [bar]',

77	'Tank 4 - IS PRESSURE [mbar]',	197	'Tank 3 - Spraying Pump - DISCH V/V [%]',
78	'Tank 4 - IS SUPPLY V/V [%]',	198	'Tank 4 - Cargo Pump 1 - CURRENT [A]',
79	'Tank 4 - IS EXHAUST V/V [%]',	199	'Tank 4 - Cargo Pump 1 - DISCH V/V [%]',
80	'Tank 4 - N2 differential IBS/IS [mbar]',	200	'Tank 4 - Cargo Pump 2 - CURRENT [A]',
	# Compressor diagnostic details — technical data not related to vessel consumption	201	'Tank 4 - Cargo Pump 2 - DISCH PRESS [bar]',
81	'LD compressor 1 - L.O FILTER DIFF PRESS [bar]',	202	'Tank 4 - Spraying Pump - DISCH PRESS [bar]',
82	'LD compressor 2 - L.O FILTER DIFF PRESS [bar]',	203	'Tank 4 - Spraying Pump - DISCH V/V [%]',
83	'HD compressor 1 - IGV POSITION [%]',	204	'LD compressor 2 - INLET PRESS [bara]',
84	'HD compressor 1 - Orifice Plate Diffrencial Press [mbar]',	205	'LD compressor 2 - OUTLET PRESS [barg]',
85	'HD compressor 2 - OUTLET TEMP A [°C].1',	206	'LD compressor 2 - INLET TEMP [°C]',
86	'HD compressor 2 - OUTLET TEMP B [°C]',	207	'LD compressor 2 - OUTLET TEMP A [°C]',
87	'HD compressor 2 - L.O FILTER DIFF PRESS [bar]',	208	'HD compressor 2 - INLET PRESS [bar]',
88	'HD compressor 2 - IGV POSITION [%]',	209	'HD compressor 2 - OUTLET PRESS [bar]',

89	'HD compressor 2 - Orifice Plate Diffrencial Press [mbar]',	210	'HD compressor 2 - INLET TEMP [°C].1',
	# Vaporizer raw input/output pressures and temperatures — not related to vessel consumption”	211	'Tank 1 - Spray Inlet temperature [°C]',
90	'FORCING Vaporizer - OUTLET PRESS [barg*100]',	212	'Tank 2 - Spray Inlet temperature [°C]',
91	'LNG Vaporizer - OUTLET TEMP [°C]',	213	'Tank 3 - Spray Inlet temperature [°C]',
92	'LNG Vaporizer - INLET TEMP [°C]',	214	'Tank 4 - Spray Inlet temperature [°C]',
	# System fault flags — binary indicators best used as event markers	215	'1 COFFERDAM AFT PORT UPPER TEMP [°C]',
93	'NO.1 N2 GEN SYSTEM FAULT [True/False]',	216	'1 COFFERDAM AFT STBD LOWER TEMP [°C]',
94	'NO.2 N2 GEN SYSTEM FAULT [True/False]',	217	'2 COFFERDAM FWD MIDDLE TEMP [°C]',
	# Duplicate or less meaningful boil-off gas measurements — redundant when totals are available	218	'2 COFFERDAM FWD LOWER TEMP [°C]',
95	'ME1 BOG [MT/day]',	219	'2 COFFERDAM AFT UPPER TEMP [°C]',
96	'ME2 BOG [MT/day]',	220	'2 COFFERDAM AFT MIDDLE TEMP [°C]',
97	'ME1 HFO [MT/d]',	221	'2 COFFERDAM AFT LOWER TEMP [°C]',

98	'ME2 HFO [MT/d]',	222	'3 COFFERDAM FWD UPPER TEMP [°C]',
99	'ME1 MGO/MDO [MT/d]',	223	'3 COFFERDAM FWD MIDDLE TEMP [°C]',
100	'ME2 MGO/MDO [MT/d]',	224	'3 COFFERDAM FWD LOWER TEMP [°C]',
101	'Relative wind speed [m/s]',	225	'3 COFFERDAM AFT UPPER TEMP [°C]',
102	'Relative wind direction [°]',	226	'3 COFFERDAM AFT MIDDLE TEMP [°C]',
103	'DG Total BOG [MT]',	227	'4 COFFERDAM FWD UPPER TEMP [°C]',
104	'DG Total HFO [MT]',	228	'4 COFFERDAM FWD MIDDLE TEMP [°C]',
105	'DG Total MGO/MDO [MT]',	229	'4 COFFERDAM AFT UPPER TEMP [°C]',
106	'Ambient air pressure [mbar]',	230	'4 COFFERDAM AFT MIDDLE TEMP [°C]',
107	'Ambient air temperature [°C]',	231	'4 COFFERDAM AFT LOWER TEMP [°C]',
108	'Seawater temperature [°C]',	232	'5 COFFERDAM FWD MIDDLE TEMP [°C]',
109	'ME BOG [MT]',	233	'5 COFFERDAM FWD STBD UPPER TEMP [°C]',
110	'ME HFO [MT]',	234	'5 COFFERDAM FWD PORT LOWER TEMP [°C]',

111	'ME MGO/MDO [MT]',	235	'5 COFFERDAM FWD STBD LOWER TEMP [°C]',
112	'DG Port HFO [MT/day]',	236	'NO.1 N2 GENERATOR PRODUCT DEW POINT [°C]',
113	'DG Port MGO/MDO [MT/day]',	237	'NO.2 N2 GENERATOR PRODUCT DEW POINT [°C]',
114	'DG STBD HFO [MT/day]',		
115	'DG STBD MGO/MDO [MT/day]',		
116	'Total BOG consumption [MT/day]',		
117	'Total NBOG [MT/day]',		

Appendix 9 - Remaining features

	Column 1		Column 2
1	ShipName	55	Tank 1 - Vapour temperature [°C]
2	IMONo	56	Tank 2 - Vapour pressure [mbarg]
3	DateTime	57	Tank 2 - Vapour temperature [°C]
4	Latitude	58	Tank 3 - Vapour pressure [mbarg]
5	Longitude	59	Tank 3 - Vapour temperature [°C]
6	DG consumed [MT]	60	Tank 4 - Vapour pressure [mbarg]
7	ME consumed [MT]	61	Tank 4 - Vapour temperature [°C]
8	DG electrical power [kW]	62	BOG to GCU [kg/h]
9	Shaft power [kW]	63	LNG Vaporizer - DISCH FLOW [kg/h]
10	Shaft rpm [rpm]	64	LNG Vaporizer - INLET PRESS [bar]
11	Draft fore [m]	65	LNG Vaporizer - OUTLET PRESS [bar]
12	Draft aft [m]	66	FORCING Vaporizer - DISCH FLOW [kg/h]
13	COG heading [°]	67	FORCING Vaporizer - INLET PRESS [barg*100]
14	GPS speed [knots]	68	FORCING Vaporizer - INLET TEMP [°C]
15	Log speed [knots]	69	FORCING Vaporizer - OUTLET TEMP [°C]
16	DG1 Power [kW]	70	Reliquefaction - Inlet flow [kg/h]
17	DG2 Power [kW]	71	Reliquefaction - Inlet temperature [°C]

18	DG3 Power [kW]	72	Reliquefaction - Inlet pressure [mbara]
19	DG4 Power [kW]	73	Reliquefaction - Electrical consumption [kW]
20	Roll average [°]	74	LD compressor 1 - INLET PRESS [bara]
21	Pitch average [°]	75	LD compressor 1 - OUTLET PRESS [barg]
22	Yaw average [°]	76	LD compressor 1 - INLET TEMP [°C]
23	ME1 RPM [rpm]	77	LD compressor 1 - OUTLET TEMP A [°C]
24	ME1 Shaft Power [kW]	78	LD compressor 1 - OUTLET TEMP B [°C]
25	ME1 Torque [knm]	79	LD compressor 1 - DISCH FLOW [kg/h]
26	ME2 RPM [rpm]	80	LD compressor 2 - OUTLET TEMP B [°C]
27	ME2 Shaft Power [kW]	81	HD compressor 1 - INLET PRESS [bar]
28	ME2 Torque [knm]	82	HD compressor 1 - OUTLET PRESS [bar]
29	Total impacts all tanks []	83	HD compressor 1 - INLET TEMP [°C]
30	Impacts tank 5 []	84	HD compressor 1 - OUTLET TEMP A [°C]
31	Impacts tank 6 []	85	HD compressor 1 - OUTLET TEMP B [°C]
32	Roll max starboard (Sloshield) [°]	86	HD compressor 1 - L.O FILTER DIFF PRESS [bar]

33	Pitch max fore (Sloshield) [°]	87	Liquid MAIN - FWD temperature [°C]
34	Roll avarage (Sloshield) [°]	88	Liquid MAIN - AFT temperature [°C]
35	Pitch avarage (Sloshield) [°]	89	Liquid Cross-Over - FWD pressure [mbar]
36	Impacts per minute overall [Impact/min]	90	Liquid Cross-Over - AFT pressure [mbarg]
37	Impact alarm overall []	91	Liquid Cross-Over - FWD temperature [°C]
38	RHO LNG [Kg/m^3]	92	Liquid Cross-Over - AFT temperature [°C]
39	LNG tank volume [m^3]	93	Vapour MAIN - Gauge pressure [mbarg]
40	BOR alarm low [%]	94	Vapour MAIN - FWD temperature [°C]
41	BOR alarm high [%]	95	Vapour MAIN - AFT temperature [°C]
42	Tank 1 - Average Liquid temp [°C]	96	Vapour Cross-Over - Pressure [barG]
43	Tank 2 - Average Liquid temp [°C]	97	Spray MAIN - FWD temperature [°C]
44	Tank 3 - Average Liquid temp [°C]	98	Spray MAIN - AFT temperature [°C]
45	Tank 4 - Average Liquid temp [°C]	99	LNG supply HDR - Pressure [mbarg]
46	Tank 1 - Liquid level corrected [m]	100	Draft mid portside [m]
47	Tank 1 - Liquid Volume [m^3]	101	Draft mid starboard [m]
48	Tank 2 - Liquid level corrected [m]	102	DG1 energy production [kWh]
49	Tank 2 - Liquid Volume [m^3]	103	DG1 running hours [h]
50	Tank 3 - Liquid level corrected [m]	104	DG2 energy production [kWh]
51	Tank 3 - Liquid Volume [m^3]	105	DG2 running hours [h]

52	Tank 4 - Liquid level corrected [m]	106	DG3 energy production [kWh]
53	Tank 4 - Liquid Volume [m^3]	107	DG3 running hours [h]
54	Tank 1 - Vapour pressure [mbarg]	108	DG4 energy production [kWh]

Appendix 10 - Imputation process of Vessel 1

1	IMONo: 0 NaNs (0.0%)	55	Tank 2 - Vapour temperature [°C]: 0 NaNs (0.0%)
2	Latitude: 0 NaNs (0.0%)	56	Tank 3 - Vapour pressure [mbarg]: 0 NaNs (0.0%)
3	Longitude: 0 NaNs (0.0%)	57	Tank 3 - Vapour temperature [°C]: 0 NaNs (0.0%)
4	DG consumed [MT]: 2 NaNs (0.0%)	58	Tank 4 - Vapour pressure [mbarg]: 0 NaNs (0.0%)
5	ME consumed [MT]: 171 NaNs (0.24%)	59	Tank 4 - Vapour temperature [°C]: 0 NaNs (0.0%)
6	DG electrical power [kW]: 0 NaNs (0.0%)	60	BOG to GCU [kg/h]: 0 NaNs (0.0%)
7	Shaft power [kW]: 1022 NaNs (1.46%)	61	LNG Vaporizer - DISCH FLOW [kg/h]: 26292 NaNs (37.47%)
8	Shaft rpm [rpm]: 41 NaNs (0.06%)	62	LNG Vaporizer - INLET PRESS [bar]: 26292 NaNs (37.47%)
9	Draft fore [m]: 0 NaNs (0.0%)	63	LNG Vaporizer - OUTLET PRESS [bar]: 26292 NaNs (37.47%)
10	Draft aft [m]: 0 NaNs (0.0%)	64	FORCING Vaporizer - DISCH FLOW [kg/h]: 0 NaNs (0.0%)
11	COG heading [°]: 0 NaNs (0.0%)	65	FORCING Vaporizer - INLET PRESS [barg*100]: 26292 NaNs (37.47%)
12	GPS speed [knots]: 7 NaNs (0.01%)	66	FORCING Vaporizer - INLET TEMP [°C]: 26292 NaNs (37.47%)
13	Log speed [knots]: 68 NaNs (0.1%)	67	FORCING Vaporizer - OUTLET TEMP [°C]: 26292 NaNs (37.47%)

14	DG1 Power [kW]: 11910 NaNs (16.97%)	68	Reliquefaction - Inlet flow [kg/h]: 0 NaNs (0.0%)
15	DG2 Power [kW]: 0 NaNs (0.0%)	69	Reliquefaction - Inlet temperature [°C]: 0 NaNs (0.0%)
16	DG3 Power [kW]: 13296 NaNs (18.95%)	70	Reliquefaction - Inlet pressure [mbara]: 0 NaNs (0.0%)
17	DG4 Power [kW]: 7987 NaNs (11.38%)	71	Reliquefaction - Electrical consumption [kW]: 0 NaNs (0.0%)
18	Roll average [°]: 26292 NaNs (37.47%)	72	LD compressor 1 - INLET PRESS [bara]: 26292 NaNs (37.47%)
19	Pitch average [°]: 26292 NaNs (37.47%)	73	LD compressor 1 - OUTLET PRESS [barg]: 26292 NaNs (37.47%)
20	Yaw average [°]: 26292 NaNs (37.47%)	74	LD compressor 1 - INLET TEMP [°C]: 26292 NaNs (37.47%)
21	ME1 RPM [rpm]: 0 NaNs (0.0%)	75	LD compressor 1 - OUTLET TEMP A [°C]: 26292 NaNs (37.47%)
22	ME1 Shaft Power [kW]: 0 NaNs (0.0%)	76	LD compressor 1 - OUTLET TEMP B [°C]: 26292 NaNs (37.47%)
23	ME1 Torque [knm]: 0 NaNs (0.0%)	77	LD compressor 1 - DISCH FLOW [kg/h]: 26292 NaNs (37.47%)
24	ME2 RPM [rpm]: 0 NaNs (0.0%)	78	LD compressor 2 - OUTLET TEMP B [°C]: 26292 NaNs (37.47%)
25	ME2 Shaft Power [kW]: 0 NaNs (0.0%)	79	HD compressor 1 - INLET PRESS [bar]: 0 NaNs (0.0%)
26	ME2 Torque [knm]: 0 NaNs (0.0%)	80	HD compressor 1 - OUTLET PRESS [bar]: 0 NaNs (0.0%)

27	Total impacts all tanks []: 26292 NaNs (37.47%)	81	HD compressor 1 - INLET TEMP [°C]: 0 NaNs (0.0%)
28	Impacts tank 5 []: 0 NaNs (0.0%)	82	HD compressor 1 - OUTLET TEMP A [°C]: 0 NaNs (0.0%)
29	Impacts tank 6 []: 0 NaNs (0.0%)	83	HD compressor 1 - OUTLET TEMP B [°C]: 0 NaNs (0.0%)
30	Roll max starboard (Sloshield) [°]: 0 NaNs (0.0%)	84	HD compressor 1 - L.O FILTER DIFF PRESS [bar]: 0 NaNs (0.0%)
31	Pitch max fore (Sloshield) [°]: 0 NaNs (0.0%)	85	Liquid MAIN - FWD temperature [°C]: 0 NaNs (0.0%)
32	Roll avarage (Sloshield) [°]: 0 NaNs (0.0%)	86	Liquid MAIN - AFT temperature [°C]: 0 NaNs (0.0%)
33	Pitch avarage (Sloshield) [°]: 0 NaNs (0.0%)	87	Liquid Cross-Over - FWD pressure [mbar]: 0 NaNs (0.0%)
34	Impacts per minute overall [Impact/min]: 0 NaNs (0.0%)	88	Liquid Cross-Over - AFT pressure [mbarg]: 0 NaNs (0.0%)
35	Impact alarm overall []: 0 NaNs (0.0%)	89	Liquid Cross-Over - FWD temperature [°C]: 0 NaNs (0.0%)
36	RHO LNG [Kg/m^3]: 0 NaNs (0.0%)	90	Liquid Cross-Over - AFT temperature [°C]: 0 NaNs (0.0%)
37	LNG tank volume [m^3]: 0 NaNs (0.0%)	91	Vapour MAIN - Gauge pressure [mbarg]: 26292 NaNs (37.47%)
38	BOR alarm low [%]: 0 NaNs (0.0%)	92	Vapour MAIN - FWD temperature [°C]: 26292 NaNs (37.47%)
39	BOR alarm high [%]: 0 NaNs (0.0%)	93	Vapour MAIN - AFT temperature [°C]: 26292 NaNs (37.47%)

40	Tank 1 - Average Liquid temp [°C]: 15120 NaNs (21.55%)	94	Vapour Cross-Over - Pressure [barG]: 0 NaNs (0.0%)
41	Tank 2 - Average Liquid temp [°C]: 20307 NaNs (28.94%)	95	Spray MAIN - FWD temperature [°C]: 26292 NaNs (37.47%)
42	Tank 3 - Average Liquid temp [°C]: 163 NaNs (0.23%)	96	Spray MAIN - AFT temperature [°C]: 26292 NaNs (37.47%)
43	Tank 4 - Average Liquid temp [°C]: 13515 NaNs (19.26%)	97	LNG supply HDR - Pressure [mbarg]: 26292 NaNs (37.47%)
44	Tank 1 - Liquid level corrected [m]: 15 NaNs (0.02%)	98	Draft mid portside [m]: 26292 NaNs (37.47%)
45	Tank 1 - Liquid Volume [m^3]: 0 NaNs (0.0%)	99	Draft mid starboard [m]: 26292 NaNs (37.47%)
46	Tank 2 - Liquid level corrected [m]: 14 NaNs (0.02%)	100	DG1 energy production [kWh]: 26292 NaNs (37.47%)
47	Tank 2 - Liquid Volume [m^3]: 0 NaNs (0.0%)	101	DG1 running hours [h]: 26292 NaNs (37.47%)
48	Tank 3 - Liquid level corrected [m]: 0 NaNs (0.0%)	102	DG2 energy production [kWh]: 26292 NaNs (37.47%)
49	Tank 3 - Liquid Volume [m^3]: 0 NaNs (0.0%)	103	DG2 running hours [h]: 26292 NaNs (37.47%)
50	Tank 4 - Liquid level corrected [m]: 57 NaNs (0.08%)	104	DG3 energy production [kWh]: 26292 NaNs (37.47%)
51	Tank 4 - Liquid Volume [m^3]: 0 NaNs (0.0%)	105	DG3 running hours [h]: 26292 NaNs (37.47%)
52	Tank 1 - Vapour pressure [mbarg]: 0 NaNs (0.0%)	106	DG4 energy production [kWh]: 26292 NaNs (37.47%)

53	Tank 1 - Vapour temperature [°C]: 0 NaNs (0.0%)	107	DG4 running hours [h]: 26292 NaNs (37.47%)
54	Tank 2 - Vapour pressure [mbarg]: 0 NaNs (0.0%)	108	ME FO supply temperature [°C]: 26292 NaNs (37.47%)
		109	ME running hours [h]: 26292 NaNs (37.47%)

Appendix 11 - Imputation process of Vessel 2

	Column 1		Column 2
1	IMONo: 0 NaNs (0.0%)	85	Tank 2 - IS AFT TRAN WALL TEMP(ST-BY) [°C]: 26285 NaNs (37.47%)
2	Latitude: 254 NaNs (0.36%)	86	Tank 2 - IS FWD TRAN WALL TEMP(ST-BY) [°C]: 26285 NaNs (37.47%)
3	Longitude: 254 NaNs (0.36%)	87	Tank 2 - IS PORT SIDE WALL TEMP(ST-BY) - (HULL) [°C]: 26285 NaNs (37.47%)
4	Boiler consumed [MT]: 41 NaNs (0.06%)	88	Tank 2 - Liquid Dome IS inlet pressure [mbar]: 0 NaNs (0.0%)
5	DG consumed [MT]: 40 NaNs (0.06%)	89	Tank 3 - IS BTM AFT MID TEMP(ST-BY) [°C]: 26285 NaNs (37.47%)
6	ME consumed [MT]: 3811 NaNs (5.43%)	90	Tank 3 - IS BTM MIDDLE TEMP(ST-BY) [°C]: 26285 NaNs (37.47%)
7	DG electrical power [kW]: 0 NaNs (0.0%)	91	Tank 3 - IS PORT LOW CHAM TEMP(ST-BY) [°C]: 26285 NaNs (37.47%)
8	Shaft power [kW]: 0 NaNs (0.0%)	92	Tank 3 - IS PORT SIDE WALL TEMP(ST-BY) [°C]: 26285 NaNs (37.47%)
9	Shaft rpm [rpm]: 1 NaNs (0.0%)	93	Tank 3 - IS PORT UPP CHAM TEMP(ST-BY) [°C]: 26285 NaNs (37.47%)

10	Draft fore [m]: 247 NaNs (0.35%)	94	Tank 3 - IS CEIL TEMP(ST-BY) [°C]: 26285 NaNs (37.47%)
11	Draft aft [m]: 224 NaNs (0.32%)	95	Tank 3 - IS AFT TRAN WALL TEMP(ST-BY) [°C]: 26285 NaNs (37.47%)
12	COG heading [°]: 254 NaNs (0.36%)	96	Tank 3 - IS FWD TRAN WALL TEMP(ST-BY) [°C]: 26285 NaNs (37.47%)
13	GPS speed [knots]: 240 NaNs (0.34%)	97	Tank 3 - IS PORT SIDE WALL TEMP(ST-BY) - (HULL) [°C]: 26285 NaNs (37.47%)
14	Log speed [knots]: 622 NaNs (0.89%)	98	Tank 3 - Liquid Dome IS inlet pressure [mbar]: 0 NaNs (0.0%)
15	DG1 Power [kW]: 224 NaNs (0.32%)	99	Tank 4 - IS BTM AFT MID TEMP(ST-BY) [°C]: 26285 NaNs (37.47%)
16	DG2 Power [kW]: 224 NaNs (0.32%)	100	Tank 4 - IS BTM MIDDLE TEMP(ST-BY) [°C]: 26285 NaNs (37.47%)
17	DG3 Power [kW]: 224 NaNs (0.32%)	101	Tank 4 - IS PORT LOW CHAM TEMP(ST-BY) [°C]: 26285 NaNs (37.47%)
18	DG4 Power [kW]: 224 NaNs (0.32%)	102	Tank 4 - IS PORT SIDE WALL TEMP(ST-BY) [°C]: 26285 NaNs (37.47%)
19	Roll average [°]: 26285 NaNs (37.47%)	103	Tank 4 - IS PORT UPP CHAM TEMP(ST-BY) [°C]: 26285 NaNs (37.47%)

20	Pitch average [°]: 26285 NaNs (37.47%)	104	Tank 4 - IS CEIL TEMP(ST-BY) [°C]: 26285 NaNs (37.47%)
21	Yaw average [°]: 26285 NaNs (37.47%)	105	Tank 4 - IS AFT TRAN WALL TEMP(ST-BY) [°C]: 26285 NaNs (37.47%)
22	Heave Average [m]: 26285 NaNs (37.47%)	106	Tank 4 - IS FWD TRAN WALL TEMP(ST-BY) [°C]: 26285 NaNs (37.47%)
23	Sway Average [m]: 26285 NaNs (37.47%)	107	Tank 4 - IS PORT SIDE WALL TEMP(ST-BY) - (HULL) [°C]: 26285 NaNs (37.47%)
24	Surge Average [m]: 26285 NaNs (37.47%)	108	Tank 4 - Liquid Dome IS inlet pressure [mbar]: 0 NaNs (0.0%)
25	ME1 RPM [rpm]: 0 NaNs (0.0%)	109	BOG to GCU [kg/h]: 0 NaNs (0.0%)
26	ME1 Shaft Power [kW]: 0 NaNs (0.0%)	110	LNG Vaporizer - DISCH FLOW [kg/h]: 26285 NaNs (37.47%)
27	ME1 Torque [knm]: 0 NaNs (0.0%)	111	LNG Vaporizer - INLET PRESS [bar]: 26285 NaNs (37.47%)
28	ME2 RPM [rpm]: 0 NaNs (0.0%)	112	LNG Vaporizer - OUTLET PRESS [bar]: 26285 NaNs (37.47%)
29	ME2 Shaft Power [kW]: 0 NaNs (0.0%)	113	FORCING Vaporizer - DISCH FLOW [kg/h]: 0 NaNs (0.0%)
30	ME2 Torque [knm]: 0 NaNs (0.0%)	114	FORCING Vaporizer - INLET PRESS [barg*100]: 26285 NaNs (37.47%)
31	Total impacts all tanks []: 38356 NaNs (54.67%)	115	FORCING Vaporizer - INLET TEMP [°C]: 26285 NaNs (37.47%)

32	Roll max starboard (Sloshield) [°]: 29917 NaNs (42.64%)	116	Reliquefaction - Outlet temperature [°C]: 0 NaNs (0.0%)
33	Pitch max fore (Sloshield) [°]: 29917 NaNs (42.64%)	117	Reliquefaction - Inlet flow [kg/h]: 0 NaNs (0.0%)
34	Roll avarage (Sloshield) [°]: 29917 NaNs (42.64%)	118	Reliquefaction - Inlet temperature [°C]: 0 NaNs (0.0%)
35	Pitch avarage (Sloshield) [°]: 29917 NaNs (42.64%)	119	Reliquefaction - Inlet pressure [mbara]: 0 NaNs (0.0%)
36	Impacts per minute overall [Impact/min]: 29917 NaNs (42.64%)	120	Reliquefaction - Electrical consumption [kW]: 0 NaNs (0.0%)
37	Impact alarm overall []: 29917 NaNs (42.64%)	121	LD compressor 1 - OUTLET TEMP B [°C]: 26285 NaNs (37.47%)
38	RHO LNG [Kg/m^3]: 0 NaNs (0.0%)	122	LD compressor 1 - SPRAY AFT. CLR. TEMP VV POS. [%]: 26285 NaNs (37.47%)
39	LNG tank volume [m^3]: 0 NaNs (0.0%)	123	LD compressor 2 - SPRAY AFT. CLR. TEMP VV POS. [%]: 26285 NaNs (37.47%)
40	BOR alarm low [%]: 0 NaNs (0.0%)	124	HD compressor 1 - INLET PRESS [bar]: 0 NaNs (0.0%)
41	BOR alarm high [%]: 0 NaNs (0.0%)	125	HD compressor 1 - OUTLET PRESS [bar]: 0 NaNs (0.0%)
42	Daily BOR (Sloshield) [MT/Day]: 0 NaNs (0.0%)	126	HD compressor 1 - INLET TEMP [°C]: 0 NaNs (0.0%)
43	Daily BOR alarm []: 0 NaNs (0.0%)	127	HD compressor 1 - OUTLET TEMP A [°C]: 0 NaNs (0.0%)

44	BOR rate running average (Sloshield) [MT/Day]: 0 NaNs (0.0%)	128	HD compressor 1 - OUTLET TEMP B [°C]: 0 NaNs (0.0%)
45	Tank 1 - Liquid temp 75% [°C]: 0 NaNs (0.0%)	129	HD compressor 1 - L.O FILTER DIFF PRESS [bar]: 0 NaNs (0.0%)
46	Tank 1 - Average Liquid temp [°C]: 21221 NaNs (30.25%)	130	Liquid MAIN - FWD temperature [°C]: 0 NaNs (0.0%)
47	Tank 2 - Liquid temp 75% [°C]: 0 NaNs (0.0%)	131	Liquid MAIN - AFT temperature [°C]: 0 NaNs (0.0%)
48	Tank 2 - Average Liquid temp [°C]: 21303 NaNs (30.36%)	132	Liquid Cross-Over - FWD pressure [mbar]: 0 NaNs (0.0%)
49	Tank 3 - Liquid temp 75% [°C]: 0 NaNs (0.0%)	133	Liquid Cross-Over - AFT pressure [mbarg]: 0 NaNs (0.0%)
50	Tank 3 - Average Liquid temp [°C]: 2 NaNs (0.0%)	134	Liquid Cross-Over - FWD temperature [°C]: 0 NaNs (0.0%)
51	Tank 4 - Liquid temp 75% [°C]: 0 NaNs (0.0%)	135	Liquid Cross-Over - AFT temperature [°C]: 0 NaNs (0.0%)
52	Tank 4 - Average Liquid temp [°C]: 7956 NaNs (11.34%)	136	Vapour MAIN - FWD temperature [°C]: 26285 NaNs (37.47%)
53	Tank 1 - Liquid level corrected [m]: 829 NaNs (1.18%)	137	Vapour MAIN - AFT temperature [°C]: 26285 NaNs (37.47%)
54	Tank 1 - Liquid Volume [m^3]: 0 NaNs (0.0%)	138	Vapour Cross-Over - Pressure [barG]: 0 NaNs (0.0%)
55	Tank 2 - Liquid level corrected [m]: 0 NaNs (0.0%)	139	Spray MAIN - FWD temperature [°C]: 26285 NaNs (37.47%)
56	Tank 2 - Liquid Volume [m^3]: 0 NaNs (0.0%)	140	Spray MAIN - AFT temperature [°C]: 26285 NaNs (37.47%)

57	Tank 3 - Liquid level corrected [m]: 0 NaNs (0.0%)	141	Tank 1 - Spray return pressure [barg]: 26285 NaNs (37.47%)
58	Tank 3 - Liquid Volume [m^3]: 0 NaNs (0.0%)	142	Tank 2 - Spray return pressure [barg]: 26285 NaNs (37.47%)
59	Tank 4 - Liquid level corrected [m]: 9 NaNs (0.01%)	143	Tank 3 - Spray return pressure [barg]: 26285 NaNs (37.47%)
60	Tank 4 - Liquid Volume [m^3]: 0 NaNs (0.0%)	144	Tank 4 - Spray return pressure [barg]: 26285 NaNs (37.47%)
61	Tank 1 - Vapour pressure [mbarg]: 0 NaNs (0.0%)	145	LNG supply HDR - Pressure [mbarg]: 26285 NaNs (37.47%)
62	Tank 1 - Vapour temperature [°C]: 0 NaNs (0.0%)	146	LNG Heater - GAS INLET PRESS [bar]: 0 NaNs (0.0%)
63	Tank 2 - Vapour pressure [mbarg]: 0 NaNs (0.0%)	147	LNG Heater - GAS OUTLET PRESS [bar]: 0 NaNs (0.0%)
64	Tank 2 - Vapour temperature [°C]: 0 NaNs (0.0%)	148	LNG Heater - GAS INLET TEMP [°C]: 0 NaNs (0.0%)
65	Tank 3 - Vapour pressure [mbarg]: 0 NaNs (0.0%)	149	LNG Heater - GAS OUTLET TEMP [°C]: 0 NaNs (0.0%)
66	Tank 3 - Vapour temperature [°C]: 0 NaNs (0.0%)	150	Fuel Gas Heater - GAS INLET PRESS [bar]: 0 NaNs (0.0%)
67	Tank 4 - Vapour pressure [mbarg]: 0 NaNs (0.0%)	151	Fuel Gas Heater - GAS OUTLET PRESS [bar]: 0 NaNs (0.0%)
68	Tank 4 - Vapour temperature [°C]: 0 NaNs (0.0%)	152	Fuel Gas Heater - GAS INLET TEMP [°C]: 0 NaNs (0.0%)
69	Tank 1 - IS BTM AFT MID TEMP(ST-BY) [°C]: 26285 NaNs (37.47%)	153	Fuel Gas Heater - GAS OUTLET TEMP [°C]: 0 NaNs (0.0%)

70	Tank 1 - IS BTM MIDDLE TEMP(ST-BY) [°C]: 26285 NaNs (37.47%)	154	Nitrogen system - Bleeding pressure [bar]: 0 NaNs (0.0%)
71	Tank 1 - IS PORT LOW CHAM TEMP(ST-BY) [°C]: 26285 NaNs (37.47%)	155	NO.1 N2 GENERATOR PRODUCT OXYGEN CONTENT [%]: 0 NaNs (0.0%)
72	Tank 1 - IS PORT SIDE WALL TEMP(ST-BY) [°C]: 26285 NaNs (37.47%)	156	NO.2 N2 GENERATOR PRODUCT OXYGEN CONTENT [%]: 0 NaNs (0.0%)
73	Tank 1 - IS PORT UPP CHAM TEMP(ST-BY) [°C]: 26285 NaNs (37.47%)	157	Draft mid portside [m]: 26285 NaNs (37.47%)
74	Tank 1 - IS CEIL TEMP(ST-BY) [°C]: 26285 NaNs (37.47%)	158	Draft mid starboard [m]: 26285 NaNs (37.47%)
75	Tank 1 - IS AFT TRAN WALL TEMP(ST-BY) [°C]: 26285 NaNs (37.47%)	159	DG1 energy production [kWh]: 26285 NaNs (37.47%)
76	Tank 1 - IS FWD TRAN WALL TEMP(ST-BY) [°C]: 26285 NaNs (37.47%)	160	DG1 running hours [h]: 26285 NaNs (37.47%)
77	Tank 1 - IS PORT SIDE WALL TEMP(ST-BY) - (HULL) [°C]: 26285 NaNs (37.47%)	161	DG2 energy production [kWh]: 26285 NaNs (37.47%)
78	Tank 1 - Liquid Dome IS inlet pressure [mbar]: 0 NaNs (0.0%)	162	DG2 running hours [h]: 26285 NaNs (37.47%)
79	Tank 2 - IS BTM AFT MID TEMP(ST-BY) [°C]: 26285 NaNs (37.47%)	163	DG3 energy production [kWh]: 26285 NaNs (37.47%)

80	Tank 2 - IS BTM MIDDLE TEMP(ST-BY) [°C]: 26285 NaNs (37.47%)	164	DG3 running hours [h]: 26285 NaNs (37.47%)
81	Tank 2 - IS PORT LOW CHAM TEMP(ST-BY) [°C]: 26285 NaNs (37.47%)	165	DG4 energy production [kWh]: 26285 NaNs (37.47%)
82	Tank 2 - IS PORT SIDE WALL TEMP(ST-BY) [°C]: 26285 NaNs (37.47%)	166	DG4 running hours [h]: 26285 NaNs (37.47%)
83	Tank 2 - IS PORT UPP CHAM TEMP(ST-BY) [°C]: 26285 NaNs (37.47%)	167	ME running hours [h]: 26285 NaNs (37.47%)
84	Tank 2 - IS CEIL TEMP(ST-BY) [°C]: 26285 NaNs (37.47%)		

Appendix 12 - Imputation process of Vessel 3

	Column 1		Column 2
1	IMONo: 0 NaNs (0.0%)	53	Tank 1 - Vapour pressure [mbarg]: 0 NaNs (0.0%)
2	Latitude: 4 NaNs (0.01%)	54	Tank 1 - Vapour temperature [°C]: 0 NaNs (0.0%)
3	Longitude: 4 NaNs (0.01%)	55	Tank 2 - Vapour pressure [mbarg]: 0 NaNs (0.0%)
4	DG consumed [MT]: 6 NaNs (0.01%)	56	Tank 2 - Vapour temperature [°C]: 0 NaNs (0.0%)
5	ME consumed [MT]: 698 NaNs (1.0%)	57	Tank 3 - Vapour pressure [mbarg]: 0 NaNs (0.0%)
6	DG electrical power [kW]: 0 NaNs (0.0%)	58	Tank 3 - Vapour temperature [°C]: 0 NaNs (0.0%)
7	Shaft power [kW]: 0 NaNs (0.0%)	59	Tank 4 - Vapour pressure [mbarg]: 0 NaNs (0.0%)
8	Shaft rpm [rpm]: 4 NaNs (0.01%)	60	Tank 4 - Vapour temperature [°C]: 0 NaNs (0.0%)
9	Draft fore [m]: 0 NaNs (0.0%)	61	BOG to GCU [kg/h]: 0 NaNs (0.0%)
10	Draft aft [m]: 0 NaNs (0.0%)	62	LNG Vaporizer - DISCH FLOW [kg/h]: 26277 NaNs (37.51%)
11	COG heading [°]: 6 NaNs (0.01%)	63	LNG Vaporizer - INLET PRESS [bar]: 26277 NaNs (37.51%)
12	GPS speed [knots]: 4 NaNs (0.01%)	64	LNG Vaporizer - OUTLET PRESS [bar]: 26277 NaNs (37.51%)
13	Log speed [knots]: 131 NaNs (0.19%)	65	FORCING Vaporizer - DISCH FLOW [kg/h]: 0 NaNs (0.0%)

14	Under keel clearance [m]: 26277 NaNs (37.51%)	66	FORCING Vaporizer - INLET PRESS [barg*100]: 26277 NaNs (37.51%)
15	DG1 Power [kW]: 0 NaNs (0.0%)	67	FORCING Vaporizer - INLET TEMP [°C]: 26277 NaNs (37.51%)
16	DG2 Power [kW]: 0 NaNs (0.0%)	68	FORCING Vaporizer - OUTLET TEMP [°C]: 26277 NaNs (37.51%)
17	DG3 Power [kW]: 0 NaNs (0.0%)	69	Sub-Cooler - Cold power [%]: 0 NaNs (0.0%)
18	DG4 Power [kW]: 0 NaNs (0.0%)	70	Sub-Cooler - MTC1.POWER [kW]: 0 NaNs (0.0%)
19	Roll average [°]: 26277 NaNs (37.51%)	71	Sub-Cooler - MC1.POWER [kW]: 0 NaNs (0.0%)
20	Pitch average [°]: 26277 NaNs (37.51%)	72	Sub-Cooler - MC2.POWER [kW]: 0 NaNs (0.0%)
21	Yaw average [°]: 26277 NaNs (37.51%)	73	Sub-Cooler - MTC2.POWER [kW]: 0 NaNs (0.0%)
22	ME1 RPM [rpm]: 0 NaNs (0.0%)	74	Sub-Cooler - MC3.POWER [kW]: 0 NaNs (0.0%)
23	ME1 Shaft Power [kW]: 0 NaNs (0.0%)	75	Sub-Cooler - MTC3.POWER [kW]: 0 NaNs (0.0%)
24	ME1 Torque [knm]: 0 NaNs (0.0%)	76	Sub-Cooler - MC4.POWER [kW]: 0 NaNs (0.0%)
25	ME2 RPM [rpm]: 0 NaNs (0.0%)	77	LD compressor 1 - INLET PRESS [bara]: 26277 NaNs (37.51%)
26	ME2 Shaft Power [kW]: 0 NaNs (0.0%)	78	LD compressor 1 - OUTLET PRESS [barg]: 26277 NaNs (37.51%)

27	ME2 Torque [knm]: 0 NaNs (0.0%)	79	LD compressor 1 - INLET TEMP [°C]: 26277 NaNs (37.51%)
28	Roll max starboard (Sloshield) [°]: 41937 NaNs (59.87%)	80	LD compressor 1 - OUTLET TEMP A [°C]: 26277 NaNs (37.51%)
29	Pitch max fore (Sloshield) [°]: 41937 NaNs (59.87%)	81	LD compressor 1 - DISCH FLOW [kg/h]: 26277 NaNs (37.51%)
30	Roll avarage (Sloshield) [°]: 41937 NaNs (59.87%)	82	HD compressor 1 - INLET PRESS [bar]: 0 NaNs (0.0%)
31	Pitch avarage (Sloshield) [°]: 41937 NaNs (59.87%)	83	HD compressor 1 - OUTLET PRESS [bar]: 0 NaNs (0.0%)
32	Impacts per minute overall [Impact/min]: 41937 NaNs (59.87%)	84	HD compressor 1 - INLET TEMP [°C]: 0 NaNs (0.0%)
33	Impact alarm overall []: 41937 NaNs (59.87%)	85	HD compressor 1 - OUTLET TEMP A [°C]: 0 NaNs (0.0%)
34	RHO LNG [Kg/m^3]: 0 NaNs (0.0%)	86	HD compressor 1 - OUTLET TEMP B [°C]: 0 NaNs (0.0%)
35	LNG tank volume [m^3]: 0 NaNs (0.0%)	87	HD compressor 1 - L.O FILTER DIFF PRESS [bar]: 0 NaNs (0.0%)
36	BOR alarm low [%]: 0 NaNs (0.0%)	88	Liquid Cross-Over - FWD pressure [mbar]: 0 NaNs (0.0%)
37	BOR alarm high [%]: 0 NaNs (0.0%)	89	Liquid Cross-Over - AFT pressure [mbarg]: 0 NaNs (0.0%)
38	Daily BOR (Sloshield) [MT/Day]: 0 NaNs (0.0%)	90	Liquid Cross-Over - FWD temperature [°C]: 0 NaNs (0.0%)
39	Daily BOR alarm []: 0 NaNs (0.0%)	91	Liquid Cross-Over - AFT temperature [°C]: 0 NaNs (0.0%)

40	BOR rate running average (Sloshield) [MT/Day]: 0 NaNs (0.0%)	92	Vapour Cross-Over - Pressure [barG]: 0 NaNs (0.0%)
41	Tank 1 - Average Liquid temp [°C]: 650 NaNs (0.93%)	93	LNG supply HDR - Pressure [mbarg]: 26277 NaNs (37.51%)
42	Tank 2 - Average Liquid temp [°C]: 288 NaNs (0.41%)	94	Draft mid portside [m]: 26277 NaNs (37.51%)
43	Tank 3 - Average Liquid temp [°C]: 237 NaNs (0.34%)	95	Draft mid starboard [m]: 26277 NaNs (37.51%)
44	Tank 4 - Average Liquid temp [°C]: 2300 NaNs (3.28%)	96	DG1 energy production [kWh]: 26277 NaNs (37.51%)
45	Tank 1 - Liquid level corrected [m]: 0 NaNs (0.0%)	97	DG1 running hours [h]: 26277 NaNs (37.51%)
46	Tank 1 - Liquid Volume [m^3]: 0 NaNs (0.0%)	98	DG2 energy production [kWh]: 26277 NaNs (37.51%)
47	Tank 2 - Liquid level corrected [m]: 0 NaNs (0.0%)	99	DG2 running hours [h]: 26277 NaNs (37.51%)
48	Tank 2 - Liquid Volume [m^3]: 0 NaNs (0.0%)	100	DG3 energy production [kWh]: 26277 NaNs (37.51%)
49	Tank 3 - Liquid level corrected [m]: 0 NaNs (0.0%)	101	DG3 running hours [h]: 26277 NaNs (37.51%)
50	Tank 3 - Liquid Volume [m^3]: 0 NaNs (0.0%)	102	DG4 energy production [kWh]: 26277 NaNs (37.51%)
51	Tank 4 - Liquid level corrected [m]: 0 NaNs (0.0%)	103	DG4 running hours [h]: 26277 NaNs (37.51%)
52	Tank 4 - Liquid Volume [m^3]: 0 NaNs (0.0%)	104	ME running hours [h]: 26277 NaNs (37.51%)

Appendix 13 - Imputation process of Vessel 1 (Skewness)

Features	Skewness	Interpretation
LNG Vaporizer - DISCH FLOW [kg/h]	-14.8617	Highly skewed → median
HD compressor 1 - OUTLET TEMP B [°C]	-7.41024	Highly skewed → median
HD compressor 1 - OUTLET TEMP A [°C]	-7.38047	Highly skewed → median
HD compressor 1 - INLET TEMP [°C]	-6.27097	Highly skewed → median
Spray MAIN - AFT temperature [°C]	-5.37015	Highly skewed → median
Spray MAIN - FWD temperature [°C]	-4.84456	Highly skewed → median
Liquid Cross-Over - FWD temperature [°C]	-2.63694	Highly skewed → median
Liquid MAIN - FWD temperature [°C]	-2.34227	Highly skewed → median
Liquid MAIN - AFT temperature [°C]	-1.93131	Highly skewed → median
FORCING Vaporizer - INLET TEMP [°C]	-1.92014	Highly skewed → median
Liquid Cross-Over - AFT temperature [°C]	-1.80775	Highly skewed → median
FORCING Vaporizer - OUTLET TEMP [°C]	-1.68976	Highly skewed → median
Shaft rpm [rpm]	-1.31353	Highly skewed → median
ME1 RPM [rpm]	-1.31052	Highly skewed → median
Log speed [knots]	-1.30887	Highly skewed → median
ME2 RPM [rpm]	-1.30459	Highly skewed → median
GPS speed [knots]	-1.27526	Highly skewed → median
LD compressor 1 - OUTLET TEMP A [°C]	-1.22058	Highly skewed → median
LD compressor 1 - OUTLET TEMP B [°C]	-1.22055	Highly skewed → median
LD compressor 1 - OUTLET PRESS [barg]	-1.219	Highly skewed → median
Latitude	-1.06363	Highly skewed → median

Reliquefaction - Inlet temperature [°C]	-1.01657	Highly skewed → median
AirTemperatureSL	-0.93241	Moderately skewed → median
ME1 Torque [knm]	-0.76654	Moderately skewed → median
ME2 Torque [knm]	-0.7119	Moderately skewed → median
LD compressor 1 - INLET PRESS [bara]	-0.58081	Moderately skewed → median
AirPressureSL	-0.49723	Approximately symmetric → Use mean
DG3 running hours [h]	-0.41501	Approximately symmetric → Use mean
SwellPeriod	-0.37763	Approximately symmetric → Use mean
ME consumed [MT]	-0.31681	Approximately symmetric → Use mean
ME1 Shaft Power [kW]	-0.26729	Approximately symmetric → Use mean
Shaft power [kW]	-0.22828	Approximately symmetric → Use mean
ME2 Shaft Power [kW]	-0.20111	Approximately symmetric → Use mean
PackageId	-0.19667	Approximately symmetric → Use mean
Roll avarage (Sloshield) [°]	-0.17468	Approximately symmetric → Use mean
Tank 1 - Liquid level corrected [m]	-0.15931	Approximately symmetric → Use mean

Tank 1 - Liquid Volume [m^3]	-0.15529	Approximately symmetric → Use mean
DG2 energy production [kWh]	-0.14547	Approximately symmetric → Use mean
CurrentDirection	-0.07362	Approximately symmetric → Use mean
Impacts tank 6 []	0	Approximately symmetric → Use mean
LD compressor 1 - DISCH FLOW [kg/h]	0	Approximately symmetric → Use mean
RHO LNG [Kg/m^3]	0	Approximately symmetric → Use mean
BOR alarm low [%]	0	Approximately symmetric → Use mean
BOR alarm high [%]	0	Approximately symmetric → Use mean
Impacts per minute overall [Impact/min]	0	Approximately symmetric → Use mean
Total impacts all tanks []	0	Approximately symmetric → Use mean
ShipId	0	Approximately symmetric → Use mean
DG3 energy production [kWh]	0	Approximately symmetric → Use mean
Impact alarm overall []	0	Approximately symmetric → Use mean

Impacts tank 5 []	0	Approximately symmetric → Use mean
IMONo	0	Approximately symmetric → Use mean
LNG tank volume [m^3]	0	Approximately symmetric → Use mean
Tank 3 - Vapour temperature [°C]	0.021356	Approximately symmetric → Use mean
PrimaryWavePeriod	0.03974	Approximately symmetric → Use mean
DG1 running hours [h]	0.051606	Approximately symmetric → Use mean
Yaw average [°]	0.058818	Approximately symmetric → Use mean
DG3 Power [kW]	0.064504	Approximately symmetric → Use mean
Roll average [°]	0.06864	Approximately symmetric → Use mean
DG2 running hours [h]	0.074651	Approximately symmetric → Use mean
SwellDirection	0.104624	Approximately symmetric → Use mean
Draft fore [m]	0.129939	Approximately symmetric → Use mean
DG1 energy production [kWh]	0.131629	Approximately symmetric → Use mean

Draft mid portside [m]	0.141743	Approximately symmetric → Use mean
ME running hours [h]	0.169369	Approximately symmetric → Use mean
Draft mid starboard [m]	0.176727	Approximately symmetric → Use mean
DG4 running hours [h]	0.178224	Approximately symmetric → Use mean
Tank 4 - Liquid Volume [m^3]	0.22736	Approximately symmetric → Use mean
Tank 3 - Liquid Volume [m^3]	0.228657	Approximately symmetric → Use mean
Tank 4 - Liquid level corrected [m]	0.231804	Approximately symmetric → Use mean
DG4 Power [kW]	0.236793	Approximately symmetric → Use mean
Tank 3 - Liquid level corrected [m]	0.239316	Approximately symmetric → Use mean
DG1 Power [kW]	0.315796	Approximately symmetric → Use mean
Vapour MAIN - FWD temperature [°C]	0.323717	Approximately symmetric → Use mean
PrimaryWaveDirection	0.335105	Approximately symmetric → Use mean
Draft aft [m]	0.373548	Approximately symmetric → Use mean

LD compressor 1 - INLET TEMP [°C]	0.412942	Approximately symmetric → Use mean
DG2 Power [kW]	0.447307	Approximately symmetric → Use mean
WindWavePeriod	0.462699	Approximately symmetric → Use mean
Tank 2 - Liquid Volume [m^3]	0.475913	Approximately symmetric → Use mean
Tank 2 - Liquid level corrected [m]	0.477656	Approximately symmetric → Use mean
WindDirection	0.484901	Approximately symmetric → Use mean
Longitude	0.520865	Moderately skewed → median
Vapour MAIN - Gauge pressure [mbarg]	0.619799	Moderately skewed → median
LNG supply HDR - Pressure [mbarg]	0.619839	Moderately skewed → median
Reliquefaction - Inlet pressure [mbara]	0.658483	Moderately skewed → median
HD compressor 1 - INLET PRESS [bar]	0.710002	Moderately skewed → median
HD compressor 1 - L.O FILTER DIFF PRESS [bar]	0.714779	Moderately skewed → median
Tank 1 - Vapour pressure [mbarg]	0.775122	Moderately skewed → median
WindWaveDirection	0.784781	Moderately skewed → median
Tank 3 - Vapour pressure [mbarg]	0.798733	Moderately skewed → median
Tank 4 - Vapour pressure [mbarg]	0.806819	Moderately skewed → median
Reliquefaction - Electrical consumption [kW]	0.80986	Moderately skewed → median
Reliquefaction - Inlet flow [kg/h]	0.862998	Moderately skewed → median

Tank 2 - Vapour pressure [mbarg]	0.866403	Moderately skewed → median
WindWaveSwellHeight	0.871444	Moderately skewed → median
DG consumed [MT]	0.982416	Moderately skewed → median
DG4 energy production [kWh]	1.000034	Highly skewed → median
Pitch avarage (Sloshield) [°]	1.162234	Highly skewed → median
LD compressor 2 - OUTLET TEMP B [°C]	1.26553	Highly skewed → median
Tank 1 - Vapour temperature [°C]	1.28977	Highly skewed → median
WindSpeed	1.338645	Highly skewed → median
SwellHeight	1.445843	Highly skewed → median
Tank 2 - Vapour temperature [°C]	1.452173	Highly skewed → median
Pitch average [°]	1.637877	Highly skewed → median
Tank 4 - Vapour temperature [°C]	1.669671	Highly skewed → median
LNG Vaporizer - OUTLET PRESS [bar]	1.683035	Highly skewed → median
WindWaveHeight	1.686232	Highly skewed → median
DG electrical power [kW]	1.774277	Highly skewed → median
Roll max starboard (Sloshield) [°]	2.039996	Highly skewed → median
CurrentSpeed	2.045206	Highly skewed → median
ME FO supply temperature [°C]	2.117948	Highly skewed → median
FORCING Vaporizer - INLET PRESS [barg*100]	2.120409	Highly skewed → median
Vapour Cross-Over - Pressure [barG]	2.423277	Highly skewed → median
HD compressor 1 - OUTLET PRESS [bar]	2.628689	Highly skewed → median
FORCING Vaporizer - DISCH FLOW [kg/h]	3.204258	Highly skewed → median

COG heading [°]	3.62567	Highly skewed → median
Vapour MAIN - AFT temperature [°C]	3.803676	Highly skewed → median
LNG Vaporizer - INLET PRESS [bar]	4.683554	Highly skewed → median
Tank 4 - Average Liquid temp [°C]	5.721745	Highly skewed → median
Tank 2 - Average Liquid temp [°C]	5.822035	Highly skewed → median
Tank 1 - Average Liquid temp [°C]	6.156968	Highly skewed → median
Liquid Cross-Over - AFT pressure [mbarg]	6.764843	Highly skewed → median
Liquid Cross-Over - FWD pressure [mbar]	6.787815	Highly skewed → median
Tank 3 - Average Liquid temp [°C]	7.198552	Highly skewed → median
BOG to GCU [kg/h]	10.24688	Highly skewed → median
WaterTemperatureSL	16.47886	Highly skewed → median
Pitch max fore (Sloshield) [°]	64.29236	Highly skewed → median

Appendix 14 - Imputation process of Vessel 2 (Skewness)

Features	Skewness	Interpretation
Tank 1 - Average Liquid temp [°C]	-21.3244	Highly skewed → use median
LNG Heater - GAS OUTLET TEMP [°C]	-10.7404	Highly skewed → use median
LNG Heater - GAS INLET TEMP [°C]	-10.7393	Highly skewed → use median
HD compressor 1 - OUTLET TEMP B [°C]	-7.86616	Highly skewed → use median
HD compressor 1 - OUTLET TEMP A [°C]	-7.85443	Highly skewed → use median
HD compressor 1 - INLET TEMP [°C]	-6.8072	Highly skewed → use median
Liquid Cross-Over - FWD temperature [°C]	-4.2128	Highly skewed → use median
Liquid Cross-Over - AFT temperature [°C]	-3.74906	Highly skewed → use median
Liquid MAIN - AFT temperature [°C]	-3.30677	Highly skewed → use median
Liquid MAIN - FWD temperature [°C]	-3.29372	Highly skewed → use median
Spray MAIN - FWD temperature [°C]	-3.15788	Highly skewed → use median
Spray MAIN - AFT temperature [°C]	-2.09724	Highly skewed → use median
Sway Average [m]	-1.56423	Highly skewed → use median
Log speed [knots]	-1.35419	Highly skewed → use median
Shaft rpm [rpm]	-1.33165	Highly skewed → use median
ME1 RPM [rpm]	-1.33158	Highly skewed → use median
ME2 RPM [rpm]	-1.32506	Highly skewed → use median
GPS speed [knots]	-1.30548	Highly skewed → use median

Tank 3 - IS PORT SIDE WALL TEMP(ST-BY) - (HULL) [°C]	-1.10478	Highly skewed → use median
Tank 1 - IS PORT SIDE WALL TEMP(ST-BY) - (HULL) [°C]	-1.09087	Highly skewed → use median
Tank 2 - IS PORT SIDE WALL TEMP(ST-BY) - (HULL) [°C]	-1.08311	Highly skewed → use median
Tank 4 - IS PORT SIDE WALL TEMP(ST-BY) [°C]	-1.07875	Highly skewed → use median
FORCING Vaporizer - INLET TEMP [°C]	-1.01362	Highly skewed → use median
AirTemperatureSL	-1.00011	Highly skewed → use median
Nitrogen system - Bleeding pressure [bar]	-0.95412	Moderately skewed → median
Tank 3 - Vapour pressure [mbarg]	-0.94499	Moderately skewed → median
Tank 4 - Vapour pressure [mbarg]	-0.92224	Moderately skewed → median
Tank 1 - Vapour pressure [mbarg]	-0.90991	Moderately skewed → median
Tank 2 - Vapour pressure [mbarg]	-0.90572	Moderately skewed → median
Latitude	-0.75159	Moderately skewed → median
Reliquefaction - Inlet temperature [°C]	-0.74357	Moderately skewed → median
ME2 Torque [knm]	-0.69089	Moderately skewed → median
ME1 Torque [knm]	-0.66704	Moderately skewed → median
Reliquefaction - Outlet temperature [°C]	-0.38913	Approximately symmetric → Use mean
ME consumed [MT]	-0.28149	Approximately symmetric → Use mean

DG2 energy production [kWh]	-0.26567	Approximately symmetric → Use mean
Tank 3 - IS CEIL TEMP(ST-BY) [°C]	-0.25881	Approximately symmetric → Use mean
SwellPeriod	-0.25381	Approximately symmetric → Use mean
ME2 Shaft Power [kW]	-0.25248	Approximately symmetric → Use mean
Shaft power [kW]	-0.24683	Approximately symmetric → Use mean
ME1 Shaft Power [kW]	-0.24012	Approximately symmetric → Use mean
DG2 running hours [h]	-0.23662	Approximately symmetric → Use mean
PackageId	-0.1955	Approximately symmetric → Use mean
Tank 3 - IS BTM MIDDLE TEMP(ST-BY) [°C]	-0.1925	Approximately symmetric → Use mean
DG3 energy production [kWh]	-0.1435	Approximately symmetric → Use mean
CurrentDirection	-0.12737	Approximately symmetric → Use mean
DG1 running hours [h]	-0.12611	Approximately symmetric → Use mean
Tank 3 - IS BTM AFT MID TEMP(ST-BY) [°C]	-0.11851	Approximately symmetric → Use mean

COG heading [°]	-0.04326	Approximately symmetric → Use mean
ME running hours [h]	-0.01376	Approximately symmetric → Use mean
Tank 1 - Liquid level corrected [m]	-0.00618	Approximately symmetric → Use mean
LD compressor 1 - SPRAY AFT. CLR. TEMP VV POS. [%]	0	Approximately symmetric → Use mean
BOR alarm low [%]	0	Approximately symmetric → Use mean
RHO LNG [Kg/m^3]	0	Approximately symmetric → Use mean
LNG tank volume [m^3]	0	Approximately symmetric → Use mean
BOR alarm high [%]	0	Approximately symmetric → Use mean
LNG Vaporizer - DISCH FLOW [kg/h]	0	Approximately symmetric → Use mean
LD compressor 1 - OUTLET TEMP B [°C]	0	Approximately symmetric → Use mean
LD compressor 2 - SPRAY AFT. CLR. TEMP VV POS. [%]	0	Approximately symmetric → Use mean
LNG supply HDR - Pressure [mbarg]	0	Approximately symmetric → Use mean
Fuel Gas Heater - GAS OUTLET PRESS [bar]	0	Approximately symmetric → Use mean

Fuel Gas Heater - GAS INLET TEMP [°C]	0	Approximately symmetric → Use mean
Total impacts all tanks []	0	Approximately symmetric → Use mean
IMONo	0	Approximately symmetric → Use mean
ShipId	0	Approximately symmetric → Use mean
Fuel Gas Heater - GAS OUTLET TEMP [°C]	0	Approximately symmetric → Use mean
Fuel Gas Heater - GAS INLET PRESS [bar]	0	Approximately symmetric → Use mean
DG3 running hours [h]	0.002456	Approximately symmetric → Use mean
Tank 1 - Liquid Volume [m^3]	0.021242	Approximately symmetric → Use mean
Tank 1 - Liquid Dome IS inlet pressure [mbar]	0.030013	Approximately symmetric → Use mean
Daily BOR (Sloshield) [MT/Day]	0.050156	Approximately symmetric → Use mean
BOR rate running average (Sloshield) [MT/Day]	0.050156	Approximately symmetric → Use mean
Yaw average [°]	0.061097	Approximately symmetric → Use mean
Vapour MAIN - FWD temperature [°C]	0.063887	Approximately symmetric → Use mean

Draft fore [m]	0.07889	Approximately symmetric → Use mean
DG4 energy production [kWh]	0.079396	Approximately symmetric → Use mean
PrimaryWavePeriod	0.083403	Approximately symmetric → Use mean
DG4 running hours [h]	0.090073	Approximately symmetric → Use mean
DG1 energy production [kWh]	0.09035	Approximately symmetric → Use mean
Longitude	0.136737	Approximately symmetric → Use mean
SwellDirection	0.154222	Approximately symmetric → Use mean
Draft mid portside [m]	0.20878	Approximately symmetric → Use mean
Surge Average [m]	0.213643	Approximately symmetric → Use mean
Draft mid starboard [m]	0.224477	Approximately symmetric → Use mean
Tank 2 - Liquid Dome IS inlet pressure [mbar]	0.256496	Approximately symmetric → Use mean
Tank 4 - Liquid Volume [m^3]	0.294226	Approximately symmetric → Use mean
Tank 3 - Liquid Volume [m^3]	0.296229	Approximately symmetric → Use mean

Tank 2 - Liquid Volume [m^3]	0.297862	Approximately symmetric → Use mean
Tank 4 - Liquid level corrected [m]	0.299259	Approximately symmetric → Use mean
PrimaryWaveDirection	0.301925	Approximately symmetric → Use mean
Tank 3 - Liquid level corrected [m]	0.303462	Approximately symmetric → Use mean
Tank 2 - Liquid level corrected [m]	0.304197	Approximately symmetric → Use mean
Draft aft [m]	0.344229	Approximately symmetric → Use mean
Tank 3 - Vapour temperature [°C]	0.365025	Approximately symmetric → Use mean
Tank 4 - Liquid Dome IS inlet pressure [mbar]	0.391277	Approximately symmetric → Use mean
DG1 Power [kW]	0.402571	Approximately symmetric → Use mean
Reliquefaction - Inlet pressure [mbara]	0.409627	Approximately symmetric → Use mean
WindDirection	0.42292	Approximately symmetric → Use mean
Tank 3 - IS PORT UPP CHAM TEMP(ST-BY) [°C]	0.426045	Approximately symmetric → Use mean
Tank 3 - Liquid temp 75% [°C]	0.444339	Approximately symmetric → Use mean

AirPressureSL	0.446639	Approximately symmetric → Use mean
FORCING Vaporizer - INLET PRESS [barg*100]	0.44862	Approximately symmetric → Use mean
Tank 3 - Liquid Dome IS inlet pressure [mbar]	0.46402	Approximately symmetric → Use mean
WindWavePeriod	0.467478	Approximately symmetric → Use mean
DG4 Power [kW]	0.507844	Moderately skewed → median
Tank 2 - IS CEIL TEMP(ST-BY) [°C]	0.572085	Moderately skewed → median
Tank 1 - IS CEIL TEMP(ST-BY) [°C]	0.576467	Moderately skewed → median
Roll average [°]	0.59474	Moderately skewed → median
DG2 Power [kW]	0.622188	Moderately skewed → median
Reliquefaction - Electrical consumption [kW]	0.645049	Moderately skewed → median
Tank 4 - IS CEIL TEMP(ST-BY) [°C]	0.662082	Moderately skewed → median
Tank 2 - IS AFT TRAN WALL TEMP(ST-BY) [°C]	0.681333	Moderately skewed → median
Tank 2 - IS PORT UPP CHAM TEMP(ST-BY) [°C]	0.683251	Moderately skewed → median
Tank 2 - IS PORT SIDE WALL TEMP(ST-BY) [°C]	0.684704	Moderately skewed → median
Heave Average [m]	0.68499	Moderately skewed → median
Tank 2 - IS FWD TRAN WALL TEMP(ST-BY) [°C]	0.685078	Moderately skewed → median

Tank 3 - IS FWD TRAN WALL TEMP(ST-BY) [°C]	0.698037	Moderately skewed → median
Tank 1 - IS PORT UPP CHAM TEMP(ST-BY) [°C]	0.699191	Moderately skewed → median
Tank 1 - IS PORT SIDE WALL TEMP(ST-BY) [°C]	0.701524	Moderately skewed → median
Tank 1 - IS FWD TRAN WALL TEMP(ST-BY) [°C]	0.712951	Moderately skewed → median
Tank 2 - IS PORT LOW CHAM TEMP(ST-BY) [°C]	0.727933	Moderately skewed → median
WindWaveSwellHeight	0.732053	Moderately skewed → median
Tank 1 - IS AFT TRAN WALL TEMP(ST-BY) [°C]	0.735109	Moderately skewed → median
Tank 3 - IS AFT TRAN WALL TEMP(ST-BY) [°C]	0.755922	Moderately skewed → median
Tank 2 - Liquid temp 75% [°C]	0.786	Moderately skewed → median
Tank 3 - IS PORT SIDE WALL TEMP(ST-BY) [°C]	0.807543	Moderately skewed → median
Reliquefaction - Inlet flow [kg/h]	0.812863	Moderately skewed → median
HD compressor 1 - L.O FILTER DIFF PRESS [bar]	0.814186	Moderately skewed → median
HD compressor 1 - INLET PRESS [bar]	0.8244	Moderately skewed → median
WindWaveDirection	0.834898	Moderately skewed → median
Tank 1 - Liquid temp 75% [°C]	0.837121	Moderately skewed → median

Tank 2 - IS BTM MIDDLE TEMP(ST-BY) [°C]	0.846224	Moderately skewed → median
Tank 2 - Vapour temperature [°C]	0.850743	Moderately skewed → median
Tank 2 - IS BTM AFT MID TEMP(ST-BY) [°C]	0.858699	Moderately skewed → median
DG3 Power [kW]	0.860558	Moderately skewed → median
Tank 1 - Vapour temperature [°C]	0.873244	Moderately skewed → median
Roll avarage (Sloshield) [°]	0.884376	Moderately skewed → median
Pitch average [°]	0.986755	Moderately skewed → median
WindSpeed	0.996888	Moderately skewed → median
Vapour MAIN - AFT temperature [°C]	0.998282	Moderately skewed → median
Tank 1 - IS PORT LOW CHAM TEMP(ST-BY) [°C]	1.059073	Highly skewed → use median
LNG Heater - GAS OUTLET PRESS [bar]	1.060229	Highly skewed → use median
LNG Heater - GAS INLET PRESS [bar]	1.06157	Highly skewed → use median
Pitch avarage (Sloshield) [°]	1.124609	Highly skewed → use median
Tank 1 - IS BTM MIDDLE TEMP(ST-BY) [°C]	1.139678	Highly skewed → use median
Tank 1 - IS BTM AFT MID TEMP(ST-BY) [°C]	1.146357	Highly skewed → use median
Tank 4 - IS PORT UPP CHAM TEMP(ST-BY) [°C]	1.149149	Highly skewed → use median
SwellHeight	1.284035	Highly skewed → use median
Tank 3 - Spray return pressure [barg]	1.319442	Highly skewed → use median

Tank 3 - Average Liquid temp [°C]	1.342935	Highly skewed → use median
Tank 4 - IS FWD TRAN WALL TEMP(ST-BY) [°C]	1.444032	Highly skewed → use median
LNG Vaporizer - OUTLET PRESS [bar]	1.492661	Highly skewed → use median
Tank 4 - IS AFT TRAN WALL TEMP(ST-BY) [°C]	1.514079	Highly skewed → use median
Tank 4 - IS PORT SIDE WALL TEMP(ST-BY) - (HULL) [°C]	1.538535	Highly skewed → use median
Tank 4 - Spray return pressure [barg]	1.608815	Highly skewed → use median
Tank 4 - Liquid temp 75% [°C]	1.628615	Highly skewed → use median
Tank 3 - IS PORT LOW CHAM TEMP(ST-BY) [°C]	1.654506	Highly skewed → use median
Boiler consumed [MT]	1.669237	Highly skewed → use median
DG electrical power [kW]	1.676964	Highly skewed → use median
WindWaveHeight	1.687858	Highly skewed → use median
Vapour Cross-Over - Pressure [barG]	1.714727	Highly skewed → use median
FORCING Vaporizer - DISCH FLOW [kg/h]	1.786321	Highly skewed → use median
Roll max starboard (Sloshield) [°]	1.851281	Highly skewed → use median
Pitch max fore (Sloshield) [°]	1.913554	Highly skewed → use median
Tank 4 - Vapour temperature [°C]	1.922853	Highly skewed → use median
DG consumed [MT]	2.118476	Highly skewed → use median
Tank 4 - IS PORT LOW CHAM TEMP(ST-BY) [°C]	2.386833	Highly skewed → se median

CurrentSpeed	2.431995	Highly skewed → use median
HD compressor 1 - OUTLET PRESS [bar]	2.801444	Highly skewed → use median
Tank 4 - IS BTM MIDDLE TEMP(ST-BY) [°C]	3.408571	Highly skewed → use median
Tank 4 - IS BTM AFT MID TEMP(ST-BY) [°C]	3.571606	Highly skewed → use median
Tank 2 - Average Liquid temp [°C]	4.032424	Highly skewed → use median
NO.2 N2 GENERATOR PRODUCT OXYGEN CONTENT [%]	4.191823	Highly skewed → use median
Liquid Cross-Over - FWD pressure [mbar]	7.455429	Highly skewed → use median
Liquid Cross-Over - AFT pressure [mbarg]	7.457008	Highly skewed → use median
Tank 4 - Average Liquid temp [°C]	8.284883	Highly skewed → use median
Tank 2 - Spray return pressure [barg]	8.673142	Highly skewed → use median
LNG Vaporizer - INLET PRESS [bar]	10.78314	Highly skewed → use median
Daily BOR alarm []	11.543	Highly skewed → use median
Impacts per minute overall [Impact/min]	11.99171	Highly skewed → use median
Tank 1 - Spray return pressure [barg]	13.86859	Highly skewed → use median
Impact alarm overall []	14.14234	Highly skewed → use median
WaterTemperatureSL	15.98272	Highly skewed → use median
NO.1 N2 GENERATOR PRODUCT OXYGEN CONTENT [%]	17.10072	Highly skewed → use median
BOG to GCU [kg/h]	46.96074	Highly skewed → use median

Appendix 15 - Imputation process of Vessel 3 (Skewness)

Features	Skewness	Interpretation
HD compressor 1 - OUTLET TEMP B [°C]	-6.99226786	Highly skewed → use median
HD compressor 1 - OUTLET TEMP A [°C]	-6.97902989	Highly skewed → use median
Daily BOR (Sloshield) [MT/Day]	-4.67921626	Highly skewed → use median
BOR rate running average (Sloshield) [MT/Day]	-4.67921479	Highly skewed → use median
HD compressor 1 - INLET TEMP [°C]	-3.85094619	Highly skewed → use median
Liquid Cross-Over - AFT temperature [°C]	-3.08816254	Highly skewed → use median
Liquid Cross-Over - FWD temperature [°C]	-3.08641736	Highly skewed → use median
FORCING Vaporizer - INLET TEMP [°C]	-2.21120907	Highly skewed → use median
FORCING Vaporizer - OUTLET TEMP [°C]	-2.11215242	Highly skewed → use median
AirTemperatureSL	-1.14887897	Highly skewed → use median
ME1 RPM [rpm]	-1.10578484	Highly skewed → use median
ME2 RPM [rpm]	-1.1050572	Highly skewed → use median
Shaft rpm [rpm]	-1.10405398	Highly skewed → use median
Log speed [knots]	-1.07667489	Highly skewed → use median
GPS speed [knots]	-1.05380835	Highly skewed → use median
LD compressor 1 - INLET TEMP [°C]	-0.80996219	Moderately skewed → median
LNG Vaporizer - OUTLET PRESS [bar]	-0.75278999	Moderately skewed → median
Sub-Cooler - MC3.POWER [kW]	-0.63151597	Moderately skewed → median
DG1 energy production [kWh]	-0.61928419	Moderately skewed → median
ME1 Torque [knm]	-0.50860738	Moderately skewed → median

ME2 Torque [knm]	-0.50351331	Moderately skewed → median
Roll average [°]	-0.2772659	Approximately symmetric → Use mean
SwellPeriod	-0.27198238	Approximately symmetric → Use mean
Roll avarage (Sloshield) [°]	-0.24633667	Approximately symmetric → Use mean
CurrentDirection	-0.22339314	Approximately symmetric → Use mean
LD compressor 1 - OUTLET PRESS [barg]	-0.21566613	Approximately symmetric → Use mean
Latitude	-0.19885903	Approximately symmetric → Use mean
PackageId	-0.18764949	Approximately symmetric → Use mean
LD compressor 1 - OUTLET TEMP A [°C]	-0.09434082	Approximately symmetric → Use mean
PrimaryWavePeriod	-0.03894887	Approximately symmetric → Use mean
Draft mid portside [m]	-0.03474282	Approximately symmetric → Use mean
Draft fore [m]	-0.02982136	Approximately symmetric → Use mean
ME running hours [h]	-0.00639572	Approximately symmetric → Use mean
DG3 running hours [h]	-0.00076775	Approximately symmetric → Use mean
LNG tank volume [m^3]	0	Approximately symmetric → Use mean
BOR alarm low [%]	0	Approximately symmetric → Use mean
RHO LNG [Kg/m^3]	0	Approximately symmetric → Use mean
BOR alarm high [%]	0	Approximately symmetric → Use mean
IMONo	0	Approximately symmetric → Use mean
Impacts per minute overall [Impact/min]	0	Approximately symmetric → Use mean
Impact alarm overall []	0	Approximately symmetric → Use mean
LNG Vaporizer - DISCH FLOW [kg/h]	0	Approximately symmetric → Use mean
ShipId	0	Approximately symmetric → Use mean
DG4 running hours [h]	0.00225675	Approximately symmetric → Use mean

DG1 running hours [h]	0.002259273	Approximately symmetric → Use mean
Yaw average [°]	0.015965774	Approximately symmetric → Use mean
ME consumed [MT]	0.016844241	Approximately symmetric → Use mean
Draft aft [m]	0.019107394	Approximately symmetric → Use mean
Tank 2 - Liquid Volume [m^3]	0.027884233	Approximately symmetric → Use mean
Tank 3 - Liquid Volume [m^3]	0.032024214	Approximately symmetric → Use mean
Tank 2 - Liquid level corrected [m]	0.041252125	Approximately symmetric → Use mean
Draft mid starboard [m]	0.041756998	Approximately symmetric → Use mean
Tank 3 - Liquid level corrected [m]	0.043955474	Approximately symmetric → Use mean
ME2 Shaft Power [kW]	0.058320064	Approximately symmetric → Use mean
Shaft power [kW]	0.058653555	Approximately symmetric → Use mean
ME1 Shaft Power [kW]	0.061219585	Approximately symmetric → Use mean
Tank 3 - Vapour temperature [°C]	0.066835033	Approximately symmetric → Use mean
DG2 running hours [h]	0.06976165	Approximately symmetric → Use mean
COG heading [°]	0.070955184	Approximately symmetric → Use mean
DG4 Power [kW]	0.076620008	Approximately symmetric → Use mean
Tank 1 - Liquid level corrected [m]	0.093109708	Approximately symmetric → Use mean
Tank 1 - Liquid Volume [m^3]	0.096542894	Approximately symmetric → Use mean
Tank 2 - Vapour temperature [°C]	0.127080075	Approximately symmetric → Use mean
Tank 4 - Liquid Volume [m^3]	0.146816687	Approximately symmetric → Use mean
Tank 4 - Liquid level corrected [m]	0.154457592	Approximately symmetric → Use mean
DG1 Power [kW]	0.165853206	Approximately symmetric → Use mean
AirPressureSL	0.181738954	Approximately symmetric → Use mean
DG3 energy production [kWh]	0.243808405	Approximately symmetric → Use mean

Tank 1 - Vapour temperature [°C]	0.305572717	Approximately symmetric → Use mean
DG4 energy production [kWh]	0.386806879	Approximately symmetric → Use mean
DG2 energy production [kWh]	0.412463992	Approximately symmetric → Use mean
Longitude	0.475888939	Approximately symmetric → Use mean
SwellDirection	0.486568333	Approximately symmetric → Use mean
WindWavePeriod	0.593341761	Moderately skewed → median
Pitch avarage (Sloshield) [°]	0.606101355	Moderately skewed → median
PrimaryWaveDirection	0.651465178	Moderately skewed → median
LD compressor 1 - DISCH FLOW [kg/h]	0.6747292	Moderately skewed → median
WindSpeed	0.68318677	Moderately skewed → median
WindWaveSwellHeight	0.784995459	Moderately skewed → median
Pitch average [°]	0.794683298	Moderately skewed → median
WindDirection	0.798426168	Moderately skewed → median
Under keel clearance [m]	1.042781473	Highly skewed → use median
Tank 4 - Vapour pressure [mbarg]	1.060182126	Highly skewed → use median
Tank 1 - Vapour pressure [mbarg]	1.062358821	Highly skewed → use median
Tank 2 - Vapour pressure [mbarg]	1.067897462	Highly skewed → use median
Tank 3 - Vapour pressure [mbarg]	1.069041083	Highly skewed → use median
HD compressor 1 - INLET PRESS [bar]	1.07797128	Highly skewed → use median
LNG supply HDR - Pressure [mbarg]	1.105742489	Highly skewed → use median
WindWaveDirection	1.153297642	Highly skewed → use median
HD compressor 1 - L.O FILTER DIFF PRESS [bar]	1.173542951	Highly skewed → use median
DG consumed [MT]	1.336967434	Highly skewed → use median

Sub-Cooler - MTC2.POWER [kW]	1.34787859	Highly skewed → use median
Sub-Cooler - MC1.POWER [kW]	1.348696393	Highly skewed → use median
Sub-Cooler - MC2.POWER [kW]	1.349235314	Highly skewed → use median
Sub-Cooler - MTC3.POWER [kW]	1.350548083	Highly skewed → use median
Sub-Cooler - MC4.POWER [kW]	1.351688947	Highly skewed → use median
Sub-Cooler - MTC1.POWER [kW]	1.352368902	Highly skewed → use median
SwellHeight	1.36743531	Highly skewed → use median
DG2 Power [kW]	1.408379903	Highly skewed → use median
DG3 Power [kW]	1.414214775	Highly skewed → use median
Pitch max fore (Sloshield) [°]	1.654766487	Highly skewed → use median
WindWaveHeight	1.722455021	Highly skewed → use median
Sub-Cooler - Cold power [%]	1.791577297	Highly skewed → use median
DG electrical power [kW]	1.858735232	Highly skewed → use median
LNG Vaporizer - INLET PRESS [bar]	1.960691117	Highly skewed → use median
Tank 4 - Vapour temperature [°C]	2.006158116	Highly skewed → use median
Roll max starboard (Sloshield) [°]	2.15809292	Highly skewed → use median
CurrentSpeed	2.161616052	Highly skewed → use median
FORCING Vaporizer - INLET PRESS [barg*100]	2.401664795	Highly skewed → use median
HD compressor 1 - OUTLET PRESS [bar]	2.64027144	Highly skewed → use median
LD compressor 1 - INLET PRESS [bara]	2.726870319	Highly skewed → use median
Vapour Cross-Over - Pressure [barG]	3.452943126	Highly skewed → use median
BOG to GCU [kg/h]	4.094496477	Highly skewed → use median

FORCING Vaporizer - DISCH FLOW [kg/h]	5.632868901	Highly skewed → use median
Liquid Cross-Over - AFT pressure [mbarg]	6.79981741	Highly skewed → use median
Liquid Cross-Over - FWD pressure [mbar]	6.802617356	Highly skewed → use median
WaterTemperatureSL	9.635883011	Highly skewed → use median
Daily BOR alarm []	14.99291791	Highly skewed → use median
Tank 1 - Average Liquid temp [°C]	16.20806079	Highly skewed → use median
Tank 4 - Average Liquid temp [°C]	17.04148187	Highly skewed → use median
Tank 2 - Average Liquid temp [°C]	32.7044268	Highly skewed → use median
Tank 3 - Average Liquid temp [°C]	44.72007138	Highly skewed → use median

Appendix 16 - Correlation matrix corresponding to fuel consumption

Feature	Correlation_with_fuel consumption
Draft fore [m]	0,078294388
Draft aft [m]	-0,057839878
Average Draft Mid [m]	0,203963794
GPS speed [knots]	0,870320361
Shaft power [kW]	0,971776495
Shaft rpm [rpm]	0,893837227
Total DG Power [kW]	-0,141239373
Total DG Energy [kWh]	-0,063810031
ME running hours [h]	0,067460885
Total ME Torque [knm]	0,955888299
Total ME Shaft Power [kW]	0,974117577
Average ME RPM [rpm]	0,894490565
WindSpeed	0,223802767
WindWavePeriod	0,158171727
WindWaveHeight	0,207933499
CurrentSpeed	0,166182699
AirTemperatureSL	0,106550915
WaterTemperatureSL	0,161808268
AirPressureSL	-0,00244421
BOG to GCU [kg/h]	-0,194888249
Reliquefaction - Electrical consumption [kW]	-0,189378568

SwellHeight	0,279245662
SwellPeriod	0,156237464
Swell Steepness [m/s]	0,280533394
Roll average [°]	-0,064467185
Pitch average [°]	-0,085889873
Yaw average [°]	0,010900038
Roll max starboard (Sloshield) [°]	0,151113143
Pitch max fore (Sloshield) [°]	0,090174131
Roll avarage (Sloshield) [°]	-0,067476294
Pitch avarage (Sloshield) [°]	-0,019813595
Tank 1 - Liquid Volume [m^3]	0,22676545
Tank 2 - Liquid Volume [m^3]	0,212100132
Tank 3 - Liquid Volume [m^3]	0,222499597
Tank 4 - Liquid Volume [m^3]	0,226533143

Appendix 17 - Coding for the fuel prediction

Code Cell 1

```
import pandas as pd
file_path_1gb = r'C:\UsageIQ\vesselsdataset.csv'
!pip install chardet
```

Code Cell 2

```
#Print the first 5 rows of the database

df_vessel_1.head()
```

Code Cell 3

```
nan_percentage = df_vessel_1.isna().mean() * 100


# Filter columns with more than 60% NaNs
columns_to_drop_due_to_more_60_percent_nans = nan_percentage[nan_percentage > 60]


# Print columns with their NaN percentages
print("Columns with more than 60% NaNs:")
for col, pct in columns_to_drop_due_to_more_60_percent_nans.items():
    print(f"- {col}: {pct:.2f}% NaNs")
```

Code Cell 4

```
# Drop features with NaN percentage greater than or equal to 60%
df_vessel_1 = df_vessel_1.loc[:, nan_percentage < 60]
df_vessel_1.head()
```

Code Cell 5

```
columns_to_drop = [
    # Highly detailed internal tank temperatures — too specific, unlikely to affect overall ship
performance or satisfaction
    'Tank 1 - IS BTM AFT MID TEMP(MAIN) [°C]',
    'Tank 1 - IS BTM MIDDLE TEMP(MAIN) [°C]',
    'Tank 1 - IS PORT LOW CHAM TEMP(MAIN) [°C]',
    'Tank 1 - IS PORT SIDE WALL TEMP(MAIN) [°C]',
```

'Tank 1 - IS PORT UPP CHAM TEMP(MAIN) [°C]',

'Tank 1 - IS CEIL TEMP(MAIN) [°C]',

'Tank 1 - IS AFT TRAN WALL TEMP(MAIN) [°C]',

'Tank 1 - IS FWD TRAN WALL TEMP(MAIN) [°C]',

'Tank 1 - IS PORT SIDE WALL TEMP(MAIN) - (HULL) [°C]',

'Tank 2 - IS BTM AFT MID TEMP(MAIN) [°C]',

'Tank 2 - IS BTM MIDDLE TEMP(MAIN) [°C]',

'Tank 2 - IS PORT LOW CHAM TEMP(MAIN) [°C]',

'Tank 2 - IS PORT SIDE WALL TEMP(MAIN) [°C]',

'Tank 2 - IS PORT UPP CHAM TEMP(MAIN) [°C]',

'Tank 2 - IS CEIL TEMP(MAIN) [°C]',

'Tank 2 - IS AFT TRAN WALL TEMP(MAIN) [°C]',

'Tank 2 - IS FWD TRAN WALL TEMP(MAIN) [°C]',

'Tank 2 - IS PORT SIDE WALL TEMP(MAIN) - (HULL) [°C]',

'Tank 3 - IS BTM AFT MID TEMP(MAIN) [°C]',

'Tank 3 - IS BTM MIDDLE TEMP(MAIN) [°C]',

'Tank 3 - IS PORT LOW CHAM TEMP(MAIN) [°C]',

'Tank 3 - IS PORT SIDE WALL TEMP(MAIN) [°C]',

'Tank 3 - IS PORT UPP CHAM TEMP(MAIN) [°C]',

'Tank 3 - IS CEIL TEMP(MAIN) [°C]',

'Tank 3 - IS AFT TRAN WALL TEMP(MAIN) [°C]',

'Tank 3 - IS FWD TRAN WALL TEMP(MAIN) [°C]',

'Tank 3 - IS PORT SIDE WALL TEMP(MAIN) - (HULL) [°C]',

'Tank 4 - IS BTM AFT MID TEMP(MAIN) [°C]',

'Tank 4 - IS BTM MIDDLE TEMP(MAIN) [°C]',

'Tank 4 - IS PORT LOW CHAM TEMP(MAIN) [°C]',

'Tank 4 - IS PORT SIDE WALL TEMP(MAIN) [°C]',

'Tank 4 - IS PORT UPP CHAM TEMP(MAIN) [°C]',

'Tank 4 - IS CEIL TEMP(MAIN) [°C]',

'Tank 4 - IS AFT TRAN WALL TEMP(MAIN) [°C]',

'Tank 4 - IS FWD TRAN WALL TEMP(MAIN) [°C]',

'Tank 4 - IS PORT SIDE WALL TEMP(MAIN) - (HULL) [°C]',

```
# COFFERDAM temperatures — very detailed structural measurements, with negligible impact on charterer experience
'1 COFFERDAM AFT MIDDLE TEMP  [°C]',
'1 COFFERDAM AFT STBD UPPER TEMP [°C]',
'1 COFFERDAM AFT PORT LOWER TEMP  [°C]',
'2 COFFERDAM FWD UPPER TEMP  [°C]',
'3 COFFERDAM AFT LOWER TEMP  [°C]',
'4 COFFERDAM FWD LOWER TEMP  [°C]',
'5 COFFERDAM FWD PORT UPPER TEMP [°C]',

# Spray and cargo pump sensor readings — very detailed operational metrics that don’t directly impact satisfaction
'Tank 1 - Spraying Pump - CURRENT [A]',
'Tank 1 - Cargo Pump 1 - DISCH PRESS [bar]',
'Tank 1 - Cargo Pump 2 - DISCH V/V [%]',
'Tank 2 - Spraying Pump - CURRENT [A]',
'Tank 2 - Cargo Pump 1 - DISCH PRESS [bar]',
'Tank 2 - Cargo Pump 2 - DISCH V/V [%]',
'Tank 3 - Spraying Pump - CURRENT [A]',
'Tank 3 - Cargo Pump 1 - DISCH PRESS [bar]',
'Tank 3 - Cargo Pump 2 - DISCH V/V [%]',
'Tank 4 - Spraying Pump - CURRENT [A]',
'Tank 4 - Cargo Pump 1 - DISCH PRESS [bar]',
'Tank 4 - Cargo Pump 2 - DISCH V/V [%]',

# Internal valve settings and pressures — technical parameters with limited external relevance
'Tank 1 - IBS SUPPLY  V/V [%]',
'Tank 1 - IBS EXHAUST  V/V [%]',
'Tank 1 - IS PRESSURE [mbar]',
'Tank 1 - IS SUPPLY  V/V [%]',
```

'Tank 1 - IS EXHAUST V/V [%]',

'Tank 1 - N2 differential IBS/IS [mbar]',

'Tank 2 - IBS SUPPLY V/V [%]',

'Tank 2 - IBS EXHAUST V/V [%]',

'Tank 2 - IS PRESSURE [mbar]',

'Tank 2 - IS SUPPLY V/V [%]',

'Tank 2 - IS EXHAUST V/V [%]',

'Tank 2 - N2 differential IBS/IS [mbar]',

'Tank 3 - IBS SUPPLY V/V [%]',

'Tank 3 - IBS EXHAUST V/V [%]',

'Tank 3 - IS PRESSURE [mbar]',

'Tank 3 - IS SUPPLY V/V [%]',

'Tank 3 - IS EXHAUST V/V [%]',

'Tank 3 - N2 differential IBS/IS [mbar]',

'Tank 4 - IBS SUPPLY V/V [%]',

'Tank 4 - IBS EXHAUST V/V [%]',

'Tank 4 - IS PRESSURE [mbar]',

'Tank 4 - IS SUPPLY V/V [%]',

'Tank 4 - IS EXHAUST V/V [%]',

'Tank 4 - N2 differential IBS/IS [mbar]',

Compressor diagnostic details — maintenance info unlikely to impact charterer satisfaction

'LD compressor 1 - L.O FILTER DIFF PRESS [bar]',

'LD compressor 2 - L.O FILTER DIFF PRESS [bar]',

'HD compressor 1 - IGV POSITION [%]',

'HD compressor 1 - Orifice Plate Diffrencial Press [mbar]',

'HD compressor 2 - OUTLET TEMP A [°C].1',

'HD compressor 2 - OUTLET TEMP B [°C]',

'HD compressor 2 - L.O FILTER DIFF PRESS [bar]',

'HD compressor 2 - IGV POSITION [%]',

'HD compressor 2 - Orifice Plate Diffrencial Press [mbar]',

```
    # Vaporizer raw input/output pressures and temps — very technical
    'FORCING Vaporizer - OUTLET PRESS [barg*100]',
    'LNG Vaporizer - OUTLET TEMP [°C]',
    'LNG Vaporizer - INLET TEMP [°C]',

    # System fault flags — binary indicators better used as event markers, less for continuous
satisfaction prediction
    'NO.1 N2 GEN SYSTEM FAULT [True/False]',
    'NO.2 N2 GEN SYSTEM FAULT [True/False]',

    # Duplicate or less meaningful boil-off gas measurements — redundant when totals are
present
    'ME1 BOG [MT/day]',
    'ME2 BOG [MT/day]',
    'ME1 HFO [MT/d]',
    'ME2 HFO [MT/d]',
    'ME1 MGO/MDO [MT/d]',
    'ME2 MGO/MDO [MT/d]',

    # Newly added columns to drop — variables with high missing data or less direct impact
on satisfaction
    'Relative wind speed [m/s]',
    'Relative wind direction [°]',
    'DG Total BOG [MT]',
    'DG Total HFO [MT]',
    'DG Total MGO/MDO [MT]',
    'Ambient air pressure [mbar]',
    'Ambient air temperature [°C]',
    'Seawater temperature [°C]',
    'ME BOG [MT]',
    'ME HFO [MT]',
```

```
'ME MGO/MDO [MT]',
'DG Port HFO [MT/day]',
'DG Port MGO/MDO [MT/day]',
'DG STBD HFO [MT/day]',
'DG STBD MGO/MDO [MT/day]',
'Total BOG consumption [MT/day]',
'Total NBOG [MT/day]',
'Forced boil-off [MT/day]',
'BOG to ME [MT/day]',
'BOG to AUX [MT/day]',
'LBOG [MT/day]',

# Newly added based on your input
'DG1 BOG [MT/day]',
'DG2 BOG [MT/day]',
'DG3 BOG [MT/day]',
'DG4 BOG [MT/day]',
'Impacts tank 1 []',
'Impacts tank 2 []',
'Impacts tank 3 []',
'Impacts tank 4 []',
'Impact alarm critical threshold [Impact/min]',
'Impact alarm warning threshold [Impact/min]',
'Impacts per minute tank 1 [Impact/min]',
'Impact alarm tank 1 []',
'Impacts per minute tank 2 [Impact/min]',
'Impact alarm tank 2 []',
'Impacts per minute tank 3 [Impact/min]',
'Impact alarm tank 3 []',
'Impacts per minute tank 4 [Impact/min]',
'Impact alarm tank 4 []',
'Tank 1 - Liquid temp TOP [°C]',
```

'Tank 1 - Liquid temp 95% [°C]',

'Tank 1 - Liquid temp 60% [°C]',

'Tank 1 - Liquid temp 30% [°C]',

'Tank 1 - Liquid temp BTM [°C]',

'Tank 2 - Liquid temp TOP [°C]',

'Tank 2 - Liquid temp 95% [°C]',

'Tank 2 - Liquid temp 60% [°C]',

'Tank 2 - Liquid temp 30% [°C]',

'Tank 2 - Liquid temp BTM [°C]',

'Tank 3 - Liquid temp TOP [°C]',

'Tank 3 - Liquid temp 95% [°C]',

'Tank 3 - Liquid temp 60% [°C]',

'Tank 3 - Liquid temp 30% [°C]',

'Tank 3 - Liquid temp BTM [°C]',

'Tank 4 - Liquid temp TOP [°C]',

'Tank 4 - Liquid temp 95% [°C]',

'Tank 4 - Liquid temp 60% [°C]',

'Tank 4 - Liquid temp 30% [°C]',

'Tank 4 - Liquid temp BTM [°C]',

'Tank 1 - TK TRUNK DK AFT TEMP [°C]',

'Tank 1 - TK TRUNK DK MIDDLE TEMP [°C]',

'Tank 1 - TK PIPE DUCT AFT TEMP [°C]',

'Tank 1 - TK PIPE DUCT MIDDLE TEMP [°C]',

'Tank 1 - IBS PRESSURE [mbar]',

'Tank 2 - TK TRUNK DK AFT TEMP [°C]',

'Tank 2 - TK TRUNK DK MIDDLE TEMP [°C]',

'Tank 2 - TK PIPE DUCT AFT TEMP [°C]',

'Tank 2 - TK PIPE DUCT MIDDLE TEMP [°C]',

'Tank 2 - IBS PRESSURE [mbar]',

'Tank 3 - TK TRUNK DK AFT TEMP [°C]',

'Tank 3 - TK TRUNK DK MIDDLE TEMP [°C]',

'Tank 3 - TK PIPE DUCT AFT TEMP [°C]',

'Tank 3 - TK PIPE DUCT MIDDLE TEMP [°C]',

'Tank 3 - IBS PRESSURE [mbar]',

'Tank 4 - TK TRUNK DK AFT TEMP [°C]',

'Tank 4 - TK TRUNK DK MIDDLE TEMP [°C]',

'Tank 4 - TK PIPE DUCT AFT TEMP [°C]',

'Tank 4 - TK PIPE DUCT MIDDLE TEMP [°C]',

'Tank 4 - IBS PRESSURE [mbar]',

'Tank 1 - Cargo Pump 1 - CURRENT [A]',

'Tank 1 - Cargo Pump 1 - DISCH V/V [%]',

'Tank 1 - Cargo Pump 2 - CURRENT [A]',

'Tank 1 - Cargo Pump 2 - DISCH PRESS [bar]',

'Tank 1 - Spraying Pump - DISCH PRESS [bar]',

'Tank 1 - Spraying Pump - DISCH V/V [%]',

'Tank 2 - Cargo Pump 1 - CURRENT [A]',

'Tank 2 - Cargo Pump 1 - DISCH V/V [%]',

'Tank 2 - Cargo Pump 2 - CURRENT [A]',

'Tank 2 - Cargo Pump 2 - DISCH PRESS [bar]',

'Tank 2 - Spraying Pump - DISCH PRESS [bar]',

'Tank 2 - Spraying Pump - DISCH V/V [%]',

'Tank 3 - Cargo Pump 1 - CURRENT [A]',

'Tank 3 - Cargo Pump 1 - DISCH V/V [%]',

'Tank 3 - Cargo Pump 2 - CURRENT [A]',

'Tank 3 - Cargo Pump 2 - DISCH PRESS [bar]',

'Tank 3 - Spraying Pump - DISCH PRESS [bar]',

'Tank 3 - Spraying Pump - DISCH V/V [%]',

'Tank 4 - Cargo Pump 1 - CURRENT [A]',

'Tank 4 - Cargo Pump 1 - DISCH V/V [%]',

'Tank 4 - Cargo Pump 2 - CURRENT [A]',

'Tank 4 - Cargo Pump 2 - DISCH PRESS [bar]',

'Tank 4 - Spraying Pump - DISCH PRESS [bar]',

'Tank 4 - Spraying Pump - DISCH V/V [%]',

'LD compressor 2 - INLET PRESS [bara]',

'LD compressor 2 - OUTLET PRESS [barg]',

'LD compressor 2 - INLET TEMP [°C]',

'LD compressor 2 - OUTLET TEMP A [°C]',

'HD compressor 2 - INLET PRESS [bar]',

'HD compressor 2 - OUTLET PRESS [bar]',

'HD compressor 2 - INLET TEMP [°C].1',

'Tank 1 - Spray Inlet temperature [°C]',

'Tank 2 - Spray Inlet temperature [°C]',

'Tank 3 - Spray Inlet temperature [°C]',

'Tank 4 - Spray Inlet temperature [°C]',

'1 COFFERDAM AFT PORT UPPER TEMP [°C]',

'1 COFFERDAM AFT STBD LOWER TEMP [°C]',

'2 COFFERDAM FWD MIDDLE TEMP [°C]',

'2 COFFERDAM FWD LOWER TEMP [°C]',

'2 COFFERDAM AFT UPPER TEMP [°C]',

'2 COFFERDAM AFT MIDDLE TEMP [°C]',

'2 COFFERDAM AFT LOWER TEMP [°C]',

'3 COFFERDAM FWD UPPER TEMP [°C]',

'3 COFFERDAM FWD MIDDLE TEMP [°C]',

'3 COFFERDAM FWD LOWER TEMP [°C]',

'3 COFFERDAM AFT UPPER TEMP [°C]',

'3 COFFERDAM AFT MIDDLE TEMP [°C]',

'4 COFFERDAM FWD UPPER TEMP [°C]',

'4 COFFERDAM FWD MIDDLE TEMP [°C]',

'4 COFFERDAM AFT UPPER TEMP [°C]',

'4 COFFERDAM AFT MIDDLE TEMP [°C]',

'4 COFFERDAM AFT LOWER TEMP [°C]',

'5 COFFERDAM FWD MIDDLE TEMP [°C]',

'5 COFFERDAM FWD STBD UPPER TEMP [°C]',

'5 COFFERDAM FWD PORT LOWER TEMP [°C]',

'5 COFFERDAM FWD STBD LOWER TEMP [°C]',

```
    'NO.1 N2 GENERATOR PRODUCT DEW POINT [°C]',
    'NO.2 N2 GENERATOR PRODUCT DEW POINT [°C]',
]
len(columns_to_drop)
```

Code Cell 6

```
# Keep only the columns that are in both the DataFrame and the columns_to_drop list
existing_columns_to_drop = [col for col in columns_to_drop if col in df_vessel_1.columns]

# Drop those features
df_vessel_1.drop(columns=existing_columns_to_drop, inplace=True)
```

Code Cell 7

```
#Print the first 5 rows of the database

df_vessel_1.head()
```

Code Cell 8

```
#final_columns = df_vessel_1.columns.tolist()
for col in final_columns:
    print(col)
```

Code Cell 9

```
# missing values percentage per feature in list format
missing_values = df_vessel_1_merged.isnull().sum()
missing_percentage = (missing_values / len(df_vessel_1_merged)) * 100
print("Missing values percentage per feature in the merged dataset:")
for column, percentage in missing_percentage.items():
    print(f"- {column}: {percentage:.2f}%")
```

Code Cell 10

```
# Calculate skewness of numeric features
skewness = df_vessel_1_merged.skew(numeric_only=True).sort_values()
def interpret_skew(value):
    if -0.5 <= value <= 0.5:
        return "Approximately symmetric → Use mean"
```

```
    elif -1 < value < -0.5 or 0.5 < value < 1:
        return "Moderately skewed → Prefer median"
    else:
        return "Highly skewed → Definitely use median"

# Create DataFrame with skewness and interpretation
skew_df_vessel_1 = pd.DataFrame({'Skewness': skewness})
skew_df_vessel_1['Interpretation'] = skew_df_vessel_1['Skewness'].apply(interpret_skew)
# Save to Excel file
skew_df_vessel_1.to_excel(
    r"C:/UsageIQ/Vessel_1_Vessel_Skewness_Report.xlsx",
    sheet_name='Skewness Analysis',
    index=True
)
```

Code Cell 11

```
df_vessel_1_imputed = df_vessel_1_merged.copy()

# Loop through skew_df and apply appropriate imputation
for col in skew_df_vessel_1.index:
    if df_vessel_1_imputed[col].isna().any():  # Only impute if missing values exist
        interpretation = skew_df_vessel_1.loc[col, 'Interpretation']

        if "Use mean" in interpretation:
            impute_value = df_vessel_1_imputed[col].mean()
        else:  # For both "Prefer median" and "Definitely use median"
            impute_value = df_vessel_1_imputed[col].median()

        # Correct way to assign the filled column
        df_vessel_1_imputed[col] = df_vessel_1_imputed[col].fillna(impute_value)

df_vessel_1_imputed['Total consumption'] = df_vessel_1_imputed[['DG consumed [MT]',
```

```
'ME consumed [MT]']].sum(axis=1)
df_vessel_1_imputed.to_csv('C:/UsageIQ/df_vessel_1_imputed.csv', index=False)
```

Code Cell 12

```
from sklearn.cross_decomposition import PLSRegression
from sklearn.decomposition import PCA
target_col = "Total consumption"
output_file = "C:/UsageIQ/vessel_1_vessel_pca_pls_correlation_analysis.xlsx"
X = df_vessel_1_imputed.drop(columns=[target_col])
X_num = X.select_dtypes(include='number')
y = df_vessel_1_imputed[target_col]
# ================================
# 4. Full Correlation Matrix
# ================================
correlation_matrix = df_vessel_1_imputed.corr(numeric_only=True)
with pd.ExcelWriter(output_file) as writer:
    correlation_df.to_excel(writer, sheet_name="Correlation with Target")
    pls_coefficients.to_excel(writer, sheet_name="PLS Coefficients")
    pca_loadings.to_excel(writer, sheet_name="PCA Loadings")
    correlation_matrix.to_excel(writer, sheet_name="Correlation Matrix")
print(f"Analysis saved to: {output_file}")
```

Code Cell 13

```
import numpy as np
# Copy the original imputed DataFrame
df = df_vessel_1_imputed.copy()
df['SwellPeriod'] = df['SwellPeriod'].replace(0, df['SwellPeriod'].median())

# --- Derived Features ---

# Average Draft Mid
df['Average Draft Mid [m]'] = df[['Draft mid portside [m]', 'Draft mid starboard
[m]']].mean(axis=1)
```

```
# Draft ratio (portside divided by starboard)
df['Draft Ratio Port to Starboard'] = df['Draft mid portside [m]'] / df['Draft mid starboard [m]']

# Total DG Power [kW]
dg_power_cols = ['DG1 Power [kW]', 'DG2 Power [kW]', 'DG3 Power [kW]', 'DG4 Power
[kW]']
df['Total DG Power [kW]'] = df[dg_power_cols].sum(axis=1)

# Total DG Energy [kWh]
dg_energy_cols = ['DG1 energy production [kWh]', 'DG2 energy production [kWh]',
               'DG3 energy production [kWh]', 'DG4 energy production [kWh]']
df['Total DG Energy [kWh]'] = df[dg_energy_cols].sum(axis=1)

# 4. Total ME Torque [knm]
df['Total ME Torque [knm]'] = df[['ME1 Torque [knm]', 'ME2 Torque [knm]']].sum(axis=1)

# 5. Total ME Shaft Power [kW]
df['Total ME Shaft Power [kW]'] = df[['ME1 Shaft Power [kW]', 'ME2 Shaft Power
[kW]']].sum(axis=1)

# 6. Average ME RPM [rpm]
df['Average ME RPM [rpm]'] = df[['ME1 RPM [rpm]', 'ME2 RPM [rpm]']].mean(axis=1)

# 7. Swell Steepness = Height / Period
df['Swell Steepness [m/s]'] = df['SwellHeight'] / df['SwellPeriod'].replace(0, np.nan)

# --- Final Feature List ---

selected_features = [
    'ShipName', 'DateTime',
    'Total consumption',
```

```
    'Draft fore [m]', 'Draft aft [m]', 'Average Draft Mid [m]',
    'GPS speed [knots]', 'Shaft power [kW]', 'Shaft rpm [rpm]',
    'Total DG Power [kW]', 'Total DG Energy [kWh]',
    'ME running hours [h]', 'Total ME Torque [knm]',
    'Total ME Shaft Power [kW]', 'Average ME RPM [rpm]',
    'WindSpeed', 'WindWavePeriod', 'WindWaveHeight', 'CurrentSpeed',
    'AirTemperatureSL', 'WaterTemperatureSL', 'AirPressureSL',
    'BOG to GCU [kg/h]', 'Reliquefaction - Electrical consumption [kW]',
    'SwellHeight', 'SwellPeriod', 'Swell Steepness [m/s]',

    'Roll average [°]',
    'Pitch average [°]',
    'Yaw average [°]',
    'Total impacts all tanks []',
    'Roll max starboard (Sloshield) [°]',
    'Pitch max fore (Sloshield) [°]',
    'Roll avarage (Sloshield) [°]',
    'Pitch avarage (Sloshield) [°]',
    'Tank 1 - Liquid Volume [m^3]',
    'Tank 2 - Liquid Volume [m^3]',
    'Tank 3 - Liquid Volume [m^3]',
    'Tank 4 - Liquid Volume [m^3]'
]
# Filter final dataset
df_vessel_1_final = df[selected_features]
```

Code Cell 14

```
df_vessel_1_final = df_vessel_1_final.copy()

# Replace 0 in WindWavePeriod with the median
df_vessel_1_final['WindWavePeriod'] = df_vessel_1_final['WindWavePeriod'].replace(
    0, df_vessel_1_final['WindWavePeriod'].median()
```

```
)

# Calculate WaveSteepness
df_vessel_1_final['WaveSteepness'] = (
    df_vessel_1_final['WindWaveHeight'] / df_vessel_1_final['WindWavePeriod']
)

# Calculate TotalLiquidVolume
df_vessel_1_final['TotalLiquidVolume'] = (
    df_vessel_1_final['Tank 1 - Liquid Volume [m^3]'] +
    df_vessel_1_final['Tank 2 - Liquid Volume [m^3]'] +
    df_vessel_1_final['Tank 3 - Liquid Volume [m^3]'] +
    df_vessel_1_final['Tank 4 - Liquid Volume [m^3]']
)
```

Code Cell 15

```
# Add VesselCondition based on TotalLiquidVolume
df_vessel_1_final['VesselCondition'] = np.where(
    df_vessel_1_final['TotalLiquidVolume'] < 15000,
    'Ballast',
    'Laden'
)
```

Code Cell 16

```
final_features = [
    "ShipName",
    "DateTime",
    "Average Draft Mid [m]",
    "GPS speed [knots]",
    "Shaft power [kW]",
    "Shaft rpm [rpm]",
    "Total DG Power [kW]",
    "Total ME Torque [knm]",
```

```
    "Total ME Shaft Power [kW]",
    "Average ME RPM [rpm]",
    "WindSpeed",
    "CurrentSpeed",
    "WaterTemperatureSL",
    "BOG to GCU [kg/h]",
    "Reliquefaction - Electrical consumption [kW]",
    "Swell Steepness [m/s]",
    "Roll max starboard (Sloshield) [°]",
    "WaveSteepness",        # Engineered: WindWaveHeight / WindWavePeriod (period median
used for 0)
    "TotalLiquidVolume",     # Engineered: sum of tanks 1 to 4 volume
    "VesselCondition", # Engineered: 'Ballast' if TotalLiquidVolume < 15000 else 'Laden'
    "Total consumption"
]
df_vessel_1_final = df_vessel_1_final[final_features]
```

Code Cell 17

```
# Export to Excel
excel_path = r"C:\UsageIQ\df_vessel_1_final.xlsx"
df_vessel_1_final.to_excel(excel_path, index=False)
```

Code Cell 18

```
# Copy your cleaned DataFrame
df = df_vessel_1_final.copy()
# Filter rows where GPS speed >= 5
df = df[df['GPS speed [knots]'] >= 6].copy()
```

Code Cell 19

```
unseen_indices = []
# Loop through each VesselCondition group
for condition, group in df.groupby('VesselCondition'):
    sample_size = max(1, int(len(group) * 0.10))  # 10% of group, at least 1
    unseen_sample = group.sample(n=sample_size, random_state=42)
```

```
    # Save the 10% unseen data per group to an Excel file
    filename = f"C:/UsageIQ/vessel_1_unseen_{condition}.xlsx"
    unseen_sample.to_excel(filename, index=False)
    print(f"Saved unseen data for '{condition}' to {filename}")

    unseen_indices.extend(unseen_sample.index)

# Create train/test dataset by dropping unseen indices
df_vessel_1_train_test = df.drop(unseen_indices)

# Save combined train/test dataset
df_vessel_1_train_test.to_excel("C:/UsageIQ/vessel_1_train_test_data.xlsx", index=False)
print("Saved combined train/test data to train_test_data.xlsx")
```

Code Cell 20

```
import numpy as np
from sklearn.model_selection import train_test_split
from sklearn.linear_model import LinearRegression, Lasso
from sklearn.ensemble import RandomForestRegressor, GradientBoostingRegressor,
AdaBoostRegressor, HistGradientBoostingRegressor
from sklearn.metrics import mean_squared_error, R²_score, mean_absolute_error
from lightgbm import LGBMRegressor
from xgboost import XGBRegressor

# ==== Define target and features ====
target_column = "Total consumption"
exclude_cols = ["ShipName", "DateTime", "BOG to GCU [kg/h]", "TotalLiquidVolume",
"VesselCondition"]

X = df_vessel_1_train_test.drop(columns=[target_column] + exclude_cols, errors='ignore')
y = df_vessel_1_train_test[target_column]
```

```
X.columns = X.columns.str.replace(r"[\[\]<>]", "", regex=True)

# ==== Split data ====
X_train, X_test, y_train, y_test = train_test_split(X, y, test_size=0.2, random_state=42)

# ==== Define models ====
models = {
    "Linear Regression": LinearRegression(),
    "Lasso": Lasso(alpha=0.1),
    "Random Forest": RandomForestRegressor(n_estimators=200, random_state=42),
    "Gradient Boosting": GradientBoostingRegressor(random_state=42),
    "AdaBoost": AdaBoostRegressor(random_state=42),
    "XGBoost": XGBRegressor(random_state=42),
    "Hist Gradient Boosting": HistGradientBoostingRegressor(random_state=42),
    "Light GBM": LGBMRegressor(random_state=42)
}
# ==== Evaluate models on both train and test sets ====
all_results = []

for name, model in models.items():
    model.fit(X_train, y_train)

    # Training scores
    train_preds = model.predict(X_train)
    all_results.append({
        "Model": name,
        "Dataset": "Training (80%)",
        "MAE": mean_absolute_error(y_train, train_preds),
        "RMSE": np.sqrt(mean_squared_error(y_train, train_preds)),
        "R²": R²_score(y_train, train_preds)
    })
```

```
    # Testing scores
    test_preds = model.predict(X_test)
    all_results.append({
        "Model": name,
        "Dataset": "Testing (20%)",
        "MAE": mean_absolute_error(y_test, test_preds),
        "RMSE": np.sqrt(mean_squared_error(y_test, test_preds)),
        "R²": R²_score(y_test, test_preds)
    })

# ==== Convert to DataFrame ====
evaluation_df = pd.DataFrame(all_results)

# Optional: round values for neatness
evaluation_df["MAE"] = evaluation_df["MAE"].round(3)
evaluation_df["RMSE"] = evaluation_df["RMSE"].round(3)
evaluation_df["R²"] = evaluation_df["R²"].round(3)

# ==== Save to Excel  ====
output_path = "C:/UsageIQ/vessel_1_model_evaluation_results_all_models.xlsx"
evaluation_df.to_excel(output_path, index=False)

print("\n Model evaluation completed — scores saved to:", output_path)
```

Code Cell 20

```
# Tuning RandomForest Model
from sklearn.model_selection import RandomizedSearchCV

param_grid = {
    'n_estimators': [200, 500, 800],
    'max_depth': [None, 10, 20, 40],
```

```
    'min_samples_split': [2, 5, 10],
    'min_samples_leaf': [1, 2, 4],
    'max_features': ['sqrt', 'log2', None]
}
search = RandomizedSearchCV(
    RandomForestRegressor(random_state=42),
    param_distributions=param_grid,
    n_iter=20,
    scoring='R²',
    cv=5,
    n_jobs=-1
)

search.fit(X_train, y_train)
best_rf = search.best_estimator_
best_rf
```

Code Cell 21

```
# ==== Train tuned RandomForest ====
best_model = RandomForestRegressor(
    n_estimators=200,
    max_depth=40,
    max_features='sqrt',
    min_samples_leaf=2,
    random_state=42
)
best_model.fit(X_train, y_train)

# ==== Evaluate on training set ====
train_preds = best_model.predict(X_train)
train_rmse = np.sqrt(mean_squared_error(y_train, train_preds))
train_R² = R²_score(y_train, train_preds)
```

```
train_mae = mean_absolute_error(y_train, train_preds)

# ==== Evaluate on testing set ====
test_preds = best_model.predict(X_test)
test_rmse = np.sqrt(mean_squared_error(y_test, test_preds))
test_R² = R²_score(y_test, test_preds)
test_mae = mean_absolute_error(y_test, test_preds)

# ==== Create a single DataFrame for Excel export ====
scores_df = pd.DataFrame([
    {
        "Model": "Random Forest (Tuned)",
        "Dataset": "Training (80%)",
        "RMSE": train_rmse,
        "R²": train_R²,
        "MAE": train_mae
    },
    {
        "Model": "Random Forest (Tuned)",
        "Dataset": "Testing (20%)",
        "RMSE": test_rmse,
        "R²": test_R²,
        "MAE": test_mae
    }
])

# ==== Save scores to Excel ====
scores_path = "C:/UsageIQ/vessel_1_model_scores_tuned_random_forest.xlsx"
scores_df.to_excel(scores_path, index=False)

# ==== Print results nicely ====
print("\n=== Random Forest (Tuned) Scores ===")
```

```
print(scores_df)

print(f"\n Model tuned and evaluated — scores saved to: {scores_path}")

# ==== Save train predictions ====
train_results = X_train.copy()
train_results[target_column] = y_train
train_results[f"Predicted {target_column}"] = train_preds
train_results.to_excel("C:/UsageIQ/vessel_1_train_predictions_tuned_random_forest.xlsx",
index=False)

# ==== Save test predictions ====
test_results = X_test.copy()
test_results[target_column] = y_test
test_results[f"Predicted {target_column}"] = test_preds
test_results.to_excel("C:/UsageIQ/vessel_1_test_predictions_tuned_random_forest.xlsx",
index=False)

# ==== Unseen data predictions ====
for condition in ["Ballast", "Laden"]:
   file_path = f"C:/UsageIQ/vessel_1_unseen_{condition}.xlsx"
   unseen_df = pd.read_excel(file_path)

   X_unseen = unseen_df.drop(columns=[target_column] + exclude_cols, errors='ignore')
   X_unseen.columns = X_unseen.columns.str.replace(r"[\[\]<>]", "", regex=True)

   unseen_df[f"Predicted {target_column}"] = best_model.predict(X_unseen)

unseen_df.to_excel(f"C:/UsageIQ/vessel_1_unseen_{condition}_predictions_tuned_random_
forest.xlsx", index=False)

print("\n Predictions saved to C:/UsageIQ/")
```

Appendix 18 - Interviews for CSI Sensitivity analysis

Section 1: Interviews background

The following demographic and professional data were collected to contextualize responses and ensure analytical validity:

- **Position / Title: ___________________________**
- **Functional Role:** ☐ Operational ☐ Commercial ☐ Managerial
- **Sector / Industry: _________________________**
- **Years of Professional Experience: __________**
- **Operational Context:** ☐ Office-based ☐ On-board

Section 2: Customer Satisfaction Index (CSI) Classification

This categorical approach enables comparative analysis across satisfaction levels and CSI Score Range

CSI Score Range	Very Low Satisfaction	Low Satisfaction	Moderate Satisfaction	High Satisfaction	Very High Satisfaction
0–100					
100–200					
200–300					
300–400					
400+					

Section 3: Fuel Consumption Prediction Accuracy

This classification allows for direct linkage between predictive performance and CSI outcomes.

Prediction Error Range:

Prediction Error Range	**Highly Accurate**	**Acceptable Accuracy**	**Low Accuracy**	**Poor Accuracy**
0%–3%				
3%–6%				
6%–9%				
Above 9%				

Appendix 19 - CSI Sensitivity Analysis Results

Section 1: Respondent Background

The interviewers mainly come from long and practical experience in the shipping industry. Most have worked as ship captains, in office-based and on board roles. A smaller number have commercial and management backgrounds, which adds experience in business market. Together, this shows a well-experienced and balanced interview participant matrix.

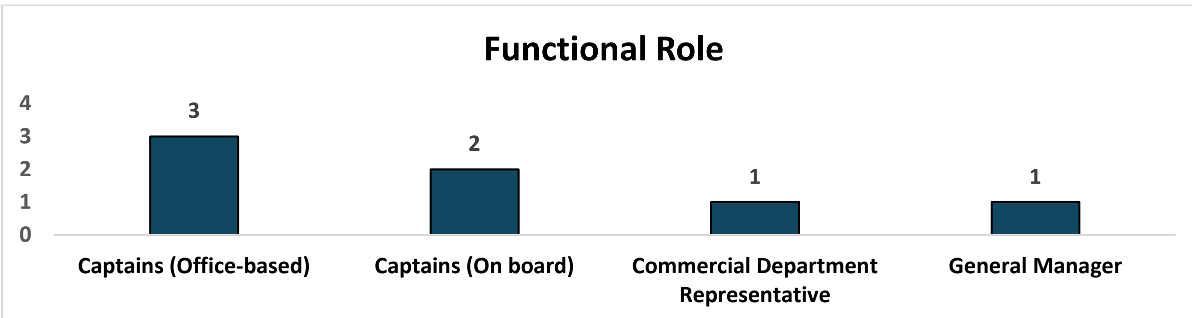

Section 2: Summary of CSI Score Range Classification

The Customer Satisfaction Index (CSI) is categorized into five distinct satisfaction levels based on score ranges. Scores above 400 represent Very High Satisfaction, indicating exceptional customer experience and strong approval. Scores between 300 and 400 correspond to High Satisfaction, reflecting consistently positive customer perceptions. A CSI range of 200 to 300 indicates Moderate Satisfaction, where customer expectations are generally met but with room for improvement. Scores between 100 and 200 fall under Low Satisfaction, suggesting noticeable dissatisfaction and service gaps. Finally, CSI scores ranging from 0 to 100 indicate Very Low Satisfaction, highlighting critical service or performance issues requiring immediate attention.

CSI Score Range	Very Low Satisfaction	Low Satisfaction	Moderate Satisfaction	High Satisfaction	Very High Satisfaction
0–100					**X**
100–200				**X**	
200–300			**X**		
300–400		**X**			
400+	**X**				

Section 3: Summary of Fuel Consumption Prediction Accuracy Classification

Fuel consumption prediction accuracy is categorized into four levels based on the magnitude of prediction error. An error range of 0%–3% is classified as Highly Accurate, indicating strong predictive reliability and minimal deviation from actual fuel usage. Errors between 3% and 6% fall under Acceptable Accuracy, reflecting reasonable performance with minor discrepancies. A prediction error range of 6%–10% is considered Low Accuracy, suggesting noticeable deviations that may affect user confidence. Errors above 10% are classified as Poor Accuracy, indicating unreliable predictions that can significantly undermine trust and satisfaction.

Prediction Error Range	Highly Accurate	Acceptable Accuracy	Low Accuracy	Poor Accuracy
0%–3%	**X**			
3%–6%		**X**		
6%–10%			**X**	
Above 10%				**X**

A. References

Abebe, M. et al., 2020. Machine learning approaches for ship speed prediction towards energy efficient shipping. *Applied Sciences,* 10(7), p. 2325.

Abreu, L. et al., 2023. A decision tree model for the prediction of the stay time of ships in Brazilian ports. *Engineering Applications of Artificial Intelligence,* Volume 117, p. 105634.

Academia.edu, 2024. *Academia.edu.* [Online] Available at: https://www.academia.edu/ [Accessed 2025 October 2025].

Adamczyk, S., Kotowicz, D., Stępień, M. & Bartnik, W., 2020. Liquefied natural gas in mobile applications—opportunities and challenges. *Energies,* Volume 13`21, p. 5673.

Adekoya, O. O. et al., 2024. Technological innovations in the LNG sector: A review: Assessing recent advancements and their impact on LNG production, transportation and usage. *World Journal of Advanced Research and Reviews,* Volume 21, p. 40–057.

Ahlgren, F., Mondejar, M. & Thern, M., 2019. Predicting dynamic fuel oil consumption on ships with automated machine learning.. *Energy Procedia,* Volume 158, pp. 6126-6131.

Ahmed, S., Li, T., Yi, P. & Chen, R., 2023. Environmental impact assessment of green ammonia-powered very large tanker ship for decarbonized future shipping operations. *Renew. Sustain. Energy Rev.,* Volume 188, p. 113774.

Ajayi, F. A. & Udeh, C. A., 2024. A comprehensive review of talent management strategies for seafarers: Challenges and opportunities. *International Journal of Science and Research Archive,* Volume 11, p. 1116–1131.

Aladwan, Z., 2020. Dual Nationality of the Ships and its Legal Impact. *Hasanuddin Law Rev.,* Volume 6, p. 109.

Aldrich, C., 2020. Process variable importance analysis by use of random forests in a Shapley regression framework. *Minerals,* Volume 10, p. 420.

Algieri, B., Aquino, A. & Succurro, M., 2022. Trade specialisation and changing patterns of comparative advantages in manufactured goods. *Italian Economic Journal,* 8(3), pp. 607-67.

Argyriou, A. S., 2023. Tanker fleet of Greece: strategy development in the conditions of sanctions against Russia-through a practice lens. *Journal of European Economy,* Volume 22, p. 375–400.

Aseel, S. et al., 2021. A model for estimating the carbon footprint of maritime transportation of liquefied natural gas under uncertainty. *Sustainable Production and Consumption,* Volume 27, p. 1602–161.

Assimenos, N., 2017. Commercial Operations Management. In: *Shipping Operations Management.* Cham: Springer International Publishing, p. 47–71.

Atieh, A. T., 2021. The next generation cloud technologies: a review on distributed cloud, fog and edge computing and their opportunities and challenges. *ResearchBerg Review of Science and Technology,* Volume 1, p. 1–15.

Baressi Šegota, S. et al., 2020. Frigate speed estimation using CODLAG propulsion system parameters and multilayer perceptron. *Nase More,* Volume 67, p. 117–125.

Bassam, A., Phillips, A., T. S. & Wilson, P., 2023. Artificial neural network based prediction of ship speed under operating conditions for operational optimization.. *Ocean Engineering,* Volume 278, , p. 114613.

Bassam, A., Phillips, A., Turnock, S. & Wilson, P., 2022. Ship speed prediction based on machine learning for efficient shipping operation. *Ocean Engineering,* Volume 245, p. 110449.

Beşikçi, E., Arslan, O., Turan, O. & Ölçer, A., 2016. An artificial neural network based decision support system for energy efficient ship operations.. *Computers & operations research,* Volume 66, pp. 393-401.

Bialystocki, N. & Konovessis, D., 2016. On the estimation of ship's fuel consumption and speed curve: A statistical approach. *J. Ocean Eng. Sci.,* Volume 1, p. 157–166.

Bicer, Y. & Dincer, I., 2018. Clean fuel options with hydrogen for sea transportation: A life cycle approach. *Int. J. Hydrogen Energy,* Volume 43, p. 1179–1193.

Botão, R. P., De Medeiros Costa, H. K. & Dos Santos, E. M., 2023. *Global gas and LNG markets: Demand, supply dynamics, and implications for the future,* s.l.: s.n.

Bouman, E., Lindstad, E., Rialland, A. & Strømman, A., 2020. Maritime Transport in a Life Cycle Perspective How Fuels, Vessel Types, and Operational Profiles Influence Energy Demand and Greenhouse Gas Emissions. *Energies,* 13(11), p. 27394.

Brandsæter, A. & Vanem, E., 2018. Ship speed prediction based on full scale sensor measurements of shaft thrust and environmental conditions. *Ocean Eng.,* Volume 162, p. 316–330.

Bui-Duy, L. & Vu-Thi-Minh, N., 2021. Utilization of a deep learning-based fuel consumption model in choosing a liner shipping route for container ships in Asia.. *The Asian Journal of Shipping and Logistics,* 37(1), pp. 1-11.

Cai, J. et al., 2024. Method for identification of aberrations in operational data of maritime vessels and sources investigation. *Sensors (Basel),* Volume 24.

Cepowski, T. & Chorab, P., 2021. The use of artificial neural networks to determine the engine power and fuel consumption of modern bulk carriers, tankers and container ships. *Energies,* Volume 14, p. 4827.

Cepowski, T. & Drozd, A., 2023. Measurement-based relationships between container ship operating parameters and fuel consumption.. *Applied Energy,* Volume 347, p. 121315.

Chaal, M., 2018. Ship operational performance modelling for voyage optimization through fuel consumption minimization.

Caterina, A.K. and Efrata, T.C. (2026) 'Influence mediation quality logistics services, service costs, customer satisfaction, and dependencies to loyalty customers in the container shipping industry', *International Journal of Review Management Business and Entrepreneurship*, 6(1), pp. 119–133.

Chao, S.L., Lin, R.Y. and Sun, Y.H. (2019) 'Mediating effects of service recovery on liner shipping users', *Transport Policy*, 84, pp. 40–49.

Chao, S.L., Yu, M.M. and Wei, S.Y. (2024) 'Ascertaining the impact of e-service quality on e-loyalty for the e-commerce platform of liner shipping companies', *Transportation Research Part E: Logistics and Transportation Review*, 184, article 103491.

Chen, Z. S., Lam, J. S. L. & Xiao, Z., 2023. Prediction of harbour vessel fuel consumption based on machine learning approach. *Ocean Eng.,* Volume 278, p. 114483.

Clarksons, 2024. *Clarksons, Shipping Intelligence Network.* [Online] Available at: https://sin.clarksons.net/ [Accessed 1 May 2024].

Coraddu, A., Oneto, L., Baldi, F. & Anguita, D., 2017. Vessels fuel consumption forecast and trim optimisation: A data analytics perspective.. *Ocean Engineering,* Volume 130, pp. 351-370.

Coraddu, A. et al., 2019. Data-driven ship digital twin for estimating the speed loss caused by the marine fouling. *Ocean Eng.,* Volume 186, p. 106063.

Cronshaw, M., 2021. *Energy in perspective.* 2021 ed. Cham(Switzerland): Springer Nature.

DeKeyser, S., Morobé, C. & Mittendorf, M., 2022. Towards improved prediction of ship performance: a comparative analysis on in-service ship monitoring data for modeling the speed-power relation.. *arXiv preprint arXiv:2212.13061.*

Dev, A. K. & Saha, M., 2021. *Weight estimation of marine propulsion and power generation machinery,* s.l.: s.n.

DNV, 2025. *FuelEU Maritime.* [Online] Available at: https://www.dnv.com/maritime/insights/topics/fueleu-maritime [Accessed 5 August 2025].

Dolzhenko, N. et al., 2025. Organization of Transport Services and Transport Process Safety. *Periodica Polytechnica Transportation Engineering*.

Domić, I., Stanivuk, T., Stazić, L. & Pavlović, I., 2022. Analysis of LNG carrier propulsion developments. *Istraz. Proj. Za Privredu,* Volume 20, p. 1122–1132.

Du, Y. et al., 2022. Data fusion and machine learning for ship fuel efficiency modeling: Part III – Sensor data and meteorological data. *Communications in Transportation Research,* Volume 2, p. 100072.

European Parliament and Council of European Union, 2003. *Directive 2003/87/EC of the European Parliament and of the Council of 13 October 2003 establishing a scheme for greenhouse gas emission allowance trading within the Community and amending Council Directive 96/61/EC,* s.l.: European Parliament and Council of the European Union.

European Parliament and Council of the European Union, 2015. *egulation (EU) 2015/757 of the European Parliament and of the Council of 29 April 2015 on the monitoring, reporting and verification of carbon dioxide emissions from maritime transport, and amending Directive 2009/16/EC. OJ L 123,* s.l.: European Parliament and Council of the European Union.

European Parliament and Council of the European Union, 2023. *egulation (EU) 2023/1805 of the European Parliament and of the Council of 13 September 2023 on the use of renewable and low-carbon fuels in maritime transport, and amending Directive 2009/16/EC (FuelEU Maritime),* s.l.: s.n.

Eyres, D. & Bruce, G., 2012. 23 - Liquefied gas carriers. In: 7th, ed. *Ship Construction..* s.l.:Oxford: Butterworth-Heinemann, pp. 279-289.

Fam, M. L., Tay, Z. Y. & Konovessis, D., 2022. An Artificial Neural Network for fuel efficiency analysis for cargo vessel operation. *Ocean Eng.,* Volume 264, p. 112437.

Fan, A. et al., 2020. A novel ship energy efficiency model considering random environmental parameters. *Journal of Marine Engineering & Technology,* 19(4), pp. 215-228.

Farag, Y. & Ölçer, A., 2020. The development of a ship performance model in varying operating conditions based on ANN and regression techniques.. *Ocean Engineering,* Volume 198, p. 106972.

Gabel-Shemueli, R., Westman, M., Chen, S. & Bahamonde, D., 2019. Does cultural intelligence increase work engagement? The role of idiocentrism-allocentrism and organizational culture in MNCs. *Cross Cult. Strateg. Manag.,* Volume 26, p. 46–66.

Gaslog Ltd., 2023. *ANNUAL REPORT PURSUANT TO SECTION 13 OR 15(d) OF THE SECURITIES EXCHANGE ACT OF 1934.* [Online]
Available at: https://www.gaslogltd.com/content/uploads/24-2242-1_GasLog-Ltd._20-F-AsFiled.pdf
[Accessed 1 May 2024].

Genç, Y. E., 2024. Competitive strategy and advantages. *J. Acc. Fin.,* Volume 24.

Gkerekos, C., Lazakis, I. & Theotokatos, G., 2019. Machine learning models for predicting ship main engine Fuel Oil Consumption: A comparative study. *Ocean Eng.,* Volume 188, p. 106282.

Gómez, R., Camarero, A. & Molina, R., 2016. Development of a vessel-performance forecasting system: Methodological framework and case study. *Journal of Waterway, Port, Coastal, and Ocean Engineering,* 142(2), p. 04015016..

Google Colaboratory, 2025. *Google Colaboratory Jupyter Notebook.* [Online] Available at: https://colab.research.google.com/

Goundar, S., 2012. *Research methodology and research method,* s.l.: Victoria University of Wellington.

Graves, S., 2021. Reflections on the evolution of operations management. *Management Science,* 67(9), pp. 5379-5388.

Gucma, S. & Gucma, M., 2019. Optimization of LNG terminal parameters for a wide range of gas tanker sizes: the case of the port of Świnoujście. *Arch. Transp.,* Volume 50, p. 91–100.

Guo, B. et al., 2022. Combined machine learning and physics-based models for estimating fuel consumption of cargo ships. *Ocean Engineering,* Volume 255, p. 111435.

He, Q., Zhang, X. & Nip, K., 2017. Speed optimization over a path with heterogeneous arc costs. *Transportation Research Part B: Methodological,* Volume 104, pp. 198-214.

Hirata, E. (2019) 'Service characteristics and customer satisfaction in the container liner shipping industry', *The Asian Journal of Shipping and Logistics*, 35(1), pp. 24–29.

Hirata, E. (2020) 'Service recovery and customer satisfaction in container liner shipping industry – an ordered logit approach', *International Journal of Shipping and Transport Logistics*, 12(6), pp. 563–575.

Hoang, A. & Choung, J., 2021. Effect of heat transfer coefficients on evaluation of temperature distribution in membrane type LNG carriers. *Ships and Offshore Structures,* pp. 1-14.

Hoang, A. D. & Choung, J., 2021. Effect of heat transfer coefficients on evaluation of temperature distribution in membrane type LNG carriers. *Ships Offshore Structures,* Volume 16, p. 204–215.

Hoang, N. & and Tran, V., 2023. Comparison of histogram-based gradient boosting classification machine, random forest, and deep convolutional neural network for pavement raveling severity classification. *Automation in Construction,* Volume 148, p. 104767.

Huang, S.T., Bulut, E. and Duru, O. (2015) ‘Service quality assessment in liner shipping industry: An empirical study on Asian shipping case’, *International Journal of Shipping and Transport Logistics*, 7(2), pp. 221–242.

Huang, S. H., Sheoran, S. K. & Keskar, H., 2005. Computer-assisted supply chain configuration based on supply chain operations reference (SCOR) model. *Computers & industrial engineering,* Volume 48, pp. 377-394.

Hu, Z. J. Y. et al., 2019. Prediction of fuel consumption for enroute ship based on machine learning.. *IEEE Access,* Volume 7, pp. 119497-119505.

Hu, Z. et al., 2021. A novel hybrid fuel consumption prediction model for ocean-going container ships based on sensor data.. *Journal of Marine Science and Engineering,* 9(4), p. 449.

Hu, Z. et al., 2022. A two-step strategy for fuel consumption prediction and optimization of ocean-going ships. *Ocean Engineering,* Volume 249, p. 110904.

IEEE Xplore, 2024. *IEEE Xplore Digital Library.* [Online] Available at: https://ieeexplore.ieee.org/ [Accessed 6 October 2025].

Ilias, L., Kapsalis, P., Mouzakitis, S. & Askounis, D., 2023. A multitask learning framework for predicting ship fuel oil consumption. *IEEE Access,* Volume 11, p. 132576–132589.

IMO, 2016. *International Gas Carrier (IGC) Code.* s.l.:IMO .

IMO, 2021. *IMO (International Maritime Organization). “EEXI and CII – Ship Carbon Intensity and Rating System.” FAQ / Guidance. IMO. Effective as of 1 January 2023,* s.l.: International Maritime Organization.

Işıklı, E., Aydın, N., Bilgili, L. & Toprak, A., 2020. Estimating fuel consumption in maritime transport. *Journal of Cleaner Production,* Volume 275, p. 124142.

Ivanov, D., Tsipoulanidis, A. & Schönberger, J., 2021. *Global Supply Chain and Operations Management: A Decision-Oriented Introduction to the Creation of Value.* s.l.:Springer.

Jeon, M. et al., 2018. Prediction of ship fuel consumption by using an artificial neural network.. *Journal of Mechanical Science and Technology,* Volume 32, pp. 5785-5796.

Ji, C., 2021. *Predicting fuel consumptions and exhaust gas emissions for LNG carriers via machine learning with hyperparameter optimization..* s.l., In SNAME Offshore Symposium. SNAME..

JSTOR, 2024. *JSTOR.* [Online] Available at: https://www.jstor.org/ [Accessed 6 October 2025].

Kano, N., Seraku, N., Takahashi, F. & Tsuji, S., 1984. Attractive quality and must-be quality. *Journal of the Japanese Society for Quality Control,* Volume 41, pp. 39-48.

Karagiannidis, P. & Themelis, N., 2021. Data-driven modelling of ship propulsion and the effect of data pre-processing on the prediction of ship fuel consumption and speed loss. *Ocean Eng.,* Volume 222, p. 108616.

Karatuğ, C, Arslanoğlu Y, 2020. *Analysis of Ship Fuel Consumption Through Multiple Linear Regression.* s.l., s.n., p. 268–271.

Kartal, G. & Bayramoğlu, G., 2024. The Safety Management System (SMS) as A tool for building safety culture in aviation: A qualitative research. *J. Aviat.,* Volume 8, p. 315–324.

Kee, K.-K., Lau Simon, B.-Y. & Yong Renco, K.-H., 2018. Prediction of ship fuel consumption and speed curve by using statistical method. *J. Comput. Sci. Comput. Math.,* Volume 8, p. 19–25.

Kim, D., Lee, S. & Lee, J., 2020. Data-driven prediction of vessel propulsion power using support vector regression with onboard measurement and ocean data. *Sensors (Basel),* Volume 20, p. 1588.

Kimmel, P., W. J. & Mitchell, J., 2022. *Survey of Accounting.* s.l.:John Wiley & Sons..

Lang, X., Wu, D. & Mao, W., 2021. *Benchmark Study of Supervised Machine Learning Methods for a Ship Speed-Power Prediction at Sea.* s.l., s.n., p. V006T06A018.

Lazakis, I., Turan, O. & Aksu, S., 2010. Increasing ship operational reliability through the implementation of a holistic maintenance management strategy. *Ships and Offshore Structures,* 5(4), pp. 337-357.

Lazakis, I. & Van Der Meer, R., 2023. Organisational structure configurations, their application and contribution to business performance in Greek shipping companies. *WMU J. Marit. Aff.,* Volume 22, p. 543–570.

Lee, H. et al., 2018. A decision support system for vessel speed decision in maritime logistics using weather archive big data. *Comput. Oper. Res.,* Volume 98, p. 330–342.

Leifsson, L., Sævarsdóttir, H., Sigurðsson, S. & Vésteinsson, A., 2008. Grey-box modeling of an ocean vessel for operational optimization. *Simulation Modelling Practice and Theory,* 16(8), pp. 923-932.

Le, L. T., Lee, G., Kim, H. & Woo, S.-H., 2020. Voyage-based statistical fuel consumption models of ocean-going container ships in Korea. *Marit. Policy Manage.,* Volume 47, p. 304–331.

Le, T. et al., 2024. Development of comprehensive models for precise prognostics of ship fuel consumption.. *Journal of Marine Engineering & Technology,* 23(6), pp. 451-465.

Liang, Q., Vanem, E., Knutsen, K. & Zhang, H., 2022. *Data-driven prediction of ship propulsion power using spark parallel random forest on comprehensive ship operation data.* s.l., IEEE.

Lin, C.-W., Hsu, W.-C. J. & Su, H.-J., 2020. Subjective and objective analysis of schedule delaying factors for container shipping lines. *J. Int. Logist. Trade,* Volume 18, p. 181–192.

Lirn, T. & Wong, R., 2013. Determinants of grain shippers' and importers' freight transport choice behaviour. *Production Planning & Control,* 24(7), pp. 575-588.

Li, S., Li, X., Zuo, Y. & Li, T., 2021. *Prediction of ship fuel consumption based on Elastic network regression model.* s.l., IEEE.

Lobo, A. (2010) 'Assessing the service quality of container shipping lines in the international supply chain network – shippers' perspective', *International Journal of Value Chain Management*, 4(3), pp. 256–266.

Mao, W., Rychlik, I., Wallin, J. & Storhaug, G., 2016. Statistical models for the speed prediction of a container ship. *Ocean Engineering,* Volume 126, pp. 152-162.

Martinić-Cezar, S., Jurić, Z., Assani, N. & Lalić, B., 2024. Optimization of fuel consumption by controlling the load distribution between engines in an LNG ship electric propulsion plant. *Energies,* Volume 17, p. 3718.

Menzel, A. & Otto, L., 2020. Connecting the dots: Implications of the intertwined global challenges to maritime security. Global Challenges in Maritime Security: An Introduction. p. 229–243.

Michail, N. A. & Melas, K. D., 2021. Market interactions between agricultural commodities and the dry bulk shipping market. *Asian J. Shipp. Logist.,* Volume 37, p. 73–81.

Mijailovi, R., V. M., Dvornik, J. & Pavasovi´c, L., 2024. Optimization of Fuel Consumption by Controlling the Load Distribution between Engines in an LNG Ship Electric Propulsion Plant. *Energies,* 17(6), p. 1415.

Milberg, W., 2008. Shifting sources and uses of profits: sustaining US financialization with global value chains. *Economy and Society,* Volume 37, pp. 420-451.

Mitroussi, 2013. Ship management: contemporary developments and implications. *The Asian Journal of Shipping and Logistics,* Volume 29, p. 229–248.

Mocerino, L. & Rizzuto, E., 2021. Statistical analysis of installed power on board modern cruise ships. In: *Lecture Notes in Civil Engineering.* Singapore: Springer Singapore, p. 769–783.

Molland, A., 2008. *The maritime engineering reference book: A guide to ship design, construction and operation..* s.l.:Oxford: Butterworth-Heinemann..

Molnar, G., 2022. Economics of gas transportation by pipeline and LNG. In: *The Palgrave Handbook of International Energy Economics.* Cham: Springer International Publishing, p. 23–57.

Moreira, L., Vettor, R. & Guedes Soares, C., 2021. Neural network approach for predicting ship speed and fuel consumption. *J. Mar. Sci. Eng.,* Volume 9, p. 119.

Nigam, A., Huising, R. & Golden, B., 2016. Explaining the selection of routines for change during organizational search. *Adm. Sci. Q.,* Volume 61, p. 551–583.

Nõmmela, K. & Kõrbe Kaare, K., 2022. Incorporated maritime policy concept: Adopting ESRS principles to support maritime sector's sustainable growth. *Sustainability,* Volume 14, p. 13593.

Notteboom, T. E., 2006. The time factor in liner shipping services. *Marit. Econ. Logist.,* Volume 8, p. 19–39.

Novaselić, M., Schiozzi, D. & Sopta, D., 2018. Strategic management in the function of adjustment of modern shipping companies to the market. *Pomor. Zb.,* Volume 54, p. 11–21.

Nwaoha, T., Ombor, G. & Okwu, M., 2017. A combined algorithm approach to fuel consumption rate analysis and prediction of sea-worthy diesel engine-powered marine vessels. *Proceedings of the Institution of Mechanical Engineers, Part M: Journal of Engineering for the Maritime Environment,* 231(2), pp. 542-554.

Odendaal, K., Alkemade, A. & Kana, A. A., 2023. Enhancing early-stage energy consumption predictions using dynamic operational voyage data: A grey-box modelling investigation. *Int. J. Nav. Archit. Ocean Eng.,* Volume 15, p. 100484.

Okumuş, F. & Ekmekçioğlu, A., 2021. MODELING OF GENERAL CARGO SHIP'S MAIN ENGINE POWERS WITH REGRESSION BASED MACHINE LEARNING ALGORITHMS: COMPARATIVE RESEARCH. *Mersin University Journal of Maritime Faculty,* 3(1), pp. 1-8.

Oliver, R., 1980. A Cognitive Model of the Antecedents and Consequences of Satisfaction Decisions. *Journal of Marketing Research,* Volume 17, pp. 460-469.

Öztürk, O. & Başar, E., 2022. Multiple linear regression analysis and artificial neural networks based decision support system for energy efficiency in shipping. *Ocean Engineering,* Volume 243, p. 110209.

Pagoropoulos, A., Møller, A. H. & McAloone, T. C., 2017. Applying Multi-Class Support Vector Machines for performance assessment of shipping operations: The case of tanker vessels. *Ocean Eng.,* Volume 140, p. 1–6.

Papageorgiou, N., 2020. Statistical analysis of marine vessel sensor data using SPM under ISO 19030. *Trans Motauto World,* Volume 5, p. 129–131.

Papandreou, C. & Ziakopoulos, A., 2022. Predicting VLCC fuel consumption with machine learning using operationally available sensor data.. *Ocean Engineering,* Volume 243, p. 110321.

Parasuraman, A., Zeithaml, V. & Berry, L., 1988. Servqual: A multiple-item scale for measuring consumer perc. *Journal of retailing,* 64(1), p. 12.

Park, J.J., Kim, S.Y., Kim, Y. *et al.* (2015) 'Study on tank shape for sloshing assessment of LNG vessels under unrestricted filling operation', *Journal of Marine Science and Technology*, 20, pp. 640–651. https://doi.org/10.1007/s00773-015-0318-1

Pavlenko, N. et al., 2020. *The climate implications of using LNG as a marine fuel,* s.l.: Swedish Environmental Protection Agency: Stockholm, Sweden.

Peace, P., Chris, J. & Victor, L., 2024. *Data Preprocessing for AI Models,* s.l.: s.n.

Peng, Y. et al., 2020. Machine learning method for energy consumption prediction of ships in port considering green ports.. *Journal of Cleaner Production,* Volume 264, p. 121564.

Perera, L. & Mo, B., 2020. Ship performance and navigation information under high-dimensional digital models.. *Journal of Marine Science and Technology,* 25(1), pp. 81-92.

Perera, L. P. & Mo, B., 2016. Marine engine operating regions under principal component analysis to evaluate ship performance and navigation behavior. *IFAC-PapersOnLine,* Volume 49, p. 512–517.

Perera, L. P. & Mo, B., 2018. Ship speed power performance under relative wind profiles in relation to sensor fault detection. *J. Ocean Eng. Sci.,* Volume 3, p. 355–366.

Petersen, J., Winther, O. & Jacobsen, D., 2012. A machine-learning approach to predict main energy consumption under realistic operational conditions. *Ship Technology Research,* 59(1), pp. 64-72.

Phan, T. M., Thai, V. V. & Vu, T. P., 2020. Port service quality (PSQ) and customer satisfaction: an exploratory study of container ports in Vietnam. *Marit. Bus. Rev.,* Volume 6, p. 72–94.

Phuong, N., 2024. Business Strategy Concept: A Systematical Review. *Journal of Knowledge Learning and Science Technology,* 3(2), pp. 128-142.

Piasecki, T., Bejger, A. & Wieczorek, A., 2021. Experimental studies of cargo tank cooldown in an LNG carrier. *European Research Studies Journal,* 24(3B), p. 886–895.

Progoulaki, M. & Theotokas, I., 2010. Human resource management and competitive advantage: An application of resource-based view in the shipping industry. *Mar. Policy,* Volume 34, p. 575–582.

Prokofieva, E., 2020. Review of research in cargo transportation reliability. *E3S Web Conf.,* Volume 157, p. 05008.

Pun, K., Yam, R. & Lewis, W., 2003. Safety management system registration in the shipping industry. *International Journal of Quality & Reliability Management,* 20(6), pp. 704-721.

Ravani, P. et al., 2008. Clinical research of kidney diseases III: Principles of regression and modelling. *Nephrology Dialysis Transplantation,* Volume 22, p. 3422–3430.

ResearchGate, 2024. *ResearchGate.* [Online] Available at: https://www.researchgate.net/ [Accessed 6 October 2025].

Ricardianto, P. et al., 2023. Enterprise risk management and business strategy on firm performance: The role of mediating competitive advantage. *Uncertain Supply Chain Manag.,* Volume 11, p. 249–260.

Rinaldy, D., 2022. *Reliability of International Safety Management (ISM) Code Implementation in Operational Risk Management of Shipping Industry.* s.l., In Proceedings of International Conference on Economics Business and Government Challenges.

Romeo, L., Vidal, L. & Rodrigo, B., 2020. Use of Small Internal Combustion Engines for LNG Boil-Off Gas Conversion An Experimental and Numerical Analysis. *Applied Sciences,* 10(24), p. 8966.

Ruan, Z. et al., 2024. A novel prediction method of fuel consumption for wing-diesel hybrid vessels based on feature construction. *Energy,* Volume 286, p. 129516.

Salah, A., Çağlar, D. & Zoubi, K., 2023. The impact of production and operations management practices in improving organizational performance: The mediating role of supply chain integration. *Sustainability,* 15(20), p. 15140.

Sanchez-Gonzalez, P.-L., Díaz-Gutiérrez, D. & Núñez-Rivas, L. R., 2022. Digitalizing maritime containers shipping companies: Impacts on their processes. *Appl. Sci. (Basel),* Volume 12, p. 2532.

Scholar, G., 2024. *Google Scholar.* [Online] Available at: https://scholar.google.com/ [Accessed 6 October 2025].

ScienceDirect, 2024. *ScienceDirect.* [Online] Available at: https://www.sciencedirect.com/ [Accessed 6 October 2025].

Shokohian, A. & Kaviani, M., 2024. *Improving machine learning models for ship fuel consumption prediction using K-fold cross validation and grid search methods,* s.l.: s.n.

SIGTTO, 2024. *Annual Report and Accounts 2024.* [Online] Available at: https://www.sigtto.com/media/4195/sigtto-annual-report-2024.pdf [Accessed 6 October 2025].

Simonsen, M., Walnum, H. J. & Gössling, S., 2018. Model for estimation of fuel consumption of cruise ships. *Energies,* Volume 11, p. 1059.

SpringerLink, 2024. *SpringerLink.* [Online] Available at: https://link.springer.com/ [Accessed 6 October 2025].

Stavroulakis, P. J. & Papadimitriou, S., 2022. Total cost of ownership in shipping: a framework for sustainability. *J. Shipp. Trade,* Volume 7.

Stopford, M., 2009. *Maritime Economics 3e.* 3 ed. London(England): Routledge.

Su, M., Lee, H., Wang, X. & Bae, S., 2025. Fuel consumption cost prediction model for ro-ro carriers: a machine learning-based application.. *Maritime Policy & Management,* 52(2), pp. 229-249.

Sun, C., Wang, H., Liu, C. & Zhao, Y., 2019. Dynamic prediction and optimization of energy efficiency operational index (EEOI) for an operating ship in varying environments. *Journal of Marine Science and Engineering,* 7(11), p. 402.

Suprapti, F., Susanto, S., Hendrawan, D. & Anggoro, R., 2023. Optimization of reliquefaction system on gas carrier to maintain the condition and temperature of cargo tank. *db,* Volume 4, p. 51–57.

Tam, K. & Jones, K. D., 2018. Maritime cybersecurity policy: the scope and impact of evolving technology on international shipping. *J. Cyber Policy,* Volume 3, p. 147–164.

Taylor & Francis Online, 2024. *Taylor & Francis Online.* [Online] Available at: https://www.tandfonline.com/ [Accessed 6 October 2025].

Thai, V.V. (2008) 'Service quality in maritime transport: Conceptual model and empirical evidence', *Asia Pacific Journal of Marketing and Logistics*, 20(4), pp. 493–518.

Thai, V., Tay, W., Tan, R. & Lai, A., 2014. Defining service quality in tramp shipping: conceptual model and empirical evidence. *The Asian Journal of Shipping and Logistics,,* 30(1), pp. 1-29.

Theotokas, I. N., Lagoudis, I. N., Syntychaki, A. & Prosilias, J., 2024. Factors affecting E-HRM practices in Greek shipping management companies: the role of organizational culture, cultural intelligence, and innovation. *J. Shipp. Trade,* Volume 9.

Tran, T., 2021. Comparative analysis on the fuel consumption prediction model for bulk carriers from ship launching to current states based on sea trial data and machine learning technique.. *Journal of Ocean Engineering and Science,* 6(4), pp. 317-339.

Tran, T. A., 2019. Design the prediction model of low-sulfur-content fuel oil consumption for M/V NORD VENUS 80,000 DWT sailing on emission control areas by artificial neural networks. *Proc. Inst. Mech. Eng. Part M: J. Eng. Marit. Environ.,* Volume 233, p. 345–362.

Tsarouhas, P., 2023. New Trends in Production and Operations Management. *Applied Sciences,* Volume 13.

Tu, H. et al., 2023. Optimum trim prediction for container ships based on machine learning. *Ocean Engineering,* Volume 277, p. 111322.

UNCTAD, 2024. *Review of maritime transport 2024.* s.l.:s.n.

Uyanik, T., Arslanoglu, Y. & Kalenderli, O., 2019. *Ship fuel consumption prediction with machine learning.* Antalya, Turkey, Proceedings of the 4th International Mediterranean Science and Engineering Congress.

Uyanık, T., Karatuğ, Ç. & Arslanoğlu, Y., 2020. Machine learning approach to ship fuel consumption: A case of container vessel. *Transp. Res. D Transp. Environ.,* Volume 84, p. 102389.

Valchev, I. et al., 2022. *Artificial Intelligence-based short-term forecasting of vessel performance parameters,* s.l.: s.n.

Vanem, E., Antão, P., Østvik, I. & Del Castillo Comas, F., 2008. Analysing the risk of LNG carrier operations. *Reliability Engineering & System Safety,* 93(9), p. 1328–1344.

Visvikis, I. D. & Panayides, P. eds., 2017. *Shipping Operations Management.* 1 ed. Cham(Switzerland): Springer International Publishing.

Wagner, N. & Wiśnicki, B., 2022. The importance of emerging technologies to the increasing of corporate sustainability in shipping companies. *Sustainability,* Volume 14, p. 12475.

Wang, E. et al., 2024. Improving Forest Above-Ground Biomass Estimation Accuracy Using Multi-Source Remote Sensing and Optimized Least Absolute Shrinkage and Selection Operator Variable Selection Method. *Remote Sensing,* Volume 16, p. 4497.

Wang, K., Yan, X., Yuan, Y. & Li, F., 2016. Real-time optimization of ship energy efficiency based on the prediction technology of working condition. *Transportation Research Part D: Transport and Environment,* Volume 46, pp. 81-93.

Wang, S. et al., 2018. Predicting ship fuel consumption based on LASSO regression. *Transp. Res. D Transp. Environ.,* Volume 65, p. 817–824.

Weiser, A.-K., Jarzabkowski, P. & Laamanen, T., 2020. Completing the adaptive turn: An integrative view of strategy implementation. *Acad. Manag. Ann.,* Volume 14, p. 969–1031.

Widodo, Santoso, A., Erwandi & Baidowi, A., 2022. Form factor prediction based on ship model test data by statistical method. *IOP Conf. Ser. Earth Environ. Sci.,* Volume 1081, p. 012017.

Wiley Online Library, 2024. *Wiley Online Library.* [Online] Available at: https://onlinelibrary.wiley.com/ [Accessed 6 October 2025].

Wood, D., 2021. Predicting saturated vapor pressure of LNG from density and temperature data with a view to improving tank pressure management. *Petroleum,* 7(1), pp. 91-101.

Wu, L. F., Huang, I. C., Huang, W. C. & Du, P. L., 2019. Aligning organizational culture and operations strategy to improve innovation outcomes: An integrated perspective in organizational management. *Journal of Organizational Change Management,* Volume 32, p. 224–250.

Wu, S. & Ju, Y., 2021. Numerical study of the boil-off gas (BOG) generation characteristics in a type c independent liquefied natural gas (LNG) tank under sloshing excitation. *Energy,* Volume 223, p. 120001.

Xie, X. et al., 2023. Fuel consumption prediction models based on machine learning and mathematical methods. *Journal of Marine Science and Engineering,* 11(4), p. 738.

Xie, X. et al., 2023. Fuel consumption prediction models based on machine learning and mathematical methods. *Journal of Marine Science and Engineering,* 11(4), p. 738.

Xie, X. et al., 2023. Fuel consumption prediction models based on machine learning and mathematical methods.. *Journal of Marine Science and Engineering,* 11(4), p. 738.

Xi, M., Chen, Y. & Zhao, S., 2021. The Role of employees' perceptions of HPWS in the HPWS-performance relationship: A multilevel perspective. *Asia Pac. J. Manag.,* Volume 38, p. 1113–1138.

Xu, L. et al., 2023. Performance and emission characteristics of an ammonia/diesel dual-fuel marine engine. *Renew. Sustain. Energy Rev.,* Volume 185, p. 113631.

Yan, R., Wang, S. & Du, Y., 2020. Development of a two-stage ship fuel consumption prediction and reduction model for a dry bulk ship. *Transp. Res. Part E: Logist. Trans. Rev.,* Volume 138, p. 101930.

Yan, R. et al., 2024. Improving ship energy efficiency: Models, methods, and applications.. *Applied Energy,* Volume 368, p. 123132.

Yan, X., S. X. & Yin, Q., 2015. Multiparameter sensitivity analysis of operational energy efficiency for inland river ships based on backpropagation neural network method. *Marine Technology Society Journal,* 49(1), pp. 148-153.

Yao, S., Zhang, Z., Wei, Y. & Liu, R., 2022. Integrated design and optimization research of LNG cold energy and main engine exhaust heat utilization for LNG powered ships. *SSRN Electron. J.*.

Yeo, G.T., Thai, V.V. and Roh, S.Y. (2015) ‘An analysis of port service quality and customer satisfaction: The case of Korean container ports’, *The Asian Journal of Shipping and Logistics*, 31(4), pp. 437–447.

Yuen, K.F. and Thai, V.V. (2015) ‘Service quality and customer satisfaction in liner shipping’, *International Journal of Quality and Service Sciences*, 7(2/3), pp. 170–183.

Yin, L. & Ju, Y., 2022. Review on the design and optimization of BOG re-liquefaction process in LNG ship. *Energy (Oxf.),* Volume 244, p. 123065.

Yoo, B. & Kim, J., 2019. Probabilistic modeling of ship powering performance using full-scale operational data. *Applied Ocean Research,* Volume 82, pp. 1-9.

Yoon, Y., Yoon, S., Ahn, B. & Kang, H., 2020. Effect of parameters on vapor generation in ship-to-ship liquefied natural gas bunkering. *Applied Sciences,* 10(19), p. 6861.

Yuen, K. & Thai, V., 2015. Service quality and customer satisfaction in liner shipping. *International Journal of Quality and Service Sciences,* 7(2/3), pp. 170-183.

Zaman, I. et al., 2017. Development of automatic mode detection system by implementing the statistical analysis of ship data to monitor the performance. *International Journal of Maritime Engineering,* Volume 159.

Zentai, B. & Toka, L., 2023. *Boat Speed Prediction in SailGP. In.* s.l., Cham: Springer Nature Switzerland., pp. 155-164.

Zhang, C., Wang, X., Hu, Y. & Song, G., 2023. Modeling and Optimization of Fuel-Mode Switching and Control Systems for Marine Dual-Fuel Engine. *Journal of Marine Science and Engineering,* 11(11), p. 2131.

Zhang, M., Tsoulakos, N., Kujala, P. & Hirdaris, S., 2024. A deep learning method for the prediction of ship fuel consumption in real operational conditions.. *Engineering Applications of Artificial Intelligence ,* Volume 130, p. p.107425.

Zhang, Z., Larranaga, A. S. & Wang, Q., 2024b. Liquefied natural gas storage and transmission. In: *Advances in Natural Gas: Formation, Processing, and Applications. Volume 6: Natural Gas Transportation and Storage.* s.l.:Elsevier, p. 51–80.

Zhao, S. et al., 2021. *Influence of different Machine learning algorithms on Prediction Model of Fuel Consumption of Inland Ships.* s.l., 6th International Conference on Transportation Information and Safety (ICTIS) .